Regulation of morphogen signalling during neural patterning in the Xenopus embryo

Tan Grahn, Hooi Min

2011

Regulation of morphogen signalling during neural patterning in the *Xenopus* embryo

Hooi Min Tan Grahn

Department of Laboratory Medicine
Laboratory Vertebrate Developmental Biology
Lund Stem Cell Center
Faculty of Medicine
Lund University, Sweden
2011

LUND UNIVERSITY
Faculty of Medicine

With permission of the Medical Faculty at Lund University,
this thesis will be publicly defended on October 14 at 13.00
in GK Salen, BMC, Solvegatan 19, Lund

Supervisor:
Dr. Edgar pera

Faculty Opponent:
Prof. Dr. Michael Kühl, Institute of Biochemistry and Molecular Biology
Ulm University, Germany

Organization LUND UNIVERSITY Department of Laboratory Medicine Lund Stem Cell Center, Laboratory Vertebrate Developmental Biology S-22184, Lund	Document name DOCTORAL DISSERTATION Date of issue 2011-10-14 Sponsor organization
Author(s) Hooi Min Tan Grahn	

Title and subtitle

Regulation of morphogen signalling during neural patterning in the *Xenopus* embryo

Abstract

Morphogens such as Hedghog, Wnt, FGF, and retinoic acid are important signals whose concentrations need to be tightly regulated in the vertebrate embryo to ensure body axis development and formation of the central nervous system. We first show that the intracellular cytoplasmic protein XSufu acts as a dual regulator of Hedgehog (Hh) and Wnt signals during neural induction and patterning in the *Xenopus* embryo. We further reveal an essential role of XSufu in the crosstalk of the two pathways, in which β-catenin activates Hh signalling upon overexpression of Gli1, and Gli inhibits Wnt signalling upon overexpression of β-catenin. A biphasic model for the role of XSufu in anteroposterior patterning of the neural plate is presented suggesting that XSufu suppresses anterior Gli and posterior β-catenin transcription factors in a dose-dependent manner.

Then we introduce the secreted serine protease xHtrA1 as feedforward stimulator of long-range FGF signalling. Fibroblast growth factor (FGF) signals activate transcription of *xHtrA1*, and xHtrA1 stimulates *FGF4* and *FGF8* gene activities, allowing positive feedback regulation. We also show that xHtrA1 triggers proteolytic cleavage of xBiglycan, xSyndecan-4, and xGlypican-4, suggesting a model, in which xHtrA1 through cleaving proteoglycans releases FGF/proteoglycan complexes that act as long-range messages during anteroposterior patterning, mesoderm induction, and neuronal differentiation.

Third, we present *Xenopus* retinol dehydrogenase-10 (XRDH10) as a critical enzyme for embryonic vitamin A metabolism and retinoic acid (RA) synthesis in the developing embryo. We show that XRDH10, which oxidizes vitamin A to retinal, is transcriptionally inhibited by RA, suggesting negative feedback regulation at the first step of RA biosynthesis. XRDH10 cooperates with XRALDH2, which further oxidizes retinal to bioactive RA, in Spemann's organizer during dorsoventral patterning of the embryo. We also show that the nested gene expression and cooperate action of XRDH10 and XRALDH2 form a biosynthetic enzyme code that establishes RA gradients along the anteroposterior neuraxis.

Key words: Suppressor-of-fused; Gli; β-Catenin; Neural; *Xenopus*; FGF; Signalling; HtrA1; RDH10; Retinol dehydrogenase; Retinoic acid; Spemann's organizer; Induction; Gradient

Classification system and/or index termes (if any): Developmental Biology

Supplementary bibliographical information: Faculty of Medicine Doctoral Dissertation Series 2011:88		Language English
ISSN and key title: 1652-8220		ISBN 978-91-86871-37-6
Recipient's notes	Number of pages 142	Price
	Security classification	

卡乐约翰

爸爸妈妈，弟弟伟伦

谢谢！

你们是我一生中最爱！

About the cover: Whole-mount *in situ* hybridization of early neurula embryo in anterior view. *nlacZ* mRNA (red nuclei) was injected as lineage tracer. *En2* dermacates posterior midbrain (top) and *FoxG1* indicates forebrain (bottom) territories.

Hooi Min Tan Grahn

Department of Laboratory Medicine
Laboratory Vertebrate Developmental Biology
Lund Stem Cell Center
Faculty of Medicine
Lund University
Klinikgatan 26,
S-22184 Lund,
Sweden

Printed by I-husets Tryckeri, Sölvegatan 14

ISSN 1652-8220

ISBN 978-91-86871-37-6

Lund University, Faculty of Medicine Doctoral Dissertation Series 2011:88

Contents

List of Papers

This thesis is written according to the following listed papers in Roman numerals.

I. **Tan Hooi Min**, Martin Kriebel, Shirui Hou and Edgar Pera (2011). The dual regulator Sufu integrates Hedgehog and Wnt signals in the early *Xenopus* embryo. *Developmental Biology*. In press.

II. Ina Strate, **Tan Hooi Min**, Dobromir Iliev, and Edgar Pera (2009). Retinol dehydrogenase 10 is a feedback regulator of retinoic acid signalling during axis formation and patterning of the central nervous system. *Development* 136, 461-472.

III. Shirui Hou, Marco Maccarana, **Tan Hooi Min**, Ina Strate, and Edgar Pera (2007). The secreted serine protease xHtrA1 stimulates long-range FGF signalling in the early *Xenopus* embryo. *Developmental Cell* 13, 226-241.

Abbreviations

APC	Adenomatous Polyposis Coli
CK1	Casein Kinase 1
GSK3	Glycogen Synthase Kinase-3
LEF/TCF	Lymphoid enhancer factor/T-cell factor
Fz	Frizzled
LRP6	Low-density lipoprotein receptor-related protein 6
Dsh	Disheveled
Ci	Cubitus interruptus
dnWnt8	Dominant-negative Wnt8
MVBs	Multivesicular bodies
GBP	GSK3-binding protein
D-V	Dorsal-ventral
BCNE	Blastula Chordin and Noggin expression
TGF-β	Transforming growth factor beta
BMP	Bone morphogenetic protein
ActRIIB	Activin receptor IIB
Xnr3	Xenopus nodal-related 3
Dkk1	Dickkopf-1
Hh	Hedgehog
Ptch	Patched
Smo	Smoothened
PKA	Protein kinase A
Shh	Sonic Hedgehog
Bhh	Banded Hedgehog
Sufu	Suppressor-of-fused
XSufu-MO	XSufu morpholino oligonucleotide
MEF	Mouse embryonic fibroblast
FGF	Fibroblast growth factor
RTK	Receptor tyrosine kinase
PI3K	Phosphatidylinositol-3-kinase
PLC-γ	Phospholipase C- gamma
Raf	Rapidly accelerated fibrosarcoma
MAPKK	Mitogen-activated protein kinase kinase
Erk	Extracellular signal-regulated protein kinase
dnFGFR4a	Dominant-negative FGF receptor 4a
IGFs	Insulin-like growth factors
Xbra	Brachyury
bFGF	Basic FGF
XeFGF	Embryonic FGF
XFD	Dominant-negative FGF receptor-1
HtrA1	High-temperature requirement factor A 1
dpERK	Diphosphorylated extracellular signal regulated kinase
xBgn	*Xenopus* Biglycan
xSyn4	*Xenopus* Syndecan-4
xGlp4	*Xenopus* Glypican-4
CS	Chondroitin sulfate
DS	Dermatan sulfate
HS	Heparan sulfate
GAG	Glycosaminoglycan

RA	Retinoic acid
CRABP	Cellular retinoic acid-binding protein
RARs	RA receptors
RDH10	Retinol dehydrogenase-10
RALDH2	Retinaldehydrogenase 2
CYP26A1	Cytochrome P450 26 A1
SDR	Short-chain dehyrogenase/reductase
ENU	N-ethyl-N-nitrosourea
ADMP	Anti-dorsalizing morphogenetic protein

Introduction

1.1 *Xenopus laevis* as model system to study early development

The South African clawed frog, *Xenopus laevis*, has several advantages for use in research: The eggs are large and can be fertilized externally. It is easily maintained in the laboratory and produces a large amount of eggs. The frog embryo has the ability to heal after microsurgery, allowing for excision and culture of blastula-derived animal caps. Animal cap explants are pluripotent and, when exposed to different growth factors, can differentiate into three germ layers: endoderm, mesoderm and ectoderm. With the use of fate mapping and embryo transplantation techniques, *Xenopus* embryos are a convenient vertebrate model system to study pattern formation and organogenesis in the early development. *Xenopus* embryos can be microinjected with *in vitro* synthesized RNA and DNA to overexpress genes. Moreover, antisense morpholino oligonucleotides can be microinjected to downregulate endogenous genes. Embryos can also be manipulated using specific drugs that act as agonists or antagonists of distinct signalling pathways. Given the high degree of conservation between genes and signalling pathways in vertebrates, *Xenopus* embryos provide an easy tool to unravel the molecular basis and mechanisms of cellular signalling and to apply the knowledge towards understanding human development.

1.2 Establishment of dorsal-ventral polarity

In amphibians, the dorsoventral axis is the first body axis to form. Cortical rotation occurs within the first cell cycle after fertilization. Upon the entry of the sperm into the animal hemisphere, the outer layer of the fertilized egg undergoes cortical-cytoplasmic rotation. This microtubule-mediated process involves the displacement of the egg's cortex relative to its cytoplasmic core by 30 degrees in an animal-vegetal direction and

transforms the polarized cylindrical symmetry of the egg into an embryo with a bilateral symmetry (Rowning et al., 1997).

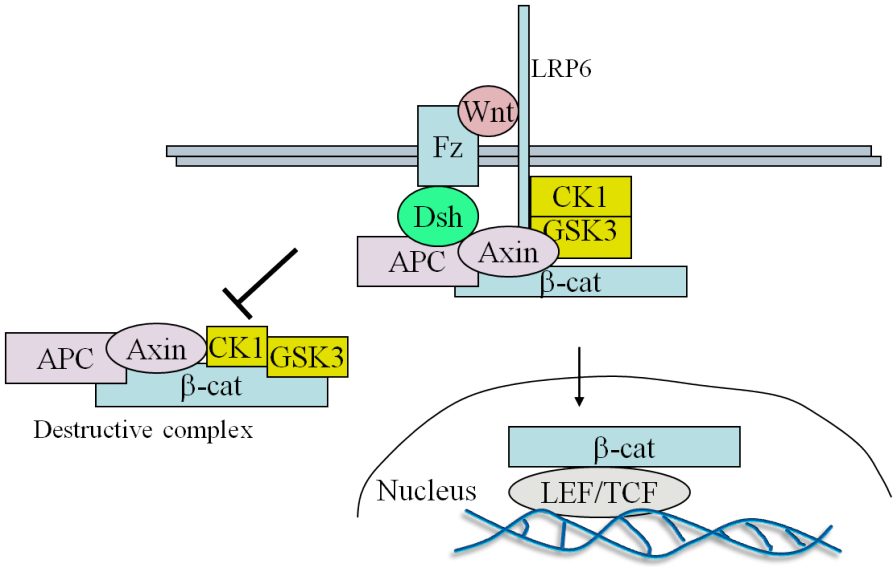

Fig. 1. Wnt/β-catenin signalling

Binding of Wnt ligands to the transmembrane receptors Frizzled (Fz) and LRP-6 stimulates recruitment of the cytoplasmic Disheveled (Dsh) protein and the β-catenin destruction complex (Axin, APC, CK1 and GSK3) that leads to a release of β-catenin. Stabilized β-catenin enters the nucleus and forms a heterodimer with the LEF/TCF transcription factor that causes activation of Wnt downstream target genes.

1.3 Canonical Wnt/β-catenin signalling in dorsoventral axis development

Wnt signals through their transcriptional effector β-catenin are critically involved in the establishment of the dorsoventral body axis (**Fig 1;** Schneider et al., 1996; Larabell et al., 1997). In resting cells, β-catenin forms with Axin, APC (Adenomatous Polyposis Coli), CK1 (Casein Kinase 1), and GSK3 (Glycogen Synthase Kinase-3) a destruction complex, in which CK1 and GSK3 phosphorylate the amino terminus of β-catenin that leads to ubiquitin-dependent degradation of β-catenin (Amit et al., 2002; Liu et al., 2002). Under these conditions, the LEF (Lymphoid enhancer factor)/TCF (T-cell factor) transcription factor acts as a transcriptional repressor and blocks the initiation of Wnt target gene transcription. Binding of Wnt ligands to the seven transmembrane receptor Frizzled (Fz) and the single-transmembrane protein LRP (Low-density lipoprotein receptor-related protein) 6, leads to activation of the intracellular Disheveled (Dsh) protein and recruitment of the β-catenin-Axin-APC-CK1-GSK3 destruction complex to the membrane. Recent studies showed that receptor internalization is required for Wnts to signal (Yamamoto et al., 2006; Blitzer and Nusse, 2006). Multiple ternary complexes of Wnt, Fz and LRP6 cluster on oligomerized Dsh protein to form endocytic signalosomes (Bilic et al., 2007). Vacuolar H+-ATPase-mediated acidification of the endocytic signalosomes is critical for Wnt signaling (Cruciat et al, 2010). CK1 and GSK3 phosphorylate LRP6 at intracellular PPPSPxP motifs (Zeng et al., 2005; 2008). LPR6 and Axin form a positive feedback loop in which Axin is required for Lrp6 phosphorylation, and Lrp6 phosphorylation at the PPPSPxS motifs in turn provides docking sites for Axin (Tamai et al., 2004; Zeng et al., 2005). GSK3 is sequestered in endosomal multivesicular bodies (MVBs) that protect cytoplasmic β-catenin from inhibitory effects of GSK3 (Taelman et al., 2010). Stabilized β-catenin is then able to enter the nucleus. β-catenin forms a heterodimer with LEF/TCF and converts this DNA binding protein into a transcriptional activator to stimulate the expression of Wnt target genes. (Yost et al., 1996; Pierce and Kimelman, 1995; Weaver et al., 2003; Rao and Kühl, 2010).

Maternally expressed *Wnt11*, *Dsh* and *GSK3-binding protein* (GBP) are dorsal determinant proteins that establish the dorsoventral body axis in the *Xenopus* embryo

(Mille et al., 1999; Weaver et al., 2003; Tao et al., 2005). Dsh and GBP form a heterotetrameric complex on microtubules and translocate to the future dorsal side of the embryo. The dorsally localized GBP and Dsh prevent GSK3 from phosphorylating β-catenin. Stabilized β-catenin enters the nucleus on the dorsal side of the embryo and provides the earliest molecular dorsal-ventral (D-V) asymmetry (Schneider et al., 1996).

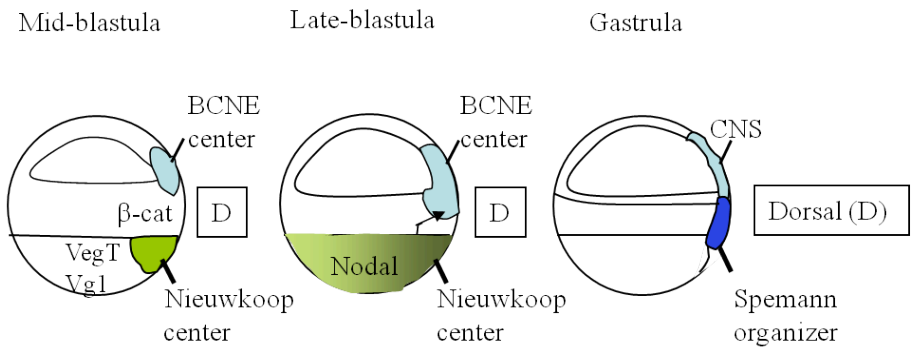

Fig. 2. Spemann organizer formation in *Xenopus*

At mid-blastula stage, formation of Nieuwkoop and BCNE centers rely on high level of β-catenin proteins on the dorsal side. The Nieuwkoop center is formed at the intersection of dorsal β-catenin and vegetally expressed *VegT* and *Vg1* genes. The BCNE center is located in the dorsal animal cap and marginal zone. Cells of the Nieuwkoop center secretes large amounts of Nodal proteins that induce Spemann's organizer in the dorsal marginal zone of the gastrula embryo.

1.4 Two signalling centers in *Xenopus* embryos

At mid-blastula transition, two signalling centers are simultaneously formed under the influence of β-catenin on the dorsal side: The Nieuwkoop center and the BCNE center (**Fig. 2**). The Nieuwkoop center is located in the dorsal-vegetal region at the intersection of dorsal β-catenin and vegetally expressed *VegT* and *Vg1* genes. VegT is a transcription factor of the T-box family and Vg1 member of the secreted TGF-β superfamily. β-

catenin and Vg1 synergistically activate the homeobox gene *Siamois* that is sufficient and required to mediate Nieuwkoop center signaling activity (Brannon and Kimelman1996). The Nieuwkoop center is fated to become dorsal endoderm. The BCNE (Blastula Chordin and Noggin expression) center is located in the dorsal and marginal zone of blastula stage embryos. In addition to Chordin and Noggin, the BCNE center expresses genes encoding Siamois, the winged-helix transcription factor *pintallavis/FoxA4/HNF3β*, and the soluble *Xenopus* nodal-related 3 (Xnr3) protein in response to β-catenin signalling (Kuroda et al., 2004; Wessely et al., 2004). BCNE cells give rise to the forebrain, midbrain and hindbrain, as well as the floor plate and notochord. Brain formation fails in embryos where the BCNE center is excised (Kuroda et al., 2004).

1.5 Nieuwkoop center and mesoderm induction

The mesoderm is formed in the equatorial region of the blastula embryo when ectodermal cells in the animal hemisphere receive signals from the underlying vegetal endoderm. When a blastula embryo is separated along the equator, neither animal nor vegetal cap forms mesodermal tissue, but the combination of both caps gives rise to mesoderm (Nieuwkoop, 1969). Mesodermal tissue further develops, from dorsal to ventral, into notochord, somite, kidney, lateral plate mesoderm, and ventral blood islands (De Robertis and Kuroda, 2004).

After mid-blastula transition, the Nieuwkoop center expresses and secretes members of the TGFβ family that induce mesoderm, including Nodal-related proteins (Xnr1, -2, -4, -5 and -6, Agius et al., 2000; Takahashi et al., 2000) and Derrière (Sun et al., 1999). *Derrière* has a similar expression pattern as *VegT* and is a direct target gene of *VegT*. Derrière is a potent mesoderm inducing signal (Sun et al., 1999). Another Nodal-related protein is the ubiquitously expressed Activin that induces mesoderm through activation of the transcription factor Brachyury (Xbra). According to the mesoderm induction model, *VegT* and *Vg1* act together with *β-catenin* to activate the Nodal-related proteins (Xnr1, 2, 4) at the late blastula stage. A gradient of Xnr1, -2, and -4 is expressed across

the endoderm, with the highest levels in the dorsal region.A high concentration of Xnrs leads to the formation of Spemann's organizer, an intermediate level of Xnrs contributes to the formation of the lateral mesoderm, while at low levels or in the absence of Xnrs ventral mesoderm formed (Agius et al., 2000).

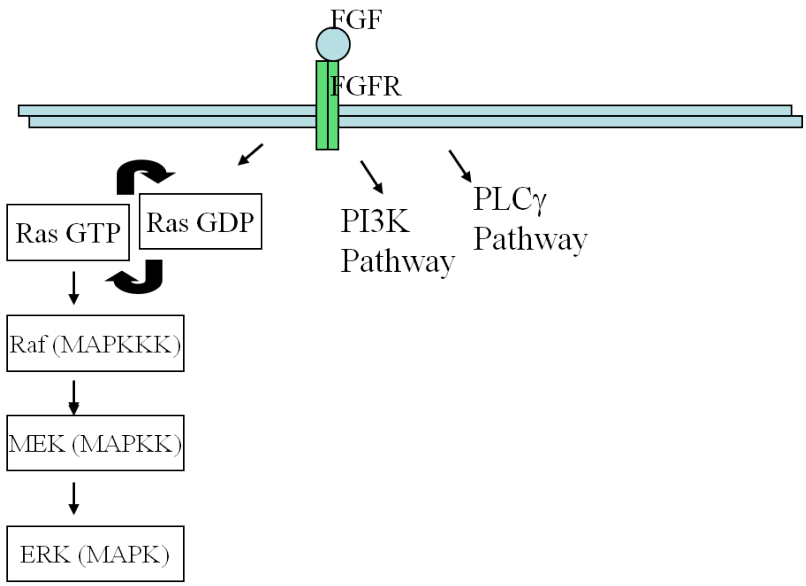

Fig. 3. FGF/ERK signalling

Fibroblast growth factor (FGF) ligands bind to FGF tyrosine kinase receptors. Dimerization of the receptor activates the Ras GTP protein. Activated Ras activates protein kinase activity of Raf. Raf phosphorylates the MEK/MAPKK, and MEK in turn activates and phosphorylates ERK/MAPK, which then enters the nucleus and activates transcription factors. Activated FGF signalling induces an inhibitory phosphorylation of Smad1 and stimulates neural induction.

1.6 Fibroblast growth factor signalling in mesoderm induction

Fibroblast growth factor (FGF) ligands bind to FGF cell surface receptors, leading to their dimerization and the activation of receptor tyrosine kinase (RTK) activity (**Fig. 3**).

RTK further activates phosphatidylinositol-3-kinase (PI3K), phospholipase C-gamma (PLC-γ), and the Ras G protein. Active Ras associates with and recruits the serine/threonine-protein kinase Raf (Rapidly accelerated fibrosarcoma) to the cell membrane. Raf phosphorylates the MAPKK (mitogen-activated protein kinase kinase) /MEK, and MEK in turn phosphorylates Erk (Extracellular signal-regulated protein kinase), which then enters the nucleus and activates downstream transcription factors.

In vertebrates, the FGF family comprises 22 ligands and 4 receptors with additional splicing variants (Ornitz et al., 2000; Zhang et al., 2006). Basic FGF (bFGF or FGF2) was first shown to induce mesoderm formation in animal explants (Kimelman et al., 1988). *Xenopus embryonic FGF* (*XeFGF* or *FGF4*) is expressed maternally and has a peak zygotic expression along the blastopore ring at the onset of gastrulation (Isaacs et al., 1992). *XeFGF* stimulates transcription of *Xbra* and, vise versa, *Xbra* activates expression of the *XeFGF* gene suggesting a positive autoregulatory loop that stabilizes mesoderm formation (Isaacs et al., 1994). FGF is a competence factor in the marginal zone and allows equatorial cells to develop into mesodermal tissue in response to activin-type TGFβ-signals (Cornell et al., 1995). A carboxyterminally truncated, dominant-negative FGF receptor-1 (XFD) inhibits the formation of notochord, muscle and ventrolateral mesoderm (Amaya et al., 1991, 1993). XFD or dominant-negative mutant constructs of c-ras and c-raf suppress Activin-mediated mesoderm induction in animal cap explants, suggesting an important function of FGF signals and the MARK/ERK pathway in the induction of mesodermal tissue (LaBonne and Whitman, 1994).

1.7 Spemann's organizer and neural induction

When transplanted into the ventral side of a host embryo, Spemann's organizer in the dorsal mesoderm of the gastrula embryo induces a secondary body axis with an ectopic central nervous system (Spemann and Mangold, 1924). Molecular studies revealed that Spemann's organizer is a source of secreted BMP antagonists such as Noggin (Lamb et al., 1993), Chordin (Sasai et al., 1994), and Follistatin (Hemmati-Brivanlou et al., 1994).

Misexpression of Noggin, Chordin, and Follistatin can convert epidermis into neural tissue in blastula and early gastrula embryos. However, dissociated animal caps can adopt a neural fate in the absence of mesodermal tissue (Grunz and Tacke, 1990; Sato and Sargent, 1989). This neuralization is reverted by members of the BMP (bone morphogenetic protein) family, including BMP2, BMP4, and BMP7 (Wilson and Hemmati-Brivanlou, 1995). A dominant-negative construct of the activin receptor IIB (ActRIIB) blocks BMP signalling and induces neural tissue in animal cap explants, leading to the idea that neural is the default state in *Xenopus* embryos (Hemmati-Brivanlou and Melton, 1992; Dale and Jones, 1999).

The Spemann organizer has trunk and head inducing activity. Inhibition of BMP signalling in the ventral marginal zone causes ectopic trunk formation, while simultaneous inhibition of BMP and Wnt signalling leads to a complete secondary axis with trunk and head structures (Glinka et al., 1997). Spemann's organizer expresses soluble Wnt antagonists, including Frzb (Leyns et al., 1997), sFRP2 (Pera and De Robertis, 2000), Crescent (Pera and De Robertis, 2000; Shibata et al., 2000), Dickkopf-1 (Dkk1; Glinka et al., 1998) and Cerberus (Bouwmeester et al., 1996; Piccolo et al., 1999). Blastocoel injection of Dkk1-neutralizing antibodies inhibits head formation, suggesting that Wnt antagonists are essential for developing anterior neural tissues in the early *Xenopus* embryo (Glinka et al., 1998). A role of Wnt inhibition in neural induction is further supported by the finding that inhibition of Wnt signaling by dominant-negative *XTcf3* constructs promotes the induction of the neural marker gene *Sox3* in early *Xenopus* embryos (Heeg-Truesdell and LaBonne, 2006).

In addition to soluble antagonists of the BMP and Wnt pathways, active signals including FGFs and IGFs contribute to neural induction. Microinjection of *FGF8* mRNA causes expansion of the neural marker *Sox2* and ectopic expression of the neuronal marker *N-tubulin*, while a dominant-negative FGF receptor 4a (*dnFGFR4a*) construct blocks neural induction and neuronal differentiation in *Xenopus* embryos (Hardcastle et al., 2000; Pera et al., 2003). Neural inducing activity requires an intact PLC-γ signalling pathway through the binding of PLC-γ at conserved tyrosine kinase residues to FGF receptors

(Umbhauer et al., 2000). Moreover, insulin-like growth factors (IGFs) are necessary and sufficient to induce head and neural tissue and act through inhibiting BMP and Wnt signalling at an intracellular step (Pera et al., 2001; Richard-Parpaillon et al., 2002; Pera et al., 2003).

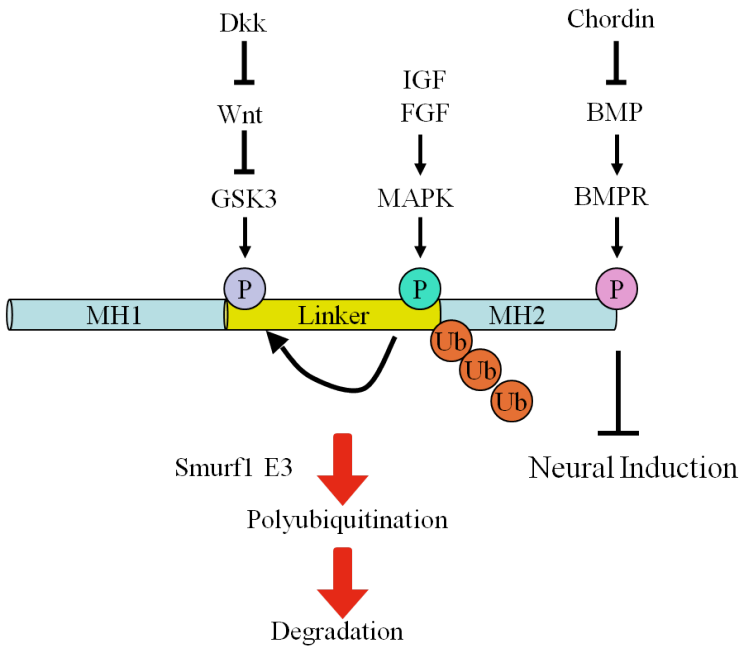

Fig. 4. Model for the integration of diverse neural inducing signals at the level of Smad1 phosphorylation

The BMP signaling intermediate Smad1 is activated through BMP receptor serine/kinase-mediated carboxyterminal phosphorylation. Chordin promotes neural induction through binding to and inhibiting BMP ligands in the extracellular space. IGF and FGF signals trigger through activation of Erk/MAPK inhibitory linker phosphorylation of Smad1. Subsequent phosphorylation by GSK3 leads to ubiquitination and degradation of Smad1. The soluble Wnt antagonist Dickkopf (Dkk) is thought to promote neural induction through derepressing GSK3 and stimulation of Smad1 degradation.

How do these diverse signals mediate neural induction? Noggin (Smith and Harland, 1992) and Chordin (Sasai et al., 1994) bind to and sequester BMPs in the extracellular space, preventing carboxyterminal phosphorylation of the BMP effector Smad1 by the BMP receptor serine/threonine kinase (Pera et al., 2003). IGF and FGF8 signals act through receptor tyrosine kinase and MAPK/ERK signaling and mediate phosphorylation of Smad1 in the central linker region, causing inhibition of Smad1 activity and promotion of neural induction (Pera et al., 2003). A recent finding shows that in response to MAPK/ERK phosphorylation, GSK3 promotes linker phosphorylation and proteosome-mediated degradation of Smad1 (Fuentealba et al., 2007). Thus multiple signals are integrated through differential phosphorylation of the BMP transducer Smad 1 during neural induction (**Fig. 4**).

1.8 Hedgehog signalling in early neural development

Hedgehog (Hh) signals act through altering the balance between activator and repressor forms of the Gli family of zinc-finger transcription factors (**Fig. 5**; Varjosalo et al., 2006; Jiang and Hui, 2008). Gli1 is a transcriptional activator, Gli2 and Gli3 can both activate and repress transcription depending on Hh signals and theirs posttranslational modification. In the absence of Hh signals, the 12-span transmembrane receptor Patched (Ptch) blocks the 7-span transmembrane protein Smoothened (Smo) (Ingham and McMahon, 2001). Protein kinase A (PKA), CK-1, and GSK3 sequentially phosphorylate and recruit the F-box-containing ubiquitin E3 ligase Slimb/β-TrCP, leading to proteolytic processing and generation of carboxyterminally truncated repressor forms of Gli2 and Gli3 that actively suppress target genes. Binding of Hh ligands to Ptc prevents Smo activity, which blocks the processing of Gli2 and Gli3, and causes transcriptional activation of Gli1, which in turn activates Hh/Gli-specific target genes (Stecca and Ruiz i Altaba, 2010). Recent studies in mice have shown that cilia containing microtubules and intraflagellar transport proteins are essential organelles for Hh/Gli signal transduction in mammals (Huangfu et al., 2003; Huangfu and Anderson, 2005).

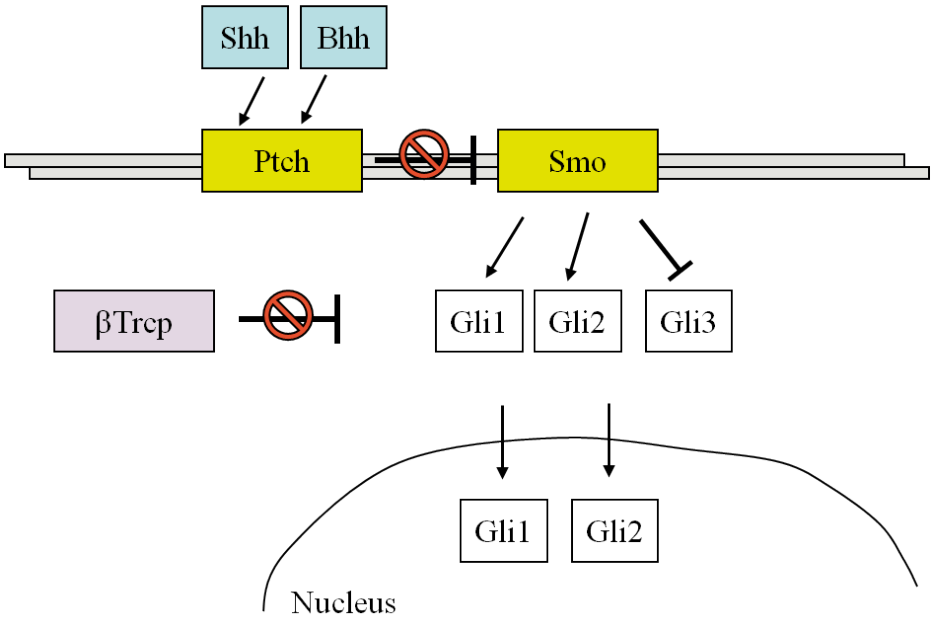

Fig. 5. Hedgehog signalling pathway

Binding of Hh ligands to Ptc blocks Smo activity and prevents kinases phosphorylation and ubiquitination by β-TrCP on Gli proteins which allows the entering of Gli proteins into the nucleus and upregulates Hh/Gli-specific target genes.

In vertebrate embryos, Sonic Hedgehog (Shh) is a well-known ventralizing signal in neural tube patterning (Marti et al., 1995). Shh null mice show defects of axial structures, lack a ventral floorplate and exhibit cyclopia (Chiang et al., 1996). It has been reported that the overexpression of Banded Hedgehog (Bhh) can stimulate anterior neural induction in *Xenopus* embryos (Lai et al., 1995), but the mechanisms of how Hh signals mediate neural induction, and whether Hh signals are required for this process is not known.

1.9 Anteroposterior patterning of the central nervous system

Nieuwkoop suggested that Spemann's organizer patterns the anteroposterior neural axis in two distinct steps. In the first step (activation), signals emanating from the early organizer and organizer-derived anterior endomesoderm induce neural tissue of forebrain-like character. In a second step (transformation), signals from the late organizer and notochord convert anterior into more posterior midbrain, hindbrain and spinal cord tissue (Nieuwkoop, 1973; 1979). Signals including Chordin, Noggin, Dkk1, Frzb1, sFRP2, Crescent, Cerberus and IGFs induce neural tissue of anterior character (Lamb et al., 1993; Sasai et al., 1995; Leyns et al., 1997; Glinka et al., 1998; Bouwmeester et al., 1996; Piccolo et al., 1999; Pera and De Robertis, 2000; Shibata et al., 2000; Pera et al., 2001). A compound knockout of Chordin and Noggin in the mouse leads to truncation of anterior forebrain structures (Bachiller et al., 2000). Dkk-1 null mutant mouse embryos show a lack of head structures (Mukhopadhyay et al., 2001). BMP, Wnt, FGF and retinoic acid signals promote posteriorization of the central nervous system (Kudoh et al., 2002; Eivers et al., 2008).

Several FGF genes, including *FGF3*, *FGF4*, *FGF8* and *FGF9* are expressed in the posterior dorsal, lateral and ventral mesoderm of early *Xenopus* embryos (Isaacs, 1997). Basic FGF (FGF2) induces gastrula ectoderm cells to express posterior neural markers in a dose-dependent manner (Kengaku and Okamoto, 1993, 1995). Similarly, activation of FGF signalling by a constitutive active chimeric FGFR1 or a constitutive active FGFR4 causes upregulation of posterior neural markers in neuralized animal cap explants (Umbhauer et al., 2000). In contrast, microinjection of the truncated dominant-negative FGF receptor-1 (XFD) causes a loss of posterior neural markers (Holowacz and Sokol, 1999). FGF8 is specifically expressed at the midbrain-hindbrain boundary in advanced gastrula-stage embryos (Christen and Slack, 1997). *Fgf8* mutant zebrafish and *Fgf8* null mice fail to form a posterior midbrain and cerebellum (Reifers et al., 1998, Meyers et al., 1998), supporting a role of FGF signals in neural patterning.

Kiecker and Niehrs demonstrate that anteroposterior patterning during gastrulation is influenced by posterioriolyenriched XWnt3A and XWnt8 sources that establish a β-catenin gradient in the neural plate (Kiecker and Niehrs, 2001). Overexpression of *XWnt3a* mRNA or *XWnt8* DNA causes a loss of forebrain markers and anteriorward expansion of posterior neural markers in neuralized ectodermal explants (McGrew et al., 1995; Fredieu et al., 1997), while dominant-negative XWnt8 construct prevents posterior gene expression in neuralized ectodermal explants (Bang et al., 1999). In mice, *Wnt3a* knockout embryos are unable to form a tail bud, and *Wnt5a* null mutants fail to extend the antero-posterior axis due to a reduction of posterior structures, (Takada et al., 1994; Yamaguchi et al., 1999), underscoring a role of Wnts as posteriorizing agents. Furthermore, Wnt1 knockout mice exhibit defects in midbrain development (McMahon and Bradley, 1990; Mastick et al., 1996), supporting a function of Wnt signals in pattern formation of the central nervous system

1.10 Retinoid acid signalling in neural patterning

The small lipophilic molecule Vitamin A (retinol) and its bioactive derivative, retinoic acid (RA), are essential for both embryonic development and homeostasis in the adult. Excessive RA leads to teratogenesis and RA-deficient mice show specific cardiac, limb, ocular, and nervous system defects (Ross et al., 2000; Duester 2008; Niederreither and Dollé, 2008). RA signals are activated upon entering of RA into the cell nucleus via carrier proteins called cellular retinoic acid-binding protein (CRABP). RA binds to the RA receptors RARs and RXRs, which control target gene expression (Mark et al., 2006).

In vertebrate embryos, RA sequentially activates Hox genes that act in a combinatorial manner (‘Hox code’) to regulate axial development in the trunk and hindbrain (Cho and De Robertis, 1990; Kessel and Gruss, 1991; Marshall et al., 1992). In *Xenopus* embryos, RA is detected in the presumptive hindbrain at the gastrula stage and is required to pattern the hindbrain (Maden and Holder, 1991). Elevated receptor activity prevents anterior neural structures while dominant negative receptor stimulates anterior

enhancement leads to transformation of the posterior hindbrain towards more rostal rhombomere identities (Blumberg et al., 1997; van der Wees et al., 1998). Similarly, mouse embryos treated with excessive RA display stage-dependet loss of rostal rhombomeres (Morriss-Kay et al., 1991; Wood et al., 1994), underscoring a posteriorizing effect of RA in the developing hindbrain. In *Xenopus*, addition of posteriorizing signals RA to neuralized animal explants leads to primary neuron induction and neuronal differentiation (Papalopulu and Kintner, 1996; Franco et al., 1999). In contrast, a dominant-negative retinoid receptor or administration of the RA synthesis inhibitor Citral reduced the number of primary neurons in neuralized animal cap explants (Sharpe and Goldstone, 2000; Sharpe and Goldstone, 2000a). Hence RA is an important inductive molecule in anteroposterior hindbrain patterning and neuronal differentiation in vertebrate embryonic development.

1.11 The morphogen concept

A morphogen is a soluble signaling molecule that acts in a concentration-dependent manner to specify positional information and cell fates in the developing embryo (Wolpert, 1969; 2011). Hh, Wnt, FGF, and RA are well-known morphogens that activate distinct sets of genes in response to varying amounts of signal supply (Freeman and Gurdon, 2002; Smith and Gurdon, 2004; Glover et al., 2006). Shh secreted from axial midline structures activate in a dose-dependent manner specific target genes and thereby specify neuronal subtypes along the dorsal-ventral axis of the developing neural tube (Marti et al., 1995; reviewed in Marti et al., 2005). Gradual Wnt signals specify positional information along the anteroposterior neural axis in vertebrates (Kiecker and Niehrs, 2001; Martinez Arias, 2003). FGF signaling regulates anteroposterior patterning through regulation of Hox genes (Liu et al., 2001; Bel-Vialar et al., 2002), and signal in a dose-dependent fashion to maintain caudal body axis entension (reviewed in Böttcher and Niehrs, 2005; Cayuso and Martí, 2005). RA has initially been suggested to act as morphogen during anteroposterior patterning of the chick limb field (Eichele et al., 1985;

Tickle et al., 1985), and later shown to differentially regulate Hox genes in the vertebrate hindbrain and spinal cord (Maden, 2002; White et al., 2007).

Aims of this study:

The main goal of this thesis is to understand the regulation and integration of key developmental signals including Fibroblast growth factor, Hedgehog, Wnt, and retinoic acid in early pattern formation, using *Xenopus* embryos as an experimental model system.

Key objectives

1. To study the regulation and integration of Hedgehog and Wnt signals by Suppressor-of-fused (Sufu) in neural induction, anteroposterior patterning and eye field development (paper I).

2. To study the regulation of FGF signalling by the secreted serine protease HtrA1 in mesoderm induction, neuronal differentiation, and body axis development (paper II).

3. To study the biosynthesis of Retinoic acid by Retinol dehydrogenase-10 (RDH10) in anteroposterior and dorsoventral patterning in the embryo (paper III).

Present investigation

Paper I

Introduction

Suppressor-of-fused (Sufu) was first identified in a genetic mutants screen for suppressing the mutant phenotype of the putative serine/threonine kinase Fused in *Drosophila melanogaster*. In the fly, Sufu shows only maternal effects with mutants being viable and displaying no striking phenotype (Preat, 1992; Pham et al., 1995). Sufu blocks the activities of the Gli homolog Cubitus interruptus (Ci) through binding to the N- and C-terminal ends of Ci (Ohlmeyer and Kalderon, 1998). The interaction between Sufu and Ci increases the stability of Ci (Zhang et al., 2006a).

In contrast to *Drosophila*, Sufu is essential for mammalian development. Sufu knockout mouse embryos die at the mid-gestation stage with severe ventralization of the neural tube and heart defects (Cooper et al., 2005; Svard et al., 2006; Varjosalo et al., 2006). The high similarity to the Patched loss-of-function phenotype (Goodrich et al., 1997) suggests that Sufu is an important negative regulator of Hh signalling. Mammalian Sufu physically interacts with all three Gli proteins by sequestering Glis in the cytoplasm and recruiting co-repressors to suppress Gli transcriptional activity in the nucleus (Kogerman et al., 1999; Ding et al., 1999; Cheng and Bishop, 2002; Barnfield et al., 2005). The binding of Sufu enhances the stability of the Gli2 and Gli3 activation forms, but not their repressor forms in mouse embryonic fibroblast cells (Wang et al., 2010). In the absence of Hh signaling, primary cilia do not participate in the inhibition of Gli proteins by Sufu (Chen et al., 2009; Jia et al., 2009; Zeng et al., 2010). Upon activation of the pathway, Sufu-Gli complexes translocate to the cilia, dissociate, and free Gli transcription factor enters the nucleus to activate downstream target genes (Humke et al., 2010; Tukachinsky et al., 2010; Chen et al., 2011). *In vitro* studies showed that Sufu can also bind to and inhibit β-catenin activity (Meng et al., 2001). However, loss-of-function studies in mice did not detect a function of Sufu as regulator of Wnt signaling (Varjosalo et al., 2006;

Svard et al., 2006). The aim of this study is to address the function of Sufu in the regulation of Hh and Wnt signalling in the *Xenopus* embryo.

Results

We compared the roles of Hh/Gli and Wnt/β-catenin signalling in early *Xenopus* embryos, concentrating on the induction of the neural plate, anteroposterior patterning and eye field development. Hh signals are able to promote the induction of neural markers (Lai et al., 1995; Franco et., 1999), but whether they exert a critical function in this process has not been established yet. We could demonstrate that microinjection of *XBhh* or *XGli1* mRNA into the animal pole of 4-cell stage embryos led to an expansion of the neural plate marker *Sox2* and concomitant reduction of the epidermal marker *Cytokeratin* in neurula embryos. Opposite effects were seen with *Gli3C'*Δ*ClaI* or *Ptc1*Δ*loop2* mRNAs, suggesting that Hh signalling may be required for neural induction. Previous studies revealed a pro-neural activity of the Wnt pathway (Sokol et al., 1995; Baker et al., 1999), while other reports suggested that Wnt signals could inhibit neural plate formation (Itoh et al., 1995; Glinka et al., 1998; Heeg-Truesdell and LaBonne, 2006). We showed that activation of zygotic Wnt signals by *Wnt3a* DNA depleted the anterior neural plate, whereas mRNA encoding dominant-negative Wnt8 (dnWnt8) expanded the neural plate. Our data suggest that Hh/Gli1 signals support neural induction while late Wnt/β-catenin signalling blocks neural plate formation.

It has previously been reported that Hh ligands have anteriorizing activity (Lai et al., 1995; Franco et al., 1999). Consistently, we could show that overexpression of *XBhh* or *XGli1* mRNA caused a posteriorward shift of the brain markers *Otx2* (forebrain/midbrain), *En2* (posterior midbrain) and *Krox20* (hindbrain). *Gli3C'*Δ*ClaI* or *Ptc1*Δ*loop2* mRNA had a very mild opposite effect. In agreement with previous observations that Wnt signals suppress anterior fates (Christian and Moon, 1993; McGrew et al., 1995; Glinka et al., 1998; Kiecker and Niehrs, 2001), we found that *XWnt3a* DNA caused an anterior shift and *dnXWnt8* mRNA a posterior shift of regional

markers along the neuraxis. Hence Hh/Gli1 promotes anteriorization and Wnt/β-catenin stimulates posteriorization of the CNS.

It has been reported that Hh signals and activated Gli proteins inhibit early eye development (Marine et al., 1997; Cornesse et al., 2005). We found that *XBhh* and *XGli1* reduced expression of the eye field marker *Rx2A*, while *Gli3C'*Δ*ClaI* or *Ptc1*Δ*loop2* mRNA enlarged its expression domain. Wnt/β-catenin are known to counteract early eye development (Kazanskaya et al., 2000; Fujii et al., 2008). *XWnt3a* DNA caused a reduction and *dnXWnt8* mRNA an expansion of the eye marker. Thus, both Hh and Wnt signals restrict the early eye field.

The well established role of Suppressor-of-fused (Sufu) as Hh inhibitor (Cooper et al., 2005; Svard et al., 2006; Varjosalo et al., 2006) and *in vitro* findings suggesting that Sufu may also inhibit Wnt signalling (Meng et al., 2001) prompted us to clone a full-length cDNA of *Xenopus Sufu* (*XSufu*). We detected maternal and zygotic expression of *XSufu* in *Xenopus* embryos. Whole-mount *in situ* hybridization analysis showed distinct transcripts in the panplacodal and anterior neural plate of gastrula embryos. Later, signals were seen in the eye field and neural crest cells. In tail bud embryos, *XSufu* transcripts were found in the forebrain, mid/hindbrain boundary, eye, ear, branchial arches, and the tail.

In gain-of-function studies, we microinjected synthetic *XSufu* mRNA into the animal pole of 4-cell stage embryos. *XSufu* mRNA reduced the size of the neural plate, shifted brain markers posteriorly and enlarged the eye field. Animal injection of an antisense morpholino oligonucleotide against *XSufu* (*XSufu*-MO) that specifically blocks XSufu translation caused an expansion of the neural plate, anteriorization and reduction of eye structures. These results suggest an important role of XSufu in restricting neural plate development, ensuring proper anteroposterior patterning and allowing eye development to occur. Downregulation of endogenous *XSufu* also led to reduction of the cement gland marker *XAG*, the neural crest markers *Slug* and *Snail*, the neuronal marker *N-tubulin*, and

the muscle marker *MyoD*, suggesting additional functions of XSufu in cement gland, neural crest, neuron, and muscle development.

In injected animal cap explants, *XSufu* mRNA reverted *XBhh*-induced expression of *XGli1*, *XPtc1* and *XPtc2* gene expression, while *XSufu*-MO increased expression of these Hh target genes. A negative role of XSufu in Hh signalling was confirmed by the demonstration that *XSufu* mRNA reduced and *XSufu*-MO increased the expression of *XPtc1* in whole embryos.

Interestingly, *XSufu* mRNA also counteracted *XWnt8*-induced expression of *Siamois* and *Xnr3* in a dose-dependent manner, whereas *XSufu*-MO elevated expression levels of these Wnt target genes in animal caps. Whole-mount *in situ* hybridization revealed that *XSufu* mRNA downregulated and *XSufu*-MO increased endogenous expression of *Xnr3* and *Chordin* in the dorsal blastopore lip. *XSufu* mRNA reverted *XWnt8*-induced ectopic expression of *Xnr3* and dorsoanterior development in animally injected whole embryos. In co-injection experiments, *XSufu* mRNA inhibited *XWnt8*-induced secondary axis induction and *XWnt3a*-induced posteriorization of the neural plate; these effects were not reverted by *XGli1* mRNA, suggesting that XSufu may act as a direct inhibitor of Wnt signalling. We also found that *XGli1* mRNA prevented *XWnt8*-mediated secondary axis induction and *XWnt3a*-induced posterior neural patterning suggesting that XGli1 may inhibit Wnt responses in the *Xenopus* embryo. Using co-immunoprecipitation, we could show that XSufu physically interacts with XGli1 and Xβ-catenin proteins. Together, our results suggest that XSufu is a dual regulator of Hh/Gli and Wnt/β-catenin signaling.

Using specific luciferase reporter assays, we analysed the role of Sufu in the interaction of Hh and Wnt signalling. In mRNA-injected *Xenopus* embryos, *Xβ-catenin* stimulated activation of the Hh reporter *8x3'Gli-Bs luc* upon overexpression of *XGli1*. In turn, *XGli1* inhibited activation of the Wnt reporter TOP-flash upon overexpression of *Xβ-catenin*. Notably, *Xβ-catenin* failed to activate the Hh pathway, and *XGli1* did not inhibit the Wnt response in *XSufu*-morphant embryos. A similar interaction of transfected mouse constructs of *β-catenin* and *Gli1* was observed in mouse embryonic fibroblasts that were

wildtype (MEF WT), but not homozygous mutant for the *Sufu* gene (MEF *Sufu* -/-). Our results suggest a conserved crosstalk in which exogeneous Wnt/β-catenin stimulates the Hh pathway under overexpression of *Gli1*, and vice versa, exogeneous Hh/Gli1 inhibits Wnt signalling under overexpression of *β-catenin.* In both *Xenopus* embryos and mouse cells, Sufu is essential for the interaction between Hh/Gli and Wnt/β-catenin signalling.

Conclusion

In this study we present *Xenopus* Sufu as a common regulator of Hh and Wnt signalling. Sufu is an essential regulator of Hh signals in the mouse (Taylor et al., 2002; Svärd et al., 2006; Varjosalo et al., 2006). Here we show that XSufu is sufficient and required to downregulate Hh target genes in *Xenopus* embryos, suggesting a conserved function of Sufu in negatively regulating the vertebrate Hh pathway. A previous *in vitro* finding suggested that Sufu could bind to and inhibit *β-catenin* signalling (Meng et al., 2001). We now provide several lines of evidence that XSufu is essential for regulating Wnt signalling in *Xenopus* embryos. (i) Overexpression of *XSufu* mRNA blocks *XWnt8*-induced target genes and dorso-anterior development. (ii) Depletion of *XSufu* by specific antisense morpholino oligonucleotides (*XSufu*-MO) elevates transcription levels of the Wnt target genes *Siamois* and *Xnr3* in ectodermal explants. (iii) XSufu is sufficient and necessary to negatively regulate *Xnr3* and the Wnt-responsive *Chordin* gene in the dorsal blastopore lip. We also show that XSufu physically interacts with XGli1and Xβ-catenin proteins. The inhibitory effect of XSufu on Wnt/β-catenin signalling is direct and not mediated through blockage of Gli signals, since co-injection of *XGli1* mRNA does not revert the repressive effects of *XSufu* on *XWnt8*-induced secondary axis induction and *XWnt3a*-induced posteriorization of the neural plate. Hence XSufu is a dual regulator of Hh and Wnt signals in *Xenopus* embryos.

Our data are in agreement with previous findings that Hh signals are potent neural inducers in *Xenopus* (Lai et al., 1995; Franco et al., 1999). We further show that inhibition of Hh signalling by *XPtcΔloop2* or *GLI3ΔClaI* mRNA promotes epidermal

Cytokeratin at the expense of neural *Sox2* expression, suggesting an important role of Hh/Gli signals in neural plate formation. Our expression and functional data support a negative role of XSufu in neural induction. *XSufu* is robustly expressed at the border of the neural plate, *XSufu* mRNA suppresses and *XSufu*-MO induces neural fate. *XSufu* may exert its anti-neural activity by inhibiting Hh signals or through negative regulation of early pro-neural Wnt/β-catenin signals. Maternal Wnt signals stimulate neural induction through inhibition of *BMP4* expression (Baker et al., 1999) and transcriptional activation of BMP antagonist (Wessely et al., 2001). We demonstrate that *XSufu* mRNA downregulates the Spemann organizer genes *Chordin* and *Xnr3*. Chordin and Xnr3 are BMP antagonists that contribute to neural induction in *Xenopus* embryos (Sasai et al., 1995; Hansen et al., 1997; Haramoto et al., 2004). Our study suggests that XSufu may restrict neural induction through inhibiting Hh/Gli and early Wnt/β-catenin signals.

Our study supports previous findings that Hh and Wnt signals negatively regulate the specification of the eye field (Marine et al., 1997; Cornesse et al., 2005). We further demonstrate that *XSufu* is not only expressed in the early eye anlage. *XSufu* mRNA expands expression of the eye-specific marker *Rx2A*, while *XSufu*-MO has the opposite effect, supporting an essential function of XSufu in eye field development. Our observation that *XSufu*-MO-mediated downregulation of *Rx2A* expression can be reverted by co-injection of either *GLI3ΔClaI* or *dnWnt8* mRNA suggests that XSufu may regulate eye specification via terminating Hh and Wnt signals.

Previous studies in *Xenopus* embryos revealed abundant expression of all three Gli proteins in the anterior neural plate (Ekker et al., 1995; Lee et al., 1997; Marine et al., 1997) and gradually increasing levels of Xβ-catenin protein towards posterior parts of the neural plate (Kiecker and Niehrs, 2001). Our observation that both overexpression and downregulation of *XSufu* causes posteriorward shifts of neural markers led us suggest a biphasic model for the role of XSufu in anteroposterior patterning of the CNS. The expression of *XSufu* at the anterolateral margin of the neural plate suggests that under normal conditions XSufu interacts rather with anterior Gli than posterior β-catenin proteins. Depletion of *XSufu* derepresses anterior XGli transcription factors leading to

anterior neural induction. In contrast, ectopically expressed *XSufu* further inhibits posterior *Xβ-catenin* activity causing suppression of posterior neural fate. Hence lowered *XSufu*-protein levels stimulate anterior Hh/Gli and elevated *XSufu* levels block posterior Wnt/β-catenin signals resulting in each case in anteriorization of the developing CNS.

An interesting problem is the interaction of Hh and Wnt signalling and a possible function of XSufu therein. Our studies show that *XGli1* mRNA counteracts *XWnt8*-induced secondary body axis and *XWnt3a*-induced posteriorization of the neural plate. In *Xenopus* embryos and mouse embryonic fibroblasts (MEFs), Gli1 blocks Wnt/β-catenin reporter activity under overexpression of *β-catenin*. A negative effect of Hh/Gli signals on Wnt signalling has previously been reported in cancer cells (Akiyoshi et al., 2006; Yanai et al., 2008), and Indian Hedgehog has been shown to inhibit Wnt transcriptional activity in intestinal cell differentiation (van den Brink et al., 2004). We observed that XSufu is critically involved in the negative regulation of Wnt/β-catenin signalling by Hh/Gli, as in *XSufu* morphant embryos and *Sufu* knock-out MEF cells, *Gli1* did no longer inhibit Wnt reporter activity, and addition of *XSufu* to MEF *Sufu*-/- cells could rescue the inhibitory effect of *Gli1* on the Wnt/β-catenin response. We notice that exogenous *β-catenin* positively regulates Hh/Gli reporter activity under overexpression of *Gli* gene in *Xenopus* embryos and MEF cells. Consistently, in human cancer cells β-catenin induces Gli1 activity independent of TCF/LEF transcription factor activity (Maeda et al., 2006). We found that *XSufu* deficient embryos and *XSufu* mutant MEF cells failed to display Hh/Gli1 activation by Wnt/β-catenin, unless exogenous *Sufu* was added. Hence the presence of XSufu is critical for the crosstalk between the two pathways. We conclude that XSufu is a dual regulator and integrator of Hh/Gli and Wnt/β-catenin signals in the *Xenopus* embryo.

Paper II

Introduction

The HtrA (high-temperature requirement factor A) family of serine proteases is conserved from bacteria to human, with four members (HtrA1-4) described in mammals (Clausen et al., 2002). Bacterial HtrA is a molecular chaperone that refolds or degrades misfolded proteins and consists of a catalytic trypsin domain followed by one or more copies of a protein-protein interacting PDZ domain (Pallen and Wren, 1997). HtrA1 was first identified as a gene downregulated in SV40-transformed human fibroblast and contains an N-terminal signal peptide, an IGF binding domain, a Kazal type serine protease inhibitor domain, a trypsin-like serine protease domain and a PDZ domain (Zumbrunn and Trueb, 1996; Pallen and Wren, 1997; Clausen et al., 2002). HtrA1 inhibits proliferation and tumor cell growth and is downregulated in many types of cancer, suggesting that HtrA1 may be a tumor suppressor (Baldi et al., 2002; Chien et al., 2004; Bowden et al., 2006). A single nucleotide polymorphism in the promoter region of HtrA1 has been identified as a risk factor for the wet form of age-related macular degeneration (Dewan et al., 2006). It has also been demonstrated that HtrA1 regulates matrix mineralization by inhibiting TGFβ/BMP signalling through the cleavage of the matrix protein decorin (Canfield et al., 2007). HtrA1 modulates Insulin-like growth factor (IGF) signals and cleaves IGF binding protein-5 (Hou et al., 2005). In a screen for secreted proteins, we isolated a full-length cDNA clone of *Xenopus HtrA1* (*xHtrA1*) from gastrula stage embryos (Pera et al., 2005). In this study, we investigated the function of *xHtrA1* and found that this protease modulates FGF signalling during anteroposterior patterning, mesoderm induction, and neuronal differentiation.

Results

Whole mount *in situ* hybridization revealed overlapping expression of *xHtrA1* and *FGF8* in several domains, including the blastopore lip at gastrula, the anterior neural plate and posterior mesoderm at neurula, and the branchial arch region at tail bud stage. RT-PCR analysis of mRNA-injected animal cap explants showed that FGF4 or FGF8 could specifically induced *xHtrA1* gene transcription.

Microinjection of *xHtrA1* mRNA into one blastomere at the 4-cell stage induced loss of head structures and formation of secondary tail-like structures. At the molecular level, *xHtrA1* mRNA reduced expression of the anterior markers *Otx2* (cement gland, forebrain, midbrain), *BF1/FoxG1* (telencephalon), *Rx2A* (eyes), *Krox20* (rhombomeres 3 and 5 of the hindbrain), *Nkx2.5* (heart) and expanded expression of the posterior marker *Sizzled* (ventral mesoderm), underscoring the posteriorizing activity of *xHtrA1*. *xHtrA1* mRNA expanded the mesoderm marker *Xbra* to the animal hemisphere indicating mesoderm inducing activity. We also observed that *xHtrA1* mRNA expanded the neural marker *Sox2* and the neuronal marker *N-tubulin* at the expense of the neural crest marker *Slug* and the epidermal marker *Cytokeratin*, suggesting that *xHtrA1* promotes neural induction and neuronal differentiation.

In loss-of-function studies, we found that a specific antisense morpholino oligonucleotide against *xHtrA1* (*xHtrA1*-MO) caused enlargement of the head and reduction of tail structures, depletion of *Xbra* (mesoderm), and reduction of *N-tubulin* expression (neurons). Similar phenotypes were observed upon blastocoel injection of a neutralizing antibody against *xHtrA1*, confirming a role of *xHtrA1* in posteriorization, mesoderm induction and neuronal differentiation.

We noted that *FGF4* DNA induced microcephaly and secondary tail structures (Pownall et al., 1996), *FGF4* mRNA ectopic mesoderm (Pownall et al., 1996), and *FGF8* mRNA ectopic neural and neuronal tissue (Hardcastle et al., 2000; Pera et al., 2003). In epistatic experiments, *xHtrA1*-induced posteriorization and mesoderm induction was blocked by

co-injection of the dominant-negative FGF receptor 1 (*XFD*), and *xHtrA1*-induced neuronal differentiation blocked by dominant-negative FGF receptor 4a (*dnFGFR4a*) mRNA, suggesting that intact FGF signalling is required to allow xHtrA1 to signal.

We found that xHtrA1 is sufficient and required to stimulate the FGF signaling intermediate dpERK (diphosphorylated extracellular signal regulated kinase). *xHtrA1* mRNA also induced ectopic *FGF4* and *FGF8* transcription in an FGF-dependent manner, suggesting that xHtrA1 and FGF form a positive feedback loop, in which each component reinforces the transcription of the other. Using an animal cap sandwich assay, we could demonstrate that *xHtrA1* mRNA stimulates *FGF4*-mediated induction of *Xbra* expression at distance, suggesting that xHtrA1 activates long-range FGF signalling.

Overexpression experiments in human 293 cells and *Xenopus* embryos revealed that xHtrA1 cleaves *Xenopus* Biglycan (xBgn), Syndecan-4 (xSyn4) and Glypican-4 (xGlp4). In contrast, *xHtrA1*-MO elevated protein level of overexpressed xBgn and xGlp4 in *Xenopus* embryos. The results suggest that xBgn, xSyn4, and xGlp4 are proteolytic targets of the xHtrA1 protease.

Biglycan is a secreted chondroitin sulfate (CS) or dermatan sulfate (DS) proteoglycan, while Syndecan and Glypican are cell-surface heparan sulfate (HS) proteoglycans. A series of experiments were done to compare the biological activities of purified HS, DS and CS. Unlike CS, HS and DS contain a high content of iduronic acid that enables conformational flexibility to the glycosaminoglycan (GAG) chain and ensures firm binding to FGF and the FGF receptor (Trowbridge et al., 2002). Upon blastocoel injection, HS and DS, but not CS, caused reduction or loss of head structures, expansion of the mesodermal marker *Xbra*, and ectopic expression of the neuronal marker *N-tubulin*. These effects were blocked by inhibition of endogenous FGF signalling through injection of *XFD* or *dnFGFR4a* mRNAs. We also found that blastocoel injection of specific enzymes that degrade HS (Heparitinase) or DS (Chondroitinase B) caused microcephaly, reduction of *Xbra*, and reduced *N-tubulin* expression, suggesting an

important role of iduronic acid-containing GAGs in anteroposterior axis development, mesoderm induction, and neuronal differentiation.

Conclusion

In this study, we introduce xHtrA1 as a modulator of FGF signalling. The similar expression of *xHtrA1* and *FGF8* transcripts indicates a possible interaction. Our demonstration that FGF signals induce *xHtrA1* transcription, and vice versa, xHtrA1 induces transcription of *FGF4* and *FGF8* transcripts suggests a functional feedback loop. Several components and regulators of the FGF pathway, such as the transmembrane proteins XFLRT3 (Böttcher et al., 2004) and Sef (similar expression of FGF; Fürthauer et al., 2002; Tsang et al., 2002) and the cytoplasmic Sprouty and Spred proteins are co-expressed with FGF genes (Sivak et al., 2005). Our findings suggest that xHtrA1 may be a new member of the *FGF8* synexpression group.

xHtrA1 and FGF signals share several similar activities in *Xenopus* embryos. The loss of head and induction of secondary tail-like structures as seen with xHtrA1 has also been reported upon ectopic expression of FGF4, XFLRT3, constitutively active FGFR1, activated Ras or the Ets-type protein ER81 (Pownall et al., 1996; Chen et al., 1999; Böttcher et al., 2004). We noticed that *xHtrA1* mRNA induced the mesodermal marker *Xbra* and thereby mimicked the ability of FGF4 or FGF signalling components to induce mesodermal differentiation (Isaacs et al., 1994; Böttcher et al., 2004). *xHtrA1* stimulates neural *Sox2* at the expense of epidermal *Cytokeratin* and neural crest *Slug* expression, and promotes the neuronal marker *N-tubulin*; similar effects on neural induction and neuronal differentiation also result from overexpression of FGF8 (Hardcastle et al., 2000; Pera et al., 2003). *xHtrA1* activates dpERK phosphorylation similar as FGF signals do (Böttcher et al., 2004) suggesting that xHtrA1 may act through activating FGF-ERK signalling.

Depletion of xHtrA1 by specific antisense morpholino oligonucleotides (*xHtrA1*-MO) or neutralizing antibodies resulted in enlarged head structures, shortened tails, and

extinction of mesodermal *Xbra* expression. Similar effects were observed after overexpression of the dominant-negative FGF receptor 1 (XFD, Amaya et al., 1991) or MAP kinase phosphatase (Umbhauer et al., 1995). Knockdown of xHtrA1 also caused downregulation on the neuronal marker *N-tubulin*, a phenotype that was previously seen upon overexpression of the dominant-negative FGF4Ra (DnFGFR4a, Hardcastle et al., 2000). The loss-of-function data underscore similarities between the roles of xHtrA1 and FGF signals during anteroposterior patterning, mesoderm induction and neuronal differentiation and suggest that xHtrA1 may be crucial to allow FGFs to signal.

Proteoglycans including Biglycan and members of the Syndecan and Glypican families bind FGF ligands through their heparan sulfate (HS) and dermatan sulfate (DS) glycosaminoglycan chains (Kramer and Yost, 2003; Trowbridge and Gallo, 2002). We could demonstrate that the secreted serine protease xHtrA1 triggers the cleavage of xBgn, xSyn4, and xGlp4. In *xHtrA1*-morphant embryos, protein levels of overexpressed *xBgn* and *xGlp4* were elevated, indicating that these proteoglycans are proteolytic targets of endogenous *xHtrA1*. We could further show that blastocoel injection of HS or DS triggers posteriorization, mesoderm induction and neuronal differentiation. Exogeneous HS and DS not only recapitulate the effects of *xHtrA1* and *FGF* overexpression, but their activities depend on intact FGF signaling. Injection of enzymes that specifically degrade HS and DS impair with mesoderm induction and neuronal differentiation, suggesting an important role of these glycosaminoglycans in mediating FGF signaling in the *Xenopus* embryo.

Based on our findings, we suggest a model that confers stimulation of long-range FGF signalling by the secreted serine protease xHtrA1. Proteoglycans normally bind to and sequester FGF ligands, facilitate interaction with nearby FGF receptors and ensure efficient FGF signalling to occur at short range (Häcker et al., 2005; Bülow and Hobert et al., 2006). In this study, we showed that a developmentally regulated protease (xHtrA1) through cleaving the proteoglycans Biglycan, Syndecan-4, or Glypican-4 releases soluble FGF-proteoglycan complexes. In this manner, FGFs can reach cells far away from their site of synthesis and activate FGF signals at distance.

Paper III

Introduction

The vitamin A-derived retinoic acid (RA) is an important signaling molecule in the vertebrate embryo whose distribution is tightly regulated by tissue-specific retinaldehydrogenases (RALDH1-3), which oxidize retinal to RA, and members of the cytochrome P450 family (CYP26s) that metabolize RA via oxidative inactivation (Niederreither and Dollé, 2008; Duester, 2008). The first step of RA synthesis can be mediated by several members of the alcohol dehydrogenase and retinol dehydrogenase families, but which one is essential for embryonic development has remained elusive for a long time.

Retinol dehydrogenase 10 (RDH10) is a member of the short-chain dehyrogenase/reductase (SDR) superfamily that catalyses the reversible oxidation of vitamin A (retinol) to retinal in an NAD+ dependent manner (Wu et al., 2002; Wu et al., 2004; Belyaeva et al., 2008). In the mouse, RDH10 exhibits tissue-specific expression at sites of RA signalling in the developing embryo and foetus (Sandell et al, 2007; Cammas et al., 2007; Romand et al., 2008). Mice with an ENU (N-ethyl-N-nitrosourea)-induced point mutation in the RDH10 locus die at E13.5 as a result of vascular defects; mutant embryos display craniofacial, limb and organ malformations that are characteristic of vitamin A or RA deficiency (Sandell et al, 2007; Farjo et al., 2011). However, the function of RDH10 in non-mammalian vertebrates has not been addressed yet and its regulation and interaction with other enzymes involved in RA metabolism is not well understood. *Xenopus* RDH10 (XRDH10) has been identified by secretion cloning (Pera et al., 2005). The aim of this study is to characterize XRDH10 in the *Xenopus* embryo with a particular focus on axis specification and pattern formation of the CNS.

Results

RT-PCR analysis revealed maternal and zygotic expression of *XRDH10* with transcripts abundant in the animal and vegetal hemisphere of *Xenopus* blastula embryos. Whole mount *in situ* hybridization showed distinct *XRDH10* expression in the dorsal blastopore lip at the gastrula stage. Signals were partially overlapping with circumblastoporal expression of *XRALDH2* (Chen et al., 2001) and complementary to two expression domains of *XCYP26A1* in the animal hemisphere and ventrolateral blastopore lip (Hollemann et al., 1998). In neurula embryos, *XRDH10* and *XRALDH2* showed nested gene expression in the paraxial mesoderm (Chen et al., 2001), with *XRDH10* localized slightly more anteriorly than *XRALDH2* RNA. In contrast, *XCYP26A1* expression was confined to the adjacent anterior and posterior parts of the neural plate (Hollemann et al., 1998). At the tail bud stage, *XRDH10* showed an additional expression domain in the eye field that coincided with that of *XRALDH2* (Chen et al., 2001) and was surrounded by *XCYP26A1* expression (Hollemann et al., 1998). Together, *XRDH10* and *XRALDH2* transcripts overlapped at several sites and showed complementary expression patterns with *XCYP26A1*.

We observed that treatment of embryos with exogeneous retinoic acid caused downregulation of *XRDH10* gene expression. Similar effects were seen in *XRALDH2* mRNA-injected embryos upon exposure to retinal. In contrast, treatment with the pharmacological inhibitors Disulfiram or Citral that block endogenous RA synthesis, or microinjection of *XCYP26A1* mRNA that triggerss degradation of RA, increased *XRDH10* expression. These data suggest that RA is sufficient and necessary to restrict *XRDH10* transcription in the embryo.

Microinjection of *XRDH10* mRNA caused a reduction of head structures and shortening of the body axis. This effect was not only mimicked by a low dosis of exogeneous RA, but *XRDH10*-induced posteriorization was also reverted by co-injection of *XCYP26A1* mRNA or Citral treatment, suggesting that *XRDH10* promotes RA signalling in the embryo. We could demonstrate that *XRDH10* mRNA upregulated *Xlim1* and *Chordin*

expression, but downregulated *Goosecoid* and *ADMP* transcripts in Spemann's organizer. Similar effects were observed upon RA treatment, suggesting that XRDH10/RA differentially affect organizer-specific gene expression.

We could also demonstrate that *XRDH10* mRNA induced an anteriorward shift of neural markers, including *HoxD1*, *Xlim1, Krox20* and *Rx2A*, and that *XRDH10* co-operated with *XRALDH2* in posteriorzing the developing CNS. Co-injection of *XRDH10* and *XCYP26A1* had the opposite effect, suggesting that XRDH10-mediated posteriorization depends on intact RA signalling.

In loss-of-function experiments, we could show that an antisense morpholino oligonucleotide against *XRDH10* (*XRDH10*-MO) caused microcephaly and enlarged belly structures, indicative of a ventralized phenotype. Concomitantly, *XRDH10* morphant embryos showed reduction of *Chordin* and *Xlim1* expression and expansion of *Goosecoid* and *ADMP* expression. Not only are these effects oppositie to those obtained in gain-of-function studies. An antisense morpholino oligonucleotide against *XRALDH2* (*XRALDH2*-MO) phenocopied the ventralization and effects on mesodermal marker genes by *XRDH10* downregulation, suggesting an important role of XRDH10 and XRALDH2 in dorsoventral patterning.

We could further show that knockdown of *XRDH10* or *XRALDH2* causes a posteriorward shift of neural markers. Importantly, the anteriorward expansion of the RA target gene *HoxD1* that is induced by exogeneous retinol treatment was blocked in *XRDH10*-morphant embryos, suggesting that XRDH10 is crucially involved in the conversion of vitamin A into bioactive RA during anteroposterior patterning of the embryo.

Conclusion

In this study, we present tissue-specific expression of *XRDH10* that partially overlaps with *XRALDH2* and is complementary to *XCYP26A1* in several domains of the

developing *Xenopus* embryo. We found that exogeneous RA reduced *XRDH10* transcription. Notably, inhibition of embryonic RA levels by the pharmacological drugs disulfiram and citral, or the RA-inactivating enzyme XCYP26A1, stimulated *XRDH10* expression, suggesting that endogenous RA counteracts XRDH10 gene activity. Previous studies in *Xenopus* and other vertebrates have shown that RA inhibits *RALDH2* expression (Niederreither et al., 1997; Chen et al., 2001; Dobbs-McAucliffe et al., 2004), and that RA in turn activates *CYP26A1* transcription (White et al., 1996; Ray et al., 1997; Hollemann et al., 1998; White et al., 2007). Hence the negative feedback regulation of XRDH10 by RA complements a regulatory network, in which RA blocks anabolic (RA-synthesizing) and stimulates catabolic (RA-degrading) enzymes.

The specific expression of *XRDH10* (this study) and *XRALDH2* (Chen et al., 2001) in Spemann's organizer coincides with active RA signalling in this region (Chen et al., 1994; Yelin et al., 2005). Our gain- and loss-of-function studies demonstrated an important role of both enzymes in activating *Chordin* and repressing *ADMP* expression. Chordin is a soluble BMP antagonist and important mediator of Spemann's organizer (Sasai et al., 1994), while ADMP (anti-dorsalizing morphogenetic protein) acts as a BMP agonist in the dorsal gastrula organizer (Moos et al., 1995; Reversade and De Robertis, 2005). The ventralized phenotype observed in *XRDH10* and *XRALDH2* morphant embryos is common to enhanced BMP/Smad1 activity (e.g. Pera et al., 2003). The positive regulation of Chordin and negative regulation of ADMP transcription by RA signals may provide a mechanism of how XRDH10 and XRALDH2 stimulate Spemann's organizer activity and dorsalization.

RA is a well-established morphogen that is gradually distributed along the anteroposterior neuraxis. According to previous models, these RA gradients were interpreted as a result of local RA production by RALDH2 in the paraxial mesoderm, diffusion of RA, and CYP26A1-mediated RA degradation at the anterior and posterior ends of the neural plate (e.g. Maden et al., 2002; White et al., 2007). We suggest that the nested gene expression of *XRDH10* and *XRALDH2* in the paraxial mesoderm, with *XRDH10* transcripts localized slightly more anterior than *XRALDH2* signals, generates a

posteriorward flow of retinal, that produces high levels of RA at the hindbrain-spinal cord boundary, and decreasing concentrations towards the posterior end. Our findings led us propose an alternative model, in which the combinatorial gene expression and cooperate action of XRDH10 and XRALDH2 constitute a „biosynthetic enzyme code“ that allows formation of a morphogen gradient already at the level of RA biosynthesis and gradual distribution of RA signals in the developing hindbrain and spinal cord.

Discussion

Morphogens are signals with key importance in embryonic development that act in a concentration-dependent manner to specify positional information. Yet the mechanisms of how morphogen signals are regulated and how their pathways integrated in the embryo are poorly understood. In Paper I, we investigated the control of Hedgehog (Hh) and Wnt signals at an intracellular level, introducing Suppressor-of-fused (Sufu) as a common regulator that binds to and inhibits Gli and β-catenin transcription factors in the *Xenopus* embryo. We also reveal a crosstalk between Hh and Wnt signalling, in which Wnt/β-catenin stimulates Hh response upon overexpression of *Gli1*, and in turn, Hh/Gli1 inhibits Wnt response upon overexpression of *β-catenin* in *Xenopus* embryos and mouse embryonic fibroblasts. Of note, activation of Hh signalling by Wnt/β-catenin, and vice versa, inhibition of Wnt signalling by Hh/Gli1 is only possible in the presence of Sufu, as *Sufu*-morphant *Xenopus* embryos and *Sufu* knockout mouse embryonic fibroblasts fail to show a crosstalk. Hence, Sufu is an important regulator and integrator of Hh and Wnt signalling.

In Papers II and III, we address the regulation of Fibroblast growth factor (FGF) and retinoic acid (RA) signals in the extracellular space. FGF ligands are known to interact with proteoglycans that sequester FGFs and thereby limit the range of FGF signalling in invertebrate and vertebrate embryos (Häcker et al., 2005; Bülow et al., 2006). In Paper II, we suggest a „proteolytic spread model“, in which the secreted protease xHtrA1 promotes long-range FGF signalling through cleaving proteoglycans, such as Biglycan, Syndecan-4 and Glypican-4, causing liberation of FGF-proteoglycan complexes and activation of FGF receptors far away from their site of origin. This is the first demonstration that proteoglycans not only mediate short-range signalling but, in the presence of a developmentally regulated protease, allow signals to act at distance (Gallagher, 2007). A „source and sink model“ has been proposed to explain the gradual distribution of RA signals in the vertebrate embryo: The adjacent and non-overlapping expression patterns of the RA synthesizing RALDH enzymes and RA degrading CYP26

hydrolases have been considered to account for the formation of RA gradients (Maden 1999; Maden, 2002; Sirbu et al., 2005; Hernandez et al., 2007; White et al., 2007). In Paper III, we suggest that the nested gene expression and co-operative actions of *XRDH10* and *XRALDH2* that act back-to-back to produce a signal gives rise to a RA gradient already at the level of RA biosysnthesis. Such a „biosynthetic enzyme code" constitutes a novel mechanism for the formation and stabilization of morphogen gradients.

Feedback regulation is an efficient mechanism to adjust the amount of signals to their need in the embryo. In Paper II, we introduce a feed-forward loop, in which FGF signals activate the transcription of *xHtrA1*, and xHtrA1 in turn stimulates the activity of the *xFGF4* and *xFGF8* genes. Such a mechanism ensures robust accumulation of growth factor signals that allows localized outgrowth of e.g. tail stuctures in the developing embryo. In Paper III, we identified the *XRDH10* gene as a target of RA signalling and showed that endogenous RA signals are critical to limit *XRDH10* expression in the embryo. Negative feedback regulation of the first step of RA biosynthesis is a very effective way to control RA levels, provides protection against exogeneous retinoid fluctuations and allows the stabilization of local RA distributions in the embryo.

Spemann's organizer is an important signalling center that mediates dorsoventral patterning in the vertebrate gastrula embryo. Soluble BMP antagonists such as Chordin inhibit ventral Bone morphogenetic proteins (BMPs) and thereby dorsalize the embryo. However, Spemann's organizer also harbors ADMP (anti-dorsalizing morphogenetic protein) that stimulates BMP signalling and ensures a self-regulating embryonic field (De Robertis, 2009). In Paper I, we show that XSufu is necessary to restrict *Chordin* expression in Spemann's organizer. *Chordin* is a target gene of Wnt/β-catenin signals, and *XSufu* may suppress *Chordin* transcription through binding to and inhibiting β-catenin. The negative regulation of *Chordin* gene activity by XSufu could account for the pro-epidermal and anti-neural role of XSufu during dorsoventral patterning of the ectoderm. In Paper III, we showed that *XRDH10* and *XRALDH2* are specifically expressed in the dorsal blastopore lip and crucially involved in establishing dorsal

identity in the embryo. In gain- and loss-of-function experiments, we demonstrated that RA signals positively regulate *Chordin* and negatively regulate *ADMP* gene activity in Spemann's organizer, suggesting a mechanism of how RA through regulating BMP signalling may affect the formation of the dorsoventral body axis.

Nieuwkoop had suggested a two-step activation/transformation model for the induction and patterning of the neural plate, in which signals from the organizer first induce anterior neural fate of forebrain character (activation), which in a subsequent transformation step is gradually converted into more posterior midbrain, hindbrain and spinal cord tissue (Nieuwkoop, 1973; 1977). In Paper I, we add Hh to the list of activation signals and show that Hh/Gli signals are sufficient and necessary to induce anterior neural induction in *Xenopus* embryos. We further suggest a "biphasic model" for the regulation of anteroposterior patterning by XSufu. Under normal conditions, *XSufu* at the anterolateral margin of the neural plate inhibits anterior Gli and less efficiently blocks posterior β-catenin activity. Depletion of XSufu derepresses anterior *Gli* activity, which causes excessive anterior neural induction. Ectopic expression of XSufu inhibits posterior *β-catenin* signaling and prevents posteriorization of the neural plate. In Paper II, we introduce the secreted serine protease xHtrA1 as a transforming signal. *xHtrA1* is expressed in the posterior mesoderm and promotes posterior neural induction through proteoglycan cleavage and release of posteriorizing FGF/proteoglycan messages. Paper III characterizes *XRDH10* as an important enzyme responsible for embryonic RA synthesis during anteroposterior patterning. The "biosynthetic enzyme code" describes a mechanism, in which the co-operation of *XRDH10* of *XRALDH2* in the trunk mesoderm generate RA gradients that are relevant for anteroposterior patterning of the hindbrain and spinal cord.

Populärvetenskaplig sammanfattning

En ordentlig bildning av det centrala nervsystemet är viktigt för ett nyfött barn eller en vuxen. Den senaste tidens kartläggning av människans arvsmassa har lett till identifiering av ungefär 23000 gener, många av dem aktiva i det utvecklande nervsystemet. Men lite är känt om deras funktion och hur de samverkar för att påverka utvecklingen av organ så komplexa som den mänskliga hjärnan. Eftersom många sjukdomar såsom neurodegenerativa sjukdomar och cancer orsakas av defekta gen-aktiviteter, är en bättre förståelse för reglering och funktion av gener under normal utveckling avgörande för att utveckla nya terapeutiska behandlingar.

Djurmodellsystem används för att besvara utvecklingsbiologiska frågor, och vårt labb valde den afrikanska grodan *Xenopus laevis*. Skäl för att använda detta djur är de producera stora mängder ägg, befruktning i en petriskål är genomförbar, och embryon utvecklas snabbt utanför moder-grodan. *Xenopus* embryon är mycket större än jämförbara skeden i musen, vilket medgör experimentella manipulationer som mikrokirurgi och mikroinjektion. Viktigt är också att 79 % av de gener som är associerade med en sjukdom i människa bevarats i grodan.

Det centrala nervsystemet utvecklas från ett fält av enhetligt utformade celler, kallat neural-platta. Molekylära markörer visar att cellerna i neural-platta redan på ett tidigt stadium förvärvar distinkta regionala identiteter längs huvud-svans axeln i embryot. Som ett resultat av denna mönsterprocess utvecklas neural-platta så småningom till framhjärna, mitthjärna, bakhjärna och ryggmärg. Att förstå de signaler som driver formandet av neural-platta är av stor fokus i denna studie.

Denna studie fokuserar på ett begränsat antal utvecklings-signaler, nämligen Hedgehog (Hh), Wnt, Fibroblast tillväxtfaktor (FGF) och retinoinsyrasignaler. Vi analyserar regleringen och integreringen av dessa signaler genom tre distinkta gener i det tidiga *Xenopus*-embryot.

I den första delen av denna studie, karakteriserar vi en gen, kallad Sufu, och visar att den spelar en viktig roll i regleringen av aktiviteten av Hh och Wnt signaler under bildning och formning av neural-platta. Vi beskriver vidare hur Hh och Wnt signalbanor kommunicera med varandra och identifierar en grundläggande funktion hos Sufu i överhörningen mellan de två signalvägar.

Vi introducerar sedan en gen, kallad xHtrA1 med viktiga funktioner i korrekt bildande av huvud- och svansstrukturer, neural mönster och bildandet av mogna nervceller i embryot. xHtrA1 aktiveras av FGF signaler och i sin tur stimulerar FGF signalering via en mekanism som innebär proteinklyvning och frisättning av aktiva FGF signaler utanför celler.

För det tredje beskriver vi en ny funktion för en gen med akronymen XRDH10 som är involverad i syntesen av retinoinsyra från vitamin A. Vi visar att XRDH10 regleras av retinoinsyra och förser embryot med lämpliga mängder av denna signal under mönstring av det centrala nervsystemet.

Genom att ge en bättre förståelse för de molekylära mekanismer som är inblandade i normal tidig neural utveckling hos *Xenopus* kan dessa resultat leda till ny kunskap för att lösa det intrikata signalnätverket för det centrala nervsystemets utveckling hos människan.

Acknowledgements

This thesis is finally approaching the end of its editing. A number of people have contributed and made this thesis possible, and I would like to acknowledge them here.
I would like to express gratitude to my supervisor, Edgar Pera, thank you so much for your endless support and enthusiasm. Thank you for your persistence and efforts in making our Sufu manuscript a final success. I appreciate your help and patience throughout these five years. It is not easy to reach this point, and I have learnt a lot from you during my PhD training, thank you for your perfectionism, critical evaluation, and high demands that may shape me in becoming a better scientist.

Thank you to my co-supervisor, Udo Häcker, for your useful advice and never-ending support. Thank you to my collaborators Marco Maccarana, Anders Malmström, Madeleine Durbeej-Hjalt and Henrik Semb, for providing me precious opinions and everlasting encouragement. I am grateful to have Stefan Baumgartner as an open and cheerful professor around. Thank you for your help when I was in a panic!

I would like to express my genuine appreciation to Katrin Mani for providing MEF WT cells, Catharina Svanborg, Nataliya Lutay, Bryndis Ragnarsdottir for allowing me to work with luminometer and sharing technical knowledge, Beata Perłowska Lindqvist for NIH3T3 cells and lovely chats. Uwe Rauch for showing me fluorescent microscope.

Of course, two main characters: Shirui Hou and Ina Strate, they are my lab mates, soul mates and best mentors. I have learnt a lot from them, from simple molecular biology to *in situ* hybridization. We three are perfect matches! I missed the time when we were together and shared happiness and sadness. They are forever my best friends.

Thanks to my hubby, Karl-Johan, my parents and brother, Karl-Johan's parents and sister, without their persisting love and support, I would not go this far. Their love has completed my PhD journey. Deep in my heart, I am thankful and grateful to have them and I love you all!

Karl-Johan, thank you for listening to me about everything, you are my hero!

Katie Chapman, for proof-reading my sticky introduction and I love your critical comments. You are one of my beloved friends! I appreciate Igor Arregi for organizing our lab and a nice person to read my thesis. Many hugs to all wonderful people including Pietro Farinelli, Sol da Rocha, Shai Mulinari, Martina Schneider, Kirsten Wunderlich, Darren Cleare, Virginie Carmignac, Bruno Oliveira, Cintia Yuri, Jian Liu, Zhi Ma, Loiuse Wong, Michael Li, Linda Elowsson, Kinga Gawlik, Anki Knutsson, Annelie Shami, Mohammed Alasel, Matthias Schneider, Khalid Fahmy and all people at B12 for their nice accompany! I would like to admit that I am a lucky person to have them as colleagues supplying constant laughter.

I want to thank the eye group members at A11, Hodan, Birgitta, Maithe Perez, Karin, Per for protocols, reagents and technical skills, Stem cell groups at B10 for antibodies and journal clubs discussion. I thank Isabella Artner for being my half time opponent.

To all former colleagues and friends, Javier Sancho, Jose Silva, Dafne Lemus, Julianne McCall, Oliver Blechet, Ingela Liljeqvist Soltic, Christian Holmgren, Emad Amed, Karina Steinkogler, Julia Griesbach, Mohsen Sagha, Dobromir Iliev, Casimiro Castillejo-Lopez and Wilma Martinez.

I want to thank Ulla Nilsson for hosting me three years and I really enjoy living with you! I enjoy having Swedish conversation with secretaries Mats, Märta, Kicki and Stina at B10.

Friends Anna and Martin Rosengren, Chan Yuan and Yi Ming, Barbara and Alexander Mlynarczyk, Ai Na and Diana, Ronald Petie and Eefje Jansen for awesome weekends relaxation and happy moments.

Last but not the least, a well-done PhD thesis will only be accomplished by never-ending support and valuable suggestions from all nice people, that may keep me forward and continue my scientific career.

Sincerely Yours,
Hooi Min Tan Grahn

References

Agius, E., Oelgeschläger, M., Wessely, O., Kemp, C., De Robertis, E.M. (2000). Endodermal Nodal-related signals and mesoderm induction in Xenopus. Development. 127, 1173-83.

Akiyoshi, T., Nakamura, M., Koga, K., Nakashima, H., Yao, T., Tsuneyoshi, M., Tanaka, M., Katano, M. (2006). Gli1, downregulated in colorectal cancers, inhibits proliferation of colon cancer cells involving Wnt signalling activation. Gut. 55, 991-9.

Amaya, E., Musci, T.J., Kirschner, M.W. (1991). Expression of a dominant negative mutant of the FGF receptor disrupts mesoderm formation in Xenopus embryos. Cell. 66, 257-70.

Amaya, E., Stein, P.A., Musci, T.J., Kirschner, M.W. (1993). FGF signalling in the early specification of mesoderm in Xenopus. Development. 118, 477-87.

Amit, S., Hatzubai, A., Birman, Y., Andersen, J.S., Ben-Shushan, E., Mann, M., Ben-Neriah, Y., Alkalay, I. (2002). Axin-mediated CKI phosphorylation of beta-catenin at Ser 45: a molecular switch for the Wnt pathway. Genes Dev. 16, 1066-76.

Bachiller, D., Klingensmith, J., Kemp, C., Belo, J.A., Anderson, R.M., May, S.R., McMahon, J.A., McMahon, A.P., Harland, R.M., Rossant, J., De Robertis, E.M. (2000). The organizer factors Chordin and Noggin are required for mouse forebrain development. Nature. 403, 658-61.

Baker, J.C., Beddington, R.S., Harland, R.M. (1999). Wnt signaling in Xenopus embryos inhibits bmp4 expression and activates neural development. Genes Dev. 1999 Dec 1;13(23):3149-59.

Baldi, A., De Luca, A., Morini, M., Battista, T., Felsani, A., Baldi, F., Catricalà, C., Amantea, A., Noonan, D.M., Albini, A., Natali, P.G., Lombardi, D., Paggi, M.G. (2002). The HtrA1 serine protease is down-regulated during human melanoma progression and represses growth of metastatic melanoma cells. Oncogene. 21, 6684-8.

Bachiller, D., Klingensmith, J., Kemp, C., Belo, J.A., Anderson, R.M., May, S.R., McMahon, J.A., McMahon, A.P., Harland, R.M., Rossant, J., De Robertis, E.M. (2000). The organizer factors Chordin and Noggin are required for mouse forebrain development. Nature. 403, 658-61.

Baker, J.C., Beddington, R.S., Harland, R.M. (1999). Wnt signaling in Xenopus embryos inhibits bmp4 expression and activates neural development. Genes Dev. 1999 Dec 1;13(23):3149-59.

Bang, A.G., Papalopulu, N., Goulding, M.D., Kintner, C. (1999). Expression of Pax-3 in the lateral neural plate is dependent on a Wnt-mediated signal from posterior nonaxial mesoderm. Dev. Biol. 212, 366-80.

Barnfield, P.C., Zhang, X., Thanabalasingham, V., Yoshida, M., Hui, C.C. (2005). Negative regulation of Gli1 and Gli2 activator function by Suppressor of fused through multiple mechanisms. Differentiation. 2005 Oct;73(8):397-405.

Bel-Vialar, S., Itasaki, N., Krumlauf, R. (2002). Initiating Hox gene expression: in the early chick neural tube differential sensitivity to FGF and RA signaling subdivides the HoxB genes in two distinct groups. Development. 129, 5103-15.

Belyaeva, O.V., Johnson, M.P., Kedishvili, N.Y. (2008). Kinetic analysis of human enzyme RDH10 defines the characteristics of a physiologically relevant retinol dehydrogenase. J. Biol. Chem. 283, 20299-308.

Bilic, J., Huang, Y.L., Davidson, G., Zimmermann, T., Cruciat, C.M., Bienz, M., Niehrs, C. (2007). Wnt induces LRP6 signalosomes and promotes dishevelled-dependent LRP6 phosphorylation. Science. 316, 1619-22.

Blitzer, J.T., Nusse, R. (2006). A critical role for endocytosis in Wnt signaling. BMC Cell Biol. 7, 28.

Blumberg, B., Bolado, J. Jr., Moreno, T.A., Kintner, C., Evans, R.M., Papalopulu, N. (1997). An essential role for retinoid signaling in anteroposterior neural patterning. Development. 124, 373-9.

Bouwmeester, T., Kim, S., Sasai, Y., Lu, B., De Robertis, E.M. (1996). Cerberus is a head-inducing secreted factor expressed in the anterior endoderm of Spemann's organizer. Nature. 382, 595-601.

Böttcher, R.T., Pollet, N., Delius, H., Niehrs, C. (2004). The transmembrane protein XFLRT3 forms a complex with FGF receptors and promotes FGF signalling. Nat. Cell Biol. 6, 38-44.

Bowden, M.A., Di Nezza-Cossens, L.A., Jobling, T., Salamonsen, L.A., Nie, G. (2006). Serine proteases HTRA1 and HTRA3 are down-regulated with increasing grades of human endometrial cancer. Gynecol. Oncol. 103, 253-60.

Brannon, M., Kimelman, D. (1996). Activation of Siamois by the Wnt pathway. Dev. Biol. 180, 344-7.

Bülow, H.E., Hobert, O. (2006). The molecular diversity of glycosaminoglycans shapes animal development. Annu. Rev. Cell Dev. Biol. 22, 375-407.

Cammas, L., Romand, R., Fraulob, V., Mura, C., Dollé, P. (2007). Expression of the murine retinol dehydrogenase 10 (Rdh10) gene correlates with many sites of retinoid signalling during embryogenesis and organ differentiation. Dev Dyn. 236, 2899-908.

Canfield, A.E., Hadfield, K.D., Rock, C.F., Wylie, E.C., Wilkinson, F.L. (2007). HtrA1: a novel regulator of physiological and pathological matrix mineralization? Biochem. Soc. Trans. .35, 669-71.

Cayuso, J., Martí, E. (2005). Morphogens in motion: growth control of the neural tube. J. Neurobiol. 64, 376-87.

Chen, M.H., Wilson, C.W., Li, Y.J., Law, K.K., Lu, C.S., Gacayan, R., Zhang, X., Hui, C.C., Chuang, P.T. (2009). Cilium-independent regulation of Gli protein function by Sufu in Hedgehog signaling is evolutionarily conserved. Genes Dev. 23, 1910-28.

Chen, Y., Hollemann, T., Grunz, H., Pieler, T. (1999). Characterization of the Ets-type protein ER81 in Xenopus embryos. Mech. Dev. 80, 67-76.

Chen, Y., Huang, L., Solursh, M. (1994). A concentration gradient of retinoids in the early Xenopus laevis embryo. Dev Biol. 161, 70-6.

Chen, Y., Pollet, N., Niehrs, C., Pieler, T. (2001). Increased XRALDH2 activity has a posteriorizing effect on the central nervous system of Xenopus embryos. Mech. Dev. 101, 91-103.

Chen, Y., Yue, S., Xie, L., Pu, X.H., Jin, T., Cheng, S.Y. (2011). Dual Phosphorylation of suppressor of fused (Sufu) by PKA and GSK3beta regulates its stability and localization in the primary cilium. J. Biol. Chem. 286, 13502-11.

Cheng, S.Y., Bishop, J.M. (2002). Suppressor of Fused represses Gli-mediated transcription by recruiting the SAP18-mSin3 corepressor complex. Proc. Natl. Acad. Sci. U. S. A. 99, 5442-7.

Chiang, C., Litingtung, Y., Lee, E., Young, K.E., Corden, J.L., Westphal, H., Beachy, P.A.(1996). Cyclopia and defective axial patterning in mice lacking Sonic hedgehog gene function. Nature. 383, 407-13.

Chien, J., Staub, J., Hu, S.I., Erickson-Johnson, M.R., Couch, F.J., Smith, D.I., Crowl, R,M., Kaufmann, S.H., Shridhar, V. (2004). A candidate tumor suppressor HtrA1 is downregulated in ovarian cancer. Oncogene. 23, 1636-44.

Cho, K.W., De Robertis, E.M. (1990). Differential activation of Xenopus homeo box genes by mesoderm-inducing growth factors and retinoic acid. Genes Dev. 4, 1910-6.

Christian, J.L., Moon, R.T. (1993). Interactions between Xwnt-8 and Spemann organizer signaling pathways generate dorsoventral pattern in the embryonic mesoderm of Xenopus. Genes Dev. 7, 13-28.

Christen, B., Slack, J.M. (1997). FGF-8 is associated with anteroposterior patterning and limb regeneration in Xenopus. Dev. Biol. 192, 455-66.

Clausen, T., Southan, C., Ehrmann, M. (2002). The HtrA family of proteases: implications for protein composition and cell fate. Mol. Cell. 10, 443-55.

Cooper, A.F., Yu, K.P., Brueckner, M., Brailey, L.L., Johnson, L., McGrath, J.M., Bale, A.E. (2005). Cardiac and CNS defects in a mouse with targeted disruption of suppressor of fused. Development. 132, 4407-17.

Cornell, R.A., Musci, T.J., Kimelman, D. (1995). FGF is a prospective competence factor for early activin-type signals in Xenopus mesoderm induction. Development. 121, 2429-37.

Cornesse, Y., Pieler, T., Hollemann, T. (2005). Olfactory and lens placode formation is controlled by the hedgehog-interacting protein (Xhip) in Xenopus. Dev Biol. 2005 Jan 15;277(2):296-315.

Cruciat, C.M., Ohkawara, B., Acebron, S.P., Karaulanov, E., Reinhard, C., Ingelfinger, D., Boutros, M., Niehrs, C. (2010). Requirement of prorenin receptor and vacuolar H+-ATPase-mediated acidification for Wnt signaling. Science. 327, 459-63.

Dale, L., Jones, C.M. (1999). BMP signalling in early Xenopus development. Bioessays. 21, 751-60.

De Robertis, E.M. (2009). Spemann's organizer and the self-regulation of embryonic fields. Mech. Dev. 126, 925-41.

De Robertis, E.M., Kuroda, H. (2004). Dorsal-ventral patterning and neural induction in Xenopus embryos. Annu. Rev. Cell Dev. Biol. 20, 285-308.

Dewan, A., Liu, M., Hartman, S., Zhang, S.S., Liu, D.T., Zhao, C., Tam, P.O., Chan, W.M., Lam, D.S., Snyder, M., Barnstable, C., Pang, C.P., Hoh, J. (2006). HTRA1 promoter polymorphism in wet age-related macular degeneration. Science. 2006 314, 989-92.

Ding, Q., Fukami, S., Meng, X., Nishizaki, Y., Zhang, X., Sasaki, H., Dlugosz, A., Nakafuku, M., Hui, C. (1999). Mouse suppressor of fused is a negative regulator of sonic hedgehog signaling and alters the subcellular distribution of Gli1. Curr. Biol. 9, 1119-22.

Duester, G. (2008). Retinoic acid synthesis and signaling during early organogenesis. Cell 134, 921-31.

Eichele, G., Tickle, C., Alberts, B.M. (1985). Studies on the mechanism of retinoid-induced pattern duplications in the early chick limb bud: temporal and spatial aspects. J. Cell Biol. 101, 1913-20.

Eivers, E., Fuentealba, L.C., De Robertis, E.M. (2008). Integrating positional information at the level of Smad1/5/8. Curr. Opin Genet. Dev. 18, 304-10.

Ekker, S.C., McGrew, L.L., Lai, C.J., Lee, J.J., von Kessler, D.P., Moon, R.T., Beachy, P.A. (1995). Distinct expression and shared activities of members of the hedgehog gene family of Xenopus laevis. Development. 121, 2337-47.

Farjo, K.M., Moiseyev, G., Nikolaeva, O., Sandell, L.L., Trainor, P.A., Ma, J.X. (2011). RDH10 is the primary enzyme responsible for the first step of embryonic Vitamin A metabolism and retinoic acid synthesis. Dev. Biol. In press.

Fredieu, J.R., Cui, Y., Maier, D., Danilchik, M.V., Christian, J.L. (1997). Xwnt-8 and lithium can act upon either dorsal mesodermal or neurectodermal cells to cause a loss of forebrain in Xenopus embryos. Dev. Biol. 186, 100-14.

Franco, P.G., Paganelli, A.R., López, S.L., Carrasco, A.E. (1999). Functional association of retinoic acid and hedgehog signaling in Xenopus primary neurogenesis. Development. 126, 4257-65.

Freeman, M., Gurdon, J.B. (2002). Regulatory principles of developmental signaling. Annu. Rev. Cell Dev. Biol. 18, 515-39

Fuentealba, L.C., Eivers, E., Ikeda, A., Hurtado, C., Kuroda, H., Pera, E.M., De Robertis, E.M. (2007). Integrating patterning signals: Wnt/GSK3 regulates the duration of the BMP/Smad1 signal. Cell. 131, 980-93.

Fujii, H., Sakai, M., Nishimatsu, S., Nohno, T., Mochii, M., Orii, H., Watanabe, K. (2008). VegT, eFGF and Xbra cause overall posteriorization while Xwnt8 causes eye-level restricted posteriorization in synergy with chordin in early Xenopus development. Dev. Growth Differ. 50, 169-80.

Fürthauer, M., Lin, W., Ang, S.L., Thisse, B., Thisse, C. (2002). Sef is a feedback-induced antagonist of Ras/MAPK-mediated FGF signalling. Nat. Cell Biol. 4, 170-4.

Gallagher, J. (2007). Messages in the matrix: proteoglycans go the distance. Dev. Cell. 13, 166-7.

Glinka, A., Wu, W., Delius, H., Monaghan, A.P., Blumenstock, C., Niehrs, C. (1998). Dickkopf-1 is a member of a new family of secreted proteins and functions in head induction. Nature. 391, 357-62.

Glinka, A., Wu, W., Onichtchouk, D., Blumenstock, C., Niehrs, C. (1997). Head induction by simultaneous repression of Bmp and Wnt signalling in Xenopus. Nature 389, 517-9.

Glover, J.C., Renaud, J.S., Rijli, F.M. (2006). Retinoic acid and hindbrain patterning. J. Neurobiol. 66, 705-25.

Goodrich, L.V., Milenković, L., Higgins, K.M., Scott, M.P. (1997). Altered neural cell fates and medulloblastoma in mouse patched mutants. Science. 277, 1109-13.

Grunz, H., Tacke, L. (1990). Extracellular matrix components prevent neural differentiation of disaggregated Xenopus ectoderm cells. Cell Differ. Dev. 32, 117-23.

Häcker, U., Nybakken, K., Perrimon, N. (2005). Heparan sulphate proteoglycans: the sweet side of development. Nat. Rev. Mol. Cell Biol. 6, 530-41.

Hansen, C.S., Marion, C.D., Steele, K., George, S., Smith, W.C. (1997). Direct neural induction and selective inhibition of mesoderm and epidermis inducers by Xnr3. Development. 124, 483-92.

Haramoto, Y., Tanegashima, K., Onuma, Y., Takahashi, S., Sekizaki, H., Asashima, M. (2004). Xenopus tropicalis nodal-related gene 3 regulates BMP signaling: an essential role for the pro-region. Dev. Biol. 265, 155-68.

Hardcastle, Z., Chalmers, A.D., Papalopulu, N. (2000). FGF-8 stimulates neuronal differentiation through FGFR-4a and interferes with mesoderm induction in Xenopus embryos. Curr. Biol. 10, 1511-4.

Heeg-Truesdell E, LaBonne C. (2006). Neural induction in Xenopus requires inhibition of Wnt-beta-catenin signaling. Dev. Biol. 298, 71-86.

Hemmati-Brivanlou, A., Kelly, O.G., Melton, D.A. (1994). Follistatin, an antagonist of activin, is expressed in the Spemann organizer and displays direct neuralizing activity. Cell. 77, 283-95.

Hemmati-Brivanlou, A., Melton, D.A. (1992). A truncated activin receptor inhibits mesoderm induction and formation of axial structures in Xenopus embryos. Nature. 359, 609-14.

Hernandez, R.E., Putzke, A.P., Myers, J.P., Margaretha, L., Moens, C.B. (2007). Cyp26 enzymes generate the retinoic acid response pattern necessary for hindbrain development. Development. 134, 177-87.

Hollemannyy, T., Chen, Y., Grunz, H., Pieler, T. (1998). Regionalized metabolic activity establishes boundaries of retinoic acid signalling. EMBO J. 17, 7361-72.

Holowacz, T., Sokol, S. (1999). FGF is required for posterior neural patterning but not for neural induction. Dev. Biol. 205, 296-308.

Hou, J., Clemmons, D.R., Smeekens, S. (2005). Expression and characterization of a serine protease that preferentially cleaves insulin-like growth factor binding protein-5. J. Cell Biochem. 94, 470-84.

Huangfu, D., Anderson, K.V. (2005). Cilia and Hedgehog responsiveness in the mouse. Proc. Natl. Acad. Sci. U. S. A. 102, 11325-30.

Huangfu, D., Liu, A., Rakeman, A.S., Murcia, N.S., Niswander, L., Anderson, K.V. (2003). Hedgehog signalling in the mouse requires intraflagellar transport proteins. Nature. 426, 83-7.

Humke, E.W., Dorn, K.V., Milenkovic, L., Scott, M.P., Rohatgi, R. (2010). The output of Hedgehog signaling is controlled by the dynamic association between Suppressor of Fused and the Gli proteins. Genes Dev. 2010 Apr 1;24(7):670-82.

Ingham, P.W., McMahon, A.P. (2001). Hedgehog signaling in animal development: paradigms and principles. Genes Dev. 15, 3059-87.

Isaacs, H.V. (1997). New perspectives on the role of the fibroblast growth factor family in amphibian development. Cell Mol. Life Sci. 53, 350-61.

Isaacs, H.V., Pownall, M.E., Slack, J.M. (1994). eFGF regulates Xbra expression during Xenopus gastrulation. EMBO J. 13, 4469-81.

Isaacs, H.V., Tannahill, D., Slack, J.M. (1992). Expression of a novel FGF in the Xenopus embryo. A new candidate inducing factor for mesoderm formation and anteroposterior specification. Development. 114, 711-20.

Itoh, K., Tang, T.L., Neel, B.G., Sokol, S.Y. (1995). Specific modulation of ectodermal cell fates in Xenopus embryos by glycogen synthase kinase. Development. 121, 3979-88.

Jia, J., Kolterud, A., Zeng, H., Hoover, A., Teglund, S., Toftgård, R., Liu, A. (2009). Suppressor of Fused inhibits mammalian Hedgehog signaling in the absence of cilia. Dev. Biol. 330, 452-60.

Jiang, J., and Hui, C.C. (2008). Hedgehog signaling in development and cancer. Dev. Cell 15, 801-12.

Kazanskaya, O., Glinka, A., Niehrs, C. (2000). The role of Xenopus dickkopf1 in prechordal plate specification and neural patterning. Development. 127, 4981-92.

Kengaku, M., Okamoto, H. (1993). Basic fibroblast growth factor induces differentiation of neural tube and neural crest lineages of cultured ectoderm cells from Xenopus gastrula. Development. 119, 1067-78.

Kengaku, M., Okamoto, H. (1995). bFGF as a possible morphogen for the anteroposterior axis of the central nervous system in Xenopus. Development. 121, 3121-30.

Kessel, M., Gruss, P. (1991). Homeotic transformations of murine vertebrae and concomitant alteration of Hox codes induced by retinoic acid. Cell. 67, 89-104.

Kiecker, C., Niehrs, C. (2001). A morphogen gradient of Wnt/beta-catenin signalling regulates anteroposterior neural patterning in Xenopus. Development. 128, 4189-201.

Kimelman, D., Abraham, J.A., Haaparanta, T., Palisi, T.M., Kirschner, M.W. (1988). The presence of fibroblast growth factor in the frog egg: its role as a natural mesoderm inducer. Science. 242, 1053-6.

Kogerman, P., Grimm, T., Kogerman, L., Krause, D., Undén, A.B., Sandstedt, B., Toftgård, R., Zaphiropoulos, P.G. (1999). Mammalian suppressor-of-fused modulates nuclear-cytoplasmic shuttling of Gli-1. Nat. Cell Biol. 1, 312-9.

Kramer, K.L., Yost, H.J. (2003). Heparan sulfate core proteins in cell-cell signaling. Annu. Rev. Genet. 37, 461-84.

Kudoh, T., Wilson, S.W., Dawid, I.B. (2002). Distinct roles for Fgf, Wnt and retinoic acid in posteriorizing the neural ectoderm. Development. 129, 4335-46.

Kuroda, H., Wessely, O., De Robertis, E.M. (2004). Neural induction in Xenopus: requirement for ectodermal and endomesodermal signals via Chordin, Noggin, beta-Catenin, and Cerberus. PLoS Biol. 2, E92.

LaBonne, C., Whitman, M. (1994). Mesoderm induction by activin requires FGF-mediated intracellular signals. Development. 120, 463-72.

Lai, C. J., Ekker, S. C., Beachy, P. A., Moon, R. T. (1995). Patterning of the neural ectoderm of Xenopus laevis by the amino-terminal product of hedgehog autoproteolytic cleavage. Development 121, 2349-60.

Lamb, T.M., Knecht, A.K., Smith, W.C., Stachel, S.E., Economides, A.N., Stahl, N., Yancopolous, G.D., Harland, R.M. (1993). Neural induction by the secreted polypeptide noggin. Science. 262, 713-8.

Larabell, C.A., Torres, M., Rowning, B.A., Yost, C., Miller, J.R., Wu, M., Kimelman, D., Moon, R,T. (1997). Establishment of the dorso-ventral axis in Xenopus embryos is presaged by early asymmetries in beta-catenin that are modulated by the Wnt signaling pathway. J. Cell Biol. 136, 1123-36.

Lee, J., Platt, K.A., Censullo, P., Ruiz i Altaba, A. (1997). Gli1 is a target of Sonic hedgehog that induces ventral neural tube development. Development. 124, 2537-52.

Leyns, L., Bouwmeester, T., Kim, S.H., Piccolo, S., De Robertis, E.M. (1997). Frzb-1 is a secreted antagonist of Wnt signaling expressed in the Spemann organizer. Cell. 88, 747-56.

Liu, C., Li, Y., Semenov, M., Han, C., Baeg, G.H., Tan, Y., Zhang, Z., Lin, X., He, X. (2002). Control of beta-catenin phosphorylation/degradation by a dual-kinase mechanism. Cell. 108, 837-47.

Liu, J.P., Laufer, E., Jessell, T.M. (2001). Assigning the positional identity of spinal motor neurons: rostrocaudal patterning of Hox-c expression by FGFs, Gdf11, and retinoids. Neuron. 32, 997-1012.

Maeda, O., Kondo, M., Fujita, T., Usami, N., Fukui, T., Shimokata, K., Ando, T., Goto, H., Sekido, Y. (2006). Enhancement of GLI1-transcriptional activity by beta-catenin in human cancer cells. Oncol. Rep. 16, 91-6.

Maden, M. (1999). Heads or tails? Retinoic acid will decide. Bioessays. 21, 809-12.

Maden, M. (2002). Retinoid signalling in the development of the central nervous system. Nat. Rev. Neurosci. 3, 843-53.

Maden, M., Holder, N. (1991). The involvement of retinoic acid in the development of the vertebrate central nervous system. Development. Suppl 2, 87-94.

Marine, J.C., Bellefroid, E.J., Pendeville, H., Martial, J.A., Pieler, T. (1997). A role for Xenopus Gli-type zinc finger proteins in the early embryonic patterning of mesoderm and neuroectoderm. Mech. Dev. 63, 211-25.

Mark, M., Ghyselinck, N.B., Chambon, P. (2006). Function of retinoid nuclear receptors: lessons from genetic and pharmacological dissections of the retinoic acid signaling pathway during mouse embryogenesis. Annu. Rev. Pharmacol. Toxicol. 46, 451-80.

Marshall, H., Nonchev, S., Sham, M.H., Muchamore, I., Lumsden, A., Krumlauf, R. (1992). Retinoic acid alters hindbrain Hox code and induces transformation of rhombomeres 2/3 into a 4/5 identity. Nature. 360, 737-41.

Marti, E., Takada, R., Bumcrot, D. A., Sasaki, H., McMahon, A.P. (1995). Distribution of Sonic hedgehog peptides in the developing chick and mouse embryo. Development 121: 2537-2547.

Martinez Arias, A. (2003). Wnts as morphogens? The view from the wing of Drosophila. Nat Rev Mol Cell Biol. 4, 321-5.

Mastick, G.S., Fan, C.M., Tessier-Lavigne, M., Serbedzija, G.N., McMahon, A.P., Easter, S.S. Jr. (1996). Early deletion of neuromeres in Wnt-1-/- mutant mice: evaluation by morphological and molecular markers. J. Comp. Neurol. 374, 246-58.

McGrew, L.L., Lai C.J., Moon, R.T. (1995). Specification of the anteroposterior neural axis through synergistic interaction of the Wnt signaling cascade with noggin and follistatin. Dev. Biol. 172, 337-42.

McMahon, A.P., Bradley, A. (1990). The Wnt-1 (int-1) proto-oncogene is required for development of a large region of the mouse brain. Cell. 62, 1073-85.

Meng, X., Poon, R., Zhang, X., Cheah A., Ding, Q., Hui, C.C., Alman, B. (2001). Suppressor of fused negatively regulates beta-catenin signaling. J. Biol. Chem. 276, 40113-9.

Meyers, E.N., Lewandoski, M., Martin, G.R. (1998). An Fgf8 mutant allelic series generated by Cre- and Flp-mediated recombination. Nat. Genet. 18, 136-41.

Miller, J.R., Rowning, B.A., Larabell, C.A., Yang-Snyder, J.A., Bates, R.L., Moon, R.T. (1999). Establishment of the dorsal-ventral axis in Xenopus embryos coincides with the dorsal enrichment of dishevelled that is dependent on cortical rotation. J. Cell Biol. 146(2):427-37.

Moos, M. Jr., Wang, S., Krinks, M. (2005). Anti-dorsalizing morphogenetic protein is a novel TGF-beta homolog expressed in the Spemann organizer. Development. 121, 4293-301.

Morriss-Kay, G.M., Murphy, P., Hill, R.E., Davidson, D.R. (1991). Effects of retinoic acid excess on expression of Hox-2.9 and Krox-20 and on morphological segmentation in the hindbrain of mouse embryos. EMBO J. 10, 2985-95.

Mukhopadhyay, M., Shtrom, S., Rodriguez-Esteban, C., Chen, L., Tsukui, T., Gomer, L., Dorward, D.W., Glinka, A., Grinberg, A., Huang, S.P., Niehrs, C., Izpisúa Belmonte, J.C., Westphal, H. (2001). Dickkopf1 is required for embryonic head induction and limb morphogenesis in the mouse. Dev. Cell. 1, 423-34.

Niederreither, K., Dollé, P. (2008). Retinoic acid in development: towards an integrated view. Nat. Rev. Genet. 9, 541-53.

Niederreither, K., McCaffery, P., Dräger, U.C., Chambon, P., Dollé, P. (1997). Restricted expression and retinoic acid-induced downregulation of the retinaldehyde dehydrogenase type 2 (RALDH-2) gene during mouse development. Mech. Dev. 62, 67-78.

Nieuwkoop, P.D. (1969). The formation of the mesoderm in urodelean amphibians I. The induction by the endoderm. W. Roux´Arch. Ent. Org. 162, 341-373.

Nieuwkoop, P.D. (1973). The organization center of the amphibian embryo: its origin, spatial organization, and morphogenetic action. Adv. Morphog. 10, 1-39.

Nieuwkoop, P.D. (1977). Origin and establishment of embryonic polar axes in amphibian development. Curr. Top. Dev. Biol. 11, 115-32.

Ohlmeyer, J.T., Kalderon, D. (1998). Hedgehog stimulates maturation of Cubitus interruptus into a labile transcriptional activator. Nature. 396, 749-53.

Ornitz, D.M. (2000). FGFs, heparan sulfate and FGFRs: complex interactions essential for development. Bioessays. 22, 108-12.

Pallen, M.J., Wren, B.W. (1997). The HtrA family of serine proteases. Mol Microbiol. 26, 209-21.

Papalopulu, N., Kintner, C. (1996). A posteriorising factor, retinoic acid, reveals that anteroposterior patterning controls the timing of neuronal differentiation in Xenopus neuroectoderm. Development. 122, 3409-18.

Pera, E.M., De Robertis, E.M. (2000). A direct screen for secreted proteins in Xenopus embryos identifies distinct activities for the Wnt antagonists Crescent and Frzb-1. Mech. Dev. 96, 183-95.

Pera, E.M., Hou, S., Strate, I., Wessely, O., De Robertis, E.M. (2005). Exploration of the extracellular space by a large-scale secretion screen in the early Xenopus embryo. Int. J. Dev. Biol. 49, 781-96.

Pera, E.M., Ikeda, A., Eivers, E., De Robertis, E.M. (2003). Integration of IGF, FGF, and anti-BMP signals via Smad1 phosphorylation in neural induction. Genes Dev. 17, 3023-8.

Pera, E.M., Wessely, O., Li, S.Y., De Robertis, E.M. (2001). Neural and head induction by insulin-like growth factor signals. Dev. Cell 1, 655-65.

Pham, A., Therond, P., Alves, G., Tournier, F.B., Busson, D., Lamour-Isnard, C., Bouchon, B.L., Préat, T., Tricoire, H. (1995). The Suppressor of fused gene encodes a novel PEST protein involved in Drosophila segment polarity establishment. Genetics. 140, 587-98.

Piccolo, S., Agius, E., Leyns, L., Bhattacharyya, S., Grunz, H., Bouwmeester, T., De Robertis, E.M. (1999). The head inducer Cerberus is a multifunctional antagonist of Nodal, BMP and Wnt signals. Nature. 397, 707-10.

Pierce, S.B., Kimelman, D. (1995). Regulation of Spemann organizer formation by the intracellular kinase Xgsk-3. Development. 121, 755-65.

Pownall, M.E., Tucker, A.S., Slack, J.M., Isaacs, H.V. (1996). eFGF, Xcad3 and Hox genes form a molecular pathway that establishes the anteroposterior axis in Xenopus. Development 122, 3881-92.

Préat, T. (1992). Characterization of Suppressor of fused, a complete suppressor of the fused segment polarity gene of Drosophila melanogaster. Genetics. 132, 725-36.

Rao, T.P., Kühl, M. (2010). An updated overview on Wnt signaling pathways: a prelude for more. Circ. Res. 106, 1798-806.

Ray, W.J., Bain, G., Yao, M., Gottlieb, D.I. (1997). CYP26, a novel mammalian cytochrome P450, is induced by retinoic acid and defines a new family. J. Biol. Chem. 272, 18702-8.

Reifers, F., Böhli, H., Walsh, E.C., Crossley, P.H., Stainier, D.Y., Brand, M. (1998). Fgf8 is mutated in zebrafish acerebellar (ace) mutants and is required for maintenance of midbrain-hindbrain boundary development and somitogenesis. Development. 125, 2381-95.

Reversade, B., De Robertis, E.M. (2005). Regulation of ADMP and BMP2/4/7 at opposite embryonic poles generates a self-regulating morphogenetic field. Cell. 123, 1147-60.

Richard-Parpaillon, L., Héligon, C., Chesnel, F., Boujard, D., Philpott, A. (2002). The IGF pathway regulates head formation by inhibiting Wnt signaling in Xenopus. Dev Biol. 244, 407-17.

Romand, R., Kondo, T., Cammas, L., Hashino, E., Dollé, P. (2008). Dynamic expression of the retinoic acid-synthesizing enzyme retinol dehydrogenase 10 (rdh10) in the developing mouse brain and sensory organs. J. Comp. Neurol. 508, 879-92.

Ross, S.A., McCaffery, P.J., Drager, U.C., De Luca, L.M. (2000). Retinoids in embryonal development. Physiol. Rev. 80, 1021-54.

Rowning, B.A., Wells, J., Wu, M., Gerhart, J.C., Moon, R.T., Larabell, C.A. (1997). Microtubule-mediated transport of organelles and localization of beta-catenin to the future dorsal side of Xenopus eggs. Proc. Natl. Acad. Sci. U. S. A. 94, 1224-9.

Sandell, L.L., Sanderson, B.W., Moiseyev, G., Johnson, T., Mushegian, A., Young, K., Rey, J.P., Ma, J.X., Staehling-Hampton, K., Trainor, P.A. (2007). RDH10 is essential for synthesis of

embryonic retinoic acid and is required for limb, craniofacial, and organ development. Genes Dev. 21, 1113-24.

Sasai, Y., Lu, B., Steinbeisser, H., De Robertis, E.M. (1995). Regulation of neural induction by the Chd and Bmp-4 antagonistic patterning signals in Xenopus. Nature. 376, 333 - 336.

Sasai, Y., Lu, B., Steinbeisser, H., Geissert, D., Gont, L.K., De Robertis, E.M. (1994). Xenopus chordin: a novel dorsalizing factor activated by organizer-specific homeobox genes. Cell. 79, 779-90.

Sato, S.M., Sargent, T.D. (1989). Development of neural inducing capacity in dissociated Xenopus embryos. Dev. Biol. 134, 263-6.

Schneider, S., Steinbeisser, H., Warga, R.M., Hausen, P. (1996). Beta-catenin translocation into nuclei demarcates the dorsalizing centers in frog and fish embryos. Mech. Dev. 57, 191-8.

Sharpe, C., Goldstone, K. (2000). The control of Xenopus embryonic primary neurogenesis is mediated by retinoid signalling in the neurectoderm. Mech. Dev. 91, 69-80.

Sharpe, C., Goldstone, K. (2000a). Retinoid signalling acts during the gastrula stages to promote primary neurogenesis. Int. J. Dev. Biol. 44, 463-70.

Shibata, M., Ono, H., Hikasa, H., Shinga, J., Taira, M. (2000). Xenopus crescent encoding a Frizzled-like domain is expressed in the Spemann organizer and pronephros. Mech. Dev. 96, 243-6.

Sirbu, I.O., Gresh, L., Barra, J., Duester, G. (2005). Shifting boundaries of retinoic acid activity control hindbrain segmental gene expression. Development. 132, 2611-22.

Sivak, J.M., Petersen, L.F., Amaya, E. (2005). FGF signal interpretation is directed by Sprouty and Spred proteins during mesoderm formation. Dev. Cell. 8, 689-701.

Smith, J.C., Gurdon, J.B. (2004). Many ways to make a gradient. Bioessays. 26, 705-6.

Smith, W.C., Harland, R.M. (1992). Expression cloning of noggin, a new dorsalizing factor localized to the Spemann organizer in Xenopus embryos. Cell. 70, 829-40.

Spemann, H., Mangold, H. (1924). Ueber Induktion von Embryonalanlagen durch Implantation artfremder Organisatoren. Roux's Arch. Entw. Mech. Org. 100, 599-638. Reprinted and transl. Int. J. Dev. Biol. 45, 13-18.

Sokol, S.Y., Klingensmith, J., Perrimon, N., Itoh, K. (1995). Dorsalizing and neuralizing properties of Xdsh, a maternally expressed Xenopus homolog of dishevelled. Development. 121, 3487.

Stecca, B., Ruiz I Altaba, A. (2010). Context-dependent regulation of the GLI code in cancer by HEDGEHOG and non-HEDGEHOG signals. J. Mol. Cell Biol. 2, 84-95.

Sun, B.I., Bush, S.M., Collins-Racie, L.A., LaVallie, E.R., DiBlasio-Smith, E.A., Wolfman, N.M., McCoy, J.M., Sive, H.L. (1999). derrière: a TGF-beta family member required for posterior development in Xenopus. Development. 126, 1467-82.

Svärd, J., Heby-Henricson, K., Persson-Lek, M., Rozell, B., Lauth, M., Bergström, A., Ericson, J., Toftgård, R., Teglund, S. (2006). Genetic elimination of Suppressor of fused reveals an essential repressor function in the mammalian Hedgehog signaling pathway. Dev Cell. 10, 187-97.

Taelman, V.F., Dobrowolski, R., Plouhinec, J.L., Fuentealba, L.C., Vorwald, P.P., Gumper, I., Sabatini, D.D., De Robertis, E.M. (2010). Wnt signaling requires sequestration of glycogen synthase kinase 3 inside multivesicular endosomes. Cell. 143, 1136-48.

Takada, S., Stark, K.L., Shea, M.J., Vassileva, G., McMahon, J.A., McMahon, A.P. (1994). Wnt-3a regulates somite and tailbud formation in the mouse embryo. Genes Dev. 8, 174-89.

Takahashi, S., Yokota, C., Takano, K., Tanegashima, K., Onuma, Y., Goto, J., Asashima, M. (2000). Two novel nodal-related genes initiate early inductive events in Xenopus Nieuwkoop center. Development. 127, 5319-29.

Tamai, K., Zeng, X., Liu, C., Zhang, X., Harada, Y., Chang, Z., He, X. (2004). A mechanism for Wnt coreceptor activation. Mol. Cell. 2004 Jan 16;13(1):149-56.

Tao, Q., Yokota, C., Puck, H., Kofron, M., Birsoy, B., Yan, D., Asashima, M., Wylie, C.C., Lin, X., Heasman, J. (2005). Maternal wnt11 activates the canonical wnt signaling pathway required for axis formation in Xenopus embryos. Cell. 2005 120, 857-71.

Taylor, M.D., Liu, L., Raffel, C., Hui, C.C., Mainprize, T.G., Zhang, X., Agatep, R., Chiappa, S., Gao, L., Lowrance, A., Hao, A., Goldstein, A.M., Stavrou, T., Scherer, S.W., Dura, W.T., Wainwright, B., Squire, J.A., Rutka, J.T., Hogg, D. (2002). Mutations in SUFU predispose to medulloblastoma. Nat. Genet. 31, 306-10.

Tickle, C., Lee, J., Eichele, G. (1985). A quantitative analysis of the effect of all-trans-retinoic acid on the pattern of chick wing development. Dev. Biol. 109, 82-95.

Trowbridge, J.M., Gallo, R.L. (2002). Dermatan sulfate: new functions from an old glycosaminoglycan. Glycobiology. 12, 117R-25R.

Trowbridge, J.M., Rudisill, J.A., Ron, D., Gallo, R.L. (2002). Dermatan sulfate binds and potentiates activity of keratinocyte growth factor (FGF-7). J. Biol. Chem. 277, 42815-20.

Tsang, M., Dawid, I.B. (2004). Promotion and attenuation of FGF signaling through the Ras-MAPK pathway. 2004, pe17.

Tsang, M., Friesel, R., Kudoh, T., Dawid, I.B. (2002). Identification of Sef, a novel modulator of FGF signalling. Nat. Cell Biol. 4, 165-9.

Tukachinsky, H., Lopez, L.V., Salic, A. (2010). A mechanism for vertebrate Hedgehog signaling: recruitment to cilia and dissociation of SuFu-Gli protein complexes. J. Cell Biol. 191, 415-28.

Umbhauer, M., Marshall, C.J., Mason, C.S., Old, R.W., Smith, J.C. (1995). Mesoderm induction in Xenopus caused by activation of MAP kinase. Nature. 376, 58-62.

Umbhauer, M., Penzo-Méndez, A., Clavilier, L., Boucaut, J., Riou, J. (2000). Signaling specificities of fibroblast growth factor receptors in early Xenopus embryo. J. Cell Sci. 113, 2865-75.

van den Brink, G.R., Bleuming, S.A., Hardwick, J.C., Schepman, B.L., Offerhaus, G.J., Keller, J.J., Nielsen, C., Gaffield, W., van Deventer, S.J., Roberts, D.J., Peppelenbosch, M.P. (2004). Indian Hedgehog is an antagonist of Wnt signaling in colonic epithelial cell differentiation. Nat. Genet. 36, 277-82.

van der Wees, J., Schilthuis, J.G., Koster, C.H., Diesveld-Schipper, H., Folkers, G.E., van der Saag, P.T., Dawson, M.I., Shudo, K., van der Burg, B., Durston, A.J. (1998). Inhibition of retinoic acid receptor-mediated signalling alters positional identity in the developing hindbrain. Development. 125, 545-56.

Varjosalo, M., Li, S. P., and Taipale, J. (2006). Divergence of hedgehog signal transduction mechanism between Drosophila and mammals. Dev. Cell 10, 177-86.

Wang, C., Pan, Y., Wang, B. (2010). Suppressor of fused and Spop regulate the stability, processing and function of Gli2 and Gli3 full-length activators but not their repressors. Development. 137, 2001-9.

Weaver, C., Farr, G.H., Pan, W., Rowning, B.A., Wang, J., Mao, J., Wu, D., Li, L., Larabell, C.A., Kimelman, D. (2003). GBP binds kinesin light chain and translocates during cortical rotation in Xenopus eggs. Development. 130, 5425-36.

Wessely, O., Agius, E., Oelgeschläger, M., Pera, E.M., De Robertis, E.M. (2001). Neural induction in the absence of mesoderm: beta-catenin-dependent expression of secreted BMP antagonists at the blastula stage in Xenopus. Dev. Biol. 234, 161-73.

Wessely, O., Kim, J.I., Geissert, D., Tran, U., De Robertis, E.M. (2004). Analysis of Spemann organizer formation in Xenopus embryos by cDNA macroarrays. Dev. Biol. 269, 552-66.

White, J.A., Guo, Y.D., Baetz, K., Beckett-Jones, B., Bonasoro, J., Hsu, K.E., Dilworth, F.J., Jones, G., Petkovich, M. (1996). Identification of the retinoic acid-inducible all-trans-retinoic acid 4-hydroxylase. J. Biol. Chem. 271, 29922-7.

White, R.J., Nie, Q., Lander, A.D., Schilling, T.F. (2007). Complex regulation of cyp26a1 creates a robust retinoic acid gradient in the zebrafish embryo. PLoS. Biol. 5, e304.

Wilson, P.A., Hemmati-Brivanlou, A. (1995). Induction of epidermis and inhibition of neural fate by Bmp-4. Nature. 376, 331-3.

Wolpert, L. (1969). Positional information and the spatial pattern of cellular differentiation. J. Theor. Biol. 25, 1-47.

Wolpert, L. (2011). Positional information and patterning revisited. J. Theor. Biol. 269, 359-65.

Wood, H., Pall, G., Morriss-Kay, G. (1994). Exposure to retinoic acid before or after the onset of somitogenesis reveals separate effects on rhombomeric segmentation and 3' HoxB gene expression domains. Development. 120, 2279-85.

Wu, B.X., Chen, Y., Chen, Y., Fan, J., Rohrer, B., Crouch, R.K., Ma, J.X. (2002). Cloning and characterization of a novel all-trans retinol short-chain dehydrogenase/reductase from the RPE. Invest. Ophthalmol. Vis. Sci. 43, 3365-72.

Wu, B.X., Moiseyev, G., Chen, Y., Rohrer, B., Crouch, R.K., Ma, J.X. (2004). Identification of RDH10, an All-trans Retinol Dehydrogenase, in Retinal Muller Cells. Invest Ophthalmol. Vis. Sci. 45, 3857-62.

Yamaguchi, T.P., Bradley, A., McMahon, A.P., Jones, S. (1999). A Wnt5a pathway underlies outgrowth of multiple structures in the vertebrate embryo. Development. 126, 1211-23.

Yamamoto, H., Komekado, H., Kikuchi, A. (2006). Caveolin is necessary for Wnt-3a-dependent internalization of LRP6 and accumulation of beta-catenin. Dev. Cell. 11, 213-23.

Yanai, K., Nakamura, M., Akiyoshi, T., Nagai, S., Wada, J., Koga, K., Noshiro, H., Nagai, E., Tsuneyoshi, M., Tanaka, M., Katano, M. (2008). Crosstalk of hedgehog and Wnt pathways in gastric cancer. Cancer Lett. 263, 145-56.

Yelin, R., Schyr, R.B., Kot, H., Zins, S., Frumkin, A., Pillemer, G., Fainsod, A. (2005). Ethanol exposure affects gene expression in the embryonic organizer and reduces retinoic acid levels. Dev. Biol. 279, 193-204.

Yost, C., Torres, M., Miller, J.R., Huang, E., Kimelman, D., Moon, R.T. (1996). The axis-inducing activity, stability, and subcellular distribution of beta-catenin is regulated in Xenopus embryos by glycogen synthase kinase 3. Genes Dev. 10, 1443-54.

Zeng, H., Jia, J., Liu, A. (2010). Coordinated translocation of mammalian Gli proteins and suppressor of fused to the primary cilium. PLoS One 5, e15900.

Zeng, X., Huang, H., Tamai, K., Zhang, X., Harada, Y., Yokota, C., Almeida, K., Wang, J., Doble, B., Woodgett, J., Wynshaw-Boris, A., Hsieh, J.C., He, X. (2008). Initiation of Wnt signaling: control of Wnt coreceptor Lrp6 phosphorylation/activation via frizzled, dishevelled and axin functions. Development. 135, 367-75.

Zeng, X., Tamai, K., Doble, B., Li, S., Huang, H., Habas, R., Okamura, H., Woodgett, J., He, X. (2005). A dual-kinase mechanism for Wnt co-receptor phosphorylation and activation. Nature. 438, 873-7.

Zhang, Q., Zhang, L., Wang, B., Ou, C.Y., Chien, C.T., Jiang, J. (2006a). A hedgehog-induced BTB protein modulates hedgehog signaling by degrading Ci/Gli transcription factor. Dev. Cell 10, 719-29.

Zhang, X., Ibrahimi, O.A., Olsen, S.K., Umemori, H., Mohammadi, M., Ornitz, D.M. (2006). Receptor specificity of the fibroblast growth factor family. The complete mammalian FGF family. J. Biol. Chem. 281, 15694-700.

Zumbrunn, J., Trueb, B. (1996). Primary structure of a putative serine protease specific for IGF-binding proteins. FEBS Lett. 398, 187-92.

Paper I

ARTICLE IN PRESS
YDBIO-05414; No. of pages: 15; 4C: 3, 4, 5, 6, 8, 9, 10, 13
Developmental Biology xxx (2011) xxx–xxx

Contents lists available at ScienceDirect

Developmental Biology

journal homepage: www.elsevier.com/developmentalbiology

The dual regulator Sufu integrates Hedgehog and Wnt signals in the early *Xenopus* embryo

Tan H. Min [a], Martin Kriebel [b], Shirui Hou [c], Edgar M. Pera [a,*]

[a] Stem Cell Center, Lund University, 221 84 Lund, Sweden
[b] Natural and Medical Sciences Institute at the University of Tuebingen, 72770 Reutlingen, Germany
[c] The Jackson Laboratory, Bar Harbor, ME 04609, USA

ARTICLE INFO

Article history:
Received for publication 3 January 2011
Revised 1 July 2011
Accepted 28 July 2011
Available online xxxx

Keywords:
Suppressor-of-fused
Gli
β-Catenin
Neural
Xenopus

ABSTRACT

Hedgehog (Hh) and Wnt proteins are important signals implicated in several aspects of embryonic development, including the early development of the central nervous system. We found that *Xenopus* Suppressor-of-fused (XSufu) affects neural induction and patterning by regulating the Hh/Gli and Wnt/β-catenin pathways. Microinjection of *XSufu* mRNA induced expansion of the epidermis at the expense of neural plate tissue and caused enlargement of the eyes. An antisense morpholino oligonucleotide against XSufu had the opposite effect. Interestingly, both gain- and loss-of-function experiments resulted in a posterior shift of brain markers, suggesting a biphasic effect of XSufu on anteroposterior patterning. XSufu blocked early Wnt/β-catenin signaling, as indicated by the suppression of *XWnt8*-induced secondary axis formation in mRNA-injected embryos, and activation of Wnt target genes in *XSufu*-MO-injected ectodermal explants. We show that XSufu binds to XGli1 and Xβ-catenin. In *Xenopus* embryos and mouse embryonic fibroblasts, Gli1 inhibits Wnt signaling under overexpression of β-catenin, whereas β-catenin stimulates Hh signaling under overexpression of Gli1. Notably, endogenous Sufu is critically involved in this crosstalk. The results suggest that XSufu may act as a common regulator of Hh and Wnt signaling and contribute to intertwining the two pathways.

Introduction

An important question in developmental biology is how multiple signaling pathways such as those activated by Hedgehog (Hh) and Wnt proteins are integrated to generate positional identity in the embryo. Originally identified as factors affecting *Drosophila* embryogenesis, the Hh and Wnt pathways are major signaling systems during animal development, stemness and cancer (Jiang and Hui, 2008; MacDonald et al., 2009). Binding of the Hh ligand to its receptor, Patched (Ptc), alleviates an inhibition from Ptc on a downstream membrane protein, Smoothened, which ultimately activates target genes through the Gli family of zinc-finger transcription factors. Vertebrate Gli1 is mainly a transcriptional activator, whereas Gli2 and Gli3 can act both as transcriptional activators and repressors, depending on their posttranslational modification (Jiang and Hui, 2008; Koebernick and Pieler, 2002; Ruiz i Altaba et al., 2007). A central theme of the Wnt pathway is to stabilize the transcription co-activator β-catenin. Stabilized β-catenin then accumulates in the nucleus and interacts with the T cell factor (TCF)/lymphoid enhancer factor (LEF) family of DNA binding transcription factors to promote expression of target genes (Angers and Moon, 2009; MacDonald et al., 2009).

In vertebrates, the developing neural tube and telencephalon are patterned along the dorsoventral axis by opposing actions of two signaling centers with Sonic hedgehog through activation of Gli transcription factors inducing ventral cell fates and Wnt signals *via* the transcriptional co-activator β-catenin inducing dorsal identities (Danesin et al., 2009; Lee et al., 1997; Saint-Jeannet et al., 1997). Studies in *Xenopus* embryos first showed that the anteroposterior polarity of the neural tube is determined by a gradient of Wnt/β-catenin signaling (Kiecker and Niehrs, 2001). A key role for posterior Wnt signals and anterior Wnt inhibition has now been validated in most animals (Niehrs, 2010; Petersen and Reddien, 2009). Overexpression of Hh ligands can stimulate anterior neural induction in *Xenopus* embryos (Franco et al., 1999; Lai et al., 1995), but the signaling mechanism and whether Hh signals are required in this process are not known. The precise role of Wnt signals in neural induction remains a matter of debate. While earlier studies suggested that maternal Wnt/β-catenin signals induce neural fate through inhibiting *BMP4* transcription (Baker et al., 1999) and promoting the expression of secreted BMP antagonists (Wessely et al., 2001), a more recent report challenged the view of Wnts as pro-neural inducers and suggested instead that neural induction requires inhibition of Wnt/β-catenin signaling (Heeg-Truesdell and LaBonne, 2006). A possible mechanism for the anti-neural activity of Wnt signals was proposed, by which Wnts through inhibition of

* Corresponding author at: Lund Stem Cell Center, BMC, B12, Klinikgatan 26, SE-22184 Lund, Sweden. Fax: +46 46 2220855.
E-mail address: edgar.pera@med.lu.se (E.M. Pera).

0012-1606/$ – see front matter © 2011 Elsevier Inc. All rights reserved.
doi:10.1016/j.ydbio.2011.07.035

Please cite this article as: Min, T.H., et al., The dual regulator Sufu integrates Hedgehog and Wnt signals in the early *Xenopus* embryo, Dev. Biol. (2011), doi:10.1016/j.ydbio.2011.07.035

Glycogen synthase kinase 3 (GSK3) prevent phosphorylation and proteosome-mediated degradation of the BMP transducer Smad1 (Fuentealba et al., 2007). An interesting and yet unresolved question is whether Hh and Wnt signaling interconnect and whether a common regulatory mechanism may exist that integrates the two pathways in neural induction and patterning.

Suppressor-of-fused (Sufu) is an intracellular inhibitor of Hh signaling whose impact varies from being only marginally important in *Drosophila*, where it was first described (Préat, 1992), to being an absolutely necessary regulator of this pathway in mammals (Cheng and Yue, 2008). Elimination of Sufu in the mouse leads to ligand-independent activation of the Hh pathway, and *Sufu*-homozygous mutant embryos die at mid-gestation with a ventralized spinal cord (Cooper et al., 2005; Svärd et al., 2006; Varjosalo et al., 2006). Mutations of *Sufu* are linked to medulloblastoma in human (Taylor et al., 2002; 2004) and an elevated risk for the same type of brain cancer in mice (Lee et al., 2007), suggesting that Sufu is a tumor suppressor gene. Sufu directly binds to the Gli proteins and is thought to antagonize their activity through distinct mechanisms: sequestering Gli proteins in the cytoplasm or inhibiting Gli transcriptional activity in the nucleus (Barnfield et al., 2005; Cheng and Bishop, 2002; Ding et al., 1999; Kogerman et al., 1999; Merchant et al., 2004; Murone et al., 2000; Paces-Fessy et al., 2004; Stone et al., 1999). In the resting state of Hh signaling, primary cilia are not required for Sufu to inhibit Gli proteins (Chen et al., 2009; Jia et al., 2009; Zeng et al., 2010). Activation of the pathway leads to the recruitment of Sufu-Gli complexes to cilia and triggers their rapid dissociation to allow Gli activation (Humke et al., 2010; Tukachinsky et al., 2010). On the other hand, an *in vitro* study showed that overexpressed murine Sufu can bind to β-catenin, export it from the nucleus and thereby negatively regulate β-catenin-dependent transcription (Meng et al., 2001; Taylor et al., 2004). A repressor form of Gli3 (Gli3R), which is generated in the absence of Hh signaling, can physically interact with and inhibit β-catenin, suggesting that a complex between β-catenin, Gli3R and Sufu may inhibit canonical Wnt signaling (Ulloa et al., 2007). Node defects in Sufu-depleted mouse embryos have been interpreted due to possible upregulation of β-catenin signaling (Cooper et al., 2005), but increased Wnt pathway activity has not been detected upon RNAi-induced loss of *Sufu* expression or in *Sufu* mutants (Svärd et al., 2006; Varjosalo et al., 2006). Thus loss-of-function data so far support a role of Sufu only as a Hh/Gli inhibitor, and a function of Sufu as an *in vivo* regulator of Wnt/β-catenin signaling remains to be established.

In this study, we compare Hh and Wnt signals during neural induction, anteroposterior patterning and specification of the eye field. We analyze the function of Sufu in the early *Xenopus* embryo and study its interaction with Hh/Gli and Wnt/β-catenin signaling. We further investigate the crosstalk between Gli1 and β-catenin signals and the role that Sufu plays therein. The experimental approach is based on the analysis of overexpressed proteins and depletion of Sufu in *Xenopus* embryos and cultured cells. Our results suggest that Sufu acts as a common inhibitor of Hh/Gli1 and Wnt/β-catenin signals and is required for the integration of the two pathways.

Results

Hh and Wnt signals regulate neural induction, anteroposterior patterning and eye development

We set out to compare Hh and Wnt signaling in the early *Xenopus* embryo, focusing on the formation of the neural plate, anteroposterior patterning and specification of the eye field (Fig. 1). Hh signals can promote the induction of neural markers (Franco et al., 1999; Lai et al., 1995), but whether they are essential for neural induction has not been addressed yet. Previous work on the contribution of Wnt signals to neural induction has been conflicting with some reports supporting pro-neural activity (Baker et al., 1999; Sokol et al., 1995; Wessely et al., 2001) and other studies suggesting that the Wnt pathway may counteract neural induction (Glinka et al., 1998; Heeg-Truesdell and LaBonne, 2006; Itoh et al., 1995). We found that injection of *XGli1* or *XBhh* mRNA into the animal pole of one blastomere at the 4-cell stage caused an expansion of the neural plate marker *Sox2* and a concomitant retraction of the epidermal marker *Cytokeratin* (Fig. 1B,B′; see Fig. S1A,A′ in the Supplementary material). In contrast, inhibition of Hh signaling by mRNA encoding a carboxyterminally truncated Gli3 protein (*Gli3C′ΔClaI*; Ruiz i Altaba, 1999) or a dominant-negative form of the Hh receptor Patched1 (*XPtc1ΔLoop2*; Koebernick et al., 2003) promoted epidermal development at the expense of neural tissue (Fig. 1C,C′; see Fig. S1B,B′ in the Supplementary material), suggesting an important function of Hh signals in the induction of neural tissue. Microinjection of a CMV promoter plasmid containing *XWnt3a* DNA that is expressed at the onset of zygotic transcription at mid-blastula stage depleted the neural plate and expanded the epidermis primarily in anterior territories of the embryo (Fig. 1D,D′). Injection of mRNA encoding a hormone-inducible Tcf (*THVGR*; Wu et al., 2005) followed by addition of Dexamethasone at stage 10 caused downregulation of *Sox2* expression (see Fig. S2A′ in the Supplementary material) suggesting that neural plate formation can be abrogated by Wnt signaling at the onset of gastrulation. On the contrary, inhibition of Wnt signaling by *dnXWnt8* mRNA (Hoppler et al., 1996) had the opposite effect and supported neural at the expense of epidermal fate (Fig. 1E,E′). Together, these data suggest that Hh signals through activation of the transcription factor Gli1 have a positive role in the induction of neural tissue, whereas zygotic Wnt/β-catenin signals exert a negative function in neural plate formation (Fig. 1F).

Overexpression of Hh ligands can induce anterior markers in neuralized explants (Lai et al., 1995) and affect anteroposterior hindbrain patterning *in vivo* (Franco et al., 1999). Wnt signals repress anterior cell fates and induce posterior neural development (Christian and Moon, 1993; Glinka et al., 1998; Kiecker and Niehrs, 2001; McGrew et al., 1995), but temporal aspects of Wnt signaling in neural patterning have not been thoroughly addressed yet. We observed that *XGli1* or *XBhh* mRNA induced posteriorward displacement of the brain markers *Otx2* (forebrain and anterior midbrain), *En2* (posterior midbrain), and *Krox20* (hindbrain rhombomeres 3 and 5) in injected embryos (Fig. 1H–H″; see Fig. S1C–C″ in the Supplementary material). On the other hand, *Gli3C′ΔClaI* or *XPtc1ΔLoop2* mRNA caused a very subtle anteriorward shift of these markers (Fig. I–I″; see Fig. S1D–D″ in the Supplementary material), suggesting that Hh/Gli signals although potent may only be of minor importance for anterior neural development. *XWnt3a* DNA led to an anteriorward shift of *Otx2* and an anterior expansion of *En2* expression, but consistent with a previous study (Saint-Jeannet et al., 1997) had no effect on *Krox20* expression within the hindbrain (Fig. 1J–J″). THVGR induced an anteriorward shift of *Krox20* when stimulated with Dexamethasone at stage 10 but had only a moderate effect upon activation at stage 14 (see Fig. S2B′,C′ in the Supplementary material), suggesting that activated Tcf can affect the position of this hindbrain marker rather at the onset than at the end of gastrulation. In contrast, *dnXWnt8* mRNA resulted in a robust posteriorward expansion of *Otx2* and a posterior shift of *En2* and *Krox20* expression (Fig. 1K–K″), confirming a role of Wnt signals in posterior neural development. In most of the experiments, the anterior borders of the telencephalon marker *FoxG1* and the spinal cord marker *HoxC6* were not affected (Fig. 1H′–K′,H″–K″; see Fig. S1C,C',D,D' in the Supplementary material), suggesting that the effects of altering Hh and Wnt signaling were confined to the forebrain, midbrain and hindbrain territories of the neural plate. To investigate whether the effects of Hh and Wnt signals on neural plate patterning correlate with changes in the mesoderm, we performed double-*in situ* hybridization with *Otx2* and the paraxial mesoderm marker *MyoD*. We found that animal injection of *XGli1* mRNA, *Gli3C′ΔClaI* mRNA, *XWnt3a* DNA, and *dnXWnt8* mRNA affected the anteroposterior extension of the paraxial mesoderm to an extent that was less pronounced than for the neural markers (see Fig. S3 in

Please cite this article as: Min, T.H., et al., The dual regulator Sufu integrates Hedgehog and Wnt signals in the early *Xenopus* embryo, Dev. Biol. (2011), doi:10.1016/j.ydbio.2011.07.035

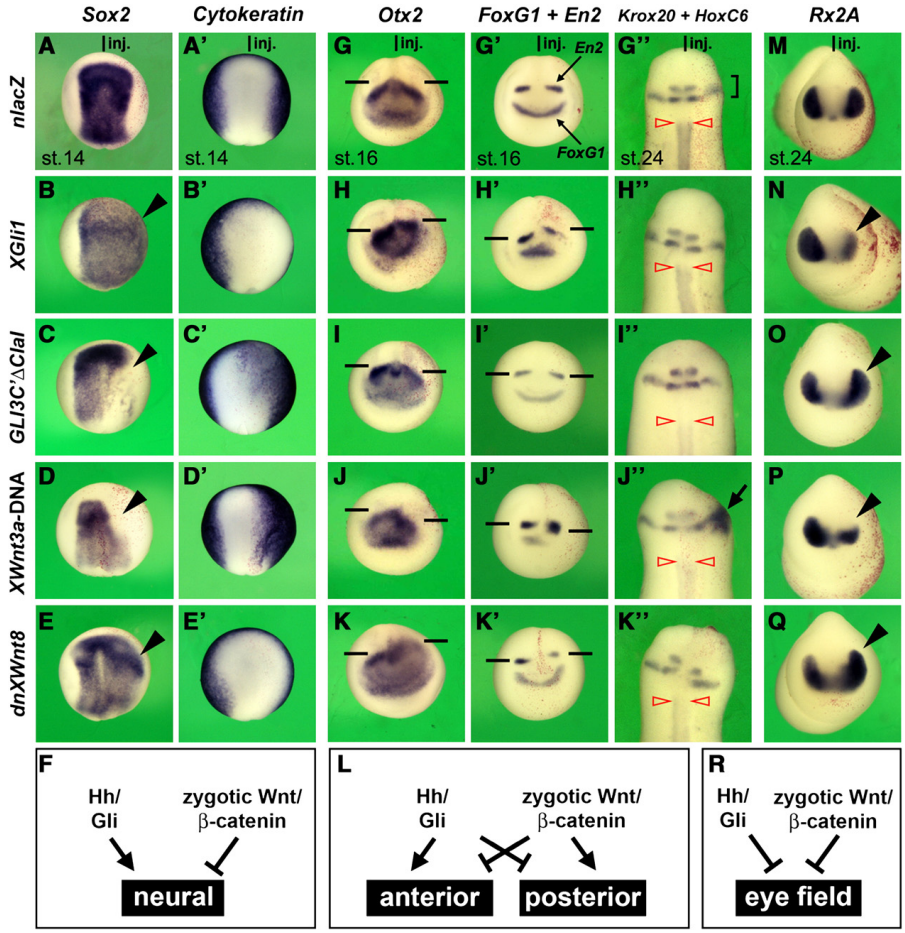

Fig. 1. Function of Hh and Wnt signals during neural induction, anteroposterior patterning and eye field development. *Xenopus* embryos were injected into the animal pole of a single blastomere at the 4-cell stage with the indicated constructs and *nlacZ* mRNA as a lineage tracer (red nuclei on injected right side). (A,A′) Control late gastrula in dorsal view depicting the neural plate marker *Sox2* and the epidermal marker *Cytokeratin*. (B,B′,C,C′) *XGli1* mRNA expands neural at the expense of epidermal tissue, while *Gli3C′ΔClaI* mRNA causes the opposite effect. (D,D′,E,E′) *XWnt3a* DNA promotes epidermal and *dnXWnt8* mRNA neural development. (G–G″) Control embryos at neurula stage in anterior view (G,G′) and at tail bud stage in dorsal view (G″). *Otx2* demarcates the developing cement gland, forebrain and midbrain (horizontal line), *FoxG1* the telencephalon, *En2* the posterior midbrain, and *Krox20* the hindbrain rhombomeres 3 and 5 (bracket). Open arrowhead points to the anterior border of *HoxC6* expression in the spinal cord. (H–H″,I–I″) *XGli1* mRNA anteriorizes the brain, whereas *Gli3C′ΔClaI* causes very subtle posteriorization. (J–J″) *XWnt3a* DNA has posteriorizing activity. The arrow points to an expansion of *Krox20* expression in neural crest cells. (K–K″) *dnXWnt8* mRNA leads to anteriorization. (M) Control tail bud embryo in anterior view, showing *Rx2A* expression in the bilateral eyes. (N–O) *XGli1* mRNAs diminish, whereas *Gli3C′ΔClaI* mRNAs expand the eye anlage. (P,Q) *XWnt3a* DNA leads to a smaller and *dnXWnt8* mRNA to a larger eye anlage. (F,L,R) Summary of effects of Hh and zygotic Wnt signals on neural induction (F), anteroposterior patterning (L), and specification of the eye field (R). The indicated gene expression patterns were obtained in: B, 43/46; B′, 24/26; C, 48/49; C′, 41/52; D, 36/40; D′, 17/19; E, 57/57; E′, 64/68, H, 9/10; H′, 12/12 (*FoxG1*), 8/12 (*En2*); H″, 7/7 (*Krox20*), 11/11 (*HoxC6*); I, 11/13; I′, 18/20 (*FoxG1*), 15/20 (*En2*); I″, 17/26 (*Krox20*), 45/49 (*HoxC6*); J, 44/44; J′, 34/34 (*FoxG1*), 29/34 (*En2*); J″, 43/50 (*Krox20*), 12/17 (*HoxC6*); K, 42/45; K′, 37/37 (*FoxG1*), 29/37 (*En2*); K″, 15/15 (*Krox20*), 13/13 (*HoxC6*); N, 8/10; O, 17/20; P, 8/9; Q, 11/11 (*Rx2A*).

the Supplementary material), suggesting that cell fate changes rather than morphogenetic defects account for the observed effects on neural plate patterning. Hence Hh/Gli are potent anteriorizing signals, whereas Wnt/β-catenin signals exert important roles in suppressing anterior and stimulating posterior neural development (Fig. 1L).

The bilateral eyes are ectodermally-derived organs that originate from the anterior neural plate. Overexpression of a constitutively activated Gli protein or Sonic Hedgehog can impair with early eye development (Cornesse et al., 2005; Marine et al., 1997), but it is not well understood whether Hh/Gli signals have a function in the specification of the eye field. In addition, little is known about temporal aspects of canonical Wnt signals in eye field specification. We found that *XGli1* or *XBhh* mRNAs decreased the eye size on the injected side, while *Gli3C′ΔClaI* and *XPtc1ΔLoop2* mRNAs enlarged the *Rx2A*-positive eye anlagen (Fig. 1N,O; see Fig. S1E,F in the Supplementary material). *XWnt3a* DNA reduced *Rx2A* expression particularly in the posterior

Please cite this article as: Min, T.H., et al., The dual regulator Sufu integrates Hedgehog and Wnt signals in the early *Xenopus* embryo, Dev. Biol. (2011), doi:10.1016/j.ydbio.2011.07.035

domain (Fig. 1P). THVGR also downregulated this marker when activated at stage 10 or at stage 14 (see Fig. S2D′,E′ in the Supplementary material), suggesting that Wnt/Tcf signals can suppress the formation of the eye field in gastrula and early neurula embryos. It is noteworthy that the activation of Wnt signaling at stage 14 caused a robust anteriorward shift of *Rx2A* expression, while the posteriorizing effects on the hindbrain marker *Krox20* had only been moderate (Fig. S2C′,E′ in the Supplementary material), supporting the idea that the eye and hindbrain fields may be independently regulated. In contrast, *dnXWnt8* mRNA caused an expansion of *Rx2A* expression (Fig. 1Q). These observations allow the conclusion that both Hh/Gli and Wnt/β-catenin signals negatively regulate the eye field (Fig. 1R).

Cloning and expression of Xenopus Sufu

Because of the well-established role of Suppressor-of-fused (Sufu) in the regulation of Hh/Gli signaling in the mouse (Cooper et al., 2005; Svärd et al., 2006; Varjosalo et al., 2006) and a previous *in vitro* report that links Sufu to Wnt/β-catenin signaling (Meng et al., 2001), we cloned the homolog of Sufu in *Xenopus laevis* (*XSufu*; see Fig. S4 in the Supplementary material and Supplemental experimental procedures). RT-PCR revealed abundant *XSufu* transcripts from the 4-cell to tadpole stage, indicating maternal and zygotic expression (Fig. 2A). Equal *XSufu* mRNA levels were seen in animal and vegetal portions of blastula embryos (Fig. 2B), and comparable amounts were detected in dorsal and ventral marginal zone explants of early gastrula embryos (Fig. 2C). *In situ* hybridization showed robust *XSufu* expression in advanced gastrula embryos in a crescent-shaped anterior ectoderm domain comprising the panplacodal primordium (Fig. 2D,E). Moderate expression levels were also found in the neural plate with exclusion of the midline. During neurulation, distinct *XSufu* signals were observed in the anterior neural plate, neural crest, and in a bilateral row of cells adjacent to the neural groove (Fig. 2F–I). After closure of the neural tube, *XSufu* is expressed in the anterior brain, eye field, and migrating neural crest cells (Fig. 2J). In tailbud embryos, transcripts were localized in the forebrain, midbrain–hindbrain boundary, eye and ear vesicles, branchial arches, and tailbud (Fig. 2K–M). Together, these data show that *XSufu* is ubiquitously expressed in embryos up to the early gastrula stage and later restricted to distinct ectodermal derivatives.

Overexpression of XSufu suppresses neural fate, affects anteroposterior patterning, and promotes eye specification

To investigate the activity of XSufu during *Xenopus* development, we microinjected *XSufu* mRNA into the animal pole of a single dorsal blastomere at the 4-cell stage (Fig. 3). In early neurula embryos, *XSufu* mRNA led to a significant reduction of *Sox2* expression in the neural plate concomitant with an expansion of the epidermis marker *Cytokeratin* (Fig. 3A′,B′). *XSufu* mRNA caused a posteriorward displacement of *Otx2* (forebrain and midbrain anlage), *FoxG1* (telencephalon), *En2* (posterior midbrain), and *Krox20* expression (hindbrain) (Fig. 3C′–E′). A clear dose-dependent effect could be observed, with 100 pg *XSufu* mRNA causing only a little posteriorward shift, and 1600 pg *XSufu* mRNA resulting in shifts of up to two rhombomeric units (see Fig. S5 in the Supplementary material). Co-injection of *XSufu* mRNA and *XWnt3a* DNA restored normal expression of *Otx2*, *FoxG1*, *En2*, and *Krox20* (Fig. 3C″,D″,E″), suggesting that the anteriorization observed upon XSufu overexpression may be mediated through inhibition of Wnt signaling. Animal injection of *XSufu* mRNA did not alter mesodermal *MyoD* expression (Fig. 3F′), suggesting that overexpression of XSufu may directly affect ectodermal patterning. In tailbud embryos, *XSufu* mRNA caused an enlargement of the eye-specific *Rx2A* expression domain (Fig. 3G′). We also observed an enlargement of pigmented eye vesicles and thickening of the neural retina at the tadpole stage (Fig. 3H,I,I′,J,J′), supporting a positive effect of XSufu on eye development.

Knockdown experiments support roles of XSufu in regulation of neural fate, anteroposterior patterning and eye development

To study the endogenous function of XSufu, we designed a specific 25-mer morpholino oligonucleotide sequence directed against the translation initiation site of the *XSufu* gene (*XSufu*-MO, Fig. 4A). In an *in vitro* transcription–translation assay, the *XSufu*-MO effectively blocked protein synthesis of XSufu, whereas a non-specific control-MO had no effect (Fig. 4B, lanes 1–3). The specificity of the *XSufu*-MO was corroborated by its inability to suppress translation of a recombinant *XSufu** construct, which lacks the 5′UTR target sequence and therefore is not targeted by the *XSufu*-MO (Fig. 4A,B, lanes 4 and 5). Microinjection of *XSufu*-MO into the animal pole of 2-cell stage embryos led to microcephaly and shortened tail structures

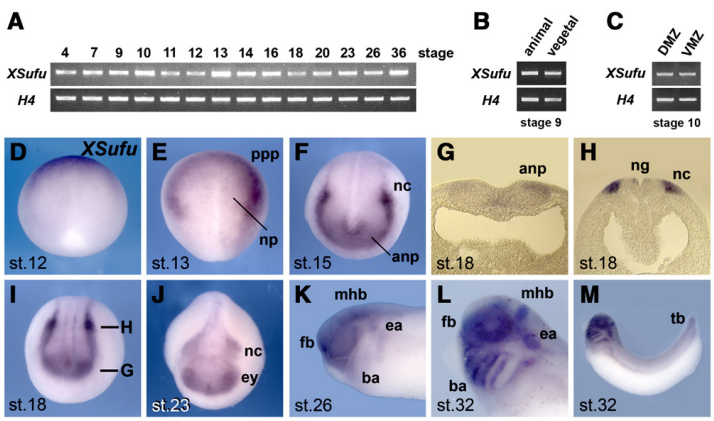

Fig. 2. Gene expression of *XSufu* in *Xenopus* embryos. (A–C) RT-PCR of whole embryos (A) and embryonic explants (B,C). *Histone H4* was used as RNA loading control. DMZ, dorsal marginal zone; VMZ, ventral marginal zone. (D–M) Whole-mount *in situ* hybridization of embryos shown in dorsal (D,E), anterior (F,I,J), and lateral views (K–M). Panels (G) and (H) are transversal sections of embryo in (I). anp, anterior neural plate; ba, branchial arch; ea, ear; ey, eye; fb, forebrain; mhb, mid–hindbrain boundary; nc, neural crest; ng, neural groove; np, neural plate; ppp, panplacodal primordium, tb, tail bud.

Please cite this article as: Min, T.H., et al., The dual regulator Sufu integrates Hedgehog and Wnt signals in the early *Xenopus* embryo, Dev. Biol. (2011), doi:10.1016/j.ydbio.2011.07.035

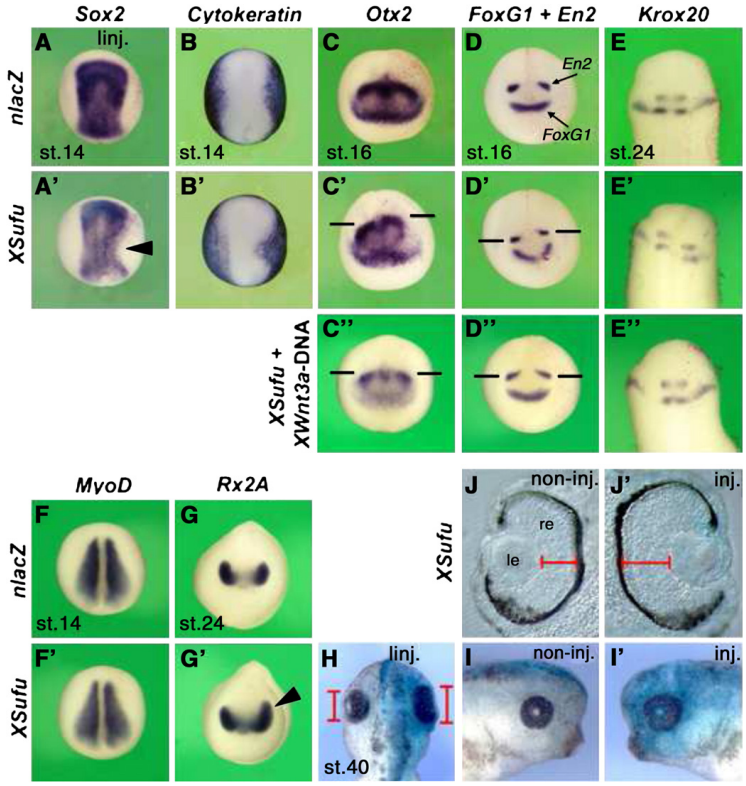

Fig. 3. Microinjection of *XSufu* mRNA suppresses neural plate formation, stimulates anterior neural markers and promotes eye development. Embryos were animally injected at the 4-cell stage with *nlacZ* mRNA as control or *XSufu* mRNA. All specimens were injected into a single blastomere. Embryos are shown in dorsal (A,A′,B,B′,E–E″,F,F′,H), anterior (C–C″,D–D″,G,G′), lateral views (I,I′), or as transversal section (J,J′). (A,B,A′,B′) *XSufu* mRNA causes reduction of *Sox2* and concomitant expansion of *Cytokeratin* expression on the injected right side (arrowhead). (C–E,C′–E′) *XSufu* mRNA causes posteriorward expansion of *Otx2* expression and a posterior shift of *En2* and *Krox20* expression, while *FoxG1* expression remains unaffected. (C″–E″) Co-injection of *XSufu* mRNA and *Wnt3a* DNA restores normal expression of *Otx2*, *En2*, and *Krox20*. (F,F′) *XSufu* mRNA has no effect on *MyoD* expression upon animal injection. (G,G′,H–J,J′,J′) *XSufu* mRNA leads to an enlargement of *Rx2A* expression, enlarged eye structures and expansion of the neural retina. Frequency of embryos with the indicated phenotype was: A′, 44/46; B′, 61/62; C′, 7/10; C″, 12/12; D′, 46/51; D″, 19/21; E′, 116/125; E″, 32/40; F′, 19/21; G′, 95/108; H, 56/115.

(Fig. 4C′). XSufu-morphant tadpoles did not swim and failed to show avoidance reflexes (data not shown). A single injection of *XSufu*-MO caused a significant expansion of *Sox2* at the expense of *Cytokeratin* expression (Fig. 4D′,E′). These effects are opposite to those obtained with *XSufu* mRNA (Fig. 3A′,B′) and suggest an important function of XSufu in restricting neural plate development. Depletion of *XSufu* resulted in an expansion of *Otx2* expression concomitant with a reduction of *En2* and posterior shift of *En2* and *Krox20* expression in the developing brain (Fig. 4F′–H′). These effects are similar to those observed in gain-of-function studies (Fig. 3C′–E′), suggesting that XSufu may regulate anteroposterior patterning of the neural plate in a biphasic manner (see Discussion). Of note, knockdown of *XSufu* led to a reduction and posteriorward retraction of the mesodermal marker *MyoD* (Fig. 4I′), raising the question of whether the change in the position of neural markers may be linked to indirect effects through changes in the mesoderm? We therefore injected *XSufu*-MO into neural-fated A1 blastomeres at the 32-cell stage to avoid an effect on mesoderm. A posteriorward expansion of *Otx2* was observed, while *MyoD* expression remained unaffected (see Fig. S6 in the Supplementary material), suggesting that XSufu may exert its anteriorizing function directly in the neural plate. Furthermore, *XSufu*-MO caused a reduction of the eye-specific *Rx2A* expression domain at the early tailbud stage (Fig. 4J′) and microphthalmy in tadpole embryos (Fig. 4L,L′). These results contrast the enlarged eye structures obtained in overexpression experiments (Fig. 3G′,H,I,I′,J,J′), supporting a positive function of XSufu during eye development. Microinjection of control-MO showed no phenotype (Fig. 4C–K,K′), and co-injection of *XSufu** mRNA with *XSufu*-MO restored normal expression of selected marker genes (*Sox2*, *FoxG1*, *En2*, and *Krox20*) and eye structures (Fig. 4D″,G″,H″,M,M′), verifying the specificity of the loss-of-function experiments.

We next addressed the impact of Hh and Wnt signaling on mediating the effects of XSufu depletion. Inhibition of Hh signals by *GLI3C′ΔClaI* mRNA in *XSufu*-morphant embryos restored normal expression of *Sox2*, *Otx2*, *FoxG1*, *En2*, and *Krox20* (see Fig. S7A–D in the Supplementary material), suggesting a role of XSufu as negative regulator of Hh signaling during neural induction and anteroposterior patterning. On the other hand, co-injection of *XSufu*-MO with either

Please cite this article as: Min, T.H., et al., The dual regulator Sufu integrates Hedgehog and Wnt signals in the early *Xenopus* embryo, Dev. Biol. (2011), doi:10.1016/j.ydbio.2011.07.035

GLI3C′ΔClaI or *dnXWnt8* mRNA restored normal *Rx2A* expression (see Fig. S7E,F in the Supplementary material), implying that the function of XSufu in the specification of the eye field may be mediated through inhibition of both Hh and Wnt signals. Together, XSufu has critical functions in suppressing neural fate, ensuring proper anteroposterior patterning, and promoting eye specification.

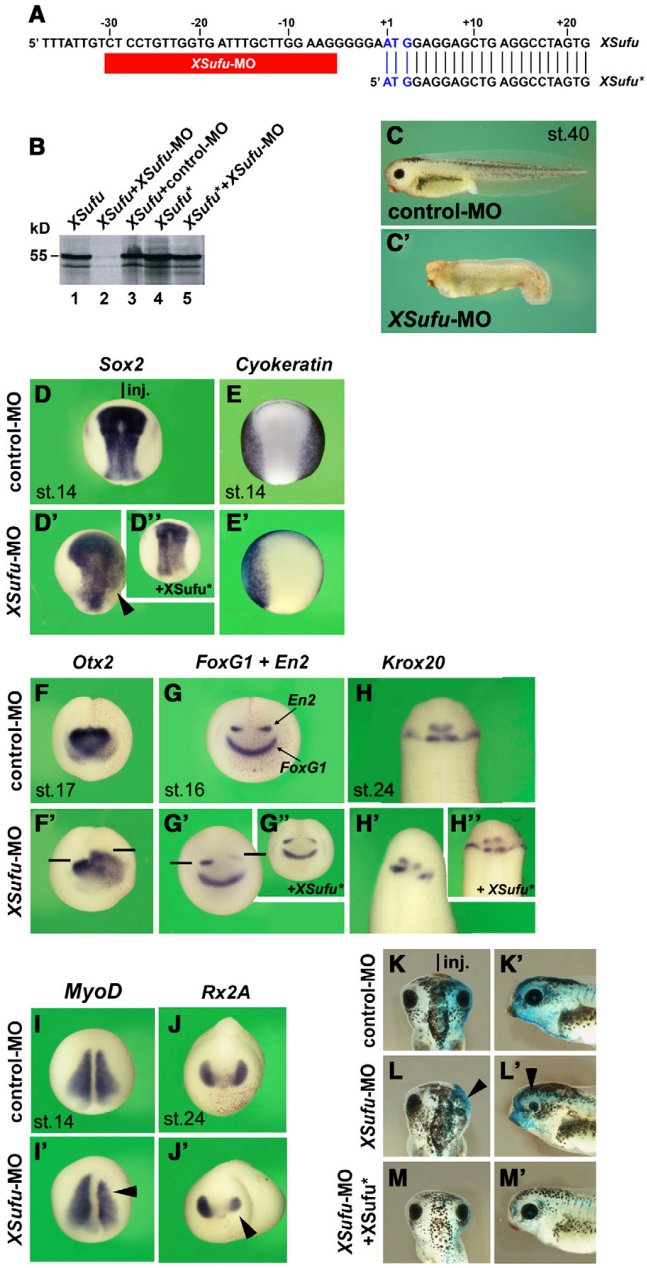

Please cite this article as: Min, T.H., et al., The dual regulator Sufu integrates Hedgehog and Wnt signals in the early *Xenopus* embryo, Dev. Biol. (2011), doi:10.1016/j.ydbio.2011.07.035

XSufu regulates cement gland, neural crest, neuron, and muscle development

Formation of the cement gland is inhibited by Wnt signals (Christian and Moon, 1993), but dependent on Hh signals (Lai et al., 1995). A single animal injection of *XSufu* mRNA resulted in reduction of the cement gland marker *XAG*, an effect that was also obtained upon injection of *XSufu*-MO (Fig. 5A′,B′), suggesting that proper levels of XSufu protein are important for cement gland formation.

Induction of neural crest cells is negatively regulated by Hh/Gli signals (Brewster et al., 1998; Franco et al., 1999; Marine et al., 1997), but dependent on Wnt signals (Deardorff et al., 2001; LaBonne and Bronner-Fraser, 1998; Wu et al., 2005). Both upregulation and downregulation of XSufu caused reduction of the neural crest markers *Slug* and *Snail* (Fig. 5C′,D′,E′,F′). The rescue of *Slug* and *Snail* expression by co-injected *XSufu** mRNA underscored the specificity of the *XSufu*-MO effect (Fig. 5D″,F″). To investigate of whether effects on neural crest markers are a secondary consequence of changes in the mesoderm, we microinjected *XSufu*-MO at the 32-cell stage into animal A2 blastomeres fated to become neural crest cells. We observed reduction of *Slug* and *Snail* expression (see Fig. S6B′,C′ in the Supplementary material) suggesting that XSufu may directly promote neural crest fate. In *XSufu*-morphant embryos, co-injected *GLI3C′ΔClaI* mRNA restored normal *Slug* and *Snail* expression (see Fig. S7G,H in the Supplementary material), suggesting a role of XSufu as inhibitor of Hh signaling during neural crest development.

Activation of Hh/Gli signaling has a negative impact on primary neurogenesis and myogenesis (Franco et al., 1999; Marine et al., 1997). In contrast, Wnt/β-catenin signals are required for sensory neuron (Garcia-Morales et al., 2009; Marcus et al., 1998) and muscle development (Hoppler et al., 1996; Leyns et al., 1997; Salic et al., 1997). Animal injection of *XSufu* mRNA slightly expanded *N-tubulin* expression (Fig. 5G′), while knockdown of *XSufu* led to loss of *N-tubulin*-positive neurons (Fig. 5H′). We also observed reduction of the muscle-specific marker *MyoD* and impaired somite formation at the tailbud stage (Fig. 5I′), indicating that the paralysis observed in *XSufu* morphant larvae (Fig. 4C′) might be caused by a failure of proper innervation and/or muscle formation. The results suggest that XSufu exerts a critical role in promoting primary neuron and muscle development likely through inhibiting Hh/Gli signaling.

We note that *XSufu*-MO and *XSufu* mRNA had no detectable effect on proliferation and apoptosis in neurula and tailbud embryos, as shown by immunohistochemical pH3 staining and the TUNEL assay (see Figs. S8 and S9 in the Supplementary material). In sum, XSufu is essential for the specification of cement gland, neural crest, neuronal and muscle cell fate.

XSufu blocks Hh/Gli and Wnt/β-catenin signaling

We next analyzed the interaction of XSufu with Hh and Wnt signaling (Figs. 6, 7). RT-PCR analysis showed that *XSufu* lowered *XBhh*-induced expression of *Xenopus Patched 1* (*XPtc1*), *XPtc2*, and *XGli1* in mRNA-injected animal caps (Fig. 6A, compare lanes 3 and 4). As the *XSufu* gene is expressed in the animal hemisphere at blastula stage (Fig. 2B), we investigated of whether endogenous XSufu is needed to suppress Hh/Gli signaling. *XSufu*-MO, but not the unspecific control-MO, elevated transcript levels of the Hh target genes in animal cap explants (Fig. 6A, compare lanes 5 and 6). Whole-mount *in situ* hybridization of neurula stage embryos further revealed that animally injected *XSufu* mRNA reduced and *XSufu*-MO expanded *XPtc1* expression in anterior and paraxial domains of the neural plate (Fig. 6B,B′,C,C′), suggesting that XSufu is not only a potent, but necessary inhibitor of Hh signaling.

RT-PCR analysis of animal cap explants at the gastrula stage revealed that *XSufu* mRNA inhibited *XWnt8*-induced expression of *Siamois* and *Xenopus nodal-related 3* (*Xnr3*) in a dose-dependent manner (Fig. 7A, compare lanes 3–5). In contrast, *XSufu*-MO, but not control-MO, caused robust induction of *Siamois, Xnr3* and *Chordin* expression (Fig. 7B, compare lanes 3 and 4). In whole-mount embryos, marginal injection of *XSufu* mRNA reduced *Xnr3* and *Chordin* transcripts in the dorsal blastopore lip, whereas animally injected *XSufu*-MO led to an expansion of these organizer markers (Fig. 7C–F,C′–F′). *XSufu* mRNA also reduced ectopic expression of *Xnr3* and counteracted dorso-anteriorizing development induced by animal injection of *XWnt8* mRNA (Fig. 7G–G″; see Fig. S10 in the Supplementary material).

A recent study proposed that Gli proteins may promote Wnt signaling in *Xenopus* embryos through a mechanism in which XGli2 and XGli3 induce transcription of *XWnt8* and other Wnt genes (Mullor et al., 2001). To investigate whether the inhibitory effect of XSufu on Wnt signaling is direct or mediated through modulation of Gli proteins, we studied the interaction of XWnt8, XSufu and XGli in *Xenopus* embryos (Fig. 7H–M). Co-injection of *XWnt8* and *XSufu* mRNAs into a single ventral blastomere at the 4-cell stage reverted the formation of a secondary body axis that is induced by *XWnt8* mRNA injection alone (Fig. 7H–J,N, lanes 1–3). A triple injection of *XWnt8*, *XSufu* and *XGli1* mRNAs did not restore but further suppressed second axis induction (Fig. 7K,N, lanes 4,5), suggesting that XSufu may not antagonize Wnt signaling through inhibition of XGli1. Interestingly, *XGli1* mRNA alone also impaired *XWnt8*-induced axis duplication, as indicated by the shortening or absence of second axes upon co-injection of *XWnt8* with increasing amounts of *XGli1* mRNA (Fig. 7L,M, N, lanes 6,7). We had previously shown that *XSufu* mRNA caused a posteriorward shift of the brain markers *Otx2*, *En2*, and *Krox20* in neurula and tailbud embryos (Fig. 3C′–E′), and that co-injection of *XSufu* mRNA and *XWnt3a* DNA reverted the anterior shift of these marker genes (Fig. 3C″–E″) that was induced by *XWnt3a* DNA alone (Fig. 1J–J″). We now found that overexpression of *XGli1* mRNA did not rescue the inhibition of *XSufu* mRNA on *XWnt3a* DNA-induced posteriorization of the neural plate (see also Fig. S11A–C in the Supplementary material). Moreover, *XGli1* mRNA caused a posterior shift of *Otx2*, *En2*, and *Krox20* expression not only when injected alone (Fig. 1H–H″) but also when *XGli1* mRNA was co-injected with *XWnt3a* DNA (see also Fig. S11A′–C′ in the Supplementary material). We conclude that XSufu may directly regulate Wnt signaling and that XGli1 can inhibit Wnt responses during secondary axis induction and neural patterning. Together, our data suggest that XSufu is a dual regulator of Hh/Gli1 and Wnt/β-catenin signaling in the *Xenopus* embryo.

Fig. 4. Depletion of XSufu induces expansion of the neural plate, stimulates anterior neural markers and suppresses eye development. (A) Targeting sequence of the *XSufu* morpholino oligonucleotide (*XSufu*-MO). The non-targeted *XSufu** mRNA construct lacks the 5′ untranslated region. Blue letters indicate start codon. (B) *In vitro* transcription–translation assay. The *XSufu*-MO, but not an unspecific control-MO, inhibits XSufu protein synthesis. *XSufu*-MO does not reduce translation of *XSufu** mRNA. (C,C′) At the tadpole stage, *XSufu*-MO-injected embryos have reduced head and tail structures. (D–D″) Dorsal view of early neurula embryos. Injection was performed animally into one blastomere at the 2-cell stage together with *nlacZ* mRNA as tracer. *XSufu*-MO, but not control-MO, causes expansion of *Sox2* expression on the injected side (arrowhead); this effect is reverted by co-injection with *XSufu** mRNA. (E,E′) *XSufu*-MO leads to a reduction of *Cytokeratin* expression. (F–H,F′–H′,G″,H″) Anterior view of neurula (F,F′,G–G″) and dorsal view of tailbud embryo (H–H″). *XSufu*-MO causes expansion of *Otx2*, reduced intensity of *En2*, and a posterior shift of *En2* and *Krox20* expression, while *FoxG1* expression remains unaffected. Co-injection of *XSufu*-MO and *XSufu** mRNA rescues normal *En2* and *Krox20* expression. (I,I′) Dorsal view of early neurula. *XSufu*-MO induces reduction of *MyoD* expression (arrowhead). (J,J′) Anterior view of tail bud embryo. *XSufu*-MO leads to a reduction of *Rx2A* expression. (K–M,K′–M′) A single injection of *XSufu*-MO causes reduction of eye structures (arrowheads), which is reverted by co-injection of *XSufu** mRNA. The indicated phenotypes were observed in: C, 70/83; C′, 21/43; J, 22/24; D, 50/50; D′, 71/77; D″, 82/87; E, 24/27; E′, 39/40; F, 23/24; F′, 20/20; G, 39/39 (*FoxG1*), 55/55 (*En2*); G′, 42/42 (*FoxG1*), 54/54 (*En2*); G″, 31/31; H, 65/67; H′, 79/79; H″, 34/40; I, 24/26; I′, 27/28; J, 40/42; J′, 67/73; L,L′, 25/25; M,M′, 21/43.

Please cite this article as: Min, T.H., et al., The dual regulator Sufu integrates Hedgehog and Wnt signals in the early *Xenopus* embryo, Dev. Biol. (2011), doi:10.1016/j.ydbio.2011.07.035

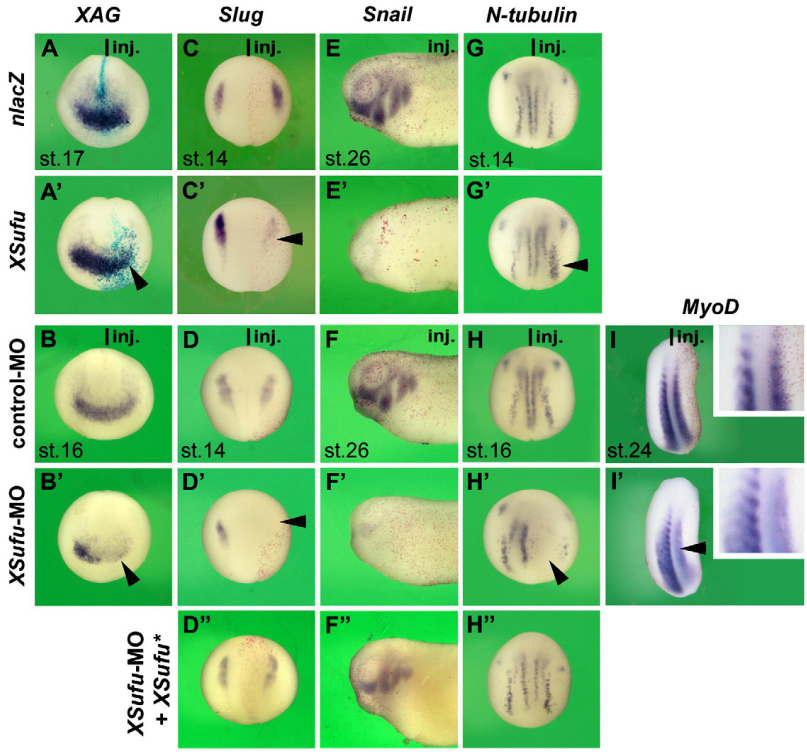

Fig. 5. *XSufu* is important for cement gland, neural crest, neuronal and paraxial mesoderm development. Embryos were injected together with *nlacZ* mRNA as tracer animally into one blastomere at the 2- or 4-cell stage. (A,A′,B,B′) Whole-mount *in situ* hybridization of early neurula embryos in anterior view. *XSufu* mRNA and *XSufu*-MO lead to a reduction of the cement gland marker *XAG* while a non-specific control-MO has no effect. (C–F,C′–F′,D″,F″) Late gastrulae in dorsal and tail bud embryo in lateral view. *XSufu* mRNA and *XSufu*-MO cause a reduction of the neural crest markers *Slug* and *Snail*. Co-injection of *XSufu*-MO and *XSufu** mRNA reverts to normal *Slug* and *Snail* expression. (G,G′,H–H″) Early neurulae in dorsal view. *XSufu* mRNA causes slight expansion of the neuronal marker *N-tubulin*. *XSufu*-MO reduces *N-tubulin* expression. Normal *N-tubulin* expression is seen after co-injection of *XSufu*-MO with *XSufu** mRNA. (I–I′) Tail bud embryos in dorsal view. *XSufu*-MO inhibits formation of *MyoD*-positive segmented somites (see also magnification in inset). Indicated effects were observed in: A′, 9/16; B, 40/45; B′, 7/7; C′, 70/70; D, 65/68; D′, 14/15; D″, 62/64; E′, 62/65; F, 13/13; F′, 19/19; F″, 30/33; G′, 66/81; H, 102/105; H′, 78/84; H″, 31/39; I, 15/20; I′, 17/17.

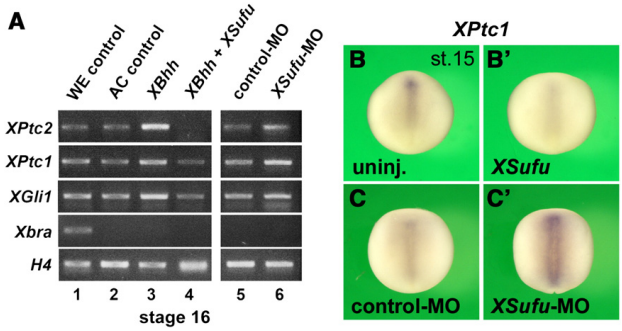

Fig. 6. XSufu inhibits Hh/Gli signaling in the *Xenopus* embryo. (A) Molecular analysis by RT-PCR of animal cap (AC) explants cultured until stage 16. Animal injection of 500 pg *XBhh* mRNA elevates the expression of *XPtc2*, *XPtc1*, and *XGli1*, and this effect is reverted by co-injection of 16 ng *XSufu* mRNA. *XSufu*-MO, but not control-MO, increases the expression of these Hh target genes. *H4* was used for normalization. (B,B′,C,C′) Whole-mount *in situ* hybridization of early neurula embryos in dorsal view. Animal injection of 15 ng *XSufu* mRNA reduces, while *XSufu*-MO, but not control-MO, expands the expression of *XPtc1* expression. Indicated effects were observed in: B, 61/61; B′, 29/38; C, 58/58; C′, 32/37.

Please cite this article as: Min, T.H., et al., The dual regulator Sufu integrates Hedgehog and Wnt signals in the early *Xenopus* embryo, Dev. Biol. (2011), doi:10.1016/j.ydbio.2011.07.035

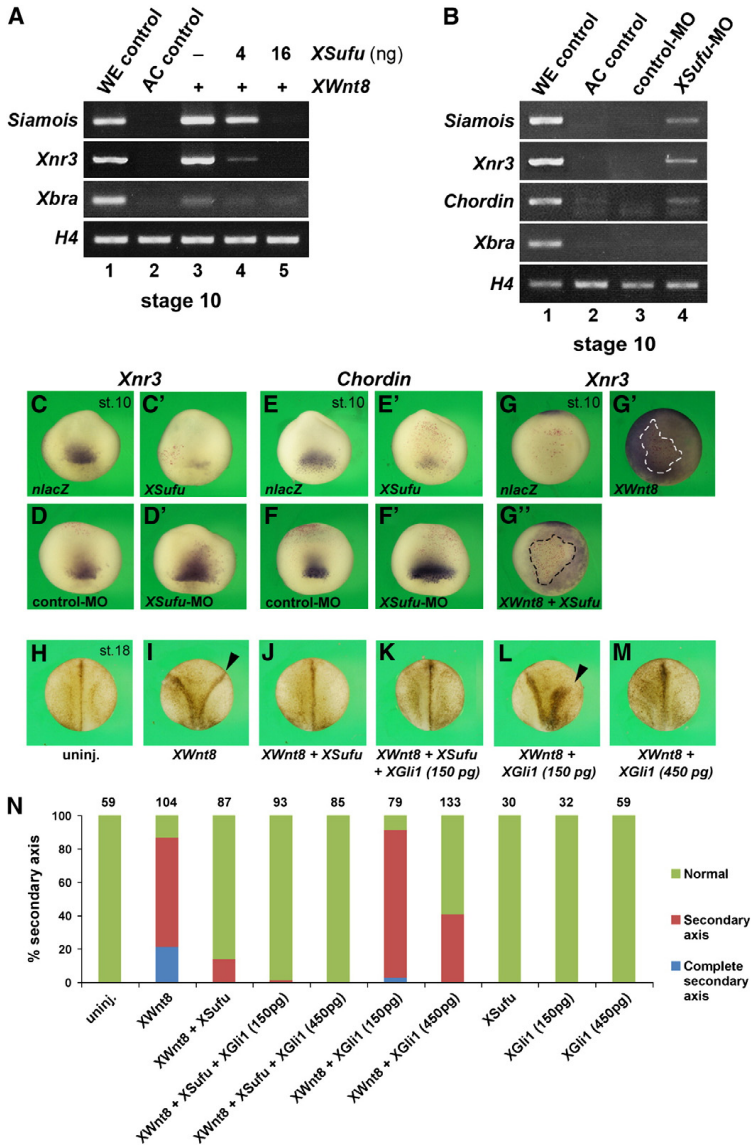

Fig. 7. XSufu inhibits Wnt/β-catenin signaling in the *Xenopus* embryo. (A) Molecular analysis by RT-PCR of animal cap (AC) explants cultured until stage 10. Embryos were animally injected with 25 pg *XWnt8* mRNA either alone or in combination with the indicated amount of *XSufu* mRNA. *H4* was used for normalization. *XSufu* mRNA downregulates *XWnt8*-induced transcription of *Siamois* and *Xnr3* in a dose-dependent manner. (B) *XSufu*-MO, but not control-MO, induced expression of the Wnt target genes *Siamois*, *Xnr3*, and *Chordin* in injected AC explants at stage 10. (C–F,C′–F′) Whole-mount *in situ* hybridization of early gastrula embryos in dorsal view. A single marginal injection of *XSufu* mRNA at the 4-cell stage reduces, while a single animal injection of *XSufu*-MO, but not of control-MO, at the 2-cell stage expands endogenous expression of *Xnr3* and *Chordin*. (G–G″) Animal view of early gastrulae. A single animal injection of 12 pg *XWnt8* mRNA at the 4-cell stage induces ectopic *Xnr3* expression (G′) that is reduced by co-injection of *XWnt8* and *XSufu* mRNA (G″). Injected *nlacZ*-positive cells are highlighted with a strippled line. (H) Dorsal view of uninjected neurula embryo. Condensed natural pigmentation at the site of neural tube closure delineates the main body axis. (I–M) A single ventral injection of 4 pg *XWnt8* mRNA induces a complete secondary body axis (arrowhead in I) that is blocked by co-injection with 4 ng *XSufu* mRNA (J) or by co-injection with a combination of *XSufu* and 150 pg *XGli1* mRNA (K). Note that *XWnt8*-induced secondary axis formation is partly reversed by co-injection of 150 pg *XGli1* mRNA (arrowhead in L) and inhibited by co-injection of 450 pg *XGli1* mRNA (M). (N) Quantification of secondary axis formation. Indicated effects were observed in: C, 14/14; C′, 8/10; D, 15/18; D′, 24/36; E, 13/13; E′, 7/8; F, 24/26; F′, 21/28; G, 47/47; G′, 14/14; G″, 55/55.

Please cite this article as: Min, T.H., et al., The dual regulator Sufu integrates Hedgehog and Wnt signals in the early *Xenopus* embryo, Dev. Biol. (2011), doi:10.1016/j.ydbio.2011.07.035

Physical interaction of XSufu with XGli1 and Xβ-catenin proteins

In view of these lines of embryological evidence linking XSufu to Hh and Wnt signaling, we addressed the biochemical interaction of XSufu with intracellular components of the pathways that transduce the signals to the nucleus. XGli1 is the main transactivator of Hh signaling in *Xenopus* (Lee et al., 1997), and mammalian Sufu has been shown to physically associate with Gli1 (Dunaeva et al., 2003; Kogerman et al., 1999; Merchant et al., 2004). In response to the activation of the Wnt signaling pathway, stabilized β-catenin regulates the transcription of Wnt target genes, and mammalian Sufu inhibits β-catenin activity through complex formation (Meng et al., 2001). In HEK293 cells, we expressed flag-tagged

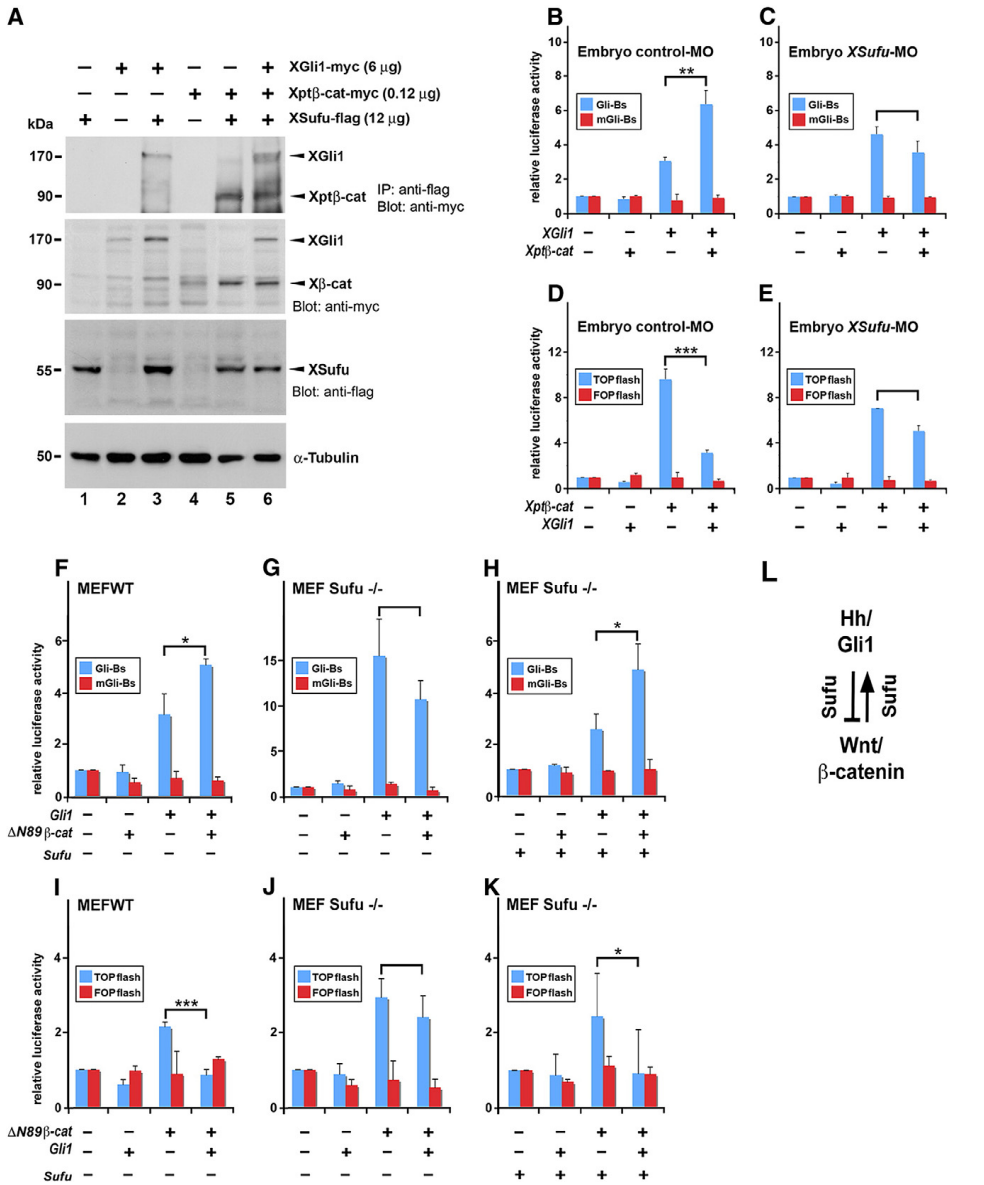

Please cite this article as: Min, T.H., et al., The dual regulator Sufu integrates Hedgehog and Wnt signals in the early *Xenopus* embryo, Dev. Biol. (2011), doi:10.1016/j.ydbio.2011.07.035

XSufu (XSufu-flag), myc-tagged XGli1 (XGli1-myc), and myc-tagged Xβ-catenin that is stabilized by four point mutations in aminoterminal GSK-3 phosphorylation sites (Xptβ-catenin-myc; Yost et al., 1996). Careful titration of plasmid DNA amounts and adjustment of culture conditions allowed us to obtain equivalent protein levels of XGli1-myc and Xptβ-catenin-myc as judged by Western blot analysis with anti-myc antibodies (Fig. 8A, middle panel, compare lanes 3 and 5). Using co-immunoprecipitation, we found that XSufu-flag immunoprecipitated with comparable levels of XGli1-myc and Xptβ-catenin-myc (Fig. 8A, upper panel). Hence XSufu can bind to XGli1 and Xptβ-catenin proteins.

Sufu is essential for the crosstalk between Hh/Gli and Wnt/β-catenin signaling

We investigated the interaction of Hh/Gli and Wnt/β-catenin signaling and asked of whether Sufu plays a role in regulating the crosstalk between the two pathways. To this end we microinjected *XGli1* and Xptβ-*catenin* mRNAs with specific luciferase reporter constructs into the animal pole of *Xenopus* embryos at the 4-cell stage that were independently injected with control-MO or *XSufu*-MO at the 2-cell stage. At the early gastrula stage, *XGli1*-induced activation of the Hh reporter construct *8x3′Gli-BS luc* (Sasaki et al., 1997) was further increased 2-fold by overexpressing *XGli1* with *Xptβ-catenin* in control-MO-injected embryos (Fig. 8B). However, *Xptβ-catenin* failed to increase *XGli1*-induced Hh pathway activation in *XSufu*-morphant embryos (Fig. 8C). On the other hand, *Xptβ-catenin*-induced activation of the Wnt reporter TOP-flash (Upstate Biotechnology) was reduced to one third by overexpressing *XGli1* with *Xptβ-catenin* in control-MO-injected embryos (Fig. 8D). Of note, *XGli1* did not significantly reduce *Xptβ-catenin*-induced Wnt pathway activation in *XSufu*-morphants (Fig. 8E). We did not observe activation of the *8x3′mGli-BS luc* reporter in which the Gli binding sites are mutated (Sasaki et al., 1997) nor activation of *FOP-flash* (Upstate Biotechnology), an altered *TOP-flash* construct in which the Tcf binding sites are inactivated by point mutations (Fig. 8B–E). Next we transfected mouse *Gli1* and stabilized mouse *ΔN89β-catenin* (Meng et al., 2001) with the luciferase reporter constructs into MEF cells that were wild type (MEF WT) or homozygous mutant for the *Sufu* gene (MEF *Sufu*−/−; Svärd et al., 2006). We found that *ΔN89β-catenin* increased *Gli1*-induced *8x3′Gli-BS luc* activity in MEF WT (Fig. 8F), but not in MEF *Sufu*−/− cells (Fig. 8G). Co-transfection of MEF *Sufu*−/− cells with a moderate amount of mouse *Sufu* plasmid restored the stimulating effect of *ΔN89β-catenin* on *Gli1*-induced Hh reporter activity (Fig. 8H). In turn, *Gli1* suppressed *ΔN89β-catenin*-induced *TOP-flash* activity in MEF WT (Fig. 8I), but not significantly in MEF *Sufu*−/− cells (Fig. 8J). Addition of *Sufu* to MEF *Sufu*−/− rescued the inhibitory effect of *Gli1* on *ΔN89β-catenin*-induced Wnt reporter activity (Fig. 8K). Similarly, *Xptβ-catenin* stimulated Hh pathway activation by *XGli1* and, vice versa, *XGli1* inhibited Wnt pathway activation by *Xptβ-catenin* in transfected NIH3T3 cells (Fig. S12A,B in the Supplementary material). Western blot analysis verified the presence of endogenous Sufu protein in NIH3T3 and MEF WT, and confirmed its absence in MEF *Sufu*−/− cells (see Fig. S12C in the Supplementary material). In sum, our data suggest a conserved crosstalk in which exogenous Wnt/β-catenin stimulates Hh/Gli signaling under overexpression of Gli1, and in turn exogenous Hh/Gli inhibits Wnt/β-catenin signaling under overexpression of stabilized β-catenin. In both *Xenopus* embryos and mammalian cells, Sufu is critically involved in the interaction between Hh/Gli and Wnt/β-catenin signaling (Fig. 8L).

Discussion

In this study, we investigated the role of *Xenopus* Sufu (XSufu) in the early embryo. Our gain- and loss-of-function studies revealed essential functions of XSufu in diverse aspects of ectodermal patterning, including the restriction of the neural plate, positioning of brain compartments along the anteroposterior body axis, and stimulation of eye development. Additional functions of XSufu could be described for cement gland, neural crest, neuronal, and muscle development. We provided evidence that XSufu acts as an inhibitor of Hh and Wnt signaling in the *Xenopus* embryo. Our data further show that Gli1 suppresses Wnt signaling under overexpression of β-catenin, and β-catenin in turn stimulates Hh signaling under overexpression of Gli1. Importantly, the presence of endogenous Sufu is vital for the crosstalk between the two signals. Based on these results, we suggest that XSufu exerts its diverse roles as a mediator and dual inhibitor of Hh/Gli and Wnt/β-catenin signaling.

XSufu is a dual regulator of Hh and Wnt signaling

In agreement with previous studies that have characterized Sufu as an essential regulator of mammalian Hh signaling (Cooper et al., 2005; Svärd et al., 2006; Taylor et al., 2002; Varjosalo et al., 2006), we show that XSufu is sufficient and required to reduce Hh target gene expression. A previous report challenged the concept of Sufu as exclusive regulator of Hh signaling and suggested instead that mammalian Sufu may directly inhibit Wnt signaling through a mechanism where Sufu binds to β-catenin and transports it out of the nucleus (Meng et al., 2001). In medulloblastoma patients a germline mutation in the human Sufu gene has been identified that prevents the protein from inhibiting Wnt signaling (Taylor et al., 2004). Yet whether Sufu-mediated suppression of Wnt signaling is relevant for embryonic development has remained elusive. We provide evidence that XSufu is a potent and critical inhibitor of Wnt/β-catenin signaling in *Xenopus*. First, overexpression of *XSufu* mRNA inhibits *in vitro* and *in vivo XWnt8*-induced target gene expression and dorso-anterior development. Then, antisense morpholino oligonucleotide (MO)-mediated knockdown of XSufu induces the direct Wnt targets *Siamois* and *Xnr3* in animal cap explants. Third, XSufu is sufficient and required to restrict endogenous expression of *Xnr3* and the Wnt-responsive *Chordin* gene in the early gastrula embryo. We note that the microcephaly observed in *XSufu*-morphant embryos may result from derepressing late Wnt signals that posteriorize the embryonic axis at more advanced stages of development. The suppression of the Wnt pathway by *XSufu* is not mediated through inhibition of Hh/Gli1 signals, as overexpression of *XGli1* fails to reverse the suppressive effect of *XSufu* on *XWnt8*-induced secondary axis induction and *XWnt3a*-induced posteriorization of the neural plate. Our observation that XSufu can be co-immunoprecipitated with Xβ-

Fig. 8. Biochemical interaction and function of Sufu in the cross-talk of Hh/Gli1 and Wnt/β-catenin signaling. (A) XSufu-flag immunoprecipitates with XGli1-myc and Xptβ-catenin-myc in HEK293 cells 36 h after co-transfection. Proteins in cell lysates were analyzed by Western blot with antibodies against myc (for XGli1 and Xptβ-catenin), flag (for XSufu) and mouse Sufu. α-Tubulin was used as the loading control. (B–K) Luciferase reporter assays in lysates of *Xenopus* embryos at stage 10.5 following injection of morpholino oligonucleotides (MOs) and mRNAs of *Xptβ-catenin* and *XGli1*, using the *8xGli-Bs-luc* reporter to monitor Hh/Gli signaling (with *8x3′mGli-Bs-luc* as negative control) and the *TOP-flash* reporter to monitor Wnt/β-catenin signaling (with *FOP-flash* as negative control). Reporter (firefly) activities were normalized to pRL-TK (*Renilla*) activities to control for transfection/injection efficiencies. Error bars represent standard deviation from three representative experiments. Control embryos are injected with reporter plasmid + pRL-TK. (B,C) *Xptβ-catenin* upregulates the *XGli1*-induced Hh reporter in control-MO-, but not in *XSufu*-MO-injected embryos. (D,E) *XGli1* downregulates the *Xptβ-catenin*-induced Wnt reporter in control-MO-, but has no significant effect in *XSufu*-MO-injected embryos. (F–K) Hh and Wnt reporter assays in lysates of MEF WT, and MEF *Sufu*−/− cells 48 h after transfection with mouse *ΔN89β-catenin*, *Gli1* and *Sufu* cDNA plasmids. Control cells are transfected with empty vector. (F–H) *ΔN89β-catenin* promotes the *Gli1*-activated Hh reporter in MEF WT (F), but not in MEF *Sufu*−/− cells (G). Addition of *Sufu* cDNA restores the stimulating effect of *ΔN89β-catenin* on Gli1-induced Hh reporter activity (H). *Gli1* inhibits the *ΔN89β-catenin*-activated Wnt reporter in MEF WT (I), but has no significant effect in MEF *Sufu*−/− cells (J). Addition of *Sufu* cDNA rescues the inhibitory effect of *Gli1* on *ΔN89β-catenin*-induced Wnt reporter activity (K). Asterisks denote statistical significance: *, $p<0.05$; **, $p<0.01$; ***, $p<0.001$. (L) Summary of protein interactions.

Please cite this article as: Min, T.H., et al., The dual regulator Sufu integrates Hedgehog and Wnt signals in the early *Xenopus* embryo, Dev. Biol. (2011), doi:10.1016/j.ydbio.2011.07.035

catenin suggests regulation through direct interaction instead. Previous studies did not detect a function of Sufu in inhibiting Wnt signaling in the mouse (Svärd et al., 2006; Varjosalo et al., 2006). Other Wnt pathway regulators may compensate for the loss of Sufu in knockout mice. In mouse embryonic fibroblasts, Gli1 or Gli2 proteins suppress Wnt signaling *via* transcriptional activation of the soluble Wnt antagonist sFRP1 (secreted frizzled-related protein-1, Katoh and Katoh, 2006; He et al., 2006), suggesting that increased levels of active Gli proteins in Sufu knockout mice may mask a possible role of Sufu in inhibiting Wnt signaling. It may be worthwhile to monitor Wnt signaling in mice with a compound knockout of Sufu, Gli1, and Gli2. Our study suggests that XSufu is a dual inhibitor of Hh and Wnt signaling in the *Xenopus* embryo, and future studies are needed to carefully investigate a possible function of Sufu as negative regulator of Wnt signaling in mammalian development.

Roles of Hh, Wnt and XSufu in neural induction and eye specification

This study supports previous findings that overexpression of Hh ligands promotes neural fate in *Xenopus* embryos (Franco et al., 1999; Lai et al., 1995). Our observation that *XGli1* phenocopies the effect of *XBhh* mRNA suggests that Hh signals favor neural induction through activation of Gli transcription factors. The demonstration that inhibition of Hh signaling at the receptor (*XPtc1Δloop2*) or transcription factor level (*GLI3′CΔClal*) impair with neural plate development point to a crucial role of the Hh/Gli pathway in this process. How Hh/Gli signals may contribute to neural induction remains an open question, and a possible integration with other neural inducing pathways needs to be further investigated. Our observation that late Wnt/β-catenin signals prevent formation of neural tissue is in agreement with a previous work (Heeg-Truesdell and LaBonne, 2006) and may occur through a mechanism involving sequestration of GSK3 in multivesicular bodies and sustained BMP/Smad1 signaling (Fuentealba et al., 2007; Taelman et al., 2010). In accordance with elevated expression levels of XSufu at the border of the neural plate, our functional experiments showed that XSufu is necessary and sufficient to restrict the neural plate marker *Sox2*. XSufu may exert its anti-neural function through inhibiting Hh/Gli1 signals. Alternatively, XSufu could regulate early pro-neural β-catenin signals. In the *Xenopus* blastula, dorsal β-catenin signals induce neural tissue *via* extinction of *BMP4* transcription (Baker et al., 1999) and the transcriptional activation of secreted BMP antagonists (Wessely et al., 2001). We identified XSufu as negative regulator of the organizer-specific *Chordin* and *Xnr3* genes. Chordin and Xnr3 are secreted BMP antagonists that induce neural differentiation (Hansen et al., 1997; Haramoto et al., 2004; Sasai et al., 1995), and a recent genome-wide screen in *Xenopus* found these genes as most strongly induced by maternal β-catenin signals (Wessely et al., 2004). We suggest that in the blastula embryo, XSufu may restrict Spemann′s organizer formation by reducing dorsal β-catenin signaling. Hence XSufu may impair with neural induction through inhibiting Hh/Gli and early Wnt/β-catenin signals.

In gain- and loss-of-function experiments, we could extend previous findings (Cornesse et al., 2005; Marine et al., 1997) and show that Hh and Wnt signals impair with the development of the eye field. Our temporal analysis revealed that an inducible Tcf construct (*THVGR*) can suppress eye fate when activated at the onset of neurulation. At this stage, XSufu is expressed in the eye field and continues to be abundant in the optic vesicles at later stages of embryogenesis. We show that overexpression of XSufu causes an expansion of the eye-specific marker *Rx2A* and enlargement of eye structures, while downregulation of XSufu has the opposite effect. We did not observe changes in cell proliferation and apoptosis suggesting that XSufu directly affects cell fate. The observation that in *XSufu*-morphant embryos suppression of the Hh or Wnt pathways restores normal *Rx2A* expression suggests that XSufu may represent a mechanism to terminate Hh and Wnt signaling in early eye anlage. A conditional knockout of Sufu in the mouse eye recently introduced a role of Sufu in maintaining multipotency of neural progenitor cells in the retina (Cwinn et al., 2011). Interestingly, Sufu-depleted retinal progenitor cells exhibited sustained expression of *Sox2* and downregulation of *Rax/Rx*, suggesting a conserved function of Sufu in the regulation of these transcription factors in the developing CNS of *Xenopus* and the mouse.

Biphasic model for XSufu in anteroposterior patterning

In loss-of-function experiments, depletion of XSufu by antisense morpholino oligonucleotides caused a posterior shift of the brain-specific markers *Otx2*, *En2* and *Krox20*. Similar results were obtained in gain-of-function experiments, with increasing doses of *XSufu* mRNA causing a proportional increase in the posteriorward shift of hindbrain rhombomeres. How can this apparent paradox be explained that up- and downregulation of one gene elicit the same response? In Fig. 9, we suggest a biphasic model for the role of XSufu in anteroposterior patterning of the developing CNS. The abundant expression of *XSufu* at the anterolateral margin of the neural plate suggests that under normal conditions XSufu interacts rather with anterior XGli proteins (Ekker et al., 1995; Lee et al., 1997; Marine et al., 1997) than with posterior Xβ-catenin (Kiecker and Niehrs, 2001). We propose that knockdown of XSufu may cause anteriorization through releasing active XGli proteins in the anterior neural plate. In contrast, ectopically expressed XSufu may suppress posterior fate by binding to and inhibiting Xβ-catenin in posterior locations of the neural plate. Regulation of the Wnt/β-catenin pathway by XSufu is supported by the rescue of normal anteroposterior pattern of brain markers upon overexpression of XSufu and simultaneous inhibition of Wnt/β-catenin signaling. Hence lowered XSufu concentration appears to stimulate anterior Hh/Gli signaling and high XSufu protein levels to downregulate posterior Wnt/β-catenin signaling, leading in each case to anteriorization of the CNS. Recent studies in mouse embryonic fibroblasts introduced a novel positive role of Sufu in regulating Hh signaling through promoting the stability of Gli2 and Gli3 full-length activators (Chen et al., 2009; Jia et al., 2009; Wang et al., 2010). Future studies will need to address the impact of XSufu on XGli protein stability and its relevance for pattern formation in the *Xenopus* embryo.

XSufu mediates the crosstalk between Hh and Wnt signals

Of particular interest is the interplay of Hh/Gli1 and Wnt/β-catenin signaling as well as the role that Sufu plays herein. We observed that *XGli1* counteracted *XWnt8*-induced secondary axis formation and *XWnt3a*-induced posteriorization of the neural plate. In mRNA-injected *Xenopus* embryos and mouse embryonic fibroblasts (MEFs), exogenous *Gli1* inhibited Wnt reporter activity under overexpression of *β-catenin*. A similar inhibition of Wnt/β-catenin transcriptional activity by Hh/GLI1 overexpression has been reported for human cancer cells (Akiyoshi et al., 2006; Yanai et al., 2008), and Indian Hedgehog has been described as a negative regulator of Wnt signaling in colonic epithelial cell differentiation (van den Brink et al., 2004). SHH-N has been shown to inhibit Wnt signaling through transcriptional activation of *sFRP2* during somite development in the mouse (Lee et al., 2000). We found that the negative regulation of the canonical Wnt pathway by Hh/Gli1 signals depends on the presence of Sufu since in *XSufu*-morphant *Xenopus* embryos and *Sufu* knockout MEF cells, *Gli1* fails to block *β-catenin*-induced Wnt reporter activity, and addition of exogenous *Sufu* to MEF *Sufu*−/− cells could restore the inhibitory effect of *Gli1* on the Wnt/β-catenin response. We also observed that exogenous *β-catenin* stimulated Hh reporter activity under overexpression of *Gli1* in *Xenopus* embryos and MEFs. Similarly, *β-catenin* enhances *Gli1*-transcriptional activity in human cancer cells in a TCF/LEF-independent manner (Maeda et al., 2006). We noted that in *XSufu*-deficient *Xenopus* embryos and *Sufu*-depleted MEF cells, *β-catenin* did

Please cite this article as: Min, T.H., et al., The dual regulator Sufu integrates Hedgehog and Wnt signals in the early *Xenopus* embryo, Dev. Biol. (2011), doi:10.1016/j.ydbio.2011.07.035

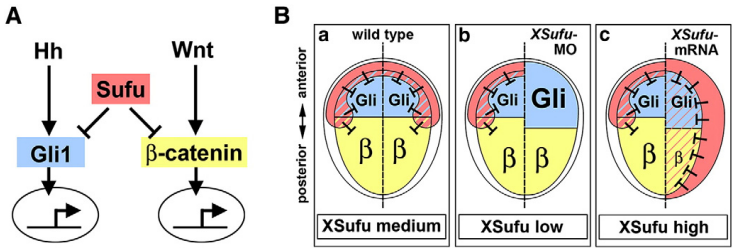

Fig. 9. Sufu as a dual repressor of Hh/Gli and Wnt/β-catenin signaling. (A) Interactions of XSufu with Gli1 and β-catenin. (B) Biphasic model for regulation of anteroposterior patterning by XSufu in late *Xenopus* gastrulae. (a) Under normal conditions, XSufu at the anterolateral margin of the neural plate suppresses anterior Gli and less efficiently posterior β-catenin activity. (b) Depletion of XSufu derepresses anterior Gli activity, which causes excessive anterior neural induction. (c) Ectopic expression of XSufu suppresses posterior β-catenin activity and prevents posteriorization of the neural plate.

not further stimulate *Gli1*-induced Hh reporter activity unless exogenous *Sufu* was added, suggesting that the levels of endogenous Sufu protein may be critical for the positive effects of Wnt/β-catenin signals on the Hh/Gli pathway. The mechanism of how Sufu may facilitate the inhibition of Wnt/β-catenin signaling by Gli1 and the activation of Hh/Gli1 response to β-catenin is not understood and needs to be addressed in future studies. In conclusion, Sufu acts as a dual regulator and may have an integrating role in linking Hh/Gli and Wnt/β-catenin signaling in the *Xenopus* embryo.

Materials and methods

Injections of RNA, DNA, and morpholino oligonucleotides

Sense RNA for microinjection was synthesized using the mMessage Machine kit (Ambion). DNA templates were linearized, transcribed and mRNAs injected per blastomere as follows: pXEX-*nlacZ* (*Xba*I, T7, 100 pg), pT7TS-*XBhh* (*Bam*HI, T7, 500 pg; Ekker et al., 1995), pCS-*XGli1-myc* (*Not*I, Sp6, 150 pg; Lee et al., 1997), pCS-*XPtc1ΔLoop2* (*Not*I, Sp6, 1 ng; Koebernick et al., 2003), pCS-*Gli3C′ΔClaI-myc* (*Not*I, Sp6, 100 pg; Ruiz i Altaba, 1999), pSP64T-*XWnt8-myc* (*Bam*HI, Sp6, 12.5 pg; Christian and Moon, 1993), pCS-*dnXWnt8* (*Asp*718, Sp6, 100 pg; Hoppler et al., 1996), pCS-*XSufu* (*Not*I, Sp6, 750 pg), pCS-*XSufu** (*Not*I, Sp6, 300 pg), pCS-*Xptβ-catenin-HA* (*Not*I, Sp6; Yost et al., 1996), and pCS-*THVGR* (*Not*I, Sp6, 20 pg; Wu et al., 2005). pCS-*XWnt3a* DNA (Saint-Jeannet et al., 1997) was injected at 30 pg per blastomere. The *XSufu*-MO (CTT CCA AGC AAA TCA CCA ACA GGA G) and standard control-MO were obtained from Gene Tools LLC and injected at 25 ng per blastomere.

Embryo manipulations and RT-PCR

X. laevis embryos and explants were obtained, cultured, microinjected and subjected to whole-mount *in situ* hybridization and lineage tracing as described (Hou et al., 2007). Gelatin/albumin sections (40 μm) were done using a Leica VT1200S vibratome. RT-PCR assays were as reported (Hou et al., 2007). For gene-specific primers and PCR conditions, see Supplemental experimental procedures.

Western blot analysis

Western blots were performed with monoclonal antibodies against c-myc (1:2000; Santa Cruz, sc-47694), α-Tubulin (1:1000; Sigma, T9026), anti-flag-HRP conjugate (1:1000; Sigma, A8592), and a polyclonal antibody against mouse Sufu (1:5000; Kise et al., 2009). For immunoprecipitation and additional Western blot methods, see Supplemental experimental procedures.

Reporter luciferase assays

NIH3T3, MEF WT and MEF *Sufu*−/− cells (Svärd et al., 2006) were transfected in 6-well plates with Fugene HD (Roche), 0.8 μg reporter constructs and the following plasmid DNAs: pCS-*XGli1-myc* (0.2 μg; Lee et al., 1997), pCS-*Xptβcatenin-HA* (0.1 μg; Yost et al., 1996), pCS2-*XSufu-Flag* (0.5 μg), pCDNA3-*mGli1-His* (2 μg; Sasaki et al., 1999), pCDNA3-*mΔ89β-catenin* (2 μg; Meng et al., 2001), pCMV5-*mSufu-myc* (0.5 μg; Ding et al., 1999), pRL-TK (2.5 ng, Promega), and empty pCS2+. Embryos were animally injected at the 2-cell stage with 50 ng MOs and at the 4-cell stage with 400 pg *Xptβ-catenin-HA* mRNA, 2 ng *XGli1-myc* mRNA, 100 pg reporter construct, and 10 pg pRL-TK. Luciferase activities were measured using the Dual luciferase reporter assay system (Promega).

Acknowledgments

We are indebted to S. Teglund and R. Toftgård for generous gifts of *Sufu*−/− MEFs and to Dr. Y. Kibe for mouse Sufu antibody. Drs. B. Alman, I. Dawid, R. Harland, C.-C. Hui, P. S. Klein, R. Moon, T. Pieler, P. Polakis, A. Ruiz i Altaba, H. Sasaki, and J. Yang kindly provided plasmids. We thank C. Holmgren for support with the pH3 analysis and Drs. O. Wessely, I. Arregi, U. Haecker, H. Semb, and three anonymous reviewers for valuable comments on the manuscript. E.M.P. was supported by the Swedish Research Council, the Swedish Child Cancer Foundation, and the Novo Nordisk Foundation.

Appendix A. Supplementary data

Supplementary data to this article can be found online at doi:10.1016/j.ydbio.2011.07.035.

References

Akiyoshi, T., Nakamura, M., Koga, K., Nakashima, H., Yao, T., Tsuneyoshi, M., Tanaka, M., Katano, M., 2006. Gli1, downregulated in colorectal cancers, inhibits proliferation of colon cancer cells involving Wnt signalling activation. Gut 55, 991–999.
Angers, S., Moon, R.T., 2009. Proximal events in Wnt signal transduction. Nat. Rev. Mol. Cell Biol. 10, 468–477.
Baker, J.C., Beddington, R.S., Harland, R.M., 1999. Wnt signaling in *Xenopus* embryos inhibits bmp4 expression and activates neural development. Genes Dev. 13, 3149–3159.
Barnfield, P.C., Zhang, X., Thanabalasingham, V., Yoshida, M., Hui, C.C., 2005. Negative regulation of Gli1 and Gli2 activator function by Suppressor of fused through multiple mechanisms. Differentiation 73, 397–405.
Brewster, R., Lee, J., Ruiz i Altaba, A., 1998. Gli/Zic factors pattern the neural plate by defining domains of cell differentiation. Nature 393, 579–583.
Chen, M.H., Wilson, C.W., Li, Y.J., Law, K.K., Lu, C.S., Gacayan, R., Zhang, X., Hui, C.C., Chuang, P.T., 2009. Cilium-independent regulation of Gli protein function by Sufu in Hedgehog signaling is evolutionarily conserved. Genes Dev. 23, 1910–1928.
Cheng, S.Y., Bishop, J.M., 2002. Suppressor of Fused represses Gli-mediated transcription by recruiting the SAP18-mSin3 corepressor complex. Proc. Natl. Acad. Sci. U. S. A. 99, 5442–5447.

Please cite this article as: Min, T.H., et al., The dual regulator Sufu integrates Hedgehog and Wnt signals in the early *Xenopus* embryo, Dev. Biol. (2011), doi:10.1016/j.ydbio.2011.07.035

Cheng, S.Y., Yue, S., 2008. Role and regulation of human tumor suppressor SUFU in Hedgehog signaling. Adv. Cancer Res. 101, 29–43.
Christian, J.L., Moon, R.T., 1993. Interactions between Xwnt-8 and Spemann organizer signaling pathways generate dorsoventral pattern in the embryonic mesoderm of *Xenopus*. Genes Dev. 7, 13–28.
Cooper, A.F., Yu, K.P., Brueckner, M., Brailey, L.L., Johnson, L., McGrath, J.M., Bale, A.E., 2005. Cardiac and CNS defects in a mouse with targeted disruption of suppressor of fused. Development 132, 4407–4417.
Cornesse, Y., Pieler, T., Hollemann, T., 2005. Olfactory and lens placode formation is controlled by the hedgehog-interacting protein (Xhip) in *Xenopus*. Dev. Biol. 277, 296–315.
Cwinn, M.A., Mazerolle, C., McNeill, B., Ringuette, R., Thurig, S., Hui, C.C., Wallace, V.A., 2011. Suppressor of fused is required to maintain the multipotency of neural progenitor cells in the retina. J. Neurosci. 31, 5169–5180.
Danesin, C., Peres, J.N., Johansson, M., Snowden, V., Cording, A., Papalopulu, N., Houart, C., 2009. Integration of telencephalic Wnt and hedgehog signaling center activities by Foxg1. Dev. Cell 16, 576–587.
Deardorff, M.A., Tan, C., Saint-Jeannet, J.P., Klein, P.S., 2001. A role for frizzled 3 in neural crest development. Development 128, 3655–3663.
Ding, Q., Fukami, S., Meng, X., Nishizaki, Y., Zhang, X., Sasaki, H., Dlugosz, A., Nakafuku, M., Hui, C., 1999. Mouse suppressor of fused is a negative regulator of sonic hedgehog signaling and alters the subcellular distribution of Gli1. Curr. Biol. 9, 1119–1122.
Dunaeva, M., Michelson, P., Kogerman, P., Toftgard, R., 2003. Characterization of the physical interaction of Gli proteins with SUFU proteins. J. Biol. Chem. 278, 5116–5122.
Ekker, S.C., McGrew, L.L., Lai, C.J., Lee, J.J., von Kessler, D.P., Moon, R.T., Beachy, P.A., 1995. Distinct expression and shared activities of members of the hedgehog gene family of *Xenopus laevis*. Development 121, 2337–2347.
Franco, P.G., Paganelli, A.R., López, S.L., Carrasco, A.E., 1999. Functional association of retinoic acid and hedgehog signaling in *Xenopus* primary neurogenesis. Development 126, 4257–4265.
Fuentealba, L.C., Eivers, E., Ikeda, A., Hurtado, C., Kuroda, H., Pera, E.M., De Robertis, E.M., 2007. Integrating patterning signals: Wnt/GSK3 regulates the duration of the BMP/Smad1 signal. Cell 131, 980–993.
Garcia-Morales, C., Liu, C.H., Abu-Elmagd, M., Hajihosseini, M.K., Wheeler, G.N., 2009. Frizzled-10 promotes sensory neuron development in *Xenopus* embryos. Dev. Biol. 335, 143–155.
Glinka, A., Wu, W., Delius, H., Monaghan, A.P., Blumenstock, C., Niehrs, C., 1998. Dickkopf-1 is a member of a new family of secreted proteins and functions in head induction. Nature 391, 357–362.
Hansen, C.S., Marion, C.D., Steele, K., George, S., Smith, W.C., 1997. Direct neural induction and selective inhibition of mesoderm and epidermis inducers by Xnr3. Development 124, 483–492.
Haramoto, Y., Tanegashima, K., Onuma, Y., Takahashi, S., Sekizaki, H., Asashima, M., 2004. *Xenopus* tropicalis nodal-related gene 3 regulates BMP signaling: an essential role for the pro-region. Dev. Biol. 265, 155–168.
Heeg-Truesdell, E., LaBonne, C., 2006. Neural induction in *Xenopus* requires inhibition of Wnt-beta-catenin signaling. Dev. Biol. 298, 71–86.
He, J., Sheng, T., Stelter, A.A., Li, C., Zhang, X., Sinha, M., Luxon, B.A., Xie, J., 2006. Suppressing Wnt signaling by the hedgehog pathway through sFRP-1. J. Biol. Chem. 281, 35598–35602.
Hoppler, S., Brown, J.D., Moon, R.T., 1996. Expression of a dominant-negative Wnt blocks induction of MyoD in *Xenopus* embryos. Genes Dev. 10, 2805–2817.
Hou, S., Maccarana, M., Min, T.H., Strate, I., Pera, E.M., 2007. The secreted serine protease xHtrA1 stimulates long-range FGF signaling in the early *Xenopus* embryo. Dev. Cell 13, 226–241.
Humke, E.W., Dorn, K.V., Milenkovic, L., Scott, M.P., Rohatgi, R., 2010. The output of Hedgehog signaling is controlled by the dynamic association between Suppressor of Fused and the Gli proteins. Genes Dev. 24, 670–682.
Itoh, K., Tang, T.L., Neel, B.G., Sokol, S.Y., 1995. Specific modulation of ectodermal cell fates in *Xenopus* embryos by glycogen synthase kinase. Development 121, 3979–3988.
Jia, J., Kolterud, A., Zeng, H., Hoover, A., Teglund, S., Toftgård, R., Liu, A., 2009. Suppressor of Fused inhibits mammalian Hedgehog signaling in the absence of cilia. Dev. Biol. 330, 452–460.
Jiang, J., Hui, C.C., 2008. Hedgehog signaling in development and cancer. Dev. Cell 15, 801–812.
Katoh, Y., Katoh, M., 2006. WNT antagonist, SFRP1, is Hedgehog signaling target. Int. J. Mol. Med. 17, 171–175.
Kiecker, C., Niehrs, C., 2001. A morphogen gradient of Wnt/beta-catenin signalling regulates anteroposterior neural patterning in *Xenopus*. Development 128, 4189–4201.
Kise, Y., Morinaka, A., Teglund, S., Miki, H., 2009. Sufu recruits GSK3beta for efficient processing of Gli3. Biochem. Biophys. Res. Commun. 387, 569–574.
Koebernick, K., Pieler, T., 2002. Gli-type zinc finger proteins as bipotential transducers of hedgehog signaling. Differentiation 70, 69–76.
Koebernick, K., Hollemann, T., Pieler, T., 2003. A restrictive role for Hedgehog signalling during otic specification in *Xenopus*. Dev. Biol. 260, 325–338.
Kogerman, P., Grimm, T., Kogerman, L., Krause, D., Unden, A.B., Sandstedt, B., Toftgård, R., Zaphiropoulos, P.G., 1999. Mammalian suppressor-of-fused modulates nuclear-cytoplasmic shuttling of Gli-1. Nat. Cell Biol. 1, 312–319.
LaBonne, C., Bronner-Fraser, M., 1998. Neural crest induction in *Xenopus*: evidence for a two-signal model. Development 125, 2403–2414.
Lai, C.J., Ekker, S.C., Beachy, P.A., Moon, R.T., 1995. Patterning of the neural ectoderm of *Xenopus laevis* by the amino-terminal product of hedgehog autoproteolytic cleavage. Development 121, 2349–2360.
Lee, J., Platt, K.A., Censullo, P., Ruiz i Altaba, A., 1997. Gli1 is a target of Sonic hedgehog that induces ventral neural tube development. Development 124, 2537–2552.
Lee, C.S., Buttitta, L.A., May, N.R., Kispert, A., Fan, C.M., 2000. SHH-N upregulates Sfrp2 to mediate its competitive interaction with WNT1 and WNT4 in the somitic mesoderm. Development 127, 109–118.
Lee, Y., Kawagoe, R., Sasai, K., Li, Y., Russell, H.R., Curran, T., McKinnon, P.J., 2007. Loss of suppressor-of-fused function promotes tumorigenesis. Oncogene 26, 6442–6447.
Leyns, L., Bouwmeester, T., Kim, S.H., Piccolo, S., De Robertis, E.M., 1997. Frzb-1 is a secreted antagonist of Wnt signaling expressed in the Spemann organizer. Cell 88, 747–756.
MacDonald, B.T., Tamai, K., He, X., 2009. Wnt/beta-catenin signalling: components, mechanisms, and diseases. Dev. Cell 17, 9–26.
Maeda, O., Kondo, M., Fujita, T., Usami, N., Fukui, T., Shimokata, K., Ando, T., Goto, H., Sekido, Y., 2006. Enhancement of GLI1-transcriptional activity by beta-catenin in human cancer cells. Oncol. Rep. 16, 91–96.
Marcus, E.A., Kintner, C., Harris, W., 1998. The role of GSK3beta in regulating neuronal differentiation in *Xenopus laevis*. Mol. Cell. Neurosci. 12, 269–280.
Marine, J.C., Bellefroid, E.J., Pendeville, H., Martial, J.A., Pieler, T., 1997. A role for *Xenopus* Gli-type zinc finger proteins in the early embryonic patterning of mesoderm and neuroectoderm. Mech. Dev. 63, 211–225.
McGrew, L.L., Lai, C.J., Moon, R.T., 1995. Specification of the anteroposterior neural axis through synergistic interaction of the Wnt signaling cascade with noggin and follistatin. Dev. Biol. 172, 337–342.
Meng, X., Poon, R., Zhang, X., Cheah, A., Ding, Q., Hui, C.C., Alman, B., 2001. Suppressor of fused negatively regulates beta-catenin signaling. J. Biol. Chem. 276, 40113–40119.
Merchant, M., Vajdos, F.F., Ultsch, M., Maun, H.R., Wendt, U., Cannon, J., Desmarais, W., Lazarus, R.A., de Vos, A.M., de Sauvage, F.J., 2004. Suppressor of fused regulates Gli activity through a dual binding mechanism. Mol. Cell. Biol. 24, 8627–8641.
Mullor, J.L., Dahmane, N., Sun, T., Ruiz i Altaba, A., 2001. Wnt signals are targets and mediators of Gli function. Curr. Biol. 11, 769–773.
Murone, M., Luoh, S.M., Stone, D., Li, W., Gurney, A., Armanini, M., Grey, C., Rosenthal, A., de Sauvage, F.J., 2000. Gli regulation by the opposing activities of fused and suppressor of fused. Nat. Cell Biol. 2, 310–312.
Niehrs, C., 2010. On growth and form: a Cartesian coordinate system of Wnt and BMP signaling specifies bilaterian body axes. Development 137, 845–857.
Paces-Fessy, M., Boucher, D., Petit, E., Paute-Briand, S., Blanchet-Tournier, M.F., 2004. The negative regulator of Gli, Suppressor of fused (Sufu), interacts with SAP18, Galectin3 and other nuclear proteins. Biochem. J. 378, 353–362.
Petersen, C.P., Reddien, P.W., 2009. Wnt signaling and the polarity of the primary body axis. Cell 139, 1056–1068.
Préat, T., 1992. Characterization of Suppressor of fused, a complete suppressor of the fused segment polarity gene of *Drosophila melanogaster*. Genetics 132, 725–736.
Ruiz i Altaba, A., 1999. Gli proteins encode context-dependent positive and negative functions: implications for development and disease. Development 126, 3205–3516.
Ruiz i Altaba, A., Mas, C., Stecca, B., 2007. The Gli code: an information nexus regulating cell fate, stemness and cancer. Trends Cell Biol. 17, 438–447.
Saint-Jeannet, J.P., He, X., Varmus, H.E., Dawid, I.B., 1997. Regulation of dorsal fate in the neuraxis by Wnt-1 and Wnt-3a. Proc. Natl. Acad. Sci. U. S. A. 94, 13713–13718.
Salic, A.N., Kroll, K.L., Evans, L.M., Kirschner, M.W., 1997. Sizzled: a secreted Xwnt8 antagonist expressed in the ventral marginal zone of *Xenopus* embryos. Development 124, 4739–4748.
Sasai, Y., Lu, B., Steinbeisser, H., De Robertis, E.M., 1995. Regulation of neural induction by the Chd and Bmp-4 antagonistic patterning signals in *Xenopus*. Nature 376, 333–336.
Sasaki, H., Hui, C., Nakafuku, M., Kondoh, H., 1997. A binding site for Gli proteins is essential for HNF-3beta floor plate enhancer activity in transgenics and can respond to Shh *in vitro*. Development 124, 1313–1322.
Sasaki, H., Nishizaki, Y., Hui, C., Nakafuku, M., Kondoh, H., 1999. Regulation of Gli2 and Gli3 activities by an amino-terminal repression domain: implication of Gli2 and Gli3 as primary mediators of Shh signaling. Development 126, 3915–3924.
Sokol, S.Y., Klingensmith, J., Perrimon, N., Itoh, K., 1995. Dorsalizing and neuralizing properties of Xdsh, a maternally expressed *Xenopus* homolog of dishevelled. Development 121, 1637–1647.
Stone, D.M., Murone, M., Luoh, S., Ye, W., Armanini, M.P., Gurney, A., Phillips, H., Brush, J., Goddard, A., de Sauvage, F.J., Rosenthal, A., 1999. Characterization of the human suppressor of fused, a negative regulator of the zinc-finger transcription factor Gli. J. Cell Sci. 112, 4437–4448.
Svärd, J., Heby-Henricson, K., Persson-Lek, M., Rozell, B., Lauth, M., Bergstrom, A., Ericson, J., Toftgård, R., Teglund, S., 2006. Genetic elimination of Suppressor of fused reveals an essential repressor function in the mammalian Hedgehog signaling pathway. Dev. Cell 10, 187–197.
Taelman, V.F., Dobrowolski, R., Plouhinec, J.L., Fuentealba, L.C., Vorwald, P.P., Gumper, I., Sabatini, D.D., De Robertis, E.M., 2010. Wnt signaling requires sequestration of glycogen synthase kinase 3 inside multivesicular endosomes. Cell 143, 1136–1148.
Taylor, M.D., Liu, L., Raffel, C., Hui, C.C., Mainprize, T.G., Zhang, X., Agatep, R., Chiappa, S., Gao, L., Lowrance, A., Hao, A., Goldstein, A.M., Stavrou, T., Scherer, S.W., Dura, W.T., Wainwright, B., Squire, J.A., Rutka, J.T., Hogg, D., 2002. Mutations in SUFU predispose to medulloblastoma. Nat. Genet. 31, 306–310.
Taylor, M.D., Zhang, X., Liu, L., Hui, C.C., Mainprize, T.G., Scherer, S.W., Wainwright, B., Hogg, D., Rutka, J.T., 2004. Failure of a medulloblastoma-derived mutant of SUFU to suppress WNT signaling. Oncogene 23, 4577–4583.
Tukachinsky, H., Lopez, L.V., Salic, A., 2010. A mechanism for vertebrate Hedgehog signaling: recruitment to cilia and dissociation of SuFu-Gli protein complexes. J. Cell Biol. 191, 415–428.
Ulloa, F., Itasaki, N., Briscoe, J., 2007. Inhibitory Gli3 activity negatively regulates Wnt/beta-catenin signaling. Curr. Biol. 17, 545–550.
van den Brink, G.R., Bleuming, S.A., Hardwick, J.C., Schepman, B.L., Offerhaus, G.J., Keller, J.J., Nielsen, C., Gaffield, W., van Deventer, S.J., Roberts, D.J., Peppelenbosch, M.P.,

Please cite this article as: Min, T.H., et al., The dual regulator Sufu integrates Hedgehog and Wnt signals in the early *Xenopus* embryo, Dev. Biol. (2011), doi:10.1016/j.ydbio.2011.07.035

2004. Indian Hedgehog is an antagonist of Wnt signaling in colonic epithelial cell differentiation. Nat. Genet. 36, 277–282.
Varjosalo, M., Li, S.P., Taipale, J., 2006. Divergence of hedgehog signal transduction mechanism between *Drosophila* and mammals. Dev. Cell 10, 177–186.
Wang, C., Pan, Y., Wang, B., 2010. Suppressor of fused and Spop regulate the stability, processing and function of Gli2 and Gli3 full-length activators but not their repressors. Development 137, 2001–2009.
Wessely, O., Agius, E., Oelgeschläger, M., Pera, E.M., De Robertis, E.M., 2001. Neural induction in the absence of mesoderm: beta-catenin-dependent expression of secreted BMP antagonists at the blastula stage in *Xenopus*. Dev. Biol. 234, 161–173.
Wessely, O., Kim, J.I., Geissert, D., Tran, U., De Robertis, E.M., 2004. Analysis of Spemann organizer formation in *Xenopus* embryos by cDNA macroarrays. Dev. Biol. 269, 552–566.
Wu, J., Yang, J., Klein, P.S., 2005. Neural crest induction by the canonical Wnt pathway can be dissociated from anterior–posterior neural patterning in *Xenopus*. Dev. Biol. 279, 220–232.
Yanai, K., Nakamura, M., Akiyoshi, T., Nagai, S., Wada, J., Koga, K., Noshiro, H., Nagai, E., Tsuneyoshi, M., Tanaka, M., Katano, M., 2008. Crosstalk of hedgehog and Wnt pathways in gastric cancer. Cancer Lett. 263, 145–156.
Yost, C., Torres, M., Miller, J.R., Huang, E., Kimelman, D., Moon, R.T., 1996. The axis-inducing activity, stability, and subcellular distribution of beta-catenin is regulated in *Xenopus* embryos by glycogen synthase kinase 3. Genes Dev. 10, 1443–1454.
Zeng, H., Jia, J., Liu, A., 2010. Coordinated translocation of mammalian Gli proteins and suppressor of fused to the primary cilium. PLoS One 5 (12), e15900. doi:10.1371/journal.pone.0015900.

Please cite this article as: Min, T.H., et al., The dual regulator Sufu integrates Hedgehog and Wnt signals in the early *Xenopus* embryo, Dev. Biol. (2011), doi:10.1016/j.ydbio.2011.07.035

Supplementary material

The dual regulator Sufu integrates Hedgehog and Wnt signals in the early *Xenopus* embryo

Tan H. Min, Martin Kriebel, Shirui Hou, and Edgar M. Pera

Supplementary data

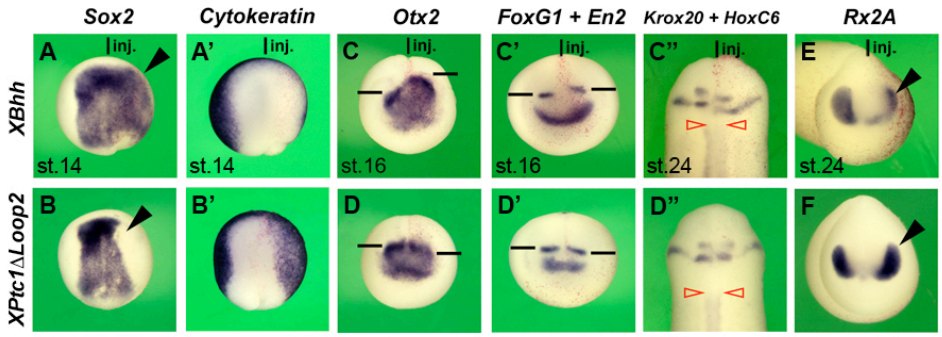

Figure S1. Hh signals during neural induction, anteroposterior patterning and eye field development.

Whole-mount *in situ* hybridization of early gastrula embryos in dorsal view (A,A',B,B'), advanced neurulae in anterior view (C,C',D,D'), and tail bud embryos in dorsal (C'',D'') and anterior views (E,F). Embryos were injected into the animal pole of one blastomere at the 4-cell stage with the indicated mRNAs. *nlacZ* mRNA (100 pg) was co-injected as lineage tracer, so that the injected side (red nuclei) can be compared with the non-injected control side within each embryo.

(A,A',B,B') *XBhh* mRNA (500 pg) expands the neural plate marker *Sox2* (arrowhead) at the expense of epidermis-specific *Cytokeratin* expression, while *XPtc1ΔLoop2* mRNA causes the opposite effect.

(C-C'') *XBhh* mRNA (500 pg) anteriorizes the brain as evident from the posteriorward shift of the regional markers *Otx2* (forebrain and anterior midbrain; horizontal line), *En2* (posterior midbrain; horizontal line), and *Krox20* (hindbrain rhombomeres 3 and 5). Note that the anterior borders of *FoxG1* (telencephalon) and *HoxC6* (spinal cord; open arrowhead) are not affected.

(D-D'') *XPtc1ΔLoop2* mRNA (1 ng) causes a very subtle posteriorization of the brain.

(E,F) *XBhh* mRNA (500 pg) reduces, whereas *XPtc1ΔLoop2* mRNA (1 ng) increases expression of the eye-specific marker *Rx2A*.

The indicated effects on gene expression were observed in: A, 35/35; A', 32/35; B, 27/32; B', 25/26; C, 26/26; C', 27/27 (*FoxG1*), 24/27 (*En2*); C'', 15/15 (*Krox20*), 18/18 (*HoxC6*); D, 23/29; D', 29/31 (*FoxG1*), 24/31 (*En2*); D'', 13/25 (*Krox20*), 22/23 (*HoxC6*); E, 34/37; F, 14/15.

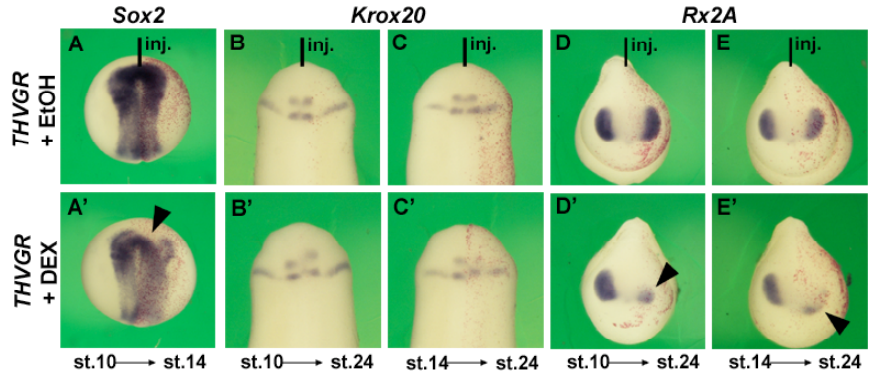

Figure S2. Temporal influences of activated Wnt signalling on neural plate, antero-posterior patterning and eye field development.

Whole-mount *in situ* hybridization of early neurula embryos in dorsal view (A,A'), tail bud embryos in dorsal (B,B',C,C') and anterior view (D,D',E,E'). All embryos were injected into the animal pole of one blastomere at the 4-cell stage with hormone-inducible Tcf mRNA (*THVGR,* 20 pg) and *nlacZ* mRNA as a lineage tracer. Embryos were then treated with 0.1% Ethanol as control (A-E) or 10 µM Dexamethasone (DEX, dissolved in 0.1% Ethanol; A'-E') at the indicated stages until fixation.

(A,A') *THVGR* induces downregulation of the neural plate marker *Sox2* in the anterior domain (arrowhead) when activated by DEX at stage 10.

(B,B',C,C') *THVGR* causes an anteriorward shift of the hindbrain marker *Krox20* upon activation at stage 10 and to a lower degree upon activation at stage 14.

(D,D',E,E') *THVGR* leads to robust downregulation and anteriorward shift of the eye-specific marker *Rx2A* following activation at stage 10 or stage 14.

The observed effects on gene expression were obtained in: A, 11/11; A', 9/13; B, 10/12; B', 5/5; C, 11/11; C', 8/8; D, 7/7; D', 8/8; E, 12/12; E', 8/8.

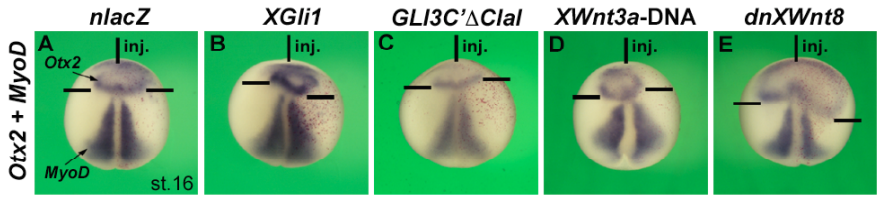

Figure S3. Hh and Wnt signals directly affect neural plate patterning.

Whole-mount *in situ* hybridization of neurula embryos in dorsal view. Embryos were animally injected into one blastomere at the 4-cell stage with the indicated mRNAs and *nlacZ* mRNAs as lineage tracer.

(A) Control embryo showing expression of the forebrain/midbrain marker *Otx2* (horizontal line depicts posterior border) and the paraxial mesoderm marker *MyoD*.

(B) *XGli1* mRNA (150 pg) causes posteriorward expansion of *Otx2*, but only moderate posterior retraction of *MyoD* expression.

(C) *Gli3C'ΔClaI* mRNA (100 pg) shifts the posterior border of *Otx2* slightly anteriorwards without obviously affecting the *MyoD* marker.

(D) *XWnt3a* DNA (30 pg) causes robust reduction of anterior *Otx2* and only minor anteriorward extension of *MyoD* expression.

(E) *dnXWnt8* mRNA (100 pg) results in posteriorly expanded *Otx2* and subtle posterior reduction of *MyoD* expression.

The indicated effects on gene expression were shown in: A, 31/34; B, 16/28; C, 9/9; D, 8/9; E, 41/41.

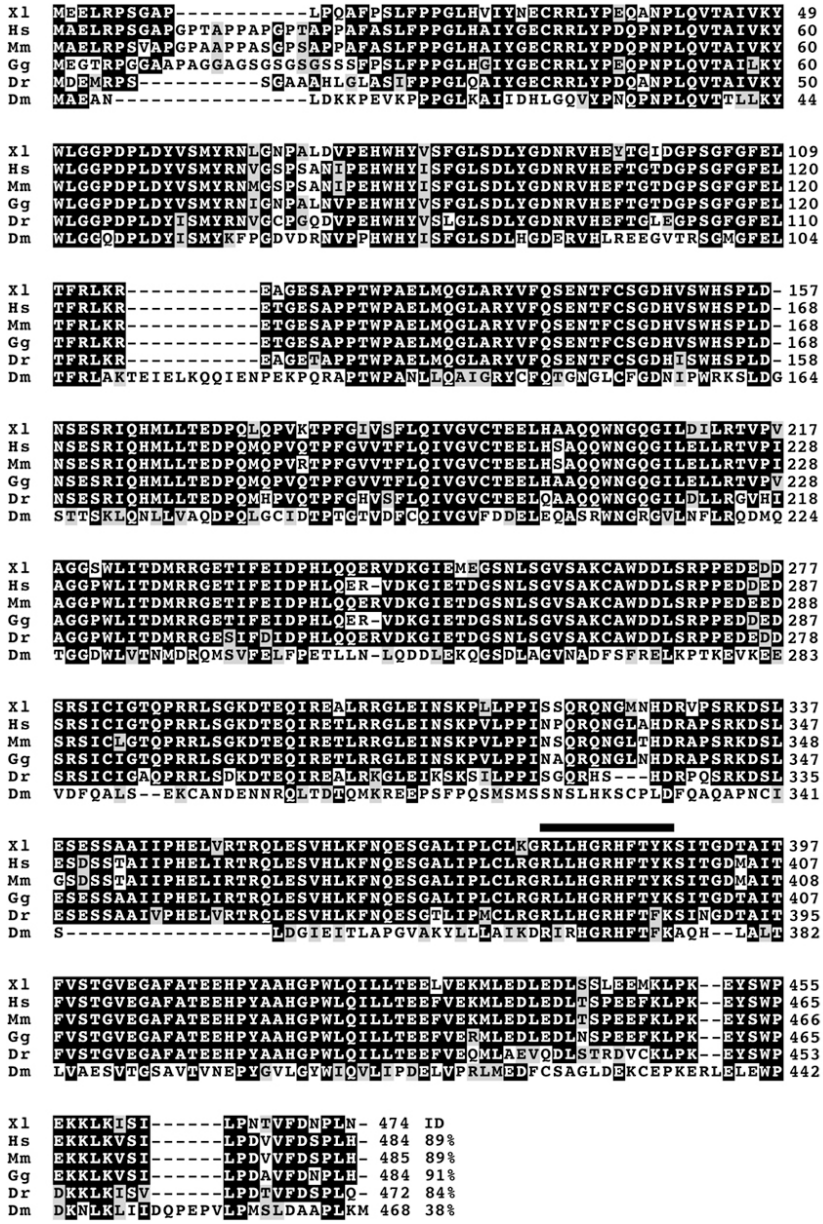

Figure S4. Comparison of Suppressor-of-fused amino acid sequences.

The sequence alignment was performed using the ClustalW server (http://www.ch.embnet.org/software/ClustalW.html) and Boxshade 3.21 server (http://www.ch.embnet.org/software/BOX_form.html). Identical amino acids are indicated in black and similar residues in grey. The black bar indicates a conserved Gli protein binding sequence (Merchant et al., 2004). ID, identity. GenBank accession numbers are Xl (*Xenopus laevis*, NP_001086013), Hs (*Homo sapiens*, NP_057353), Mm (*Mus musculus*, NP_056567), Gg (*Gallus gallus*, NP_989595), Dr (*Danio rerio*, AAI55826), and Dm (*Drosophila melanogaster*, CAA64954).

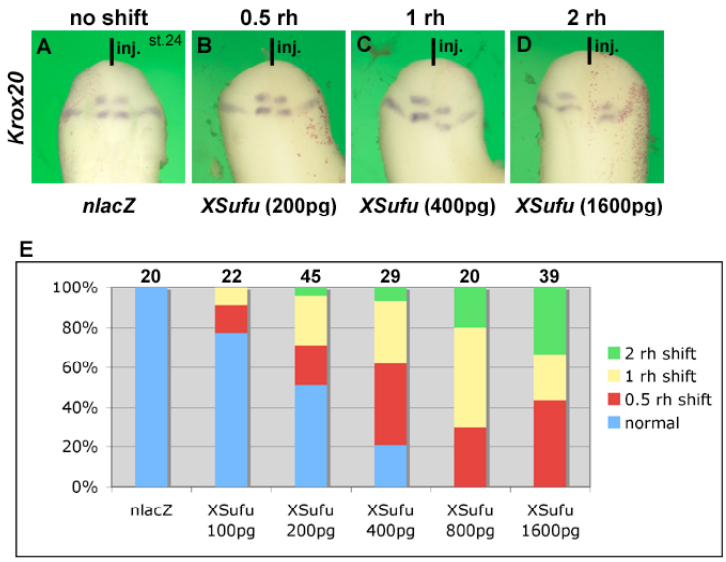

Figure S5. *XSufu* mRNA affects antero-posterior patterning in a dose-dependent manner

Embryos were animally injected into a single blastomere at the 4-cell stage with the indicated amounts of *XSufu* mRNA together with *nlacZ* mRNA as lineage tracer.
(A-D) Dorsal view of representative tailbud embryos after whole-mount *in situ* hybridization. Note that *XSufu* mRNA induces a posteriorward shift of the hindbrain marker *Krox20* (rhombomeres 3 and 5) with a displacement of up to 2 rhombomere units at the highest amount of 1600 pg.
(E) Quantification of the posteriorward rhombomeric shifts induced by the indicated doses of *XSufu* mRNA. The numbers of analyzed specimens are indicated above the columns. rh, rhombomere

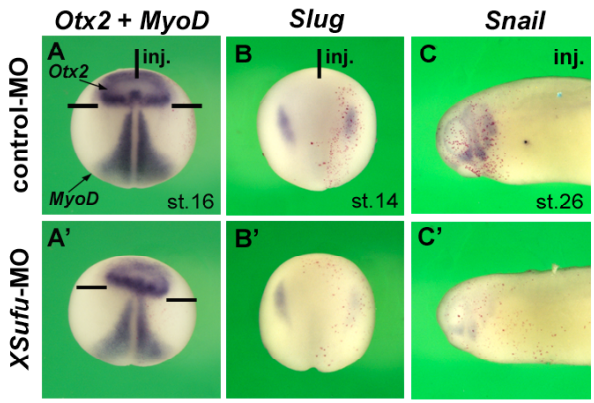

Figure S6. Direct effects of XSufu depletion on neural plate patterning and neural crest development.

Whole-mount *in situ* hybridization of embryos injected at the 32-cell stage with non-specific control-MO (25 ng) or *XSufu*-MO (25 ng) into the dorsal animal A1 blastomere to specifically target the neural plate (A,A') and A2 blastomere to target the neural crest anlage (B,B',C,C'). *nlacZ* mRNA was co-injected as a lineage tracer.

(A) Control-MO-injected neurula embryo in dorsal view showing normal expression of the forebrain/midbrain marker *Otx2* and the paraxial mesoderm marker *MyoD*.

(A') *XSufu*-MO causes posterior displacement of *Otx2*, but no effect on *MyoD* expression.

(B) Control-MO-injected neurula embryo in dorsal view exhibiting normal *Snail* expression in prospective neural crest cells.

(B') *XSufu*-MO causes reduction of *Slug* expression.

(C) Control-MO-injected tailbud embryo in lateral view showing normal *Snail* expression in migrating neural crest cells.

(C') *XSufu*-MO leads to reduction of *Snail* expression.

The observed effects on gene expression were obtained in: A, 21/21; A', 9/11; B, 55/55; B', 9/12; C, 32/32; C', 8/8.

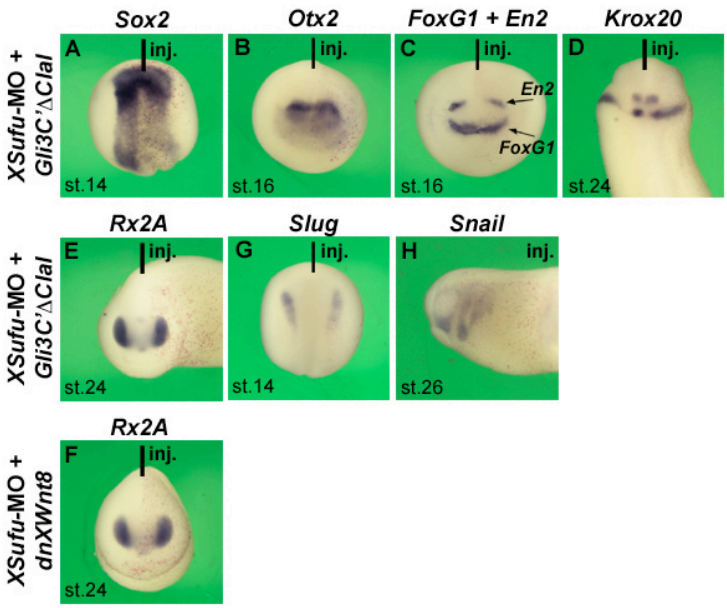

Figure S7. Rescue of embryonic patterning in XSufu-morphant embryos by inhibition of Hh and Wnt signalling.

Whole-mount *in situ* hybridization of embryos in dorsal (A,D,G), anterior (B,C,E,F), and lateral views (H). *XSufu*-MO (25 ng) and *nlacZ* mRNA as lineage tracer were co-injected into the animal pole of one blastomere at the 2-cell stage together with 3 pg *GLI3C'ΔClaI* mRNA or 3 pg *dnXWnt8* mRNA.

(A) Inhibition of Hh signals by *GLI3C'ΔClaI* mRNA restores normal expression of the neural plate marker *Sox2* in *XSufu*-MO-injected embryo.

(B-D) Blockage of the Hh pathway in *XSufu*-morphants results in normal expression of the brain markers *Otx2* (forebrain/midbrain), *FoxG1* (telencephalon), *En2* (posterior midbrain), and *Krox20* (hindbrain rhombomeres 3 and 5).

(E) Abrogation of Hh signalling in *XSufu*-depleted embryo displays normal expression of the eye-specific marker *Rx2A*.

(F) Inhibition of Wnt signals by *dnXWnt8* mRNA restores normal *Rx2A* expression in *XSufu*-MO-injected embryo.

(G,H) Blockage of the Hh pathway in *XSufu*-morphants reverts to normal expression of the neural crest markers *Slug* and *Snail*. The observed effects on gene expression were obtained in: A, 14/16; B, 11/13; C, 7/8; D, 23/28; E, 20/27; F, 20/31; G, 19/20; H, 33/43.

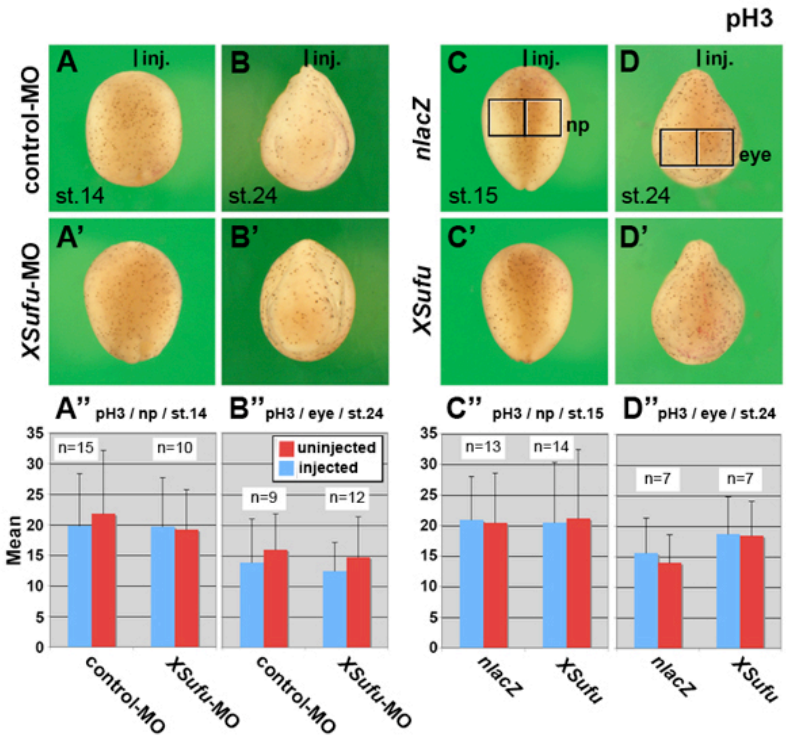

Figure S8. Knockdown and overexpression of XSufu has no effect on proliferation in early *Xenopus* embryos.

(A-D,A'-D') Cell proliferation was determined by whole-mount immunostaining using an antibody against phosphorylated Histone 3 (pH3). Embryos are shown in dorsal view at the early neurula stage (A,A',C,C') and in anterior view at the early tail bud stage (B,B',D,D'). Embryos were injected into the animal pole of one blastomere at the 2- to 4-cell stage with the indicated constructs and *nlacZ* mRNA as lineage tracer. The dark spots label pH3-positive cells. Note that 25 ng control-MO (A,B), 25 ng *XSufu*-MO (A',B'), 100 pg *nlacZ* mRNA (C,D), and 750 pg *XSufu* mRNA (C',D') do not significantly affect the number of pH3-positive cells.

(A'',B'',C'',D'') The pH3 signals on uninjected and injected sides were counted within the indicated frames representing the neural plate (C) and eye field (D). The signals were analysed using *t* test with Microsoft Excel. *P* value of <0.05 was considered significant.

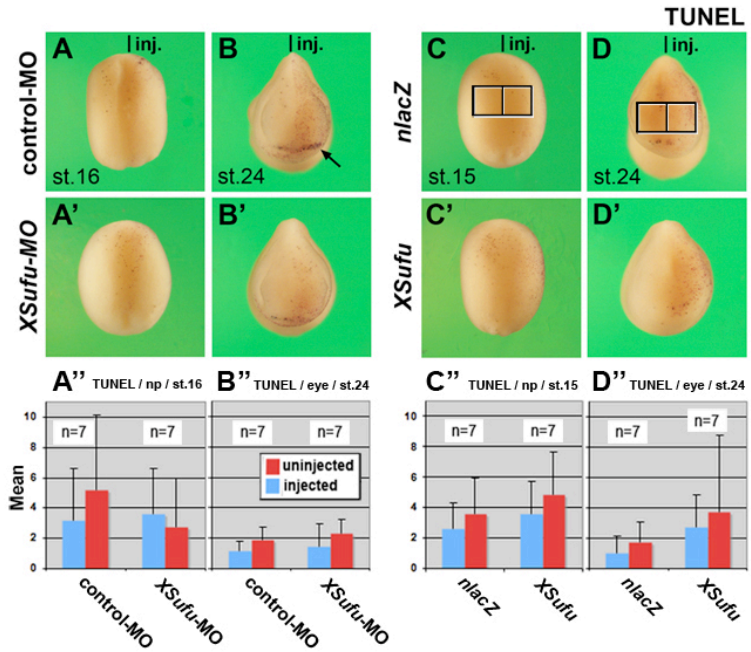

Figure S9. Modulation of XSufu protein levels has no effect on apoptosis in early *Xenopus* embryos.

Apoptosis was analyzed by whole-mount *in situ* DNA end labelling using the TUNEL protocol (Hensey and Gautier, 1998). Embryos are shown in dorsal view at the early neurula stage (A,A',C,C') and in anterior view at the early tail bud stage (B,B',D,D'). Embryos were injected into the animal pole of one blastomere at the 2-4 cell stage, using *nlacZ* mRNA as lineage tracer (red nuclei). The dark spots label TUNEL-positive apoptotic cells. The arrowhead indicates an accumulation of signals in the developing stomodeum. Note that 25 ng control-MO (A,B), 25 ng *XSufu*-MO (A',B'), 100 pg *nlacZ* mRNA (C,D), and 750 pg *XSufu* mRNA (C',D') do not significantly affect the number of TUNEL-positive cells. The indicated effects were observed in A, 32/34; A', 54/62; B, 26/29; B', 25/30; C, 25/28; C', 36/40; D, 17/20; D' 20/21.

(A'',B'',C'',D'') The TUNEL signals on uninjected and injected sides were counted within the indicated frames representing the neural plate (C) and eye field (D). The signals were analysed using *t* test with Microsoft Excel. *P* value of <0.05 was considered significant.

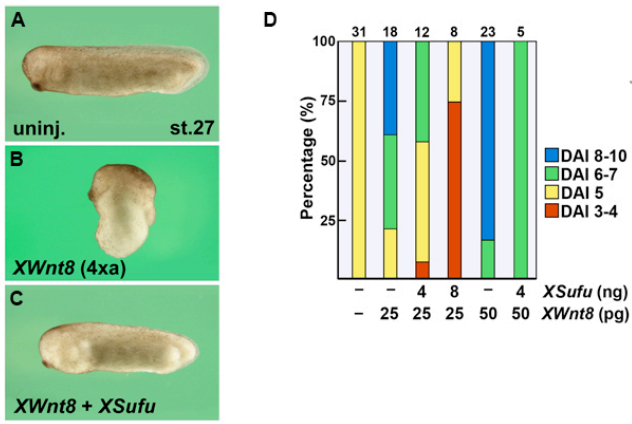

Figure S10. *XSufu* inhibits Wnt/β-catenin-induced dorsoanteriorization in *Xenopus* embryos.

(A-C) Dorsoanteriorization induced by animal injection of 50 pg *XWnt8* mRNA is partially restored by co-injection of 4 ng *XSufu* mRNA in tail bud embryos.
(D) Dorsoanterior index (DAI; Kao and Elinson, 1988) determined in stage 27 embryos following animal injection of *XWnt8* and *XSufu* mRNAs. DAI 5 is normal, DAI>5 dorso-anteriorized, and DAI<5 ventro-posteriorized.

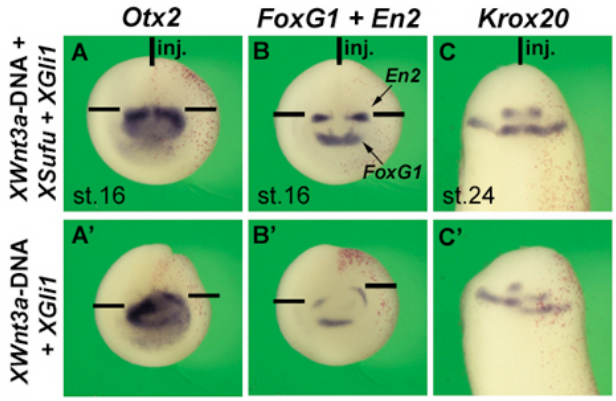

Fig S11. Interaction of *XSufu*, Wnt and Hh signals during neural plate patterning.

Whole-mount *in situ* hybridization of neurula embryos in anterior view (A, A', B, B') and tail bud embryos in dorsal view (C, C'). Embryos were injected animally into one blastomere at the 4-cell stage with the indicated mRNAs and *nlacZ* mRNA as lineage tracer.
(A-C) Co-injection of *XSufu* mRNA (750 pg), *XWnt3a* DNA (30 pg) and *XGli1* mRNA (150 pg) has no effect on the expression of *Otx2* (forebrain/midbrain), *FoxG1* (telencephalon), *En2* (posterior midbrain) and *Krox20* (hindbrain rhombomeres 3 and 5).
(A'-C') Embryos co-injected with *XWnt3a* DNA (30 pg) and *XGli1* mRNA (150 pg) show a posteriorward expansion of *Otx2* and posterior shift of *En2* and *Krox20* expression domains. Frequency of embryos with the indicated phenotype was: A, 32/33; B, 32/40; C, 32/47; A', 11/18; B', 9/15; C', 13/23.
Compare these to embryos injected with *XGli1* mRNA, *XWnt3a* DNA, *XSufu* mRNA, or a combination of *XSufu* mRNA and *XWnt3a* DNA (Fig. 1H-H'', J-J'' and Fig. 3C'-E', C''-E'').

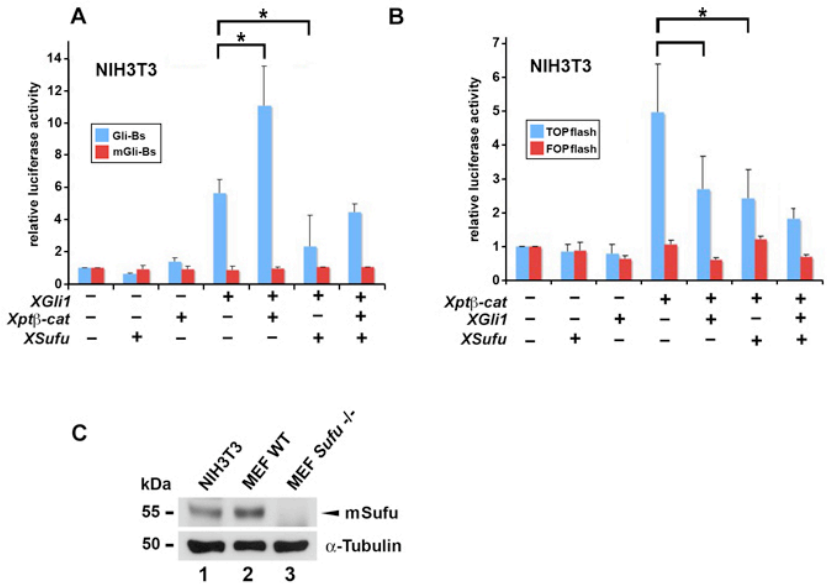

Figure S12. Effect of Gli1, β-catenin, and Sufu on Hh and Wnt signalling activities in NIH3T3 cells.

(A,B) NIH3T3 cells were transfected with *XGli1-myc*, *Xptβ-catenin-HA*, and empty vector to adjust DNA amounts together with specific luciferase reporter constructs and pRL-TK for normalization. Luciferase activities in cell lysates were determined 48 hours after transfection. P value of <0.05 was considered significant.

(A) The *8xGli-Bs-luc* reporter was used to monitor Hh/Gli signalling, and *8xmGli-Bs-luc* with mutated Gli binding sites served as a negative control. Note that *XSufu* inhibits and *Xptβ-catenin* promotes Hh pathway activation under overexpression of *XGli1*.

(B) The *TOP-flash* reporter was used to monitor Wnt/β-catenin signalling, and *FOP-flash* with mutated Lef/Tcf binding sites served as a negative control. Note that *XSufu* inhibits Wnt pathway activation under overexpression of *Xptβ-catenin*. The ability of *XGli1* to suppress *Xptβ-catenin*-induced Wnt pathway activation is close to significant.

(C) Western blot of lysates derived from NIH3T3, MEF WT, and MEF Sufu -/- cells with an antibody against mouse Sufu. α-Tubulin was used as protein loading control.

Supplemental experimental procedures

Plasmid constructs

The open reading frame (ORF) and 198 nucleotides 5' untranslated region of *XSufu* were amplified based on an NCBI sequence entry (GenBank Accession number NM_001092544) by RT-PCR and subcloned into the pCS2+ vector (Turner and Weintraub, 1994), using total RNA from stage 20 embryos and the primers *XSufu*-F-*BamH*I: AAA GGA TCC CGC TCC AGC AAC AAG CTG and *XSufu*-R-*Xho*I: AAA CTC GAG TTA ATT GAG TGG GTT ATC AAA TAC. To generate pCS-*XSufu-Flag*, the insert from pCS-*XSufu* was amplified by PCR with the primers *XSufu*-F-*BamH*I and *XSufu-Flag*-R-*Xho*I: AAA CTC GAG TTA CTT GTC ATC GTC GTC CTT GTA GTC ATT GAG TGG GTT ATC AAA TAC and inserted into pCS2+. To generate pGEMT-*XSufu*, the ORF of *XSufu* was amplified by RT-PCR and subcloned into pGEMT (Promega), using total RNA from stage 13 embryos and the primers *XSufu*-F: ATG GAG GAG CTG AGG CCT AG and *XSufu*-R: TTA ATT GAG TGG GTT ATC AAA. To generate pCS2-*XSufu**, the insert from pGEMT-*XSufu* was amplified by PCR with the primers *XSufu*-F-*Cla*I: GCA TCG ATA TGG AGG AGC TGA GGC CTA GTG and *XSufu*-R-*Xho*I: GCC TCG AGT TAA TTG AGT GGG TTA TCA AAT AC and inserted into pCS2+. To generate pCS2-Xpt*β-catenin-HA*, the myc-tag in pCS2-*Xpt-βcatenin-myc* (Yost et al., 1996) was replaced by the haemagglutinin (HA) tag using PCR with the primers β-catenin-F-*Pst*I: AAA CTG CAG ACC TTG GTC TTG ATA and β-catenin-*HA*-R-*Eco*RI: AAA GAA TTC TTA TGC GTA GTC GGG GAC GTC GTA GGG GTA CAA GTC AGT GTC AAA CCA. All plasmid constructs were prepared with *Pfu* Ultra DNA Polymerase (Stratagene) and fully sequenced. Expression constructs were further checked by the TNT Quick Coupled Transcription/Translation Systems (Promega) or Western blot analysis.

Whole-mount inmmunostaining with pH3

Cell proliferation was determined by immunocytochemistry using an antibody against phosphorylated Histone 3 (pH3) as described in Saka and Smith (2001) with the following modifications: Embryos were incubated at 4°C overnight in Dents solution (80% methanol, 20% DMSO), rehydrated (75%, 50%, 25% methanol) and blocked

with horse serum in PBS (phosphate buffered saline). Embryos were incubated with anti-pH3 rabbit polyclonal antibody (1:200, Upstate Biotechnology, 06-570) for 5 hours and subsequently with anti-rabbit conjugated alkaline phosphatase antibody (1:1000, Abcam) for another 5 hours. After serial washing with PBS-TB (0.05% Tween20 and 0.2% BSA in PBS), embryos were stained with NBT (nitro blue tetrazolium) and BCIP (5-bromo-4-chloro-3-indolyl phosphate substances).

Immunoprecipitation

HEK293 cells were grown in 10-cm plates until 60% confluency, and transient transfection was performed with Turbofect (Fermentas), the indicated expression plasmids (*XGli1-myc*, *Xptβ-catenin-myc*, *XSufu-flag*), and the empty pCS2+ vector to keep the total DNA amount in each sample constant. After 36 hours, cells were lysed with 500 µl lysis buffer containing 50 mM Tris pH 7.4, 150 mM NaCl, 0.5% Triton X-100, 1 mM EDTA and protease inhibitor cocktail (Roche). For immunoprecipitation, cleared lysates containing 1 mg of extracted proteins were incubated with 50 µl ProteinG-Sepharose beads (Genscript) crosslinked to 15 µg anti-flag IgG (AbD Serotec, 4497-1010) using the crosslinker DSS (Sigma). After overnight incubation, the beads were washed in lysis buffer, and pulled-down flag-tag proteins were released by boiling in SDS sample buffer.

Table S1. Oligonucleotides for RT-PCR

Gene	Forward	Reverse	Cycles	Annealing Temperature	References
Histone H4	5'-CGG GAT AAC ATT CAG GGT ATC ACT	5'-CAT GGC GGT AAC TGT CTT CCT	25	56°C	Hou et al., 2007
XSiamois	5'-AAA CCA CTG ATT CAG GCA GAG G	5'-GTA GGG CTG TGT ATT TGA AGG G	35	60°C	Cornesse et al., 2005
Xnr3	5'-ATG GCA TTT CTG AAC CTG TTC TTC	5'-AGG TGG AAC GGT GCT CAC ATG GAT	35	50°C	Cornesse et al., 2005
Xbra	5'-GGA TCG TTA TCA CCT CTG	5'-GTG TAG TCT GTA GCA GCA	28	50°C	Hou et al., 2007
XSufu	5'-TAC AGC CAG TGA AGA CGC	5'-CAA TGC CTT TAT CAA CTC TC	30	50°C	This study
XGli1	5'-GAC CAA CAG TGG GGA TGA TG	5'-GAG GCT GAA TTG GAG GAA GG	30	60°C	Moriishi et al., 2005
Xptc1	5'-GGA CAA GAA TCG CAG AGC TG	5'-GGA TGC TCA GGG AAC CTT AC	30	55°C	Takabatake et al., 2000
Xptc2	5'-TTG TTC ATT GGA TTG CTG GTG	5'-CTC TTC CTG GTA GAT ATG CAG	30	55°C	Takabatake et al., 2000

Statistics

Statistical analyses for the luciferase reporter assays were carried out using unpaired *t* tests with GraphPad Instat3 version 3.06. All results were reported as means ± SD and a *P* value of <0.05 was considered significant.

Animal experiments

All experiments reported here with *Xenopus laevis* have been approved by the Lund/Malmö Animal Ethics Committee (Dnr M147-08).

Supplemental references

Hensey, C. and Gautier, J., 1998. Programmed cell death during Xenopus development: a spatio-temporal analysis. Dev. Biol. 203, 36-48.

Kao, K. R. and Elinson, R. P., 1988. The entire mesodermal mantle behaves as Spemann's organizer in dorsoanterior enhanced Xenopus laevis embryos. Dev. Biol. 127, 64-77.

Moriishi, T., Shibata, Y., Tsukazaki, T., Yamaguchi, A., 2005. Expression profile of Xenopus banded hedgehog, a homolog of mouse Indian hedgehog, is related to the late development of endochondral ossification in Xenopus laevis. Biochem. Biophys. Res. Commun. 328, 867-873.

Saka, Y. and Smith, J. C., 2001. Spatial and temporal patterns of cell division during early Xenopus embryogenesis. Dev. Biol. 229, 307-318.

Takabatake, T., Takahashi, T.C., Takabatake, Y., Yamada, K., Ogawa, M., Takeshima, K., 2000. Distinct expression of two types of Xenopus Patched genes during early embryogenesis and hindlimb development. Mech. Dev. 98, 99-104.

Turner, D. L. and Weintraub, H., 1994. Expression of achaete-scute homolog 3 in Xenopus embryos converts ectodermal cells to a neural fate. Genes Dev. 8, 1434-1447.

Paper II

Developmental Cell
Article

The Secreted Serine Protease xHtrA1 Stimulates Long-Range FGF Signaling in the Early *Xenopus* Embryo

Shirui Hou,[1,2] Marco Maccarana,[3] Tan H. Min,[2] Ina Strate,[1,2] and Edgar M. Pera[1,2,*]
[1] Department of Developmental Biochemistry, Institute of Biochemistry and Cell Biology, Georg August University Göttingen, 37077 Göttingen, Germany
[2] Laboratory of Vertebrate Developmental Biology, Lund Strategic Research Center for Stem Cell Biology and Cell Therapy
[3] Department of Experimental Medical Science
Lund University, 22184 Lund, Sweden
*Correspondence: edgar.pera@med.lu.se
DOI 10.1016/j.devcel.2007.07.001

SUMMARY

We found that the secreted serine protease xHtrA1, expressed in the early embryo and transcriptionally activated by FGF signals, promotes posterior development in mRNA-injected *Xenopus* embryos. *xHtrA1* mRNA led to the induction of secondary tail-like structures, expansion of mesoderm, and formation of ectopic neurons in an FGF-dependent manner. An antisense morpholino oligonucleotide or a neutralizing antibody against xHtrA1 had the opposite effects. xHtrA1 activates FGF/ERK signaling and the transcription of FGF genes. We show that *Xenopus* Biglycan, Syndecan-4, and Glypican-4 are proteolytic targets of xHtrA1 and that heparan sulfate and dermatan sulfate trigger posteriorization, mesoderm induction, and neuronal differentiation via the FGF signaling pathway. The results are consistent with a mechanism by which xHtrA1, through cleaving proteoglycans, releases cell-surface-bound FGF ligands and stimulates long-range FGF signaling.

INTRODUCTION

Fibroblast growth factor (FGF) signaling is involved in many aspects of early embryonic development (Böttcher and Niehrs, 2005). Studies in *Xenopus* have first demonstrated a role of FGFs in the induction and migration of mesoderm during trunk and tail development. Inhibition of FGF signaling by a dominant-negative FGF receptor disrupts the development of mesodermal derivatives and prevents posterior cells from undergoing proper gastrulation movements (Amaya et al., 1991). In mice, FGF4 and FGF8 are required for the migration of cells out of the primitive streak and thus for the formation of mesoderm (Sun et al., 1999). FGF signals are also essential for the migration and patterning of mesoderm in *Drosophila* (Huang and Stern, 2005). In *Xenopus* and other vertebrates, FGFs participate in the induction and posteriorization of neural tissue (De Robertis and Kuroda, 2004). In addition, FGFs are involved in many later cell interactions, acting in the developing forebrain and at the midbrain-hindbrain boundary (Dono, 2003), during bone formation (Ornitz, 2005), angiogenesis, and in cancer (Grose and Dickson, 2005).

Proteoglycans are abundant extracellular molecules that consist of a protein core to which highly sulfated glycosaminoglycan chains are covalently attached. According to their sugar composition, the glycosaminoglycans are classified as heparan sulfate, chondroitin sulfate, or dermatan sulfate (Iozzo, 1998; Kramer and Yost, 2003). Syndecans and Glypicans are two main groups of cell-surface heparan sulfate proteoglycans. Biglycan, a soluble molecule of the small leucine-rich proteoglycan family, is a chondroitin or dermatan sulfate proteoglycan. Biochemical and cell culture experiments have identified proteoglycans as coregulators of FGF signaling. Binding of FGFs to heparin or heparan sulfate is crucial for efficient receptor stimulation (Kramer and Yost, 2003). Similarly, dermatan sulfate binds to FGF and potentiates its activity (Trowbridge and Gallo, 2002). In *Drosophila* and mice, phenotypic analyses of mutations that alter the glycosaminoglycan biosynthesis have underscored the importance of proteoglycans for efficient FGF signaling during development (Lin et al., 1999; García-García and Anderson, 2003).

HtrA1 belongs to the HtrA (*H*igh *t*emperature *r*equirement-*A*) family of serine proteases that is well conserved from bacteria to humans (Clausen et al., 2002). HtrA1 was originally isolated as a gene downregulated in SV40-transformed human fibroblasts (Zumbrunn and Trueb, 1996). Overexpression of HtrA1 in cancer cells suppresses growth and proliferation in vivo, suggesting that HtrA1 is a candidate tumor suppressor (Baldi et al., 2002). More recently, a single nucleotide polymorphism in the HtrA1 promoter has been presented as a major risk factor for age-related macular degeneration (DeWan et al., 2006; Yang et al., 2006). HtrA1 binds to and inactivates members of the TGFβ family (Oka et al., 2004) and

modulates insulin-like growth factor (IGF) signals (Hou et al., 2005), but its biological function is not yet known.

We have recently identified the *Xenopus* homolog of HtrA1 (xHtrA1) in a direct screen for secreted proteins (Pera et al., 2005). Here, we introduce xHtrA1 as a modulator of FGF signaling that participates in axial development, mesoderm formation, and neuronal differentiation. xHtrA1 is activated by FGF signals and induces ectopic *FGF4* and *FGF8* transcription. We could identify Biglycan, Syndecan-4, and Glypican-4 as proteolytic targets of xHtrA1 and show that pure heparan sulfate and dermatan sulfate phenocopy xHtrA1 and FGF activities in *Xenopus* embryos. The results suggest that xHtrA1 acts as a positive regulator of FGF signals and, through proteolytic cleavage of proteoglycans, allows long-range FGF signaling in the extracellular space.

RESULTS

Xenopus HtrA1 Is Coexpressed with *FGF8* and Activated by FGF Signals

In an unbiased screen for proteins secreted from early *Xenopus* embryos, we recently isolated a full-length cDNA clone homologous to the extracellular serine protease HtrA1 (Pera et al., 2005). We detected *Xenopus* HtrA1 (xHtrA1) as a 50 kDa protein in the supernatant of transfected and metabolically labeled HEK293T cells (Figure 1A). xHtrA1 has a cleavable signal peptide followed by an IGF-binding domain, a Kazal-type trypsin inhibitor motif, a trypsin-like serine protease, and a carboxyterminal PDZ domain (Figure 1B). xHtrA1 has 68% identity to human and mouse HtrA1 (see Figure S1 in the Supplemental Data available with this article online) and significant conservation of the trypsin and PDZ domains to a *Drosophila* serine protease and *E. coli* HtrA (Figure 1B).

Expression studies using RT-PCR identified initial transcripts of *Xenopus HtrA1* after midblastula transition with elevated RNA levels during gastrulation and neurulation (Figure S2). Whole-mount in situ hybridization revealed a dynamic expression pattern of *xHtrA1* (Figures 1C–1F) that showed striking similarities to sites of FGF signaling (Figures 1G–1J; Christen and Slack, 1997; 1999). Overlapping expression domains with *FGF8* included the blastopore lip at gastrula stage (Figures 1C and 1G), the posterior mesoderm and anterior neural plate after involution (Figures 1D and 1H), the early forebrain and midbrain-hindbrain boundary at the neurula stage (Figures 1E and 1I), and the branchial arch region in tail bud stage embryos (Figures 1F and 1J). In addition, the expression of *xHtrA1* matched with activation of the FGF signaling intermediate ERK in the neural folds (Figure 1E; Christen and Slack, 1999). Even though *xHtrA1* did not perfectly coincide with *FGF8*/ERK activity—transcripts of the protease were more broadly expressed in the anterior neural plate and did not persist in the developing brain—*xHtrA1* gene expression was still affected by FGF signals (Figure 1K). RT-PCR showed that *xHtrA1* transcripts were induced in animal cap explants injected with either *FGF8* or *FGF4* mRNA (Figure 1K, lanes 3 and 4). This activation by members of the FGF family was specific, as *BMP4* mRNA failed to induce *xHtrA1* (Figure 1K, lane 5). In mRNA-injected marginal zone explants, xHtrA1 expression was not reduced by dominant-negative FGF receptors (Figure S3). We conclude that FGF signaling is sufficient, but not required, for *xHtrA1* transcription.

xHtrA1 Induces Secondary Tail-like Structures

To investigate the activity of xHtrA1, synthetic mRNA was injected into *Xenopus* embryos (Figure 2). In early tail bud stage embryos, *xHtrA1* mRNA caused an overall shortening of the embryo and the formation of a second body axis that was anteriorly fused with the primary axis (Figures 2A and 2B). At the swimming tadpole stage, injected *xHtrA1* mRNA led to loss of head structures, including cement gland and eyes, and induced ectopic tail-like outgrowths with dorsal and ventral fins (Figures 2C and 2D). Histologically, the secondary tail-like structures contained spinal cord, notochord and somite tissue (Figure 2E). *xHtrA1* mRNA induced ectopic expression of the neuronal marker *N-tubulin* (Figures 2F and 2G), the axial marker *Sonic hedgehog* (*Shh*; Figures 2H and 2I) and the paraxial mesoderm marker *MyoD* (Figures 2J and 2K).

To determine whether xHtrA1 can induce ectopic structures on neighboring cells, we used the green fluorescent protein (GFP) as a lineage marker. After coinjection of *xHtrA1* and *GFP* mRNA into one ventral blastomere, GFP-positive cells were found in the secondary tail region (Figures 2L and 2L′). Remarkably, dorsal injection of *xHtrA1* and *GFP* mRNA also generated secondary tail-like structures on the belly (Figures 2M and 2M′). These ectopic tail outgrowths arising at the opposite pole of the embryo were devoid of GFP expression clearly showing that xHtrA1 exerts inductive effects at considerable distance.

To investigate the role of the proteolytic domain in the HtrA1 protein, we compared the phenotypic effects of wild-type xHtrA1 with mutant derivatives in which the entire trypsin domain was deleted (xHtrA1Δtrypsin) or the catalytic serine residue in position 307 replaced with alanine (xHtrA1 [S307A]). While wild-type *xHtrA1* mRNA caused anencephaly and secondary tail formation (Figure 2O), embryos injected with *xHtrA1Δtrypsin* or *xHtrA1 (S307A)* mRNA developed normally (Figures 2P and 2Q). Western blot analysis showed that the injected constructs generated equal amounts of proteins of the expected size (Figure 2R). We therefore conclude that the ability of xHtrA1 to induce ectopic tails depends on the integrity of a functional proteolytic domain.

xHtrA1 Stimulates Mesoderm Formation, Dorsalizes the Ectoderm, and Induces Neuronal Differentiation

We next performed whole-mount in situ hybridization with region- and tissue-specific molecular markers (Figure 3). At the early gastrula stage, *xHtrA1* mRNA blocked the anterior ectoderm marker *Otx2* (Figures 3A and 3B) and greatly expanded the pan-mesodermal marker *Xbra* into the animal hemisphere (Figures 3C and 3D), indicating

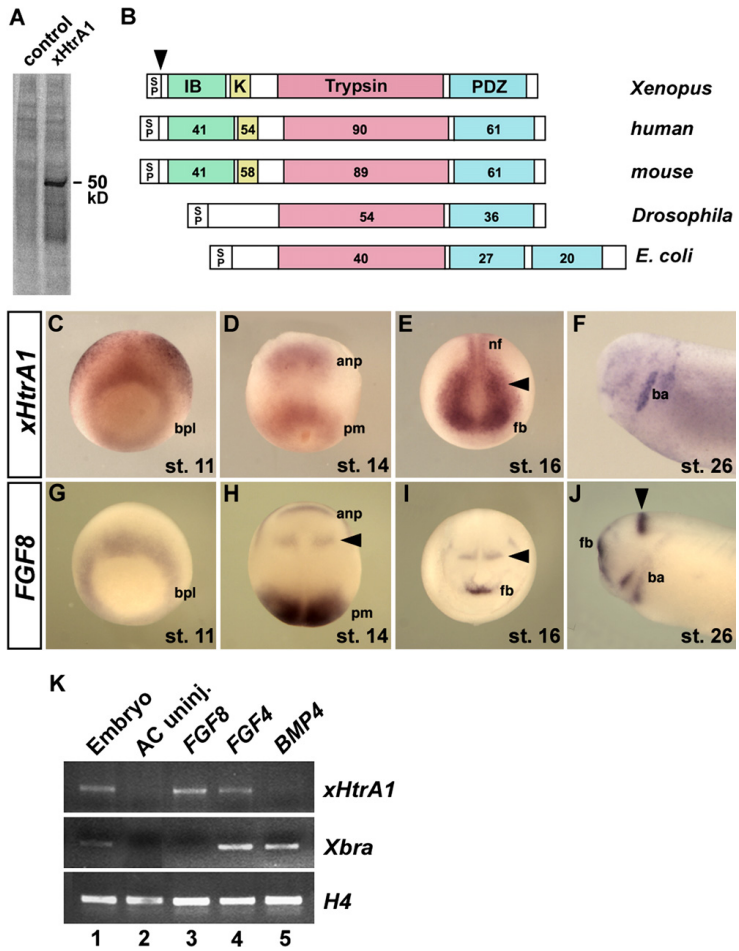

Figure 1. Protein Structure and Gene Expression of xHtrA1

(A) SDS-PAGE of supernatant from transfected and ^{35}S-methionine/cysteine-labeled HEK293T cells. The 50 kDa band corresponds to the secreted xHtrA1 protein.

(B) *Xenopus* HtrA1 and related proteins. SP, signal peptide; IB, insulin-like growth factor binding domain; K, kazal-type serine protease inhibitor domain; Trypsin, trypsin-like serine protease domain; PDZ, PDZ domain. The numbers indicate the percentages of amino acid identity with the corresponding domains in xHtrA1. The GenBank accession numbers are *Xenopus laevis* HtrA1 (EF490997), human HtrA1/L56 (NP 002766), mouse HtrA1 (AAH13516), *Drosophila* serine protease (NP 650366), and *E. coli* HtrA/DegP (X12457).

(C–J) Whole-mount in situ hybridization of *xHtrA1* (C–F) and *FGF8* (G–J) at midgastrula (C and G, vegetal view), early neurula (D and H, dorsal view), midneurula (E and I, anterior view), and tail bud stage (F and J, head). The arrowhead indicates the midbrain-hindbrain boundary. anp, anterior neural plate; ba, branchial arch; bpl, blastopore lip; fb, forebrain; nf, neural folds; pm, posterior mesoderm.

(K) RT-PCR of animal cap explants at stage 18 after injection of *FGF8* (450 pg), *FGF4* (3 pg), or *BMP4* mRNA (200 pg) at the 4-cell stage. H4, histone H4 for normalization.

a conversion of ectoderm into mesodermal tissue. During neurulation, *xHtrA1*-injected embryos failed to express *BF1* (telencephalon), *Rx2a* (eyes), and *Krox20* (rhombomeres 3 and 5 of the hindbrain; Figures 3E–3H). Analysis of isolated neural plate explants revealed that *xHtrA1* mRNA led to a suppression of anterior and upregulation

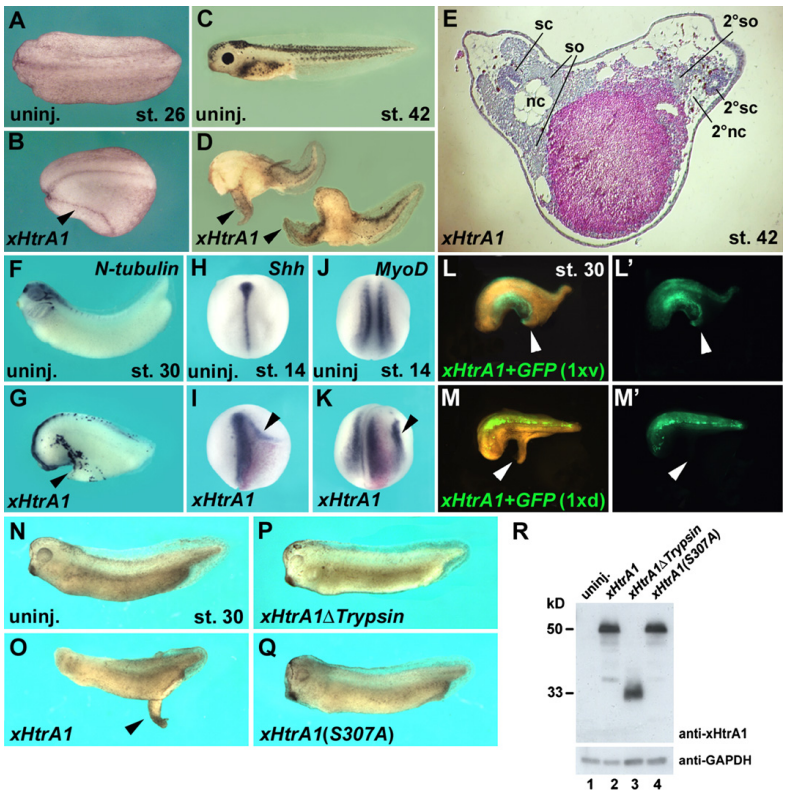

Figure 2. xHtrA1 Blocks Head Formation and Induces Ectopic Tail-like Structures

Embryos were injected into the animal pole of one blastomere at the 4-cell stage with 80 pg of the indicated mRNAs.

(A) Uninjected tail bud embryo (dorsal view, anterior to the left).

(B) *xHtrA1* mRNA induces a secondary axis (arrowhead) fused with the primary body axis at the anterior end.

(C) Uninjected embryo at tadpole stage.

(D) *xHtrA1* induces loss of head tissue and ectopic tail-like structures.

(E) Histological section of *xHtrA1*-injected tadpole embryo. sc, spinal cord; nc, notochord; so, somites.

(F and G) Ectopic *N-tubulin* expression in *xHtrA1*-induced tail outgrowth (arrowhead).

(H–K) Ectopic expression of *Shh* and *MyoD* in early neurulae (dorsal view) adjacent to cells coinjected with *xHtrA1* and nuclear *lacZ* mRNA as lineage tracer (red nuclei).

(L and L′) After a single ventral injection of *xHtrA1* and *GFP* mRNA, injected green cells populate the ectopic tail structures (arrowhead).

(M and M′) Coinjection of *xHtrA1* and *GFP* mRNA into one dorsal blastomere induces an ectopic tail outgrowth distant to injected cells.

(N–Q) While *xHtrA1* mRNA causes anencephaly and ectopic tail formation, *xHtrA1 ΔTrypsin* or *xHtrA1 (S307A)* mRNA are without effects.

(R) Western blot analysis of lysates from mRNA-injected embryos at stage 9 probed for xHtrA1. GAPDH is a loading control.

Ectopic axial structures were induced in B, 21/88; D, 61/203; G, 15/18; I, 3/15; K, 6/19; L, 3/12; M, 4/37; O, 110/124 (head reduction), 37/124 (ectopic outgrowth), P, 0/406, and Q, 0/280 embryos.

of posterior neural marker genes (Figure S4). Injected *xHtrA1* also blocked expression of the heart markers *Nkx2.5* and *Sizzled* in the anterior part of the embryo and expanded the expression domain of *Sizzled* in the ventro-posterior mesoderm (Figures 3I–3L). Moreover, *xHtrA1* mRNA caused significant expansion of *Sox2* (neural plate) concomitant with a reduction of *Slug* (neural crest) and *Cytokeratin* (epidermis; Figures 3M–3R), suggesting that xHtrA1 dorsalizes the ectoderm. In addition, *xHtrA1* induced supernumerary *N-tubulin*-positive neurons on the lateral and ventral sides of the embryo (Figures 3S and 3T). Together, xHtrA1 stimulates mesodermal and posterior fate, dorsalizes the ectoderm, and induces neuronal differentiation.

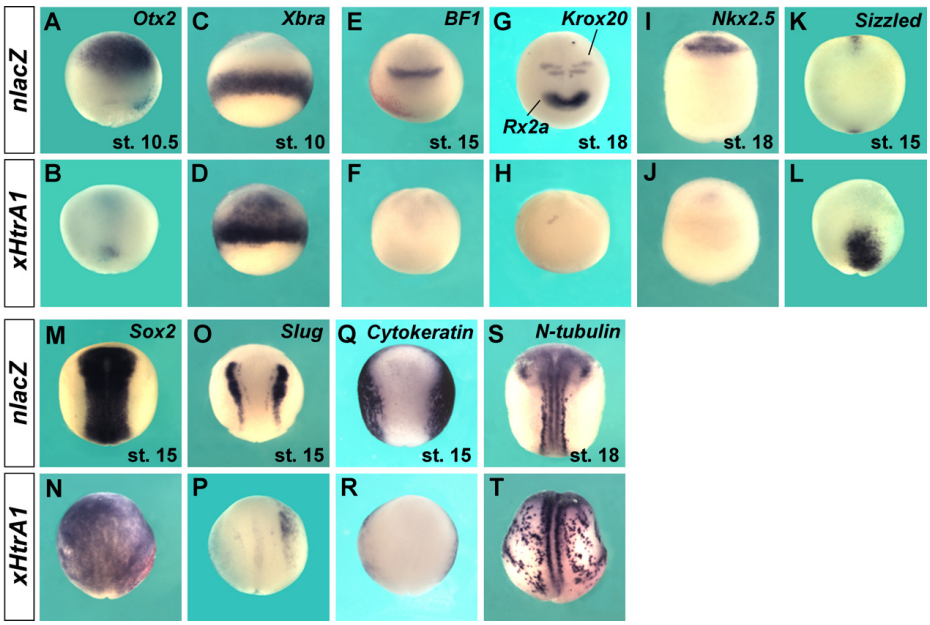

Figure 3. Effects of xHtrA1 on Early Pattern Formation

Whole-mount in situ hybridization of embryos in lateral (A–D), anterior (E–H), ventral (I–L), and dorsal view (M–T). Embryos were animally injected into one blastomere at the 4-cell stage with *nlacZ* mRNA as control or *xHtrA1* mRNA (each 80 pg).

(A–D) In early gastrula embryos, *xHtrA1* mRNA blocks expression of *Otx2* in the anterior ectoderm and expands *Xbra* expression into the animal hemisphere.

(E–L) At the neurula stage, *xHtrA1* mRNA blocks expression of *BF1*, *Rx2a*, *Krox20*, and *Nkx2.5*. *Sizzled* expression is reduced anteriorly but significantly expanded at the posterior end of the embryo.

(M–T) *xHtrA1* mRNA causes expansion of *Sox2* and downregulation of *Slug* and *Cytokeratin* expression. *N-tubulin* expression is ectopically induced. Indicated effects on gene expression were observed in B, 45/45; D, 20/23; F, 22/23; H, 16/20 (*Rx2a*) and 6/20 (*Krox20*); J, 28/36; L, 31/36; N, 62/67; P, 9/9; R, 19/30; and T, 34/49 embryos.

Knockdown of xHtrA1 Promotes Anterior Development and Impairs Mesoderm and Neuronal Differentiation

In order to investigate the endogenous function of xHtrA1, we used an antisense morpholino oligonucleotide approach (Figure 4). A 25-mer morpholino sequence was designed against the translation initiation site of the isolated *xHtrA1* gene (*xHtrA1*-MO) that also targeted a related *xHtrA1* pseudoallele (Figure 4A). Western blot analysis showed that the *xHtrA1*-MO efficiently blocked protein synthesis of injected *xHtrA1* mRNA, whereas a nonspecific control morpholino had no effect (Figure 4B, lanes 1–3). The specificity of the *xHtrA1*-MO was demonstrated by its inability to reduce translation of a recombinant *xHtrA1* construct that is not targeted by the *xHtrA1*-MO (*xHtrA1**; Figure 4B, lanes 4 and 5). By immunoprecipitation with an antibody against xHtrA1, we could show that *xHtrA1*-MO decreased the level of endogenous xHtrA1 protein significantly (Figure 4C).

Microinjection of *xHtrA1*-MO caused enlargement of the head, reduction of the eye size, and significant shortening of the tail, while the control-MO had no effect (Figures 4D–4G). *xHtrA1* morphants showed depletion of *Xbra* (mesoderm), expansion of *BF1* (telencephalon) and *En2* (boundary between mid- and hindbrain), restriction of *Rx2a* (eye field), and reduction of *N-tubulin* expression (neurons; Figures 4H–4O). The *xHtrA1*-MO also erased the posterior expression domain of *Sizzled* (ventral mesoderm), an effect that could be rescued by coinjection of nontargeted *xHtrA1** mRNA (Figures 4P–4S). Similar phenotypes were obtained upon blastocoelic injection of an immunopurified anti-xHtrA1 antibody that suppresses xHtrA1 activity in the extracellular space (Figure S5). Together, the effects of the *xHtrA1*-MO and neutralizing antibody are opposite to those observed in gain-of-function experiments (Figures 2 and 3) and suggest a restrictive function of xHtrA1 in head development, and a supportive role in tail outgrowth, mesoderm formation, and neuronal differentiation.

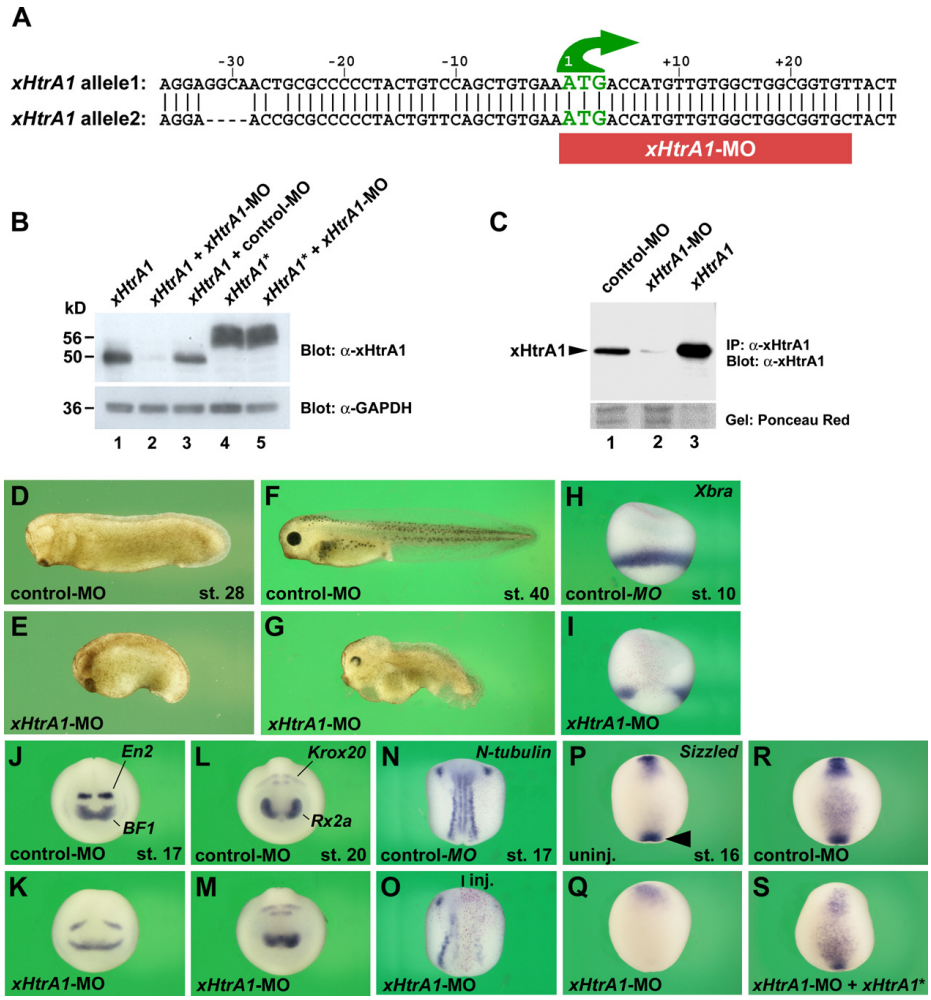

Figure 4. Knockdown of xHtrA1 Promotes Anterior Development and Impairs Mesoderm and Neuronal Differentiation

Morpholino oligonucleotides (MOs) were injected at the 2-cell stage (8 pmol per embryo); *xHtrA1* or nontargeted *xHtrA1** mRNA (see Experimental Procedures) were injected into each blastomere at the 4-cell stage (160 pg total).

(A) *xHtrA1*-MO targets both *Xenopus laevis HtrA1* pseudoalleles.

(B) *xHtrA1*-MO, but not control-MO, inhibits translation of injected *xHtrA1* mRNA at stage 9. *xHtrA1*-MO does not affect the protein synthesis of *xHtrA1** mRNA.

(C) *xHtrA1*-MO blocks endogenous xHtrA1 protein expression at stage 12.

(D–G) *xHtrA1*-MO leads to enlarged head, decreased eye and shortened tail formation after injection into the animal pole and margin of each blastomere.

(H and I) A single marginal injection of *xHtrA1*-MO blocks *Xbra* expression.

(J–M) Animally injected *xHtrA1*-MO broadens the expression domains of *BF1* and *En2*, and restricts *Rx2a* expression.

(N and O) A single animal injection of *xHtrA1*-MO reduces *N-tubulin* expression.

(P–S) Marginally injected *xHtrA1*-MO depletes the posterior *Sizzled* expression domain (arrowhead). *xHtrA1** mRNA reverts the effect of *xHtrA1*-MO. Indicated phenotypes were observed in D, 92/92; E, 60/60; F, 18/18; G, 51/51; H, 17/19; I, 22/28; J, 20/20; K, 35/57; L, 10/10; M, 42/43; N, 15/19; O, 16/18; Q, 41/74; R, 19/19; and S, 15/15 embryos.

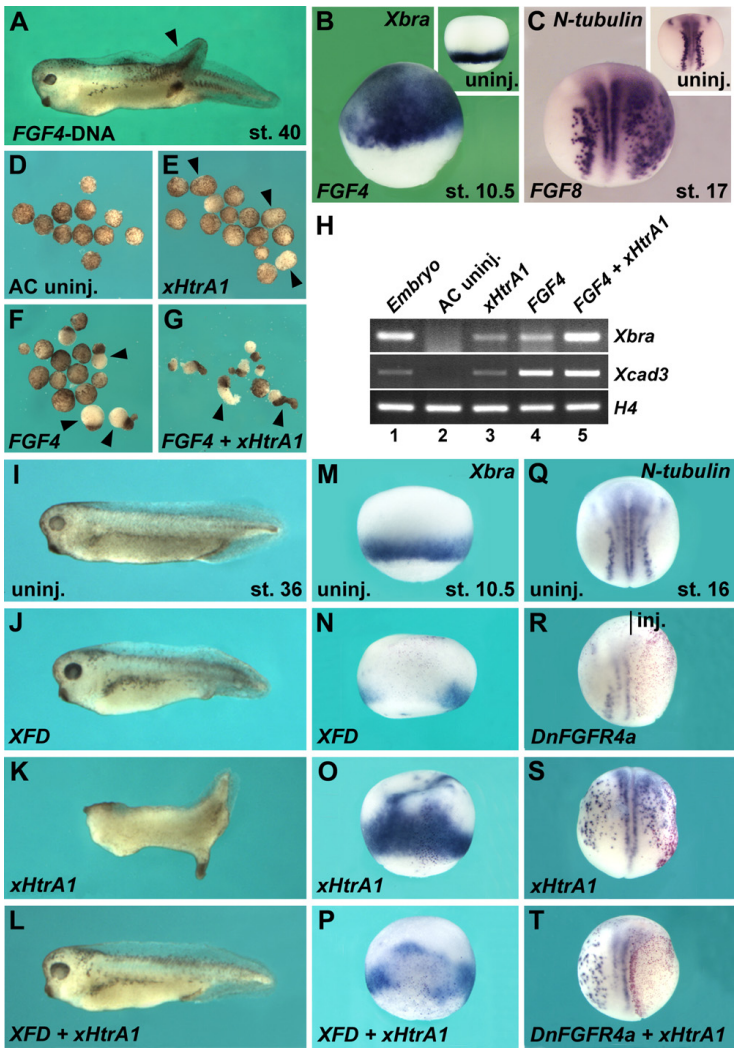

Figure 5. Cooperation between xHtrA1 and FGF Signals

(A) Ectopic tail-like outgrowth (arrowhead) induced after a single ventral injection of pCS2-*FGF4* DNA (4 pg) at the 4-cell stage.
(B) Expansion of *Xbra* expression induced by *FGF4* mRNA (6 pg).
(C) Ectopic *N-tubulin* expression induced by *FGF8* mRNA (5 pg).
(D–G) Animal caps extracted from stage 8 embryos and cultured until stage 25. Caps extend only slightly when injected with *xHtrA1* (360 pg) or *FGF4* (3.2 pg) but show robust elongation when injected with both mRNAs together.
(H) RT-PCR of animal cap explants at stage 11.
(I and J) Animal injection of *XFD* mRNA at the 4-cell stage (110 pg) causes enlargement of head structures.
(K and L) *XFD* restores head development and blocks ectopic tail outgrowth induced by *xHtrA1* mRNA (80 pg).
(M and N) A single marginal injection of *XFD* mRNA (220 pg) disrupts *Xbra* expression.
(O and P) *XFD* inhibits ectopic *Xbra* expression by *xHtrA1* mRNA (80 pg).

Requirement of FGF Signaling for the Activity of xHtrA1

The phenotypic effects observed in *xHtrA1* mRNA-injected embryos are reminiscent of those caused by FGF signals. A single injection of *FGF4* DNA induced secondary tail-like structures (Figure 5A; Pownall et al., 1996), *FGF4* mRNA caused expansion of the mesoderm marker *Xbra* (Figure 5B; Pownall et al., 1996), and *FGF8* mRNA triggered ectopic *N-tubulin*-positive neuronal differentiation (Figure 5C; Hardcastle et al., 2000). The similar activities of xHtrA1 and FGFs suggested that both proteins may functionally interact. To test this hypothesis, we analyzed mesoderm induction in animal cap explants (Figures 5D–5H). While uninjected control caps formed spherical ectodermal structures (Figure 5D), few caps elongated when injected with *xHtrA1* mRNA (Figure 5E) or a suboptimal dosis of *FGF4* mRNA (Figure 5F), indicating formation of mesoderm tissue. Strikingly, coinjection of both *FGF4* and *xHtrA1* mRNA caused dramatic elongation of all animal caps (Figure 5G). RT-PCR analysis of the injected animal caps revealed that *xHtrA1* mRNA alone activated the mesodermal marker genes *Xbra* and *Xcad3* (Figure 5H, lane 3) and, in combination with *FGF4* mRNA, further increased *Xbra* expression (Figure 5H, lane 5). The results show that xHtrA1 induces mesoderm differentiation and cooperates with FGF signals.

To test whether FGF signals are required for the actions of xHtrA1, we blocked endogenous FGF signaling using dominant-negative FGF receptor constructs (Figures 5I–5T). Microinjection of *XFD* (*DnFGFR1*) mRNA enlarged head structures at the expense of trunk and tail development (Figures 5I and 5J; Amaya et al., 1991). Notably, *XFD* restored head development and interfered with ectopic tail formation in embryos coinjected with *xHtrA1* mRNA (Figures 5K and 5L). Furthermore, *XFD* blocked endogenous expression of the mesoderm marker *Xbra* (Figures 5M and 5N; Amaya et al., 1993) and ectopic *Xbra* expression induced by *xHtrA1* (Figures 5O and 5P). An involvement of FGF signals in the formation of differentiated neurons is evident from the loss of *N-tubulin* expression by *DnFGFR4a* mRNA (Figures 5Q and 5R; Hongo et al., 1999; Hardcastle et al., 2000). While *xHtrA1* mRNA induced ectopic neurons even on the noninjected contralateral side (Figure 5S), neurogenesis was blocked in cells that were coinjected with *xHtrA1* and *DnFGFR4a* (Figure 5T). In conclusion, multiple patterning activities of xHtrA1, including axis development, mesoderm formation, and neuronal differentiation, rely on an intact FGF signaling pathway.

xHtrA1 Stimulates FGF Signaling at Distance

To investigate whether xHtrA1 affects FGF activity, we analyzed the activation of the FGF signaling intermediate ERK by immunoblotting (Figure 6A). Microinjection of *xHtrA1* mRNA led to an accumulation of diphosphorylated ERK (dpERK; Figure 6A, lanes 1 and 2). In contrast, the *xHtrA1*-MO blocked ERK phosphorylation (Figure 6A, lanes 3 and 4), indicating a requirement for xHtrA1 in the activation of FGF signaling. Immunohistochemical staining of gastrula embryos revealed an xHtrA1-induced expansion of dpERK expression from the marginal zone into the animal hemisphere (Figures 6B and 6C). In neurula embryos, *xHtrA1* also induced ectopic *FGF8* and *FGF4* transcription (Figures 6E, 6F, 6H, and 6I). The effects of *xHtrA1* were blocked by coinjection of *XFD* or *DnFGFR4a* mRNA (Figures 6D, 6G, and 6J), suggesting that xHtrA1 may stimulate ERK phosphorylation and the expression of *FGF8* and *FGF4* via the FGF receptors. Based on these and previous data (Figure 1K), we conclude that xHtrA1 and FGF may form a positive feedback loop in which overexpression of each component reinforces the gene activity of the other (Figure 6K).

We next studied whether xHtrA1 promotes long-range FGF signaling using an animal cap conjugate assay (Figures 6L–6R). Animal caps from embryos injected with *FGF4*, *xHtrA1*, and *nlacZ* mRNA as lineage tracer (''inducer'' caps) were first recombined with uninjected ''responder'' caps, incubated in vitro for 4.5 hours, and analyzed by in situ hybridization for *Xbra* expression (Figure 6L, upper half). Control conjugates injected with *nlacZ* mRNA alone were spherical and did not express *Xbra* (Figure 6M). Following microinjection of *FGF4* mRNA, the responding hemisphere slightly elongated and showed weak *Xbra* expression confined to the interface with the inducer hemisphere (Figure 6N). *xHtrA1* mRNA on its own had only a weak effect (Figure 6O) but, in combination with *FGF4* mRNA, triggered a robust outgrowth of the responder cap. Importantly, the levels of *Xbra* expression were greatly elevated and expanded to locations far away from the sites of FGF4 secretion (Figure 6P). In an independent experiment, we recombined inducer caps with *xHtrA1* mRNA-injected responder caps (Figure 6L, lower half). While *nlacZ*-injected inducer caps were without effect (Figure 6Q), juxtaposition of *FGF4* and *xHtrA1* sources triggered elongation of both hemispheres and resulted in strong and widespread *Xbra* expression (Figure 6R). The fact that *nlacZ*-labeled cells from the inducer cap did not intermingle with responder cap cells indicates that the effects of xHtrA1 were not due to cell movements. The results strongly indicate that xHtrA1 stimulates long-range signaling of FGFs.

xHtrA1 Causes Proteolytic Degradation of Biglycan, Syndecan-4, and Glypican-4

Proteoglycans are important regulators of FGF signaling that control the spread and activity of FGF ligands in the

(Q and R) A single animal injection of *DnFGFR4a* mRNA (110 pg) suppresses *N-tubulin* expression. *nlacZ* mRNA was coinjected as lineage tracer (red nuclei).
(S and T) *DnFGFR4a* blocks *N-tubulin* expression induced by *xHtrA1* mRNA (80 pg) on the injected side.
Frequency of embryos with the indicated phenotype was A, 13/66; B, 23/23; C, 118/120; J, 54/68; K, 68/80 (head reduction) and 32/80 (ectopic tail), L, 13/16; N, 38/47; O, 13/13; P, 16/18; R, 18/18; S, 10/12; and T, 10/10.

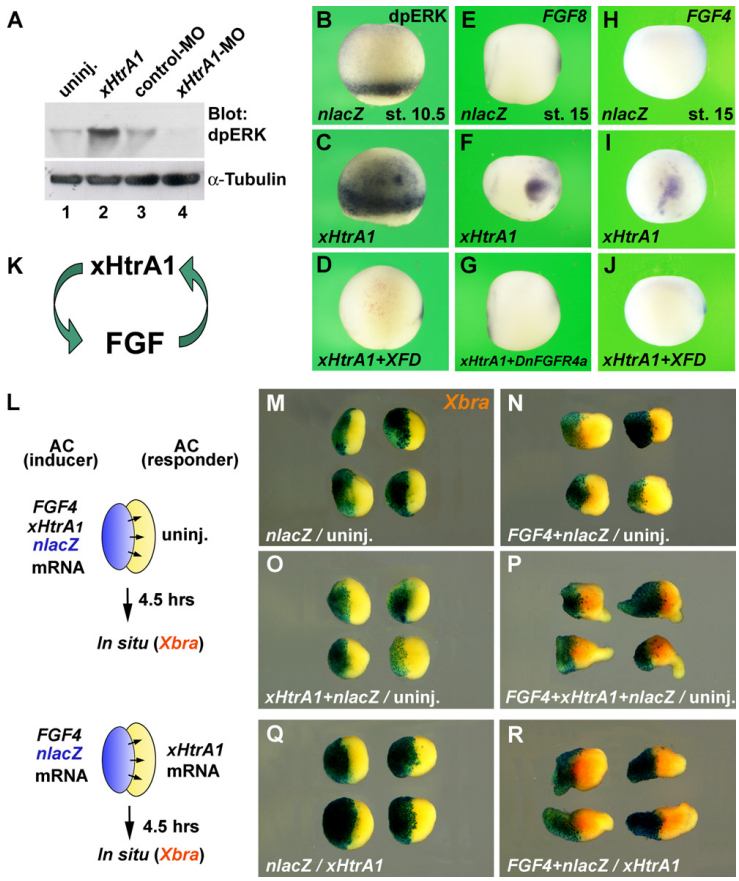

Figure 6. xHtrA1 Activates Long-Range FGF Signaling

(A) Western blot analysis of stage 14 embryos. Injection of *xHtrA1* mRNA (80 pg) induces diphosphorylated ERK (dpERK). *xHtrA1*-MO (8 pmol), but not control-MO, reduces endogenous dpERK.

(B–D) Whole-mount immunohistochemistry of early gastrula embryos probed for diphosphorylated ERK (dpERK). *xHtrA1* mRNA (80 pg) induces ectopic dpERK in the animal cap. *XFD* mRNA (220 pg) blocks endogenous and *xHtrA1*-induced dpERK expression.

(E–J) Whole-mount in situ hybridization of early neurula embryos (lateral view). *xHtrA1* mRNA (80 pg) induces robust expression of *FGF8* and *FGF4*. The effects of *xHtrA1* on *FGF8* and *FGF4* are reverted by coinjection of *DnFGFR4a* (110 pg) and *XFD* mRNA (220 pg), respectively.

(K) Reciprocal stimulation of *xHtrA1* and FGF gene activities.

(L) Experimental design of animal cap conjugate assay. The doses of mRNAs injected into each blastomere at the 4-cell stage were *FGF4* (16 pg) and *xHtrA1* (130 pg).

(M) Control animal cap conjugates with *nlacZ* mRNA-injected inducer cap (blue), and uninjected responder cap remain round and do not express *Xbra*.

(N) Slight elongation and narrow *Xbra* expression (red) in the responder cap at the interface to the inducer cap injected with *FGF4* mRNA.

(O and P) *xHtrA1* mRNA alone has only little effect but, when coinjected with *FGF4* into the inducer cap, induces significant elongation and robust *Xbra* expression in the responder cap.

(Q and R) *FGF4* in the inducer cap juxtaposed to an *xHtrA1*-injected responder cap causes significant elongation of the conjugate and *Xbra* expression far away from the signaling source.

Frequency of specimen with the indicated phenotype was B, 11/11; C, 21/21, D, 26/26; E, 10/10; F, 26/27; G, 25/27; H, 16/16; I, 12/12; J, 10/12; M, 16/16; N, 12/12; O, 10/12; P, 15/18; Q, 10/10; and R, 22/25.

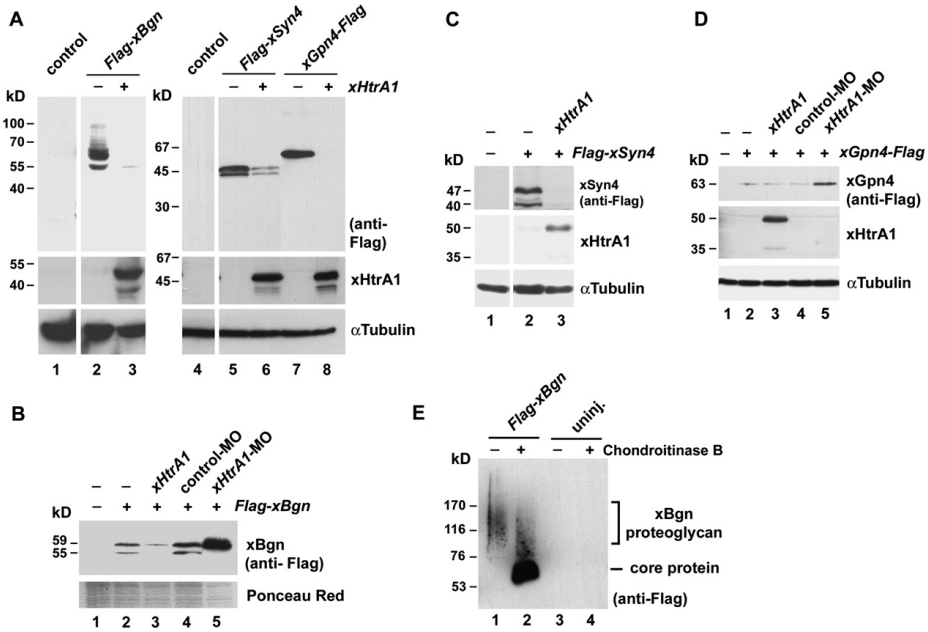

Figure 7. xHtrA1 Causes Proteolytic Cleavage of *Xenopus* Biglycan, Syndecan-4, and Glypican-4

(A) HEK293 cells were transfected with cDNAs, serum-starved for 48 h and proteins in cell lysates analyzed by Western blot with antibodies against Flag (for xBgn, xSyn4, and xGlp4), xHtrA1, and α-Tubulin.

(B–D) *Xenopus* embryos were injected at the 2-cell stage with control- or *xHtrA1*-MO (8 pmol per embryo) and at the 4-cell stage with mRNAs of *xHtrA1* (300 pg in B and 180 pg in C and D), *Flag-xBgn* (500 pg), *Flag-xSyn4* (150 pg), and *xGlp4-Flag* (60 pg). Proteins were extracted and analyzed at stage 22.

(E) *Flag-xBgn* mRNA (100 pg) was injected at the 4-cell stage; proteoglycans were extracted at stage 22, anion-exchange purified and treated with Chondroitinase B.

extracellular space (Trowbridge and Gallo, 2002; Kramer and Yost, 2003). It has previously been reported that an aminoterminally truncated mouse HtrA1 construct consisting only of the trypsin and PDZ domains degrades bovine Biglycan (Tocharus et al., 2004). *Xenopus* Biglycan (xBgn) as well as the heparan sulfate proteoglycans Syndecan-4 (xSyn4) and Glypican-4 (xGlp4) are expressed in the early embryo (Galli et al., 2003; Moreno et al., 2005; Munoz et al., 2006). We transfected full-length xHtrA1 cDNA together with flag-tagged xBgn, xSyn4, and xGlp4 constructs into HEK293 cells. Western blot analysis showed that xHtrA1 caused degradation of all three proteoglycans (Figure 7A). In *Xenopus* embryos, microinjection of *xHtrA1* mRNA decreased the protein levels of Flag-xBgn, whereas *xHtrA1*-MO had the opposite effect (Figure 7B), strongly suggesting that endogenous xHtrA1 cleaves xBgn in vivo. We also observed that injected *xHtrA1* mRNA degraded Flag-xSyn4 (Figure 7C). *xHtrA1* mRNA did not appear to affect xGlp4-Flag, but *xHtrA1*-MO led to an accumulation of this protein in the embryo (Figure 7D), indicating that endogenous xHtrA1 largely degraded xGlp4-Flag. Together, the results suggest that xBgn, xSyn4, and xGlp4 are proteolytic targets of xHtrA1 activity.

Biglycan contains one or two dermatan/chondroitin sulfate (DS/CS) chains that are released upon digestion of the protein core (Trowbridge and Gallo, 2002). DS arises from CS through epimerization of glucuronic acid into iduronic acid (Maccarana et al., 2006). As DS, but not CS, binds to and activates FGFs (Trowbridge et al., 2002), we assessed the nature of the glycosaminoglycan in xBgn. Treatment of anion exchange-purified proteoglycans from *Xenopus* embryos with Chondroitinase B caused a mobility shift of Flag-tagged xBgn (Figure 7E), confirming the presence of DS chains in *Xenopus* Biglycan.

Heparan Sulfate and Dermatan Sulfate Induce Posteriorization, Mesoderm, and Neuronal Differentiation in an FGF-Dependent Manner

We compared the biological activities of exogeneously added heparan sulfate (HS), DS, and the chondroitin sulfates CSE and CSA in early *Xenopus* embryos

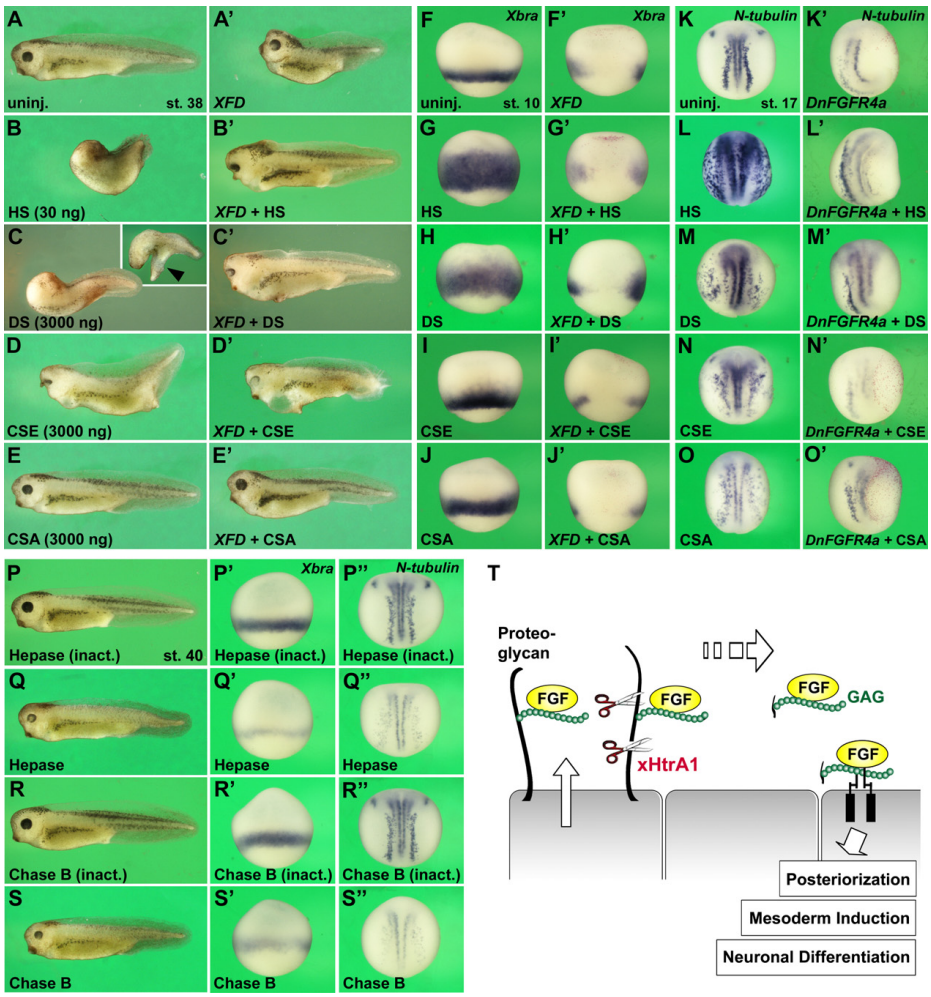

Figure 8. Heparan Sulfate and Dermatan Sulfate Induce Posteriorization, Mesoderm, and Neuronal Differentiation in an FGF-Dependent Manner

(A–E) Heparan sulfate (HS, 30 ng), dermatan sulfate (DS, 3000 ng), and the chondroitin sulfates (CSE and CSA, each 3000 ng) were injected into the blastocoel at stage 8. Note the loss or reduction of head structures by HS, DS, and CSE, and the induction of an ectopic tail-like outgrowth by DS (arrowhead).

(A′–E′) Injection of *XFD* mRNA at the 4-cell stage (110 pg/embryo) reverts the posteriorizing effects of HS, DS and CSE.

(F–J, F′–J′) HS and DS injected at stage 6.5 significantly expand *Xbra* expression, which is blocked by *XFD* mRNA (220 pg).

(K–O, K′–O′) HS, DS, CSE, and CSA injected at stage 8 expand *N-tubulin* expression, which is blocked by *DnFGFR4a* mRNA (110 pg).

(P–S, P′–S′) Blastocoelic injection at stage 6.5 of Heparitinase (16.5 microunits per embryo) or Chondroitinase B (25 microunits) affect axial development and *Xbra* expression. Heat-inactivated enzymes have no effects.

(P′′–S′′) Heparitinase or Chondroitinase B injected at stage 8 influences *N-tubulin* expression.

Frequency of embryos with the indicated phenotype was B, 63/63; C, 98/110 (anencephaly) and 20/110 (ectopic tail); D, 47/47; E, 53/53; B′, 11/11; C′, 7/7; D′, 5/6; E′, 9/13; G, 29/30; H, 48/51; I, 10/20 (slight expansion); J, 9/9; G′, 46/46; H′, 41/41; I′, 50/50; J′, 43/43; L, 63/63; M, 52/59 (slight expansion); N, 35/36 (slight expansion); O, 24/33 (slight expansion); L′, 22/22; M′, 13/13; N′, 35/35; O′, 16/17; P, 45/45; Q, 92/96; R, 48/48; S, 58/62; P′, 19/19; Q′, 27/27; R′, 29/29; S′, 26/31; P′′, 19/19; Q′′, 20/26; R′′, 35/35; and S′′, 27/27.

(Figure 8). DS contains a high proportion of iduronic acid, which is absent in chondroitin sulfates (Trowbridge and Gallo, 2002). CSE has additional 6-O-sulfate compared with CSA. Upon injection into the blastocoel, HS caused loss of head structures (Figures 8A and 8B). Likewise, DS at a 100-fold higher dosis resulted in anencephaly and occasional induction of secondary tails (Figure 8C). In contrast, CSE had little and CSA no effect on head development and failed to induce ectopic tail-like structures (Figures 8D and 8E). Importantly, defects in head development were reversed when embryos had been injected with *XFD* mRNA (Figures 8A′–8E′). In addition, HS and DS, but not CSE and CSA, caused robust expansion of mesoderm (*Xbra*; Figures 8F–8J). While HS strongly induced ectopic neurons, DS, CSE, and CSA only moderately expanded the neuronal territory (*N-tubulin*; Figures 8K–8O). These effects are strikingly similar to those induced by xHtrA1 (Figure 3) and FGF signals (Figure 5). *XFD* and *DnFGFR4* mRNA obscured ectopic mesoderm induction and neuronal differentiation, respectively (Figures 8F′–8J′ and Figures 8K′–8O′), indicating that the glycosaminoglycans require an intact FGF signaling pathway to exert their activities.

To investigate the function of endogenous glycosaminoglycans during early development, we used Heparitinase and Chondroitinase B, which specifically degrade HS and DS, respectively (Figures 8P–8S′′). In a previous study, blastocoelic injection of Heparitinase interfered with axial development and mesoderm induction (Brickman and Gerhart, 1994). Our results show that not only Heparitinase but also Chondroitinase B affected head and tail development, while embryos injected with heat-inactivated enzymes developed normally (Figures 8P–8S). In addition, Heparitinase and Chondroitinase B treatment influenced the expression of *Xbra* (Figures 8P′–S′) and *N-tubulin* (Figures 8P′′–8S′′), suggesting that HS and DS may exert a supportive role during axis development, mesoderm formation, and neurogenesis. In sum, the findings support a functional interaction between xHtrA1, proteoglycans and FGF that facilitates inductive processes in the developing embryo.

DISCUSSION

In this study, we investigated the role of the secreted serine protease HtrA1 in the early *Xenopus* embryo. By gain- and loss-of-function experiments, we have shown that xHtrA1 regulates, and is essential for, proper head and tail development, mesoderm induction, and neuronal differentiation. Our findings are consistent with a mechanism by which xHtrA1, through cleavage of proteoglycans, releases soluble FGF-glycosaminoglycan complexes that promote the range and intensity of FGF signals in the extracellular space.

Previous studies have shown that mouse HtrA1 binds to several members of the TGFβ family and inhibits BMP2 and BMP4 in cultured cells (Oka et al., 2004). Moreover, human HtrA1 modulates insulin-like growth factor (IGF) signaling by cleaving the IGF-binding protein-5 (Hou et al., 2005). These interactions may contribute to some of the effects observed for xHtrA1 in *Xenopus* embryos, as soluble BMP antagonists induce dorsalization of the ectoderm and neuronal differentiation (Pera et al., 2003; De Robertis and Kuroda, 2004), and suppression of IGF signaling causes loss of head tissue (Pera et al., 2001). However, other activities of xHtrA1, most notably the stimulation of mesoderm and induction of secondary tail structures, cannot be explained by a negative regulation of TGFβ/BMP and IGF signals. Several findings suggest instead a link of xHtrA1 to FGF signaling.

The expression pattern of *xHtrA1* is very similar to that of *FGF8* (Christen and Slack, 1997), and its transcription is induced by FGF signals (Figure 1), indicating that *xHtrA1* may be an FGF target gene. It has been proposed that genes sharing expression sites form a synexpression group and, as such, may functionally interrelate (Niehrs and Meinhardt, 2002). xHtrA1 and FGF signals have several common activities. First, anencephaly and secondary tail-like structures, as induced by *xHtrA1* mRNA (Figure 2), have also been observed after misexpression of *FGF4* (Pownall et al., 1996) or components of the FGF-MAPK pathway, such as constitutively active FGF receptor-1, activated Ras, or the Ets-type transcription factor ER81 (Chen et al., 1999; Böttcher et al., 2004). Second, *xHtrA1* stimulates mesoderm development, as shown by the formation of secondary notochord and somite tissue in mRNA-injected embryos (Figure 2), expansion of the pan-mesodermal marker *Xbra* (Figure 3), and de novo induction of mesodermal marker genes in isolated animal cap explants (Figure 5). Overexpression of *FGF4* or other activators of FGF-MAPK signaling also cause mesoderm induction (Isaacs et al., 1994; Böttcher et al., 2004). Third, xHtrA1 markedly expanded the neural plate at the expense of neural crest and epidermal tissue, and stimulated neuronal differentiation (Figure 3), a phenotype that also results from overexpression of *FGF8* through ERK-mediated repression of Smad1 activity (Pera et al., 2003). Together, the effects of xHtrA1 are indistinguishable from those caused by FGF signals, indicating that xHtrA1 may act through activating the FGF pathway. Moreover, knockdown of xHtrA1 by microinjection of specific morpholino oligonucleotides or of a neutralizing antibody resulted in enlarged head structures, shortened tails, and reduction of mesoderm and neuronal development (Figure 4). These phenotypes are reminiscent of those caused by dominant-negative FGF receptors (Amaya et al., 1991; Hardcastle et al., 2000), suggesting that xHtrA1 may play a role in allowing FGFs to signal.

(T) Model for the stimulation of long-range FGF signaling by the secreted serine protease xHtrA1. xHtrA1 cleaves the protein moiety of proteoglycans and releases biologically active FGF bound to glycosaminoglycan (GAG). The FGF-GAG complex activates the FGF receptor on cells distant to its site of origin.

Epistatic experiments demonstrated that the xHtrA1-mediated posteriorization of the embryonic axis, induction of mesoderm, and stimulation of neuronal differentiation rely on an intact FGF pathway (Figure 5). Importantly, xHtrA1 was sufficient and required for activation of the FGF signaling intermediate ERK and induced ectopic *FGF8* and *FGF4* gene expression (Figure 6). On the other hand, excessive FGF signals promoted xHtrA1 transcription (Figure 1K), suggesting that the xHtrA1 and FGF genes mutually activate each other (Figure 6K). The autoinduction of modulators is a reoccurring theme in growth factor signaling, and the FGF8 synexpression group is a paradigm therefore (Niehrs and Meinhardt, 2002; Tsang and Dawid, 2004). The transmembrane protein XFLRT3, whose gene expression is activated by FGFs, binds to the FGF receptor at the cell surface and, similarly as xHtrA1, stimulates FGF signaling (Böttcher et al., 2004). On the other hand, the membrane-bound Sef and cytosolic Sprouty and Spred proteins block the FGF pathway intracellularly and establish a negative feedback loop (Fürthauer et al., 2002; Tsang et al., 2002; Sivak et al., 2005). Hence, xHtrA1 adds to an intricate network of feedback-regulated factors that modulate the activity of this important signaling pathway. In *Xenopus*, FGF4 induces *Xbra* expression via the transcription factor Ets2 and, in turn, Xbra induces *FGF4* expression (Isaacs et al., 1994; Kawachi et al., 2003). Our results suggest that xHtrA1 is integrated in this positive feed-forward network. It has been proposed that such a self-regulated biological signaling loop contributes to the establishment of local organizing centers (Tsang and Dawid, 2004). This system of regulation may explain how misexpression of xHtrA1, FGF4, or Ets-type transcription factors eventually leads to complex secondary tail-like outgrowths.

In transfected cells and *Xenopus* embryos, xHtrA1 triggers the proteolytic cleavage of *Xenopus* Biglycan, Syndecan-4, and Glypican-4 (Figures 7A–7D). This finding supports a previous in vitro study that identified bovine Biglycan as a substrate of N-terminally truncated mouse HtrA1 (Tocharus et al., 2004). It remains to be shown whether Syndecan-4 and Glypican-4 are directly cleaved by xHtrA1 or by other proteases that are activated by xHtrA1. Interestingly, Glypican-4 binds FGF2 and modulates FGF signaling in *Xenopus* (Galli et al., 2003), underscoring the notion that proteoglycans may mediate the stimulatory effect of xHtrA1 on FGF activity.

Using blastocoelic injections, we could demonstrate that heparan sulfate and dermatan sulfate triggered posteriorization of the embryonic axis, mesoderm induction, and neuronal differentiation (Figures 8A–8O′). Not only are the effects of heparan sulfate and dermatan sulfate reminiscent of those caused by FGF signals, but they also occur in an FGF-dependent manner. Interestingly, the biological potency of a given glycosaminoglycan (GAG) correlates with its reported affinity to FGFs. Heparan sulfate and dermatan sulfate, but not chondroitin sulfate, share a high content of iduronic acid, which renders conformational flexibility to the GAG chain and facilitates tight binding to FGF and its receptor (Trowbridge et al., 2002; Kramer and Yost, 2003). Using GAG-specific degrading enzymes, we could show that abrogation of endogenous heparan sulfate and dermatan sulfate affect proper development of the primary axis, mesoderm induction, and neuronal differentiation (Figures 8P′–S′), suggesting a contribution of both heparan sulfate and dermatan sulfate to FGF signaling in the embryo.

Based on these results, we propose a model that explains of how the secreted serine protease xHtrA1 may stimulate FGF signals in the extracellular space (Figure 8T). As FGFs have high affinities for GAG side chains of proteoglycans, the FGFs are normally sequestered on or nearby to cells from which they are secreted, consistent with their function as short-range intercellular signaling molecules (Häcker et al., 2005; Bülow and Hobert, 2006). The secreted serine protease xHtrA1 triggers the cleavage of proteoglycans, such as Biglycan, Syndecan-4, or Glypican-4, thereby releasing soluble FGF-GAG complexes. In this way, FGFs are able to reach cells far away from their site of synthesis and activate FGF receptors at distance. Since GAGs strengthen the binding of FGF ligands to their receptors, the FGF-GAG complexes also increase the overall signaling intensity. This model is consistent with our observation that xHtrA1 promotes histotypic differentiation and FGF/ERK signaling over considerable distances (Figures 2, 5, and 6). Remarkably, all previously reported feedback modulators of the FGF pathway act in a cell-autonomous manner (Tsang and Dawid, 2004). To our knowledge, xHtrA1 is the first example of an FGF-induced molecule that regulates this important signaling factor over a long range.

Does the functional link between HtrA1 and FGF apply to other aspects of vertebrate development or human disease? During skeletal development, mouse HtrA1 overlaps with FGFs and their cognate receptors in precartilage condensations, ossification centers, and the bone matrix (Oka et al., 2004; Ornitz, 2005), suggesting a possible interaction between HtrA1 and FGF during growth, differentiation, and remodeling of bones. Finally, the neovascularization phenotype observed in age-related macular degeneration is associated with upregulation of HtrA1 (DeWan et al., 2006; Yang et al., 2006) and increased FGF gene expression (Kitaoka et al., 1997), suggesting a pathophysiological link for HtrA1 and angiogenic FGF signals in this eye disorder. Thus, our finding of a functional interaction between HtrA1 and FGFs may not only be relevant to answer questions related to early development, but also for understanding bone biology and the etiology of a common cause of blindness.

EXPERIMENTAL PROCEDURES

Expression Construct, Morpholino Oligos, Glycosaminoglycans, and Enzymes

A full-length cDNA clone of *xHtrA1* in pcDNA3 was obtained by secretion cloning (Pera et al., 2005) and fully sequenced (GenBank accession number EF490997). The insert was subcloned into pCS2 and used as template to construct pCS2-*xHtrA1Δtrypsin* (deletion of amino acids 151–343), pCS2-*xHtrA1 (S307A)*, and pCS2-*xHtrA1**(substitution of the leader peptide with the signal peptide of chordin and

a flag tag sequence). pCS2-Flag-xSyn4 is as described (Munoz et al., 2006). xBgn (Moreno et al., 2005) lacking the leader peptide but including the chordin signal peptide, and a flag tag at the N-terminus was subcloned to generate pCS2-Flag-xBgn. Amino acids 1–539 of xGly4 (Pera et al., 2005) were fused with a flag tag at the C terminus to generate pCS2-xGly4-Flag. The *xHtrA1*-MO (5′-ACA CCG CCA GCC ACA ACA TGG TCA T-3′) and standard control-MO were obtained from Gene Tools LLC. Heparan sulfate (HS4, from heparin byproducts), chondroitin sulfate A (chondroitin-4-sulfate, from bovine nasal cartilage), and dermatan sulfate (from bovine lung) were kindly provided by Dr. A. Malmström and prepared as described in Westergren-Thorsson et al. (1991) and below. Chondroitin sulfate E (from squid cartilage), Heparitinase (EC4.2.2.8) and Chondroitinase B (EC4.2.2) were purchased from Seikagaku.

Dermatan Sulfate Preparation

Bovine lung dermatan sulfate was prepared according to Stern et al. (1968). To be certain that heparin and heparan sulfate would not be present as contaminants, deamination at pH 1.5 (Shively and Conrad, 1976) was performed. The absence of heparin/heparan sulfate was confirmed by lack of 232 nm absorbance following extensive heparinase treatment. The preparation contains approximately 90% iduronic acid/total hexuronic acid, and the relative proportion of disaccharides according to the method of analysis by Midura et al. (1994) is: ΔA (Hex-GalNac-4-sulfated in the parent chain) 86.3%, ΔC (Hex-GalNac-6-sulfated) 4.7%, ΔE (Hex-4-sulfated-GalNac-6-sulfated) 5.5%, and ΔB (Hex-2-sulfated-GalNac-4-sulfated) 3.5%.

Antibody Production

A carboxyterminal fragment of xHtrA1 (amino acids 351–445) was produced in *E. coli* as a GST-fusion protein using the pGEX-5X-1 vector (Stratagene) and purified using Glutathione-Agarose (Sigma). Polyclonal antibody against the purified xHtrA1 fragment was raised in rabbits (Bioscience, Göttingen, Germany). Preserum and immunized serum were subjected to immunoaffinity purification using the Amino-Link Plus Immobilization Kit (Pierce). The concentration of IgG was measured with the Bradford reagent (Sigma).

Cell Culture and Immunoblotting

HEK293T cells were transiently transfected using the calcium phosphate method, labeled with ^{35}S-methionine/^{35}S-cysteine, and the supernatants were analyzed by SDS-PAGE and autoradiography as described (Pera et al., 2005). HEK293 cells were grown to 50% confluence in 6-well plates and transiently transfected with 3 μg of each DNA using Lipofectamin-2000 (Invitrogen). After 24 hr, the medium was exchanged against serum-free medium. Three days after the transfection, the cells were lysed with 200 μl lysis buffer (20 mM Tris pH8.3, 150 mM NaCl, 1% NP-40, 1 mM EDTA, 1 mM PMSF, and protease inhibitor cocktail). Embryos were lysed in the same lysis buffer (10 μl per embryo). Proteins in cleared lysates were separated by 10% SDS-PAGE and western blots performed using the following antibodies: immuno-purified anti-xHtrA1 (5 μg/ml), anti-GAPDH (1:2500, Abcam, 9485), anti-dpERK (1:1000; Cell Signaling, 9101), anti-Flag HRP-conjugated (1:1000 or 1:5000; Sigma, A8592), and anti-α-tubulin (1:2000; Sigma, T9026).

xHtrA1 Immunoprecipitation

Embryos at stage 12 were lysed in 50 mM HEPES pH 7.5, 150 mM NaCl, 1% NP40, 1 mM EDTA, 1% glycerol, 1 mM DTT, protease inhibitor cocktail. Cleared lysates containing 2 mg of extracted proteins were incubated with 10 μl ProteinA-Sepharose beads (Amersham Biosciences) crosslinked to 10 μg immunopurified anti-xHtrA1 IgG (crosslinker DSS, Pierce, used according to the manufacturer's instructions). After overnight incubation, the beads were washed in lysis buffer and the pulled down xHtrA1 released by boiling in Laemmli buffer. The western blot was stained with 2 μg/ml anti-xHtrA1 and decorated with anti-native rabbit IgG (eBioscience; 1:1000). The use of crosslinked primary antibody and anti-native IgG-conjugate reagent completely eliminated the unspecific signals coming from IgG used for the immunoprecipitation.

Embryo Manipulations

Xenopus laevis embryos and explants were obtained, cultured, microinjected, and subjected to whole-mount in situ hybridization, lineage tracing, and histology as described (Pera et al., 2001). Whole-mount immunostaining was done as described (Christen and Slack, 1999), using anti-dpERK antibody (1:250; Cell Signaling).

Proteoglycan Isolation and Lyase Treatment

Proteoglycans were extracted from approximately 100 embryos by guanidine buffer, and subsequently anion-exchange purified under denaturing conditions (Yanagishita, 2001), ethanol precipitated, and finally resuspended in TBS, containing 0.1% Triton X-100, DTT 1 mM, PMSF 1 mM, aprotinin, leupeptin, and pepstatin, each at 1 μg/ml. Samples were diluted 1:3 with Tris 20 mM pH 7.5, NaCl 50 mM, $CaCl_2$ 4 mM, followed by addition of 0.5 mU Chondroitinase B (Seikagaku), or mock treatment. After overnight incubation at 37°C, the reaction was stopped by Laemmli buffer, and the samples were subjected to western blot on premade 4%–12% acrylamide minigel (NuPAGE, Invitrogen). Flag-Biglycan was decorated by anti-Flag antibody HRP-conjugated (1:5000), and detected by ECL (AmershamBioscience).

RT-PCR

Total RNA was extracted as reported (Pera et al., 2001) and digested with DNase I (QIAGEN). The PCR reaction was carried out with the Gene Amp RNA PCR kit (Perkin Elmer) using primers and cycle numbers as listed in Table S1. The PCR products were separated on 2% agarose gels.

Supplemental Data

The Supplemental Data include five supplemental figures and one supplemental table and can be found with this article online at http://www.developmentalcell.com/cgi/content/full/13/2/226/DC1/.

ACKNOWLEDGMENTS

We thank Drs. J. Larraín, J. Yost, A. Malmström, J. Slack, E. Amaya, H. Okamoto, W. Knöchel, J. Gurdon, R. Harland, and E.M. De Robertis for the generous gifts of reagents, I. Wunderlich for her excellent technical assistance, and Oliver Wessely, Tomas Pieler, Michael Kessel, Udo Häcker, and Henrik Semb for critical review of the manuscript. We also thank Tomas Pieler and Sten-Eirik Jacobsen for generous support and continuous interest. This work was funded by the German Research Center for Molecular Physiology of the Brain and the Swedish Foundation for Strategic Research; grants from the Deutsche Forschungsgemeinschaft (Pe728/3), the Lund Stem Cell Program, and Crafoord foundation to E.M.P; and from the Swedish Science Foundation to E.M.P. (grant 5286) and M.M. (grant 7479). S.H. was a Lichtenberg Fellow at the University Göttingen. E.M.P. expresses his gratitude to Eddy De Robertis for superb training at UCLA.

Received: December 19, 2006
Revised: May 19, 2007
Accepted: July 3, 2007
Published: August 6, 2007

REFERENCES

Amaya, E., Musci, T.J., and Kirschner, M.W. (1991). Expression of a dominant negative mutant of the FGF receptor disrupts mesoderm formation in *Xenopus* embryos. Cell *66*, 257–270.

Amaya, E., Stein, P.A., Musci, T.J., and Kirschner, M.W. (1993). FGF signalling in the early specification of mesoderm in *Xenopus*. Development *118*, 477–487.

Baldi, A., De Luca, A., Morini, M., Battista, T., Felsani, A., Baldi, F., Catricala, C., Amantea, A., Noonan, D.M., Albini, A., et al. (2002). The HtrA1 serine protease is down-regulated during human melanoma progression and represses growth of metastatic melanoma cells. Oncogene *21*, 6684–6688.

Böttcher, R.T., Pollet, N., Delius, H., and Niehrs, C. (2004). The transmembrane protein XFLRT3 forms a complex with FGF receptors and promotes FGF signalling. Nat. Cell Biol. *6*, 38–44.

Böttcher, R.T., and Niehrs, C. (2005). Fibroblast growth factor signaling during early vertebrate development. Endocr. Rev. *26*, 63–77.

Brickman, M.C., and Gerhart, J.C. (1994). Heparitinase inhibition of mesoderm induction and gastrulation in *Xenopus laevis* embryos. Dev. Biol. *164*, 484–501.

Bülow, H.E., and Hobert, O. (2006). The molecular diversity of glycosaminoglycans shapes animal development. Annu. Rev. Cell Dev. Biol. *22*, 375–407.

Chen, Y., Hollemann, T., Grunz, H., and Pieler, T. (1999). Characterization of the Ets-type protein ER81 in *Xenopus* embryos. Mech. Dev. *80*, 67–76.

Christen, B., and Slack, J.M. (1997). FGF-8 is associated with anteroposterior patterning and limb regeneration in *Xenopus*. Dev. Biol. *192*, 455–466.

Christen, B., and Slack, J.M. (1999). Spatial response to fibroblast growth factor signalling in *Xenopus* embryos. Development *126*, 119–125.

Clausen, T., Southan, C., and Ehrmann, M. (2002). The HtrA family of proteases: Implications for protein composition and cell fate. Mol. Cell *10*, 443–455.

De Robertis, E.M., and Kuroda, H. (2004). Dorsal-ventral patterning and neural induction in *Xenopus* embryos. Annu. Rev. Cell Dev. Biol. *20*, 285–308.

DeWan, A., Liu, M., Hartman, S., Zhang, S.S., Liu, D.T., Zhao, C., Tam, P.O., Chan, W.M., Lam, D.S., Snyder, M., et al. (2006). HTRA1 promoter polymorphism in wet age-related macular degeneration. Science *314*, 989–992.

Dono, R. (2003). Fibroblast growth factors as regulators of central nervous system development and function. Am. J. Physiol. Regul. Integr. Comp. Physiol. *284*, R867–R881.

Fürthauer, M., Lin, W., Ang, S.L., Thisse, B., and Thisse, C. (2002). Sef is a feedback-induced antagonist of Ras/MAPK-mediated FGF signalling. Nat. Cell Biol. *4*, 170–174.

Galli, A., Roure, A., Zeller, R., and Dono, R. (2003). Glypican 4 modulates FGF signalling and regulates dorsoventral forebrain patterning in *Xenopus* embryos. Development *130*, 4919–4929.

García-García, M.J., and Anderson, K.V. (2003). Essential role of glycosaminoglycans in Fgf signaling during mouse gastrulation. Cell *114*, 727–737.

Grose, R., and Dickson, C. (2005). Fibroblast growth factor signaling in tumorigenesis. Cytokine Growth Factor Rev. *16*, 179–186.

Häcker, U., Nybakken, K., and Perrimon, N. (2005). Heparan sulphate proteoglycans: The sweet side of development. Nat. Rev. Mol. Cell Biol. *6*, 530–541.

Hardcastle, Z., Chalmers, A.D., and Papalopulu, N. (2000). FGF-8 stimulates neuronal differentiation through FGFR-4a and interferes with mesoderm induction in *Xenopus* embryos. Curr. Biol. *10*, 1511–1514.

Hongo, I., Kengaku, M., and Okamoto, H. (1999). FGF signaling and the anterior neural induction in Xenopus. Dev. Biol. *216*, 561–581.

Hou, J., Clemmons, D.R., and Smeekens, S. (2005). Expression and characterization of a serine protease that preferentially cleaves insulin-like growth factor binding protein-5. J. Cell. Biochem. *94*, 470–484.

Huang, P., and Stern, M.J. (2005). FGF signaling in flies and worms: More and more relevant to vertebrate biology. Cytokine Growth Factor Rev. *16*, 151–158.

Iozzo, R.V. (1998). Matrix proteoglycans: From molecular design to cellular function. Annu. Rev. Biochem. *67*, 609–652.

Isaacs, H.V., Pownall, M.E., and Slack, J.M. (1994). eFGF regulates *Xbra* expression during Xenopus gastrulation. EMBO J. *13*, 4469–4481.

Kawachi, K., Masuyama, N., and Nishida, E. (2003). Essential role of the transcription factor Ets-2 in *Xenopus* early development. J. Biol. Chem. *278*, 5473–5477.

Kitaoka, T., Morse, L.S., Schneeberger, S., Ishigooka, H., and Hjelmeland, L.M. (1997). Expression of FGF5 in choroidal neovascular membranes associated with ARMD. Curr. Eye Res. *16*, 396–399.

Kramer, K.L., and Yost, H.J. (2003). Heparan sulfate core proteins in cell-cell signaling. Annu. Rev. Genet. *37*, 461–484.

Lin, X., Buff, E.M., Perrimon, N., and Michelson, A.M. (1999). Heparan sulfate proteoglycans are essential for FGF receptor signaling during *Drosophila* embryonic development. Development *126*, 3715–3723.

Maccarana, M., Olander, B., Malmström, J., Tiedemann, K., Aebersold, R., Lindahl, U., Li, J.P., and Malmström, A. (2006). Biosynthesis of dermatan sulfate: Chondroitin-glucuronate C5-epimerase is identical to SART2. J. Biol. Chem. *281*, 11560–11568.

Midura, R.J., Salustri, A., Calabro, A., Yanagishita, M., and Hascall, V.C. (1994). High-resolution separation of disaccharide and oligosaccharide alditols from chondroitin sulphate, dermatan sulphate and hyaluronan using CarboPac PA1 chromatography. Glycobiology *4*, 333–342.

Moreno, M., Munoz, R., Aroca, F., Labarca, M., Brandan, E., and Larraín, J. (2005). Biglycan is a new extracellular component of the Chordin-BMP4 signaling pathway. EMBO J. *24*, 1397–1405.

Munoz, R., Moreno, M., Oliva, C., Orbenes, C., and Larraín, J. (2006). Syndecan-4 regulates non-canonical Wnt signalling and is essential for convergent and extension movements in *Xenopus* embryos. Nat. Cell Biol. *8*, 492–500.

Niehrs, C., and Meinhardt, H. (2002). Modular feedback. Nature *417*, 35–36.

Oka, C., Tsujimoto, R., Kajikawa, M., Koshiba-Takeuchi, K., Ina, J., Yano, M., Tsuchiya, A., Ueta, Y., Soma, A., Kanda, H., et al. (2004). HtrA1 serine protease inhibits signaling mediated by Tgf-beta family proteins. Development *131*, 1041–1053.

Ornitz, D.M. (2005). FGF signaling in the developing endochondral skeleton. Cytokine Growth Factor Rev. *16*, 205–213.

Pera, E.M., Wessely, O., Li, S.Y., and De Robertis, E.M. (2001). Neural and head induction by insulin-like growth factor signals. Dev. Cell *1*, 655–665.

Pera, E.M., Ikeda, A., Eivers, E., and De Robertis, E.M. (2003). Integration of IGF, FGF, and anti-BMP signals via Smad1 phosphorylation in neural induction. Genes Dev. *17*, 3023–3028.

Pera, E.M., Hou, S., Strate, I., Wessely, O., and De Robertis, E.M. (2005). Exploration of the extracellular space by a large-scale secretion screen in the early *Xenopus* embryo. Int. J. Dev. Biol. *49*, 781–796.

Pownall, M.E., Tucker, A.S., Slack, J.M., and Isaacs, H.V. (1996). eFGF, Xcad3 and Hox genes form a molecular pathway that establishes the anteroposterior axis in Xenopus. Development *122*, 3881–3892.

Shively, J.E., and Conrad, H.E. (1976). Formation of anhydrosugars in the chemical depolymerization of heparin. Biochemistry *15*, 3932–3942.

Sivak, J.M., Petersen, L.F., and Amaya, E. (2005). FGF signal interpretation is directed by Sprouty and Spred proteins during mesoderm formation. Dev. Cell *8*, 689–701.

Stern, E.L., Cifonelli, J.A., Fransson, L.-Å., Lindahl, B., Rodén, L., Schiller, S., and Spach, M.L. (1968). The linkage of dermatan sulfate to protein. I. Isolation and amino acid content of dermatan sulfate-peptides. Ark. Kemi *30*, 583–592.

Sun, X., Meyers, E.N., Lewandoski, M., and Martin, G.R. (1999). Targeted disruption of Fgf8 causes failure of cell migration in the gastrulating mouse embryo. Genes Dev. *13*, 1834–1846.

Tocharus, J., Tsuchiya, A., Kajikawa, M., Ueta, Y., Oka, C., and Kawaichi, M. (2004). Developmentally regulated expression of mouse HtrA3 and its role as an inhibitor of TGF-beta signaling. Dev. Growth Differ. *46*, 257–274.

Trowbridge, J.M., and Gallo, R.L. (2002). Dermatan sulfate: New functions from an old glycosaminoglycan. Glycobiology *12*, 117R–125R.

Trowbridge, J.M., Rudisill, J.A., Ron, D., and Gallo, R.L. (2002). Dermatan sulfate binds and potentiates activity of keratinocyte growth factor (FGF-7). J. Biol. Chem. *277*, 42815–42820.

Tsang, M., Friesel, R., Kudoh, T., and Dawid, I.B. (2002). Identification of Sef, a novel modulator of FGF signalling. Nat. Cell Biol. *4*, 165–169.

Tsang, M., and Dawid, I.B. (2004). Promotion and attenuation of FGF signaling through the Ras-MAPK pathway. Sci. STKE *228*, 1–5.

Westergren-Thorsson, G., Onnervik, P.O., Fransson, L.A., and Malmström, A. (1991). Proliferation of cultured fibroblasts is inhibited by L-iduronate-containing glycosaminoglycans. J. Cell. Physiol. *147*, 523–530.

Yanagishita, M. (2001). Isolation of Proteoglycans from Cell Cultures and Tissues. In Proteoglycan Protocols, Methods in Molecular Biology, *Volume 171*, Chapter 1 R.V. Iozzo, ed. (Towona, NJ: Humana Press), pp. 3–8.

Yang, Z., Camp, N.J., Sun, H., Tong, Z., Gibbs, D., Cameron, D.J., Chen, H., Zhao, Y., Pearson, E., Li, X., et al. (2006). A variant of the HTRA1 gene increases susceptibility to age-related macular degeneration. Science *314*, 992–993.

Zumbrunn, J., and Trueb, B. (1996). Primary structure of a putative serine protease specific for IGF-binding proteins. FEBS Lett. *398*, 187–192.

Developmental Cell *13*

Supplementary Data

The Secreted Serine Protease xHtrA1 Stimulates Long-Range FGF Signaling in the Early *Xenopus* Embryo

Shirui Hou, Marco Maccarana, Tan H. Min, Ina Strate, and Edgar M. Pera

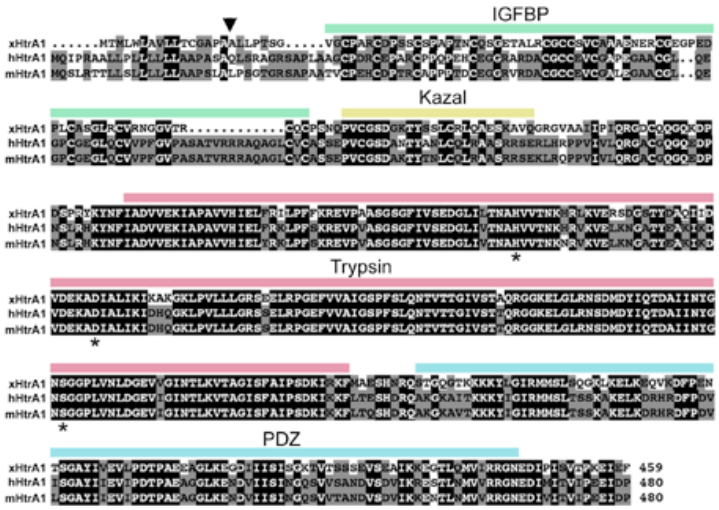

Figure S1. Protein Alignment of *Xenopus*, Human and Mouse HtrA1
The alignment was performed using the MultAlin program (Corpet, 1988). Identical amino acid residues are indicated in black, similar residues in grey. Gaps are introduced as dots. The signal peptide cleavage site is marked by an arrowhead. IGFBD, IGF-binding domain; Kazal, kazal-type serine protease inhibitor domain; Trypsin, trypsin-like serine protease domain; PDZ, PSD95 (Post-synaptic density protein-95)/DlgA (*Drosophila* disc large tumor suppressor)/ZO1 (Zona occludens-1 protein) domain. Three amino acids that constitute the catalytic triad of the trypsin domain are labeled with stars: histidine 199, aspartic acid 229, and serine 307 (referring to xHtrA1 sequence). The numbers at the end of the sequences indicate the total length of the proteins. GenBank accession numbers are: xHtrA1, EF490997; hHtrA1, NP650366; mHtrA1, AAH13516.

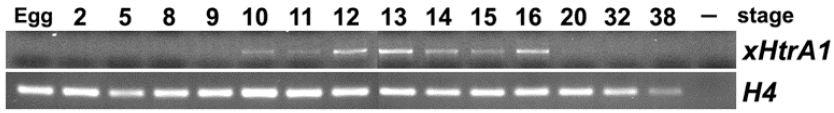

Figure S2. Temporal Expression Pattern of *xHtrA1* mRNA during *Xenopus* Development
RT-PCR analysis in embryos at the indicated stages. *H4*, histone H4 for normalization.

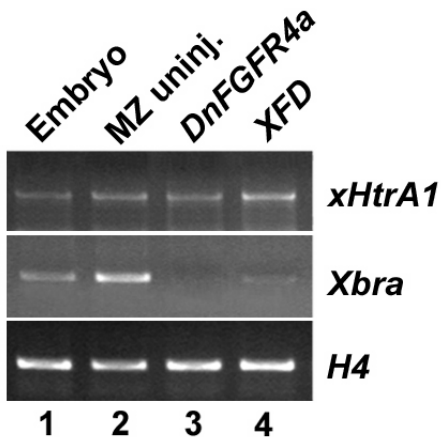

Figure S3. FGF Signalling Is Not Required for *xHtrA1* Transcription in Marginal Zone Explants
Xenopus embryos were injected into the margin of each blastomere at the 4-cell stage with *DnFGFR4a* (4 ng) or *XFD* mRNA (6 ng). Whole embryos (lane 1) and isolated marginal zone explants (lanes 2-4) were analyzed by RT-PCR at stage 11. Note that *DnFGFR4a* and *XFD* do not reduce *xHtrA1* mRNA levels at doses that significantly lower or completely erase *Xbra* expression.

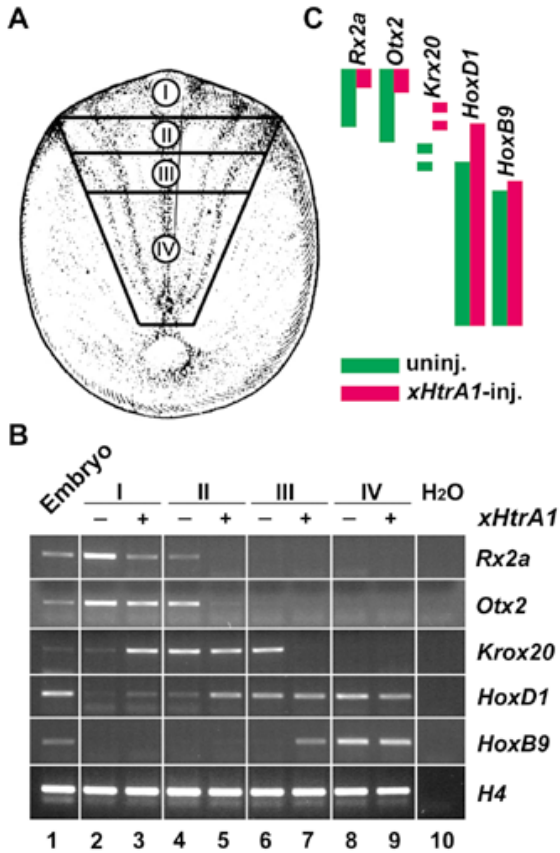

Figure S4. Posteriorization of the CNS by xHtrA1
(A) Experimental design. After injection of *Xenopus* embryos with *xHtrA1* mRNA into the animal pole of each blastomere at the 4-cell stage (20 pg total), four sections of the neural plate plus underlying mesoderm and endoderm were excised at the late gastrula stage and cultured *ex vivo* in 0.8 X MBS.
(B) RT-PCR analysis of explants (n = 5 per sample) at equivalent of embryonic stage 26 with region-specific neural markers. *Rx2a*, forebrain; *Otx2*, forebrain/midbrain; *Krox20*, rhombomeres 3 and 5 of the hindbrain; *HoxD1*, hindbrain/spinal cord; *HoxB9*, spinal cord; *H4*, histone H4 for normalization. Note that sections I-III progressively loose anterior and gain posterior marker gene expression after *xHtrA1* mRNA injection, while section IV remains unaffected.
(C) Regional fate of neural plate in uninjected and *xHtrA1*-injected embryos at stage 13 according to RT-PCR analysis at stage 26. Note that in response to *xHtrA1* mRNA injection, the expression domains of anterior genes are reduced and the domains of posterior genes expanded anteriorwards.

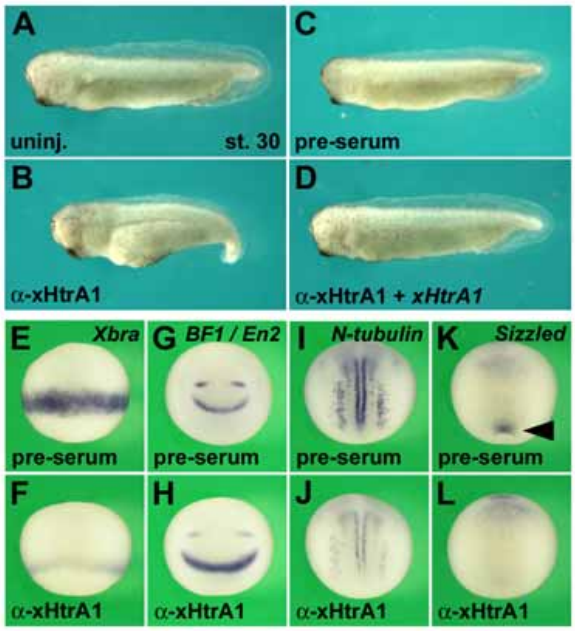

Figure S5. A Neutralizing Antibody against xHtrA1 Supports Anterior Development and Reduces Mesoderm and Neuronal Differentiation

(A) Uninjected *Xenopus* embryo at tailbud stage.

(B) Microinjection of immunopurified α-xHtrA1 antibody (200 ng in volume of 50 nl) into the blastocoel cavity at stage 8 causes enlargement of head and reduction of trunk/tail structures.

(C) Control pre-serum has no effect on axial development.

(D) The anteriorized phenotype of α-xHtrA1 is suppressed by injection at the 4-cell stage of *xHtrA1* mRNA (160 pg total), underscoring the specificity of the α-xHtrA1 effect.

(E-L) Embryos at stage 10 (E,F) and stage 16 (G-L) after whole-mount *in situ* hybridization with indicated antisense RNA probes in lateral (E,F), anterior (G,H), dorsal (I,J) and ventral views (K,L).

(E,F) Blastocoelic injection at stage 6.5 of α-xHtrA1, but not of pre-serum, reduces expression of the mesodermal marker *Xbra*.

(G-L) α-xHtrA1 injection at stage 9 broadens the expression domains of *BF1* (telencephalon) and *En2* (midbrain-hindbrain boundary), reduces the expression of *N-tubulin* (neurons) and blocks the posterior domain of the ventral mesoderm marker *Sizzled* (arrowhead).

Indicated phenotypes were observed in: B, 32/107; C, 114/121; D, 5/5; E, 19/19; F, 30/31; G, 6/6; H, 23/24; I, 16/16; J, 29/46; K, 7/11; L, 17/24 embryos.

Table S1. Oligonucleotides for RT-PCR

Gene	Forward	Reverse	Cycles
Histone H4	5'-CGG GAT AAC ATT CAG GGT ATC ACT	5'-CAT GGC GGT AAC TGT CTT CCT	24
xHtrA1	5'-TGT TGT GGC TGG CGG TGT TAC TG	5'-TCC ATC CTC CGA CAC AAT GAA TCC	43
Xbra	5'-GGA TCG TTA TCA CCT CTG	5'-GTG TAG TCT GTA GCA GCA TGC TGC TAC	28
Xcad3	5'-GGA TCA CCG AGG GAG GAA TG	5'-TAA GAG CGC TGG GTG AGT TGG	28
Rx2A	5'-CAA CAG CCC AAG AAG AAA CAC AG	5'-GAG GGC ACT CAT GGC AGA AGG	28
Otx2	5'-CCA GTC ATC TCG AGC AGC ACA	5'-CAG GAG GCC GTT TGG TCT TTG	28
Krox20	5'-CGC CCC AGT AAG ACC	5'-TCA GCC TGT CCT GTT AG	30
HoxD1	5'-CAG CCC CGA TTA CGA TTA TTA TGG	5'-CCG GGG AGG CAG GTT TTG	30
HoxB9	5'-GCC CCT GCG CAA TCT GAA C	5'-CAG CAG CGG CTC AGA CTT GAG	28

Supplemental Reference

Corpet F. (1988). Multiple sequence alignment with hierarchical clustering. Nucl. Acids Res.*16*, 10881-10890.

Paper III

Development 136, 461-472 (2009) doi:10.1242/dev.024901

Retinol dehydrogenase 10 is a feedback regulator of retinoic acid signalling during axis formation and patterning of the central nervous system

Ina Strate[1,2], Tan H. Min[1], Dobromir Iliev[1] and Edgar M. Pera[1,2,*]

Retinoic acid (RA) is an important morphogen that regulates many biological processes, including the development of the central nervous system (CNS). Its synthesis from vitamin A (retinol) occurs in two steps, with the second reaction – catalyzed by retinal dehydrogenases (RALDHs) – long considered to be crucial for tissue-specific RA production in the embryo. We have recently identified the *Xenopus* homologue of retinol dehydrogenase 10 (XRDH10) that mediates the first step in RA synthesis from retinol to retinal. *XRDH10* is specifically expressed in the dorsal blastopore lip and in other domains of the early embryo that partially overlap with *XRALDH2* expression. We show that endogenous RA suppresses *XRDH10* gene expression, suggesting negative-feedback regulation. In mRNA-injected *Xenopus* embryos, *XRDH10* mimicked RA responses, influenced the gene expression of organizer markers, and synergized with *XRALDH2* in posteriorizing the developing brain. Knockdown of XRDH10 and XRALDH2 by specific antisense morpholino oligonucleotides had the opposite effects on organizer gene expression, and caused a ventralized phenotype and anteriorization of the brain. These data indicate that the conversion of retinol into retinal is a developmentally controlled step involved in specification of the dorsoventral and anteroposterior body axes, as well as in pattern formation of the CNS. We suggest that the combinatorial gene expression and concerted action of XRDH10 and XRALDH2 constitute a 'biosynthetic enzyme code' for the establishment of a morphogen gradient in the embryo.

KEY WORDS: RDH10, Retinol dehydrogenase, Short chain dehydrogenase/reductase, Retinoic acid, Morphogen, Gradient, Spemann's organizer, Gastrulation, Induction, Pattern formation, Hindbrain, CNS, *Xenopus*

INTRODUCTION

Regional specification is a fundamental process during early development of the central nervous system. In the amphibian gastrula, a group of mesodermal cells in the dorsal blastopore lip, called the Spemann's organizer, secrete signals that induce adjacent ectodermal cells to acquire a neural fate (De Robertis, 2006). An 'activation/transformation' model has been proposed for the anteroposterior patterning of the CNS (Nieuwkoop, 1952). First, the early neurectoderm acquires an anterior (forebrain) fate. In a second inductive wave, additional signals emanating from the organizer and/or the embryonic mesoderm transform neural tissue into more posterior midbrain, hindbrain, and spinal cord fates. Studies in *Xenopus* have identified several factors that mediate the first activation step, including soluble BMP antagonists, such as Chordin and Noggin (De Robertis and Kuroda, 2004; Khoka et al., 2005), Wnt antagonists (Niehrs, 2004), and active signals, including insulin-like growth factors (Pera et al., 2001; Richard-Parpaillon et al., 2002). These diverse signals are integrated at the level of Smad1 phosphorylation and turnover (Pera et al., 2003; Fuentealba et al., 2007). Three signalling pathways, including retinoic acid, fibroblast growth factor and Wnt, contribute to the transforming signal and interact in a complex manner to specify posterior neural structures (Durston et al., 1989; Cho and De Robertis, 1990; Kudoh et al., 2002; Shiotsugu et al., 2004; Olivera-Martinez and Storey, 2007).

[1]Stem Cell Center, Lund University, 22184 Lund, Sweden. [2]Department of Developmental Biochemistry, Institute of Biochemistry and Cell Biology, Georg August University Göttingen, 37077 Göttingen, Germany.

*Author for correspondence (e-mail: edgar.pera@med.lu.se)

Accepted 30 November 2008

Retinoic acid (RA) is the most active naturally occurring member of a family of lipophilic molecules called retinoids, all of which are derived from vitamin A (Clagett-Dame and De Luca, 2002). The RA signal is transduced through nuclear retinoic acid receptors, the RARs and RXRs, which control the expression of target genes involved in vertebrate pattern formation, organogenesis and tissue homeostasis (Mark et al., 2006). Maternal insufficiency of vitamin A or excess RA cause a wide range of teratologic effects – from limb malformations and organ defects to CNS abnormalities – indicating that the embryo requires a precisely regulated supply of retinoids (Ross et al., 2000). In *Xenopus* embryos, exogenously applied RA during gastrula stages produces a concentration-dependent truncation of anterior structures and an enhancement of posterior structures (Durston et al., 1989; Sive et al., 1990) through its influence on the embryonic mesoderm and ectoderm (Ruiz i Altaba and Jessell, 1991; Papalopulu et al., 1991). RA regulates the expression of the homeotic Hox genes, which act in a combinatorial fashion ('Hox code') to specify axial identity in the trunk (Kessel and Gruss, 1991; Kessel, 1992) and the hindbrain (Marshall et al., 1992).

During embryonic development, the availability of RA is regulated by retinal dehydrogenases (RALDHs) that mediate the oxidation of retinal to RA, and by members of the cytochrome P450 family (CYP26s) that metabolize RA via oxidative inactivation (Niederreither and Dollé, 2008; Duester, 2008). In several vertebrates, the *RALDH2* gene exhibits tissue-specific expression (Niederreither et al., 1997; Swindell et al., 1999; Chen et al., 2001) at or adjacent to sites of RA signalling (Rossant et al., 1991; Mendelsohn et al., 1991; Balkan et al., 1992; Yelin et al., 2005). In *Xenopus*, overexpression of *RALDH2* mimicked RA signalling (Chen et al., 2001). Loss-of-function studies in mice and zebrafish showed that RALDH2 is not only critical for development, but that

it accounts for the majority of RA production in the embryo (Niederreither et al., 1999; Begemann et al., 2001; Grandel et al., 2002). Expression analysis in various species suggested that CYP26A1 is the major RA-degrading enzyme during gastrulation (Hollemann et al., 1998; de Roos et al., 1999; Swindell et al., 1999; Dobbs-McAuliffe et al., 2004). In *Xenopus*, overexpression of *CYP26A1* mRNA caused phenotypes resembling RA deprivation (Hollemann et al., 1998). Functional studies in mouse and zebrafish embryos revealed a crucial role for CYP26A1 in axis specification, hindbrain patterning and tail formation (Abu-Abed et al., 2001; Sakai et al., 2001; Kudoh et al., 2002; Hernandez et al., 2007).

In embryos from placental species, vitamin A (retinol) is provided from the maternal circulation (Ward et al., 1997), whereas oviparous embryos use retinoid and carotinoid stores in the egg yolk (Lampert et al., 2003). A multitude of cytosolic alcohol dehydrogenases and microsomal short-chain dehydrogenases/reductases (SDRs) (Duester et al., 2003; Lidén and Eriksson, 2006), as well as the recently identified CYP1B1 mono-oxygenase (Chambers et al., 2007), can mediate the first step of RA synthesis from vitamin A. Retinol dehydrogenase 10 (RDH10) is a member of the SDR family that oxidizes retinol into retinal (Wu et al., 2002; Wu et al., 2004) in an NAD^+-dependent manner (Belyaeva et al., 2008), and exhibits tissue-specific expression at embryonic and foetal mouse stages (Sandell et al., 2007; Cammas et al., 2007; Romand et al., 2008). Analysis of an N-ethyl-N-nitrosourea-generated mutant called *trex* suggested an essential function of murine RDH10 for RA biosynthesis during limb, craniofacial and organ development (Sandell et al., 2007). However, RDH10 has not been studied in species other than mammals, its regulation is not understood, and the interplay with other RA metabolizing enzymes, as well as its functions in early aspects of embryonic development, remain to be addressed.

In a screen for secreted proteins, we have recently identified the *Xenopus* homologue of RDH10 (Pera et al., 2005). *XRDH10* expression partially overlaps with that of *XRALDH2* in the early embryo and is subject to negative-feedback regulation by endogenous RA. *XRDH10* mimics RA signalling and modulates organizer-specific gene expression. We find that XRDH10 co-operates with XRALDH2, and that both enzymes are required to ensure proper RA signalling in the early embryo. Our data describe a novel role of RDH10 in axis formation and CNS development. We present a revised model for the generation of the RA morphogen gradient.

MATERIALS AND METHODS

Expression constructs, morpholino oligos, retinoids and citral

Full-length cDNA clones of *XRDH10* and *XRALDH2* in the expression vector pCS2 were obtained by secretion cloning (Pera et al., 2005). *XRDH10* was fully sequenced (Gene Accession Number FJ213456). To generate the rescue construct pCS2-*XRDH10**, the wobbled nucleotides in codons 2-8 were exchanged via a PCR-based two-step mutagenesis from pCS2-*XRDH10*, using the primers *XRDH10*-wob-F-1st (ATGCATATAGTCCTCGAATTCTTTCTGGTC), *XRDH10*-wob-F-2nd (GCATCGATATGCATATCGTCGTGGAATTTTTTGTGGTC) and *XRDH10*-R (GCCTCGAGTTAAAATTCCATTTTTTGTTTCATTG), and the final PCR products were inserted into the *Cla*I and *Xho*I restriction sites of pCS2. pCS2-*mRALDH2* was generated from pCMV-Sport6-*Aldh1a2* (Imagenes GmbH, Germany; IMAGE ID, 30471325) by subcloning the insert into the *Eco*RI and *Xba*I sites of pCS2. Plasmid constructs were checked by sequencing and in vitro translation (TnT-Coupled Reticulocyte Lysate System, Promega).

To prepare sense RNA, pCS2 constructs of *XRDH10*, *XRDH10**, *XRALDH2*, *mRALDH2* and *XCYP26A1* (Hollemann et al., 1998) (a kind gift of Tomas Pieler, Göttingen University, Germany) were linearized with *Not*I and transcribed with Sp6 RNA polymerase (mMessage Machine, Ambion). mRNA encoding nuclear β-galactosidase was synthesized from pXEXβgal (a kind gift of Richard Harland, UC Berkeley, CA, USA; *Xba*I digestion and T7 transcription). The *XRDH10*-MO (GGAAGAACTCGAGCACTA-TGTGCAT), *XRALDH2*-MO (GCATCTCTATTTTACTGGAAGTCAT) and standard control-MO were obtained from Gene Tools.

All-trans-retinoic acid (Sigma, R2625), all-trans-retinol (Fluka, 95144) and disulfiram (Sigma, T1132) were dissolved in DMSO as 10 mM, 50 mM and 250 mM stock solutions, respectively. All-trans-retinal (Sigma, R2500)

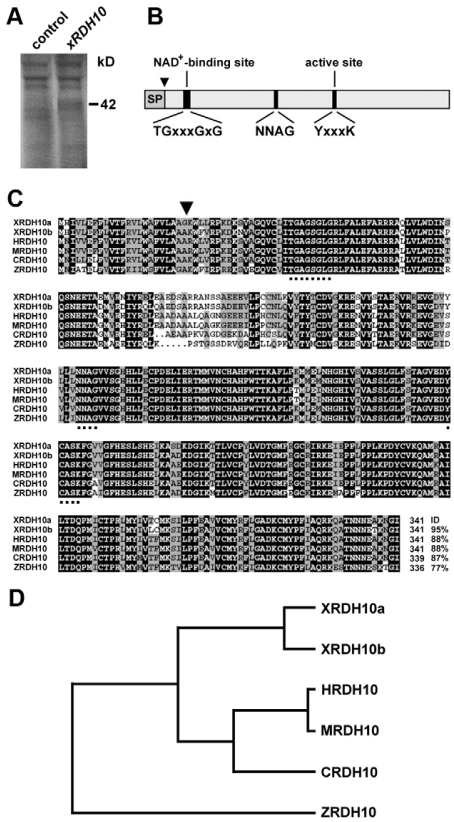

Fig. 1. *Xenopus* retinol dehydrogenase 10. (**A**) SDS-PAGE of conditioned medium from HEK 293T cells labelled with ^{35}S-methionine and ^{35}S-cysteine and mock-transfected (control) or transfected with *XRDH10* cDNA. The diffuse band at 42 kDa corresponds to the full-length XRDH10 protein. (**B**) Protein structure of XRDH10. The invariant sequences TGxxxGxG (co-factor binding; x indicates any amino acid residue), NNAG and YxxxK (active site) are characteristic for members of the short-chain dehydrogenase/reductase family (Persson et al., 2003). SP, signal peptide. (**C**) Sequence alignment of *Xenopus*, human (H), mouse (M), chick (C) and zebrafish (Z) RDH10 proteins. Two *X. laevis* RDH10 alleles (XRDH10a and XRDH10b) are shown. The arrowhead indicates the predicted signal peptide cleavage site, and dots underline conserved sequences. (**D**) Evolutionary relationship of RDH10 sequences.

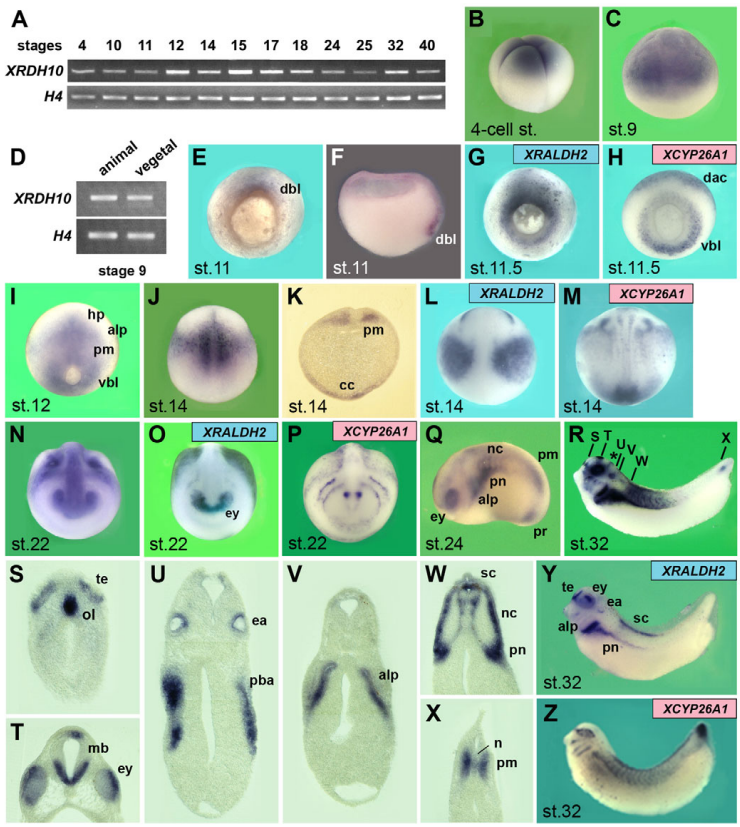

Fig. 2. Expression of *Xenopus RDH10*. (**A**,**D**) RT-PCR analysis of whole embryos (A) and embryonic explants (D). *Histone H4* was used as an RNA loading control. (**B**,**C**,**E-Z**) Whole-mount in situ hybridization with an antisense RNA probe for *XRDH10* (B,C,E,F,I-K,N,Q-X), *XRALDH2* (G,L,O,Y) and *XCYP26A1* (H,M,P,Z). Embryos are shown in lateral (B,C,Q,R,Y,Z), vegetal (E,G,H), dorsal (I,J,L,M) and anterior (N-P) views. Specimens are hemi-sectioned (F) and transversally sectioned (K,S-X). The asterisk in R indicates the midbrain-hindbrain boundary. alp, anterior lateral plate; cc, cardiac crescent; dac, dorsal animal cap; dbl, dorsal blastopore lip; ea, ear; ey, eye; hp, head process; mb, midbrain; n, notochord; nc, neural crest; ol, olfactory system; pba, posterior branchial arch; pm, presomitic mesoderm; pn, pronephros; pr, proctodeum; sc, spinal cord; te, telencephalon; vbl, ventral blastopore lip.

and citral (Sigma, W230308) were dissolved in 70% ethanol as 5 mM and 40 mM stock solutions, respectively. The stock solutions were then diluted to the final concentrations either in 0.1×MBS (for treatment of whole embryos) or in 1×MBS (for treatment of animal cap explants).

Embryo manipulations and RT-PCR

Xenopus laevis embryos and explants were obtained, cultured, microinjected and subjected to whole-mount in situ hybridization and lineage tracing as described (Hou et al., 2007). Gelatine/albumin sections (40 μm) were done using a LeicaVT1200S vibratome.

Total RNA was extracted and the PCR reaction performed as reported (Hou et al., 2007), primers and cycle numbers are available on request. The PCR products were separated on 2% agarose gels.

RESULTS

XRDH10 is dynamically expressed during early embryogenesis

We isolated a full-length cDNA clone of *Xenopus laevis* retinol dehydrogenase 10 (XRDH10) by secretion cloning from LiCl-dorsalized gastrula embryos (Pera et al., 2005). A 42-kDa protein was identified by SDS-PAGE in the supernatant of cDNA-transfected HEK293T cells after metabolic labelling with ^{35}S-methionine and ^{35}S-cysteine (Fig. 1A). XRDH10 encodes a 341 amino acid protein, containing an amino terminal cleavable signal peptide, an NAD$^+$-cofactor binding site and a catalytic site (Fig. 1B). Two pseudoalleles of *RDH10* in *X. laevis* were found, encoding XRDH10a and XRDH10b (95% amino acid identity). XRDH10a has considerable identity to human and mouse (88%), chick (87%) and zebrafish (77%) RDH10 (Fig. 1C,D).

Analysis by RT-PCR indicated that *XRDH10* is a maternal and zygotic gene with elevated expression levels at gastrula and neurula stages (Fig. 2A). Whole-mount in situ hybridization showed abundant transcripts in four-cell and blastula-stage embryos (Fig. 2B,C), and RT-PCR revealed equivalent levels of *XRDH10* mRNA at the animal and vegetal pole (Fig. 2D). At gastrula stage, distinct expression of *XRDH10* was observed in the invaginating mesoderm of the dorsal blastopore lip (Fig. 2E,F). The signals were embedded in the periblastoporal expression domain of *XRALDH2* (Fig. 2G) (Chen et al., 2001), and juxtaposed to two distinct *XCYP26A1* expression domains in the dorsal animal cap and the ventrolateral blastopore lip (Fig. 2H) (Hollemann et al., 1998). As gastrulation proceeded, *XRDH10* transcripts were observed in the head process, anterior lateral plate, presomitic mesoderm, ventral blastopore lip and cardiac crescent (Fig. 2I-K). In neural plate stage embryos, *XRDH10* and *XRALDH2* genes

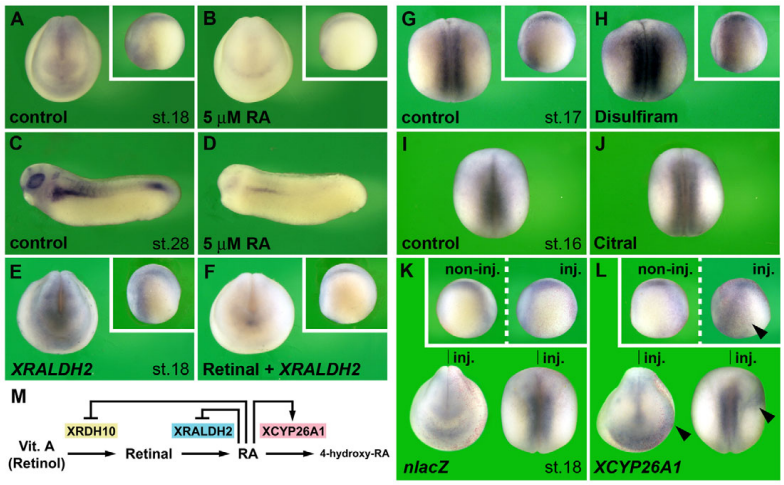

Fig. 3. Retinoic acid downregulates *XRDH10* expression. (**A-L**) Whole-mount in situ hybridization analysis of *XRDH10* transcription at neurula (A,B,E-L) and tailbud (C,D) stage. Embryos are shown in anterior (A,B,E,F,K,L), lateral (C,D, insets) and dorsal (G-L) views. (A-D) Embryos were treated from stage 11 (A,B) or stage 16 (C,D) onwards with 0.05% DMSO as a control or with 5 μM retinoic acid (RA). Note that RA induces a significant reduction in *XRDH10* expression. (E,F) Embryos were microinjected into the animal pole at the four-cell stage with 2 ng *XRALDH2* mRNA and treated from stage 11 onwards with 0.05% ethanol as a control (E) or 5 μM retinal (F). (G-J) Treatment from stage 11 onwards with the RA inhibitors disulfiram (10 μM) or citral (20 μM) causes an elevation of *XRDH10* expression. (K,L) Embryos were animally injected into a single blastomere at the four-cell stage with 300 pg *nlacZ* mRNA as lineage tracer (red nuclei) alone (K) or together with 2 ng *XCYP26A1* mRNA (L). Note that *XCYP26A1* induces an upregulation of *XRDH10* expression on the injected side (arrowhead). The indicated gene expression patterns were obtained in: A, 55/55; B, 22/31; C, 30/30; D, 37/37; E, 11/11; F, 16/17; G, 29/29; H, 49/49; I, 31/31; J, 54/57; K, 36/36; L, 48/53 embryos. (**M**) Negative-feedback regulation of RA biosynthesis.

displayed nested expression patterns in the paraxial trunk mesoderm, with *XRDH10* transcripts localized more anteriorly than *XRALDH2* signals (Fig. 2J,L) (Chen et al., 2001). These sites of expression were flanked by non-overlapping *XCYP26A1* expression domains in the anterior and posterior parts of the neural plate (Fig. 2M) (Hollemann et al., 1998). In early tailbud stage embryos, *XRDH10* mRNA overlapped with *XRALDH2* expression in the eye field (Fig. 2N,O) (Chen et al., 2001), whereas distinct *XCYP26A1* signals could be seen around the eye anlage (Fig. 2P) (Hollemann et al., 1998). Additional *XRDH10* expression domains arose in the pronephros anlage, the trunk neural crest, and the posterior inner wall of the proctodeum (Fig. 2Q). In more advanced tailbud embryos, *XRDH10* signals were seen in distinct territories of the neural tube (including in the telencephalon, midbrain, midbrain-hindbrain boundary and spinal cord), in the olfactory system, in the eyes and ears, and in the posterior branchial arch, the anterior lateral plate and the posterior notochord (Fig. 2R-X). Common *XRALDH2* expression domains were seen in the telencephalon, spinal cord, eyes, ears, anterior lateral plate and pronephros (Fig. 2Y) (Chen et al., 2001). Adjacent, but non-overlapping *XCYP26A1* expression appeared in the periocular region, in tissues that flank the pronephros, and in the tip of the tailbud (Fig. 2Z) (Hollemann et al., 1998). In conclusion, the gene expression of *XRDH10* and *XRALDH2* overlapped at several sites, with *XRDH10* expression domains being frequently embedded in those of *XRALDH2*. By contrast, *XCYP26A1* displayed a complementary, non-overlapping expression pattern.

Effects of retinoic acid on *XRDH10* gene expression

The regulation of *RDH10* gene activity has not yet been studied. The overlap of *RDH10* gene expression with sites of embryonic RA signalling in the frog and the mouse (Fig. 2) (Sandell et al., 2007; Cammas et al., 2007) raised the hypothesis that RA may regulate *RDH10* transcription. Treatment of *Xenopus* embryos with 5 μM RA induced a severe reduction of *XRDH10* expression (Fig. 3A-D). Although microinjection of *XRALDH2* mRNA alone had no effect, a combination of *XRALDH2* mRNA and treatment with 5 μM retinal caused a robust downregulation of *XRDH10* transcription (Fig. 3E,F). By contrast, exposure to the RA synthesis inhibitors disulfiram (Vermot and Pourquié, 2005) or citral (3,7-dimethyl-2,6-octadienal) (Schuh et al., 1993) increased transcript levels of *XRDH10* in the embryo (Fig. 3G-J). Similarly, microinjection of *XCYP26A1* mRNA caused local upregulation of *XRDH10* expression (Fig. 3K,L). We conclude that endogenous RA suppresses *XRDH10* gene expression and thereby controls the first enzymatic step of RA biosynthesis (Fig. 3M).

XRDH10 has retinoic acid-like activity and modulates organizer-specific gene expression

We investigated the activity of XRDH10 in *Xenopus* embryos (Fig. 4). Microinjection of *XRDH10* mRNA into the animal pole at the four-cell stage caused a moderate reduction of head structures and shortening of the primary body axis (Fig. 4A,B). This phenotype is reminiscent of the microcephaly and shortened tails obtained by

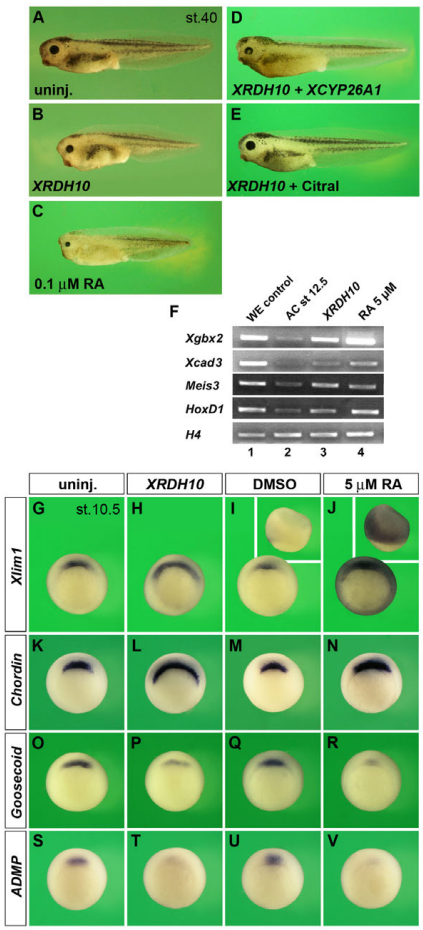

Fig. 4. XRDH10 induces retinoic acid signalling and differentially affects organizer gene expression. (**A**) Uninjected tadpole-stage embryo. (**B**) Animal injection of 4 ng *XRDH10* mRNA at the four-cell stage induces a slight reduction of head structures and a shortening of the tail. (**C**) Treatment with 0.1 μM RA between stages 9 and 12 induces microcephaly and tail shortening. (**D**) Injection of 0.5 ng *XCYP26A1* mRNA reverts the effect of *XRDH10* mRNA and restores normal head and tail development. (**E**) Treatment with 4 μM citral at stages 9-12 abrogates the activity of *XRDH10* mRNA. (**F**) RT-PCR analysis of animal caps explanted from stage 8 embryos and cultured until stage 12.5. Embryos were injected with 4 ng *XRDH10* mRNA (lane 3) and animal caps treated with 5 μM RA (lane 4). Note that *XRDH10* stimulates the transcription of all the RA target genes tested. (**G-V**) Whole-mount in situ hybridization of gastrula embryos in vegetal view. Insets depict lateral views. Embryos were injected in the margin of each blastomere at the four-cell stage with 1 ng *XRDH10* mRNA (H,L,P,T) or treated from stage 8 onwards with DMSO as a control (I,M,Q,U) or 5 μM RA (J,N,R,V). Note that *XRDH10* mRNA and RA expand the expression of *Xlim1* and *Chordin*, but reduce the expression of *Goosecoid* and *ADMP* in the dorsal blastopore lip. Frequency of embryos with the indicated phenotypes was: B, 30/39; C, 25/25; D, 30/40; E, 29/39; G, 45/45; H, 19/39; I, 31/31; J, 41/41; K, 38/38; L, 29/43; M, 30/36; N, 16/29; O, 6/8; P, 4/6; Q, 22/28; R, 15/24; S, 14/14; T, 9/13; U, 64/69; V, 38/50.

treating embryos with 0.1 μM retinoic acid (Fig. 4C) (Durston et al., 1989). Co-injection of *XRDH10* and *XCYP26A1* mRNA rescued head and tail structures (Fig. 4D), and treatment of *XRDH10*-injected embryos with citral restored axial development (Fig. 4E), suggesting that XRDH10 may elicit its activity via the RA pathway. To test whether XRDH10 affects RA signalling, we analyzed in animal cap explants a series of RA target genes, including *Xgbx2*, *Xcad3*, *Meis3* and *HoxD1* (von Bubnoff et al., 1995; Kolm et al., 1997; Dibner et al., 2004; Shiotsugu et al., 2004). RT-PCR analysis revealed that, similar to exogenous RA, injected *XRDH10* mRNA induced an upregulation of these genes (Fig. 4F). The results show that XRDH10 and RA have common activities, and that XRDH10 activity is abrogated by the inhibition of RA signals, suggesting that XRDH10 activates RA signalling in *Xenopus* embryos.

The specific expression of *XRDH10* in the dorsal blastopore lip (Fig. 2E,F) prompted us to analyze its effects on gene markers that demarcate the Spemann's organizer. To this end, we radially injected *XRDH10* mRNA at the four-cell stage and analyzed embryos at stage 10.5 by whole-mount in situ hybridization. We found that *XRDH10* overexpression led to an expansion of the *Xlim1* and *Chordin* expression domains (Fig. 4G,H,K,L), while *Goosecoid* and *ADMP* expression was reduced (Fig. 4O,P,S,T). In accordance with these results, treatment of embryos with 5 μM RA caused an upregulation of *Xlim1* (Fig. 4I,J) (Taira et al., 1994) and *Chordin* (Fig. 4M,N) expression, but a downregulation of *Goosecoid* (Fig. 4Q,R) (Cho et al., 1991) and *ADMP* (Fig. 4U,V) expression. We note that *Chordin* expression in the dorsal ectoderm of earlier blastula embryos was moderately increased by *XRDH10* mRNA injection and RA treatment (see Fig. S1 in the supplementary material). The organizer markers *Noggin*, *Frzb1*, *sFRP2* and *Crescent* were not obviously affected in gastrula embryos (see Fig. S2 in the supplementary material). We conclude that *XRDH10* overexpression mimics RA activity and differentially affects gene expression in the Spemann's organizer.

XRDH10 co-operates with XRALDH2 during axis development and CNS patterning

Next we analyzed the effects of XRDH10 on pattern formation at post-gastrulation stages (Fig. 5). At stage 12.5, *HoxD1* is expressed in the trunk mesoderm and overlying ectoderm with the anterior boundary at the level of hindbrain rhombomere 4 (Fig. 5A). Unilateral injection of *XRDH10* mRNA caused upregulation and anteriorward expansion of *HoxD1* expression (Fig. 5B). *XRALDH2* alone or upon co-injection with *XRDH10* mRNA had a similar effect (Fig. 5C,D). By contrast, *XCYP26A1* reverted the effect of co-injected *XRDH10* mRNA, as it reduced *HoxD1* expression and shifted its anterior boundary posteriorly (Fig. 5E). At stage 14, *Xlim1* labels two rows of neural expression in the trunk (arrowhead in Fig. 5F). Injected *XRDH10* or *XRALDH2* mRNA caused an anterior shift (Fig. 5G,H), and a combination of both mRNAs led to a robust expansion of these *Xlim1*-positive neural cells (Fig. 5I). *XCYP26A1* overrode the effect of co-injected *XRDH10* mRNA and suppressed *Xlim1* expression (Fig. 5J).

Previous studies had shown that overexpression of *XRALDH2* posteriorized the neural tube (Chen et al., 2001), whereas *XCYP26A1* had the opposite effect (Hollemann et al., 1998). At the tailbud stage, *XRDH10* mRNA showed little effect when injected alone (Fig. 5L,Q). However, *XRDH10* enhanced the posteriorizing effect of *XRALDH2* mRNA and caused an anterior shift of the hindbrain rhombomeres 3 and 5 (*Krox20*), and led to a distortion of the midbrain-hindbrain boundary (*En2*) and eye field (*Rx2A*) upon co-injection of both mRNAs (Fig. 5M,N,R,S). Conversely, a combination of *XRDH10* and *XCYP26A1* mRNA resulted in a pronounced posterior shift of these markers (Fig. 5O,T). The location of the telencephalon (*FoxG1*) was not affected by any of the injections (Fig. 5Q-T). The analysis of *Krox20* expression showed that the frequency and extent of rhombomeric shifts induced by a combination of *XRDH10* and *XRALDH2* exceeded the sum of effects induced by each mRNA alone (Fig. 5U). The data indicate that XRDH10 co-operates with XRALDH2 in stimulating RA signalling in the early embryo and that both enzymes exhibit synergistic effects on anteroposterior patterning of the CNS.

Retinol is a limiting factor for XRDH10 activity

The relatively mild phenotype of *XRDH10* mRNA-injected embryos raised the question of whether XRDH10 activity might be restricted by insufficient endogenous retinol concentrations. We therefore examined the effects of overexpressed XRDH10 in the presence of excessive retinol (Fig. 6). In accord with the observations of others (Durston et al., 1989), treatment of embryos between stages 9 and 12 with 50 μM retinol caused microcephaly (Fig. 6B). Although animal injection of *XRDH10* mRNA alone had little effect (Fig. 4B), *XRDH10* mRNA injection followed by treatment with retinol caused the complete loss of eye and head structures (anencephaly; Fig. 6C). The effects of *XRDH10* and retinol were reverted by co-injection of *XCYP26A1* mRNA in a dose-dependent manner (Fig. 6D,E). At the tailbud stage, retinol treatment caused a mild reduction of the eye field marker *Rx2A* (Fig. 6F,G). As shown above, injected *XRDH10* mRNA did not reduce the size of the eye field (Fig. 5L). However, a combination of *XRDH10* mRNA injection and retinol administration led to a significant downsizing of the eye anlage (Fig. 6H), which was rescued by *XCYP26A1* mRNA (Fig. 6I). Together, the results suggest that the supply of retinol may be limiting for XRDH10 activity during head development and eye formation.

Roles of XRDH10 and XRALDH2 in the embryo

To study the functional contribution of enzymes involved in RA biosynthesis, we downregulated endogenous XRDH10 and XRALDH2 proteins in *Xenopus* embryos (Fig. 7). Specific antisense morpholino oligonucleotides (MOs) directed against the translation initiation sites of the known pseudoalleles of *XRDH10* (Fig. 7A) and *XRALDH2* (Fig. 7B) reduced protein synthesis of their respective targets in an in vitro transcription-translation assay, whereas an unspecific control MO had no effect (Fig. 7C,D).

Microinjection of *XRDH10*-MO into the margin of two-cell-stage embryos caused a reduction of head structures and enlarged ventroposterior structures at the tailbud stage (Fig. 7F). In tadpole embryos, knockdown of XRDH10 led to smaller eyes and a significant shortening of the tail (Fig. 7I). Similar ventralized phenotypes were obtained with the *XRALDH2*-MO (Fig. 7G,J). To verify that the effects of the morpholino oligomers were specific, we generated a *XRDH10* rescue construct, designated *XRDH10**, in which six nucleotides in the morpholino target sequence were mutagenized (see Materials and methods). Injection of *XRDH10** mRNA rescued the phenotype caused by *XRDH10*-MO (insets in

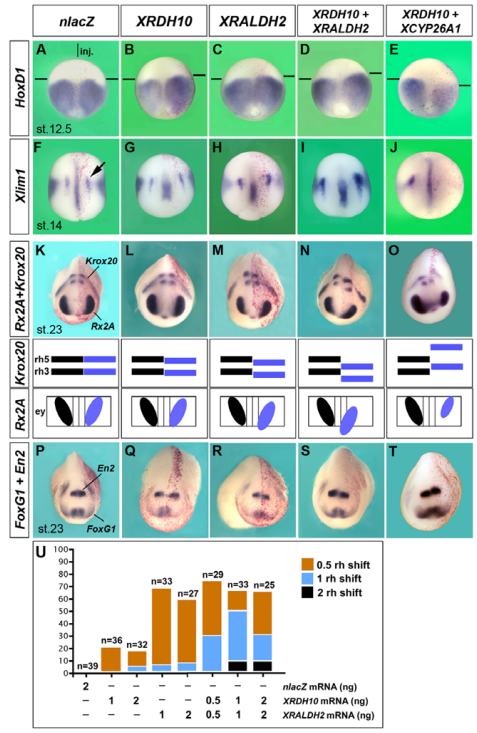

Fig. 5. Overexpression of *XRDH10* and *XRALDH2* results in an anteriorward shift of neural markers, whereas *XCYP26A1* has the opposite effect. Whole-mount in situ hybridization of embryos after microinjection of mRNA into the animal pole of one dorsal blastomere at the four-cell stage. The lineage tracer *nlacZ* (red nuclei) labels the injected right-hand side. (**A-E**) Late gastrula embryos in dorsal view (anterior to the top). *HoxD1* demarcates the ectoderm and mesoderm in the trunk with an anterior expression boundary at the level of rhombomere 4 (horizontal line). (**F-J**) Early neurula embryos in dorsal view, showing *Xlim1* expression in two lines of neural cells (arrow). (**K-O**) Early tailbud embryos in anterior view (posterior to the top) and schematic overviews demarcating *Rx2A* expression in the eyes and *Krox20* expression in rhombomeres 3 and 5 of the hindbrain. (**P-T**) *FoxG1* labels the telencephalon, and *En2* the midbrain-hindbrain boundary. (**U**) Synergistic effects of *XRDH10* and *XRALDH2* on hindbrain patterning. The anteriorward shift of *Krox20* expression is shown in response to mRNA injections at the indicated doses. Note that *XRDH10* has little effect on its own, but strongly enhances the posteriorizing effect of *XRALDH2*. *nlacZ* mRNA was injected as a control. Injected RNA amounts were (where not otherwise noted): *nlacZ* (300 pg), *XRDH10* (1 ng), *XRALDH2* (1 ng) and *XCYP26A1* (0.5 ng). ey, eye; rh, rhombomere; *R2*, *XRALDH2*; *R10*, *XRDH10*. The indicated changes in gene expression were observed in: B, 35/78; C, 43/59; D, 18/29; E, 9/9; G, 24/96; H, 45/95; I, 30/51; J, 13/13; L, 7/36; M, 22/33; N, 22/33; O, 15/15; Q, 6/56 (*En2*); R, 7/19 (*En2*); S, 8/20 (*En2*); T, 25/25 (*En2*) embryos.

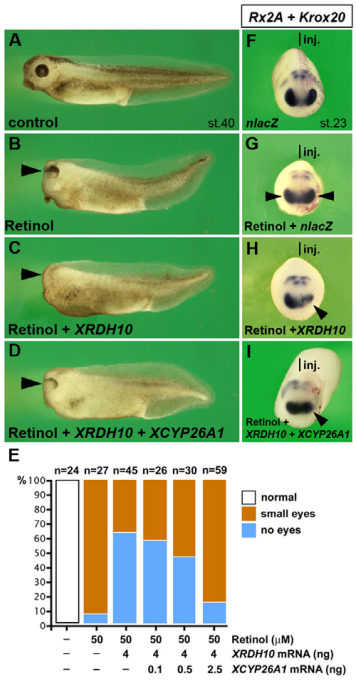

Fig. 6. XRDH10 co-operates with retinol during head development. (**A-D**) Embryos were injected into the animal pole at the four-cell stage with the indicated mRNAs and treated with DMSO or retinol at stages 9-12. (A) DMSO-treated control embryo at tadpole stage. (B) Retinol (50 μM) induces microcephaly at the tadpole stage. (C) Injection of *XRDH10* mRNA (1 ng into four blastomeres) and subsequent retinol treatment causes anencephaly. (D) *XCYP26A1* mRNA (2.5 ng) partially restores eye and head structures in retinol and *XRDH10*-treated embryos. (**E**) Eye deficiencies induced by retinol and *XRDH10*, and dose-dependent rescue by *XCYP26A1* mRNA in stage 40 embryos. (**F**) Control embryo at the tail bud stage after single injection of *nlacZ* mRNA. (**G**) Retinol (25 μM) leads to a slight reduction of the *Rx2A*-positive eye field (arrowheads). (**H**,**I**) In the retinol-treated embryos, *XRDH10* mRNA (1 ng in one dorsal blastomere) causes a unilateral collapse of *Rx2A* expression (arrowhead in H), which is rescued by the co-injection of 2.5 ng *XCYP26A1* mRNA (arrowhead in I). The indicated phenotypes were observed in: A, 24/24; B, 25/27; C, 28/45; D, 51/59; G, 13/15; H, 20/35; I, 10/13 embryos.

Fig. 7F,I). Similarly, microinjection of mRNA for mouse *RALDH2* (*mRALDH2*), which is not targeted by the morpholino oligo, neutralized the effect of *XRALDH2*-MO and restored normal axial development (insets in Fig. 7G,J).

In gastrula embryos, radially injected *XRDH10*-MO and *XRALDH2*-MO reduced *Chordin* gene expression in the dorsal blastopore lip (Fig. 7K-M). Concomitantly, depletion of XRDH10 and XRALDH2 caused a significant expansion of *Goosecoid* and *ADMP* expression (Fig. 7N-S). Despite the robust stimulation of *Xlim1* expression in gain-of-function experiments (Fig. 4G-J), depletion of XRDH10 or XRALDH2 did not affect this marker at gastrula stage (data not shown). However, *XRDH10*-MO or *XRALDH2*-MO caused a posteriorward retraction of the *Xlim1* expression domain in the pronephros anlage of neurula embryos (Fig. 7T-V).

We next investigated the effects of downregulating XRDH10 and XRALDH2 on anteroposterior patterning of the CNS (Fig. 8). At the advanced gastrula stage, unilaterally injected *XRDH10*-MO reduced transcript levels and shifted the anterior boundary of *HoxD1* expression posteriorly (Fig. 8B). The *XRALDH2*-MO (Fig. 8C), or a combination of *XRDH10*-MO and *XRALDH2*-MO (Fig. 8D), caused a similar effect. The specificity of this phenotype was underscored by the findings that a control morpholino had no effect (Fig. 8A), and that co-injection of non-targeted *XRDH10** and *mRALDH2* mRNAs with their respective MOs restored normal *HoxD1* expression (Fig. 8E,F). In neurula embryos, *XRDH10*-MO and *XRALDH2*-MO caused a slight posterior distortion of the midbrain-hindbrain boundary (*En2*), a posterior shift of hindbrain rhombomeres (*HoxB3*, *xCRABP*), but no significant effect on *HoxC6* expression in the spinal cord (Fig. 8G-L; see also Fig. S3 in the supplementary material). At the tail bud stage, *XRDH10* and *XRALDH2* morphant embryos exhibited a posterior shift of rhombomeres 3 and 5 (*Krox20*) relative to the unaffected eye field (*Rx2A*; Fig. 8M-R). Notably, the extent of the rhombomeric shift induced by 2.6 pmol *XRDH10*-MO was similar to that of an equimolar amount of *XRALDH2*-MO, and was not significantly increased when both MOs were injected together (Fig. 8S). Our results are consistent with those obtained from other loss-of-function experiments, using dominant-negative retinoid receptors (Kolm et al., 1997; Blumberg, 1997; van der Wees et al., 1998) and the RA hydroxylase CYP26A1 (Hollemann et al., 1998), supporting a contribution of XRDH10 and XRALDH2 in positioning hindbrain rhombomeres along the anteroposterior neuraxis in *Xenopus*.

To address whether XRDH10 is involved in vitamin A metabolism, we investigated the effects of downregulating the XRDH10 enzyme in the presence of exogenous retinol (Fig. 8T-W). To this end, we treated embryos with DMSO as a control or with 100 μM retinol. In advanced gastrula embryos, retinol led to an anterior expansion of *HoxD1* expression (Fig. 8T,V). The retinol-mediated anterior expansion of *HoxD1* expression was reverted by XRDH10-MO on the injected side (Fig. 8W), suggesting that the posteriorizing effect of retinol depends on XRDH10 activity. Together, the experiments demonstrate an involvement of XRDH10 in RA biosynthesis during axes formation and hindbrain patterning.

DISCUSSION

In this study, we investigated the role of RDH10 in the early *Xenopus* embryo. By gain- and loss-of-function assays, we have shown that XRDH10 upregulates retinoic acid (RA) signalling and is important for the correct specification of the dorsoventral and anteroposterior body axes. XRDH10 cooperates with XRALDH2 and participates in determining the position of the hindbrain rhombomeres. Our data suggest that XRDH10 contributes to building up the RA morphogen gradient in the embryo.

Timing and regulation of *RDH10* gene activity in the early embryo

Xenopus RDH10 exhibits tissue-specific expression with common expression domains to mouse *RDH10*; for example, in the lateral trunk mesoderm, ventral neuroepithelium, at the midbrain-hindbrain boundary, and in sensory organs (Fig. 2) (Sandell et al., 2007; Cammas et al., 2007; Romand et al., 2008). However, there are differences in the timing of induction and distribution of gene

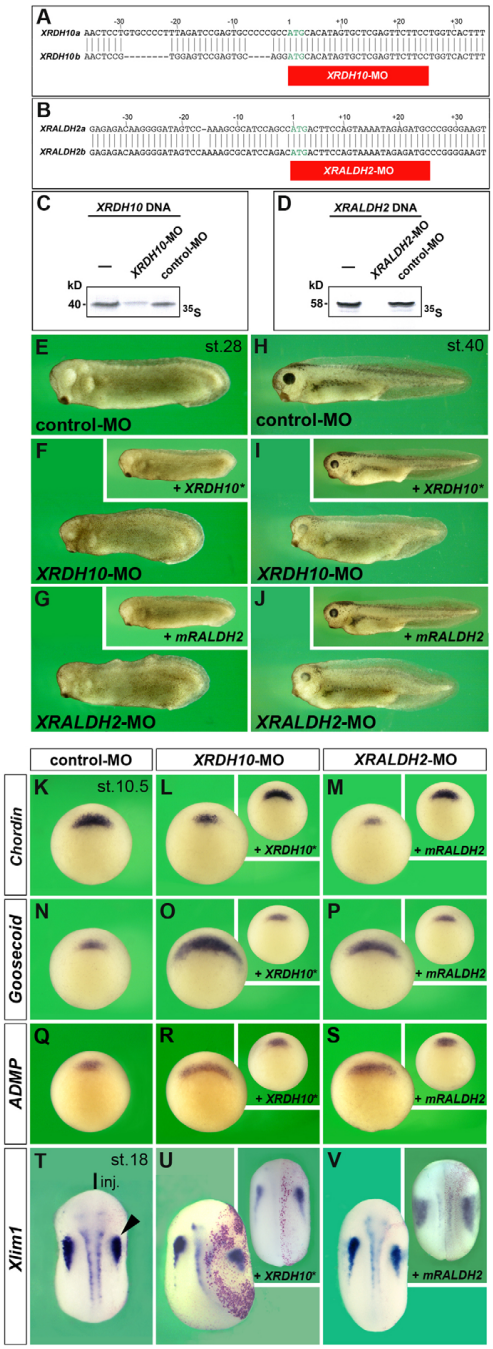

Fig. 7. Knockdown of *XRDH10* and *XRALDH2* induces ventralization and influences mesodermal gene expression. Antisense morpholino oligonucleotides (MOs) were injected marginally at the two-cell stage (5.2 pmol per blastomere), followed by injection of non-targeted mRNA constructs (*XRDH10** and *mRALDH2*) at the four-cell stage (1 ng per blastomere). (**A**,**B**) MOs target the translation initiation sites of two pseudoalleles of *Xenopus laevis RDH10* and *RALDH2*. (**C**,**D**) Protein synthesis of *XRDH10* and *XRALDH2* is specifically inhibited by *XRDH10*-MO and *XRALDH2*-MO, but not by control-MO of random sequence. (**E-J**) Microinjection of *XRDH10*-MO and *XRALDH2*-MO leads to microcephaly and enlarged ventroposterior structures in tailbud embryos (E-G), and to reduced eye structures and shortened tails in tadpoles (H-J). Normal development is restored by *XRDH10** and *mRALDH2* mRNAs, respectively (insets). (**K-S**) Gastrula embryos in dorsal view. *XRDH10*- and *XRALDH2*-morphants have reduced *Chordin* expression (K-M) and expanded expression domains of *Goosecoid* (N-P) and *ADMP* (Q-S). (**T-V**) Neurula embryos in dorsal view (anterior to the top) after a single injection of MOs with the lineage tracer *nlacZ* mRNA (red nuclei). *XRDH10*-MO and *XRALDH2*-MO reduce *Xlim1* expression in the pronephros (arrowhead). The indicated phenotypes were observed in: E, 101/117; F, 62/84 (inset, 73/98); G, 44/67 (inset, 80/84); H, 74/79; I, 39/50 (inset, 56/68); J, 18/48 (inset, 58/64); K, 33/33; L, 21/36 (inset, 19/27); M, 28/36 (inset, 20/28); N, 51/56; O, 28/38 (inset, 46/53); P, 37/49 (inset, 34/44); Q, 52/52; R, 14/26 (inset, 51/62); S, 51/62 (inset, 23/32); T, 11/15; U, 14/20 (inset, 28/32); V, 16/24 (inset, 50/51) embryos.

transcripts in both species. The earliest expression of mouse *RDH10* was reported in head-fold-stage embryos just prior to somitogenesis (Sandell et al., 2007; Cammas et al., 2007). We detected abundant maternal *XRDH10* gene products (Fig. 2A-D), which may contribute to the high levels of retinal observed in the egg and embryonic yolk (Azuma et al., 1990; Lampert et al., 2003), and robust expression levels during gastrulation (Fig. 2A,E,F,I,J), when the embryo is most sensitive to RA exposure (Durston et al., 1989; Sive et al., 1990). *XRDH10* displayed distinct expression in the dorsal blastopore lip, head process, telencephalon anlage and neural crest, which have no apparent counterpart for mouse *RDH10*.

We found that RA downregulates transcript levels of *RDH10* in *Xenopus* embryos (Fig. 3). Importantly, lowering of embryonic RA levels with the pharmacological inhibitors disulfiram and citral, or with the metabolic enzyme XCYP26A1, elevated *XRDH10* expression, suggesting that endogenous RA suppresses *XRDH10* gene activity. Previous studies have shown that RA downregulates *RALDH2* expression (Niederreither et al., 1997; Chen et al., 2001; Dobbs-McAuliffe et al., 2004) and, conversely, RA upregulated *CYP26A1* transcript levels in several species (White et al., 1996; Ray et al., 1997; Hollemann et al., 1998; White et al., 2007). Thus, the targeting of the *XRDH10* gene by RA adds to an intricate regulatory network, in which RA suppresses anabolic (RA-synthesizing) and stimulates catabolic (RA-degrading) enzymes (Fig. 3M). This fine-tuned feedback control provides protection against exogenous retinoid fluctuations and allows the stabilization of local RA distributions in the embryo.

RDH10 in the Spemann's organizer

We observed novel expression domains of *XRDH10*, most strikingly in the dorsal blastopore lip (Fig. 2E,F). This group of cells, referred to as the Spemann's organizer, plays a prominent role in the specification of the embryonic body axes, and the induction and

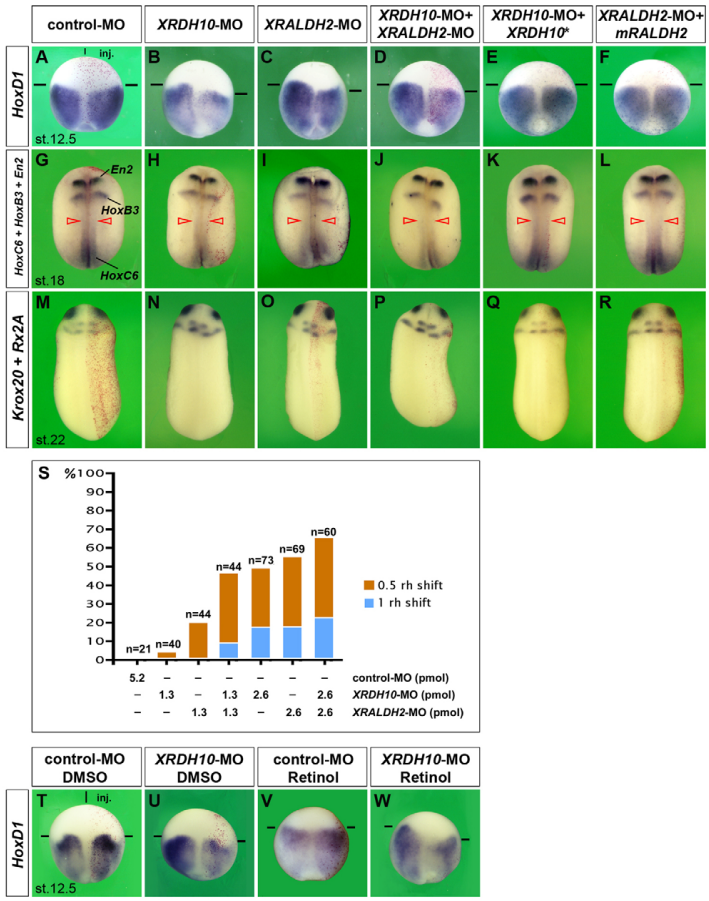

Fig. 8. XRDH10 contributes to CNS patterning and the posteriorizing effect of retinol. Morpholino oligonucleotides (MOs; each 2.6 pmol per embryo) were injected into the margin of one blastomere at the two-cell stage. The non-targeted mRNA constructs *XRDH10** and *mRALDH2* (each 1 ng) and the lineage tracer *nlacZ* mRNA were co-injected. Embryos are shown in dorsal view (anterior to the top). (**A-F**) Late gastrula embryos. *XRDH10*-MO, *XRALDH2*-MO, or a combination of both morpholinos, cause a reduction and posteriorward retraction of *HoxD1*expression, which is reverted by *XRDH10** and *mRALDH2* mRNA. (**G-L**) Neurula embryos showing expression of *En2* (midbrain-hindbrain boundary), *HoxB3* (hindbrain rhombomeres 5 and 6) and *HoxC6* (anterior spinal cord). (**M-R**) Tailbud embryos depicting expression of *Rx2A* (eyes) and *Krox20* (rhombomeres 3 and 5). (**S**) Effects of *XRDH10* and *XRALDH2* knockdown on hindbrain patterning. The posteriorward shift of *Krox20* expression is shown in response to MO injections at the indicated doses. (**T-W**) Treatment with 100 μM retinol at stages 9-12 induces a robust anterior expansion of *HoxD1* expression in late gastrula embryos (V). *XRDH10*-MO reverts the effect of retinol on the injected right-hand side (W). Frequency of embryos with the indicated phenotype was: A, 77/88; B, 55/105; C, 30/68; D, 54/88; E, 19/21; F, 23/25; G, 34/35; H, 17/31 (*En2*); H, 30/31 (*HoxB3*); H, 27/31 (*HoxC6*); I, 15/33 (*En2*); I, 31/33 (*HoxB3*); I, 32/33 (*HoxC6*); J, 6/9 (*En2*); J, 8/9 (*HoxB3*); J, 5/9 (*HoxC6*); K, 20/23; L, 39/39; M, 10/10; N, 35/73; O, 37/69; P, 38/60; Q, 10/10; R, 13/14; T, 9/9; U, 7/13; V, 9/9; W, 20/33 embryos.

pattern formation of the developing CNS (De Robertis and Kuroda, 2004). Interestingly, *XRDH10* transcripts in the organizer not only overlap with *XRALDH2* but are complementary to *XCYP26A1* expression (Fig. 2E-H) (Hollemann et al., 1998; Chen et al., 2001). *XRDH10* gene activity also coincides with active RA signalling in this region (Chen et al., 1994; Yelin et al., 2005). Our gain- and loss-of-function studies suggest a novel role for RA in positively regulating *Chordin* and negatively regulating *ADMP* expression (Figs 4, 7). Chordin is a soluble BMP antagonist and a key mediator of Spemann's organizer activity (Sasai et al., 1994; De Robertis and Kuroda, 2004). The anti-dorsalizing morphogenetic protein (ADMP) secreted from the dorsal gastrula organizer (Moos et al., 1995) induces BMP/Smad1 signalling via the ALK2 receptor (Reversade and De Robertis, 2005). Knockdown of XRDH10 and XRALDH2 cause small head and enlarged ventroposterior structures (Fig. 7), a phenotype that is commonly seen upon elevated BMP/Smad1 activity (e.g. Pera et al., 2003; Fuentealba et al., 2007). The opposite transcriptional regulation of the secreted proteins Chordin and ADMP by RA (this study) suggests a possible mechanism of how XRDH10 and XRALDH2 could promote Spemann's organizer activity and dorsal development.

Model for the establishment of the retinoic acid morphogen gradient

RA is a known morphogen that provides spatial information in various developmental contexts (Thaller and Eichele, 1987; Wolpert, 1989; Kessel and Gruss, 1991; White et al., 2007). Along the anteroposterior neuraxis, concentration-dependent gradients of RA specify positional values via the activation of Hox genes in the developing hindbrain (Gould et al., 1998; Dupé and Lumsden, 2001) and spinal cord (Muhr et al., 1999; Liu et al., 2001). Previous models have suggested that these RA gradients arise mainly as a result of local RA supply by RALDH2 in the paraxial trunk mesoderm, diffusion of RA, and CYP26A1-mediated RA decay at the anterior and posterior ends of the neural plate (Maden, 1999; Maden, 2002; Sirbu et al., 2005; Hernandez et al., 2007; White et al., 2007). During

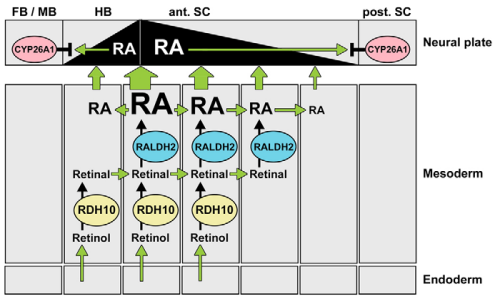

Fig. 9. Model for the establishment of retinoic acid morphogen gradients in the early embryo. The nested gene expression and combinatorial action of *RDH10* and *RALDH2* causes a posteriorward flow of retinal that generates an initial RA gradient in the trunk mesoderm with a peak at the level of the hindbrain-spinal cord boundary. Subsequent diffusion of RA creates two gradients across the hindbrain and spinal cord, which acquire their final shape through CYP26A1-mediated RA degradation at the anterior (ant.) and posterior (post.) ends of the neural plate. FB, forebrain; MB, midbrain; HB, hindbrain; SC, spinal cord.

gastrulation of lower vertebrates, retinoid stores in the yolk translocate from vegetal cells mainly to the endoderm (Azuma et al., 1990; Lampert et al., 2003). However, RALDH2 activity in the dorsal blastopore lip and trunk mesoderm may lead to a local shortage of retinal that could cause a collapse of the RA gradient. Indeed, the phenotypes of XRDH10 morphants affecting organizer-specific gene expression and hindbrain patterning (Figs 7, 8) provide strong evidence for the need of ongoing retinol conversion to retinal in the developing embryo.

Our data suggest an alternative mode of RA gradient formation based on the specific expression characteristics and on cooperation between RDH10 and RALDH2 (Fig. 9). The microsomal RDH10 enzyme in the anterior trunk mesoderm produces and secretes retinal that diffuses into posterior cells, where RALDH2 converts it into RA. The combinatorial mRNA distribution of *RDH10* and *RALDH2* (with *RDH10* being more anteriorly expressed than *RALDH2*) is crucial for the posteriorward flow of retinal. As a consequence, highest levels of RA are produced at the anterior front of the *RALDH2* expression domain, with decreasing concentrations towards its posterior end. As RDH10 ensures a continuous local supply of retinal, this enzyme also contributes to the stabilization of the RA gradient. At the neural plate stage, the peak of RA concentration is located at the hindbrain-spinal cord boundary, but as development progresses it moves concomitant with the translocation of the *RDH10* and *RALDH2* expression domains posteriorward. It is of interest that the RA-responsive Hox genes show a sharp anterior border of expression and posteriorly declining transcript levels (De Robertis et al., 1991), reflecting the gradual RA distribution generated by RDH10 and RALDH2. In conclusion, our data suggest that an initial RA gradient forms in the anterior trunk mesoderm already at the step of RA synthesis.

The combinatorial gene expression of two enzymes that act back-to-back to produce a signal, here referred to as a 'biosynthetic enzyme code', constitutes a novel mechanism for forming and stabilizing a morphogen gradient. This mechanism may apply not only to the establishment of RA gradients along the embryonic axis, but also to other areas where *RDH10* and *RALDH2* overlap, such as in the dorsal blastopore lip, the pronephros anlage, the eye field and the ear placode. In the mouse, additional sites of overlapping *RDH10* and *RALDH2* expression have been reported for the limb anlage and the foetal brain (Niederreither et al., 1997; Sandell et al., 2007; Cammas et al., 2007; Romand, 2008). Future studies need to address the significance of an interaction between the two enzymes in these morphogenetic fields. It is noteworthy that the mechanism of nested gene expression and combinatorial action has initially been found in the homeotic Hox genes, which are the most prominent targets of RA signalling in vertebrates (Kessel and Gruss, 1991). This suggests a common principle for the generation and downstream signalling events of this morphogen.

We are indebted to Drs T. Pieler, E. M. De Robertis, A. Durston, R. Harland, J. Smith, T. Hollemann, M. Taira, H. Sive, D. Wilkinson, M. Jamrich, A. Hemmati-Brivanlou, N. Papalopulu and N. Bardine for gifts of plasmids. We wish to thank J. K. Jacobsen and N. Herold for invaluable help, I. Wunderlich and I. Liljekvist-Soltic for expert technical assistance, and Drs O. Wessely, M. Kessel, T. Pieler, E. Wimmer, S. E. Jacobsen, U. Häcker, H. Semb and S. Hou for comments on the manuscript and discussions. This work was supported by grants from the German Research Foundation (PE728/3), the Swedish Research Council, the Crafoord foundation, and the Lund Stem Cell Program.

Supplementary material

Supplementary material for this article is available at http://dev.biologists.org/cgi/content/full/136/3/461/DC1

References

Abu-Abed, S., Dollé, P., Metzger, D., Beckett, B., Chambon, P. and Petkovich, M. (2001). The retinoic acid-metabolizing enzyme, CYP26A1, is essential for normal hindbrain patterning, vertebral identity, and development of posterior structures. *Genes Dev.* **15**, 226-240.

Azuma, M., Seki, T. and Fujishita, S. (1990). Changes of egg retinoids during the development of Xenopus laevis. *Vision Res.* **30**, 1395-1400.

Balkan, W., Colbert, M., Bock, C. and Linney, E. (1992). Transgenic indicator mice for studying activated retinoic acid receptors during development. *Proc. Natl. Acad. Sci. USA* **89**, 3347-3351.

Begemann, G., Schilling, T. F., Rauch, G. J., Geisler, R. and Ingham, P. W. (2001). The zebrafish neckless mutation reveals a requirement for raldh2 in mesodermal signals that pattern the hindbrain. *Development* **128**, 3081-3094.

Belyaeva, O. V., Johnson, M. P., Kedishvili, N. Y. (2008). Kinetic analysis of human enzyme RDH10 defines the characteristics of a physiologically relevant retinol dehydrogenase. *J. Biol. Chem.* **283**, 20299-20308.

Blumberg, B. (1997). An essential role for retinoid signaling in anteroposterior neural specification and neuronal differentiation. *Semin. Cell Dev. Biol.* **8**, 417-428.

Cammas, L., Romand, R., Fraulob, V., Mura, C. and Dollé, P. (2007). Expression of the murine retinol dehydrogenase 10 (Rdh10) gene correlates with many sites of retinoid signalling during embryogenesis and organ differentiation. *Dev. Dyn.* **236**, 2899-2908.

Chambers, D., Wilson, L., Maden, M. and Lumsden, A. (2007). RALDH-independent generation of retinoic acid during vertebrate embryogenesis by CYP1B1. *Development* **134**, 1369-1383.

Chen, Y., Huang, L. and Solursh, M. (1994). A concentration gradient of retinoids in the early Xenopus laevis embryo. *Dev. Biol.* **161**, 70-76.

Chen, Y., Pollet, N., Niehrs, C. and Pieler, T. (2001). Increased XRALDH2 activity has a posteriorizing effect on the central nervous system of Xenopus embryos. *Mech. Dev.* **101**, 91-103.

Cho, K. W. and De Robertis, E. M. (1990). Differential activation of Xenopus homeo box genes by mesoderm-inducing growth factors and retinoic acid. *Genes Dev.* **4**, 1910-1916.

Cho, K. W., Blumberg, B., Steinbeisser, H. and De Robertis, E. M. (1991). Molecular nature of Spemann's organizer: the role of the Xenopus homeobox gene goosecoid. *Cell* **67**, 1111-1120.

Clagett-Dame, M. and DeLuca, H. F. (2002). The role of vitamin A in mammalian reproduction and embryonic development. *Annu. Rev. Nutr.* **22**, 347-381.

De Robertis, E. M. (2006). Spemann's organizer and self-regulation in amphibian embryos. *Nat. Rev. Mol. Cell Biol.* **7**, 296-302.

De Robertis, E. M. and Kuroda, H. (2004). Dorsal-ventral patterning and neural induction in Xenopus embryos. *Annu. Rev. Cell Dev. Biol.* **20**, 285-308.

De Robertis, E. M., Morita, E. A. and Cho, K. W. (1991). Gradient fields and homeobox genes. *Development* **112**, 669-678.

de Roos, K., Sonneveld, E., Compaan, B., ten Berge, D., Durston, A. J. and van der Saag, P. T. (1999). Expression of retinoic acid 4-hydroxylase (CYP26) during mouse and Xenopus laevis embryogenesis. *Mech. Dev.* **82**, 205-211.
Dibner, C., Elias, S., Ofir, R., Souopgui, J., Kolm, P. J., Sive, H., Pieler, T. and Frank, D. (2004). The Meis3 protein and retinoid signaling interact to pattern the Xenopus hindbrain. *Dev. Biol.* **271**, 75-86.
Dobbs-McAuliffe, B., Zhao, Q. and Linney, E. (2004). Feedback mechanisms regulate retinoic acid production and degradation in the zebrafish embryo. *Mech. Dev.* **121**, 339-350.
Duester, G. (2008). Retinoic acid synthesis and signaling during early organogenesis. *Cell* **134**, 921-931.
Duester, G., Mic, F. A. and Molotkov, A. (2003). Cytosolic retinoid dehydrogenases govern ubiquitous metabolism of retinol to retinaldehyde followed by tissue-specific metabolism to retinoic acid. *Chem. Biol. Interact.* **143-144**, 201-210.
Dupé, V. and Lumsden, A. (2001). Hindbrain patterning involves graded responses to retinoic acid signalling. *Development* **128**, 2199-208.
Durston, A. J., Timmermans, J. P., Hage, W. J., Hendriks, H. F., de Vries, N. J., Heideveld, M. and Nieuwkoop, P. D. (1989). Retinoic acid causes an anteroposterior transformation in the developing central nervous system. *Nature* **340**, 140-144.
Gould, A., Itasaki, N. and Krumlauf, R. (1998). Initiation of rhombomeric Hoxb4 expression requires induction by somites and a retinoid pathway. *Neuron* **21**, 39-51.
Grandel, H., Lun, K., Rauch, G. J., Rhinn, M., Piotrowski, T., Houart, C., Sordino, P., Küchler, A. M., Schulte-Merker, S., Geisler, R., Holder, N., Wilson, S. W. and Brand, M. (2002). Retinoic acid signalling in the zebrafish embryo is necessary during pre-segmentation stages to pattern the anterior-posterior axis of the CNS and to induce a pectoral fin bud. *Development* **129**, 2851-2865.
Fuentealba, L. C., Eivers, E., Ikeda, A., Hurtado, C., Kuroda, H., Pera, E. M. and De Robertis, E. M. (2007). Integrating patterning signals: Wnt/GSK3 regulates the duration of the BMP/Smad1 signal. *Cell* **131**, 980-993.
Hernandez, R. E., Putzke, A. P., Myers, J. P., Margaretha, L. and Moens, C. B. (2007). Cyp26 enzymes generate the retinoic acid response pattern necessary for hindbrain development. *Development* **134**, 177-187.
Hollemann, T., Chen, Y., Grunz, H. and Pieler, T. (1998). Regionalized metabolic activity establishes boundaries of retinoic acid signalling. *EMBO J.* **17**, 7361-7372.
Hou, S., Maccarana, M., Min, T. H., Strate, I. and Pera, E. M. (2007). The secreted serine protease xHtrA1 stimulates long-range FGF signaling in the early Xenopus embryo. *Dev. Cell* **13**, 226-241.
Kessel, M. (1992). Respecification of vertebral identities by retinoic acid. *Development* **115**, 487-501.
Kessel, M. and Gruss, P. (1991). Homeotic transformations of murine vertebrae and concomitant alteration of Hox codes induced by retinoic acid. *Cell* **67**, 89-104.
Khokha, M. K., Yeh, J., Grammer, T. C. and Harland, R. M. (2005). Depletion of three BMP antagonists from Spemann's organizer leads to a catastrophic loss of dorsal structures. *Dev. Cell* **8**, 401-411.
Kolm, P. J., Apekin, V. and Sive, H. (1997). Xenopus hindbrain patterning requires retinoid signaling. *Dev. Biol.* **192**, 1-16.
Kudoh, T., Wilson, S. W. and Dawid, I. B. (2002). Distinct roles for Fgf, Wnt and retinoic acid in posteriorizing the neural ectoderm. *Development* **129**, 4335-4346.
Lampert, J. M., Holzschuh, J., Hessel, S., Driever, W., Vogt, K. and von Lintig, J. (2003). Provitamin A conversion to retinal via the beta,beta-carotene-15,15'-oxygenase (bcox) is essential for pattern formation and differentiation during zebrafish embryogenesis. *Development* **130**, 2173-2186.
Lidén, M. and Eriksson, U. (2006). Understanding retinol metabolism: structure and function of retinol dehydrogenases. *J. Biol. Chem.* **281**, 13001-13004.
Liu, J. P., Laufer, E. and Jessell, T. M. (2001). Assigning the positional identity of spinal motor neurons: rostrocaudal patterning of Hox-c expression by FGFs, Gdf11, and retinoids. *Neuron* **32**, 997-1012.
Maden, M. (1999). Heads or tails? Retinoic acid will decide. *BioEssays* **21**, 809-812.
Maden, M. (2002). Retinoid signalling in the development of the central nervous system. *Nat. Rev. Neurosci.* **3**, 843-853.
Mark, M., Ghyselinck, N. B. and Chambon, P. (2006). Function of retinoid nuclear receptors: lessons from genetic and pharmacological dissections of the retinoic acid signaling pathway during mouse embryogenesis. *Annu. Rev. Pharmacol. Toxicol.* **46**, 451-480.
Marshall, H., Nonchev, S., Sham, M. H., Muchamore, I., Lumsden, A. and Krumlauf, R. (1992). Retinoic acid alters hindbrain Hox code and induces transformation of rhombomeres 2/3 into a 4/5 identity. *Nature* **360**, 737-741.
Mendelsohn, C., Ruberte, E., LeMeur, M., Morriss-Kay, G. and Chambon, P. (1991). Developmental analysis of the retinoic acid-inducible RAR-beta 2 promoter in transgenic animals. *Development* **113**, 723-734.
Moos, M., Jr, Wang, S. and Krinks, M. (1995). Anti-dorsalizing morphogenetic protein is a novel TGF-beta homolog expressed in the Spemann organizer. *Development* **121**, 4293-4301.
Muhr, J., Graziano, E., Wilson, S., Jessell, T. M. and Edlund, T. (1999). Convergent inductive signals specify midbrain, hindbrain, and spinal cord identity in gastrula stage chick embryos. *Neuron* **23**, 689-702.
Niederreither, K. and Dollé, P. (2008). Retinoic acid in development: towards an integrated view. *Nat. Rev. Genet.* **9**, 541-553.
Niederreither, K., McCaffery, P., Drager, U. C., Chambon, P. and Dolle, P. (1997). Restricted expression and retinoic acid-induced downregulation of the retinaldehyde dehydrogenase type 2 (RALDH-2) gene during mouse development. *Mech. Dev.* **62**, 67-78.
Niederreither, K., Subbarayan, V., Dolle, P. and Chambon, P. (1999). Embryonic retinoic acid synthesis is essential for early mouse post-implantation development. *Nat. Genet.* **21**, 444-448.
Niehrs, C. (2004). Regionally specific induction by the Spemann-Mangold organizer. *Nat. Rev. Genet.* **5**, 425-434.
Nieuwkoop, P. (1952). Activation and organization of the central nervous system in amphibians. III. Synthesis of a new working hypothesis. *J. Exp. Zool.* **120**, 83-108.
Olivera-Martinez, I. and Storey, K. G. (2007). Wnt signals provide a timing mechanism for the FGF-retinoid differentiation switch during vertebrate body axis extension. *Development* **134**, 2125-2135.
Papalopulu, N., Clarke, J. D., Bradley, L., Wilkinson, D., Krumlauf, R. and Holder, N. (1991). Retinoic acid causes abnormal development and segmental patterning of the anterior hindbrain in Xenopus embryos. *Development* **113**, 1145-1158.
Pera, E. M., Wessely, O., Li, S. Y. and De Robertis, E. M. (2001). Neural and head induction by insulin-like growth factor signals. *Dev. Cell* **1**, 655-665.
Pera, E. M., Ikeda, A., Eivers, E. and De Robertis, E. M. (2003). Integration of IGF, FGF, and anti-BMP signals via Smad1 phosphorylation in neural induction. *Genes Dev.* **17**, 3023-3028.
Pera, E. M., Hou, S., Strate, I., Wessely, O. and De Robertis, E. M. (2005). Exploration of the extracellular space by a large-scale secretion screen in the early Xenopus embryo. *Int. J. Dev. Biol.* **49**, 781-796.
Persson, B., Kallberg, Y., Oppermann, U. and Jörnvall, H. (2003). Coenzyme-based functional assignments of short-chain dehydrogenases/reductases (SDRs). *Chem. Biol. Interact.* **143-144**, 271-278.
Ray, W. J., Bain, G., Yao, M. and Gottlieb, D. I. (1997). CYP26, a novel mammalian cytochrome P450, is induced by retinoic acid and defines a new family. *J. Biol. Chem.* **272**, 18702-18708.
Reversade, B. and De Robertis, E. M. (2005). Regulation of ADMP and BMP2/4/7 at opposite embryonic poles generates a self-regulating morphogenetic field. *Cell* **123**, 1147-1160.
Richard-Parpaillon, L., Héligon, C., Chesnel, F., Boujard, D. and Philpott, A. (2002). The IGF pathway regulates head formation by inhibiting Wnt signaling in Xenopus. *Dev. Biol.* **244**, 407-417.
Romand, R., Kondo, T., Cammas, L., Hashino, E. and Dollé, P. (2008). Dynamic expression of the retinoic acid-synthesizing enzyme retinol dehydrogenase 10 (rdh10) in the developing mouse brain and sensory organs. *J. Comp. Neurol.* **508**, 879-892.
Ross, S. A., McCaffery, P. J., Drager, U. C. and De Luca, L. M. (2000). Retinoids in embryonal development. *Physiol. Rev.* **80**, 1021-1054.
Rossant, J., Zirngibl, R., Cado, D., Shago, M. and Giguere, V. (1991). Expression of a retinoic acid response element-hsplacZ transgene defines specific domains of transcriptional activity during mouse embryogenesis. *Genes Dev.* **5**, 1333-1344.
Ruiz i Altaba, A. and Jessell, T. (1991). Retinoic acid modifies mesodermal patterning in early Xenopus embryos. *Genes Dev.* **5**, 175-187.
Sandell, L. L., Sanderson, B. W., Moiseyev, G., Johnson, T., Mushegian, A., Young, K., Rey, J. P., Ma, J. X., Staehling-Hampton, K. and Trainor, P. A. (2007). RDH10 is essential for synthesis of embryonic retinoic acid and is required for limb, craniofacial, and organ development. *Genes Dev.* **21**, 1113-1124.
Sakai, Y., Meno, C., Fujii, H., Nishino, J., Shiratori, H., Saijoh,Y., Rossant, J. and Hamada, H. (2001). The retinoic acid-inactivating enzyme CYP26 is essential for establishing an uneven distribution of retinoic acid along the anterio-posterior axis within the mouse embryo. *Genes Dev.* **15**, 213-225.
Sasai, Y., Lu, B., Steinbeisser, H., Geissert, D., Gont, L. K. and De Robertis, E. M. (1994). Xenopus chordin: a novel dorsalizing factor activated by organizer-specific homeobox genes. *Cell* **79**, 779-790.
Schuh, T. J., Hall, B. L., Kraft, J. C., Privalsky, M. L. and Kimelman, D. (1993). v-erbA and citral reduce the teratogenic effects of all-trans retinoic acid and retinol, respectively, in Xenopus embryogenesis. *Development* **119**, 785-798.
Shiotsugu, J., Katsuyama, Y., Arima, K., Baxter, A., Koide, T., Song, J., Chandraratna, R. A. and Blumberg, B. (2004). Multiple points of interaction between retinoic acid and FGF signaling during embryonic axis formation. *Development* **131**, 2653-2667.
Sirbu, I. O., Gresh, L., Barra, J. and Duester, G. (2005). Shifting boundaries of retinoic acid activity control hindbrain segmental gene expression. *Development* **132**, 2611-2622.

Sive, H. L., Draper, B. W., Harland, R. M. and Weintraub, H. (1990). Identification of a retinoic acid-sensitive period during primary axis formation in Xenopus laevis. *Genes Dev.* **4**, 932-942.
Swindell, E. C., Thaller, C., Sockanathan, S., Petkovich, M., Jessell, T. M. and Eichele, G. (1999). Complementary domains of retinoic acid production and degradation in the early chick embryo. *Dev. Biol.* **216**, 282-296.
Taira, M., Otani, H., Jamrich, M. and Dawid, I. B. (1994). Expression of the LIM class homeobox gene Xlim-1 in pronephros and CNS cell lineages of Xenopus embryos is affected by retinoic acid and exogastrulation. *Development* **120**, 1525-1536.
Thaller, C. and Eichele, G. (1987). Identification and spatial distribution of retinoids in the developing chick limb bud. *Nature* **327**, 625-628.
van der Wees, J., Schilthuis, J. G., Koster, C. H., Diesveld-Schipper, H., Folkers, G. E., van der Saag, P. T., Dawson, M. I., Shudo, K., van der Burg, B. and Durston, A. J. (1998). Inhibition of retinoic acid receptor-mediated signalling alters positional identity in the developing hindbrain. *Development* **125**, 545-556.
Vermot, J. and Pourquié, O. (2005). Retinoic acid coordinates somitogenesis and left-right patterning in vertebrate embryos. *Nature* **435**, 215-220.
von Bubnoff, A., Schmidt, J. E. and Kimelman, D. (1995). The Xenopus laevis homeobox gene Xgbx-2 is an early marker of anteroposterior patterning in the ectoderm. *Mech. Dev.* **54**, 149-160.
Ward, S. J., Chambon, P., Ong, D. E. and Båvik, C. (1997). A retinol-binding protein receptor-mediated mechanism for uptake of vitamin A to postimplantation rat embryos. *Biol. Reprod.* **57**, 751-755.
White, J. A., Guo, Y. D., Baetz, K., Beckett-Jones, B., Bonasoro, J., Hsu, K. E., Dilworth, F. J., Jones, G. and Petkovich, M. (1996). Identification of the retinoic acid-inducible all-trans-retinoic acid 4-hydroxylase. *J. Biol. Chem.* **271**, 29922-29927.
White, R. J., Nie, Q., Lander, A. D. and Schilling, T. F. (2007). Complex regulation of cyp26a1 creates a robust retinoic acid gradient in the zebrafish embryo. *PLoS Biol.* **5**, e304.
Wolpert, L. (1989). Positional information revisited. *Development* **107 Suppl.**, 3-12.
Wu, B. X., Chen, Y., Chen, Y., Fan, J., Rohrer, B., Crouch, R. K. and Ma, J. X. (2002). Cloning and characterization of a novel all-trans retinol short-chain dehydrogenase/reductase from the RPE. *Invest. Ophthalmol. Vis. Sci.* **43**, 3365-3372.
Wu, B. X., Moiseyev, G., Chen, Y., Rohrer, B., Crouch, R. K. and Ma, J. X. (2004). Identification of RDH10, an all-trans retinol dehydrogenase, in retinal Muller cells. *Invest. Ophthalmol. Vis. Sci.* **45**, 3857-3862.
Yelin, R., Schyr, R. B., Kot, H., Zins, S., Frumkin, A., Pillemer, G. and Fainsod, A. (2005). Ethanol exposure affects gene expression in the embryonic organizer and reduces retinoic acid levels. *Dev. Biol.* **279**, 193-204.

Supplementary Materials

Retinol Dehydrogenase 10 is a feedback regulator of retinoic acid signalling during axis formation and patterning of the central nervous system

Ina Strate, Tan H. Min, Dobromir Iliev, and Edgar M. Pera

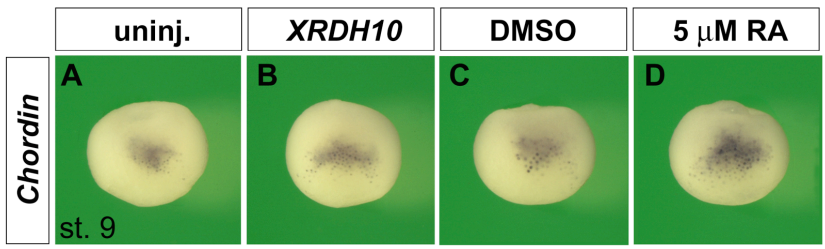

Figure S1. *XRDH10* mRNA and exogeneous RA slightly upregulate *Chordin* expression at the blastula stage.

Whole-mount *in situ* hybridization with antisense RNA against *Chordin*.

(A) Uninjected embryo at stage 9 in dorsal view.

(B) Embryo after microinjection of *XRDH10* mRNA into the margin of each blastomere at the 4-cell stage (total 4 ng).

(C,D) Embryos treated from stage 7 onwards with 0.05% DMSO (Dimethylsulfoxide) as control (C) or with 5 μM RA in DMSO (D).

Frequency of embryos with the indicated phenotypes was A, 10/11;B, 11/11; C, 31/38; D, 47/47.

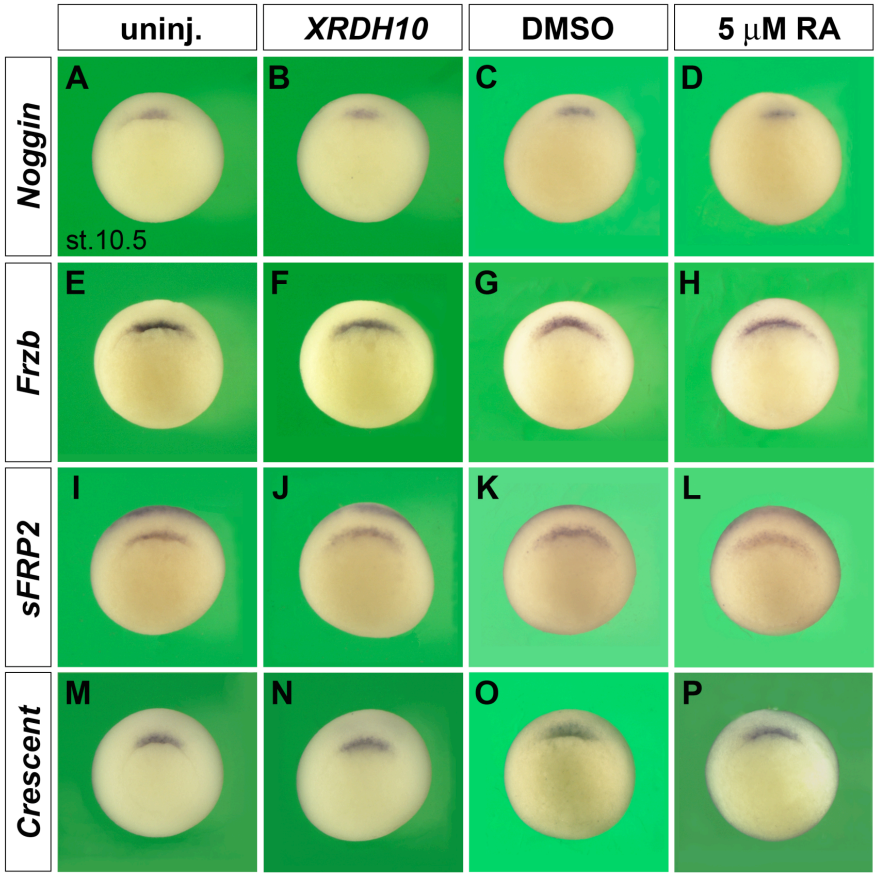

Figure S2. *XRDH10* mRNA and exogeneous RA have no effect on the organizer-specific expression of *Noggin*, *Frzb*, *sFRP2*, and *Crescent* at the early gastrula stage.

Vegetal view of embryos at stage 10.5. Embryos were uninjected (A,E,I,M), radially injected at the 4-cell stage with 4 ng *XRDH10* mRNA (B,F,J,N), treated from stage 8 onwards with DMSO (C,G,K,O) or with 5 μM RA (D,H,L,P). Note that expression of *Noggin*, *Frzb*, *sFRP2* and *Crescent* in the dorsal blastopore lip, is not affected by any of the treatments.

Frequency of embryos with the indicated phenotypes was A, 16/16;B, 24/28; C, 53/53; D, 45/45; E, 12/12; F, 27/27; G, 12/12; H, 20/20; I, 16/16; J, 25/25; K, 24/24; L, 28/28; M, 15/15; N, 28/28; O, 62/62; P, 42/46.

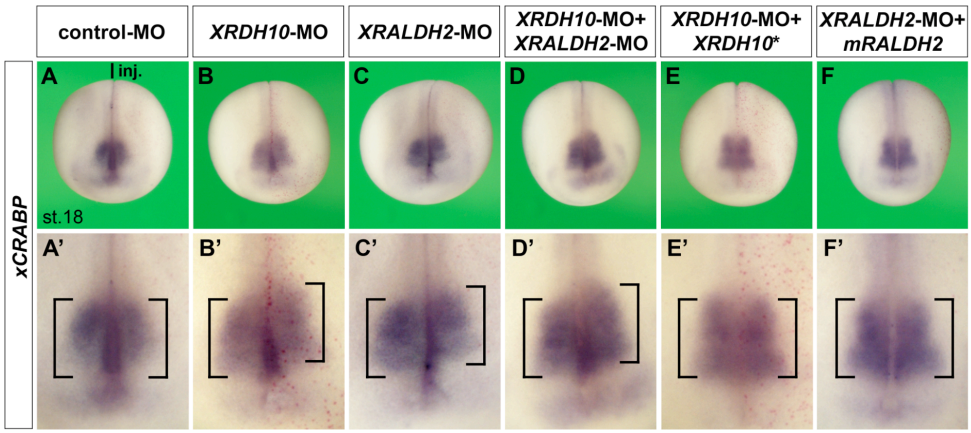

Supplementary Figure S3. Downregulation of XRDH10 and XRALDH2 causes a posteriorwards shift of the hindbrain marker *xCRABP*.

Morpholino oligonucleotides (MOs; each 2.6 pmol per embryo) were injected into the margin of a single blastomere at the 2-cell stage. The non-targeted mRNA constructs XRDH10* and mRALDH2 (each 1 ng) and the lineage tracer *nlacZ* mRNA (100 pg) were co-injected. Embryos at the advanced neurala stage are shown in anterior-dorsal view (posterior to the top). The panels A'-F' are magnifications of the embryos shown in A-F. Embryos were subjected to whole-mount *in situ* hybridization with an antisense RNA probe against xCRABP (cellular retinoic acid binding protein) that demarcates the presumptive hindbrain (square bracket). Nuclear Red-Gal staining (resulting from *nlacZ* mRNA expression) demarcates the injected right side.

(A) An unspecific control-MO does not affect *xCRABP* expression.

(B-D) *XRDH10*-MO, *XRALDH2*-MO, or a combination of both morpholinos, cause a posteriorwards shift of the *xCRABP*-expression domain.

(E,F) The effects of *XRDH10*-MO and *XRALDH2*-MO are neutralized by *XRDH10** and *mRALDH2* mRNA, respectively.

Frequency of embryos with the indicated phenotype was A, 9/11; B, 10/11; C, 18/19; D, 12/12; E, 11/11; F, 17/19.